

Alma Mater Studiorum – Università di Bologna

**DOTTORATO DI RICERCA IN
SCIENZE BIOMEDICHE**

Ciclo XXVII

Settore Concorsuale di afferenza: 06/A4

Settore Scientifico disciplinare: MED/08

**TOWARD A MOLECULAR CLASSIFICATION OF
PERIPHERAL T- CELL LYMPHOMAS: THE ROLE OF
GENE EXPRESSION PROFILING**

Presentata da: Maryam Etebari

Coordinatore Dottorato

Relatore

Prof. Lucio Cocco

Prof. Pier Paolo Piccaluga

Correlatore

Prof. Claudio Agostinelli

Esame finale anno 2016

Table of contents

1. Introduction.....	1
1.1. T lymphocyte development.....	2
1.2. T cell subsets.....	3
1.3. The World Health Organization classification of Peripheral T-cell lymphoma.....	6
1.3.1. Anaplastic large cell lymphoma.....	7
1.3.2. Angioimmunoblastic T-Cell Lymphoma.....	9
1.3.3. Peripheral T- Cell Lymphoma-not otherwise specified.....	9
1.3.3.1. Lennert lymphoma.....	11
1.3.3.2. Follicular variant of Peripheral T-cell lymphoma-not otherwise specified.....	12
1.3.3.3. T-zone variant of Peripheral T-cell lymphoma-not otherwise specified.....	12
1.4. Aim of the thesis.....	13
2. Materials and Methods.....	14
2.1. Case selection	15
2.2. Ethics statements.....	15
2.3. Gene and microRNA expression profile generation.....	15
2.4. Gene and microRNA expression analysis.....	16
2.5. High throughput massive parallel sequencing.....	18
2.6. Tissue microarray construction and Immunohistochemical analysis.....	20
2.7. Survival analyses	20
3. Results.....	22
3.1. Molecular profiling of Peripheral T-cell lymphomas-not otherwise specified identifies clinical subgroups corresponding to distinct T-cell populations.....	23
3.2. Gene and microRNA expression analysis of Lennert lymphoma reveals a unique profile and identifies novel therapeutic targets.....	39
3.3. Molecular Signature of Follicular Variant of Peripheral T-Cell Lymphoma Not Otherwise Specified Implies Distinction from Angioimmunoblastic T-cell Lymphoma.....	54
4. Discussion and Conclusion.....	62
References.....	69
Appendix (Supplementary Material).....	81

Abstract

Peripheral T-cell lymphomas-not otherwise specified (PTCL/NOS) are the most common T-cell neoplasms. This study sought to reshape the PTCL/NOS sub-classification (including its two main morphological variants, Lennert lymphoma, LL, and Follicular variant, F-PTCL) based on the correspondence between their molecular features and those of different functional T-cell subsets, also assessing the clinical impact of such an approach.

We found that PTCLs/NOS could be divided into groups corresponding to T-cell subsets differently reliant on transcription regulators including mTOR and FOXP3, and identified minimal gene sets discriminating among these groups. Notably, by grouping tumors according to their dependency on master regulators of T-lymphocyte fate, we identified three groups (T-cytotoxic, Treg/TFH, and other-T-helper) characterized by specific genetic patterns and significantly different clinical outcomes. Immunohistochemistry partially substituted for the molecular analysis by consistently recognizing only Treg and TFH cases. Finally, targeted inhibition of MTOR in T-helper cases (that were characterized by genetic lesions targeting the pathway) was proved to be effective *ex vivo*. We conclude that PTCL/NOS can be divided into subgroups corresponding to different cellular counterparts, characterized by different genetic patterns and possibly sensitivity to specific therapeutic approaches.

Furthermore, we identified different gene and microRNA signatures for LL capable of differentiating it from other PTCL/NOS and enriched in cytotoxic function. Moreover, PI3K/Akt/mTOR pathway emerged as novel therapeutic targets for LL. Additionally, LL showed some differences with other PTCL/NOS in terms of clinical features, all supporting its recognition as a distinct entity. Besides, we found that F-PTCL has a distinct molecular signature more similar to PTCL/NOS rather than AITL, and therefore cannot be included among AITLs at least based on GEP, although this necessities more genetic studies.

Overall, these results may impact on PTCL classification as well as on future studies aimed to define the more appropriate therapeutic strategy for each identified subgroup/entity.

Keywords: Peripheral T-cell lymphomas not otherwise specified, Lennert Lymphoma, Follicular Variant of PTCL, Gene expression Profiling, Normal Cell Counterpart, Classification

(1)

Introduction

1.1. T-lymphocytes development

T-lymphocytes or T-cells are a group of white blood cells that are involved in the cell-mediated immunity. They are the central element in adaptive immune system, and act different levels including primary response by naïve T-cells, followed by further processing mediated by activated T-cells, and persistence of Antigen-specific memory T-cells (1). Upon maturation in the thymus, T-cells express a unique T-cell receptor (TCR) on their cell surface that is the marker distinguishing T-cells from other lymphocytes. Two classes of mature T-cells are recognized based on the type of protein chains of TCR: Alpha–Beta ($\alpha\beta$) and Gamma–Delta ($\gamma\delta$). Alpha-Beta subtype account > 95 % of T-cells and comprise CD4+ (cluster of differentiation 4) and CD8+ (cluster of differentiation 8) T-cells, named after the expression of CD4 or CD8 glycoprotein at the cell surface, whereas $\gamma\delta$ T-cells (either CD4-CD8- or CD4-CD8+) account for < 5% of T-cells (2). T-lymphocytes leave thymus as naïve T-cells and enter to secondary (peripheral) lymph system. When naïve T-cells encounter an antigen in secondary lymphoid tissue, TCR triggers a cascade of signaling events that leads to activation of naïve T-cells, leading to their enlargement and conversion to blast T-cells with high potencies in proliferation and generating large population of clones further differentiate into effector or memory T-cells. The former perform the effector function such as cytokine production, cell-mediate cytotoxicity, and assisting B-cells. Most effector T-cells have a short life span and disappear at the end of immune response, although some would switch to memory T-cells. At the end of immune response, memory T-cells would survive for the years in peripheral and lymphoid tissues. Memory T-cells, either CD4+ or CD8+, are divided into two groups, TCM (central memory T-cells) and TEM (effector memory T-cells), recognized based on their cell surface markers. These cells would be activated in a secondary immune response, when re-exposed to their cognate antigen (3, 4). Upon reactivation, TEM and TCM cells have potency to home in the peripheral lymphoid tissues. However, TEM cells immediately perform effector functions, whether TCM cells would first proliferate and expand and then acquire effector functions (5).

1.2. T-cell subsets

As mentioned above, T-cells, either effector or memory classes, could be divided into two major classes, CD4+ and CD8+. CD4+ T-cells comprises several specialized subsets, including T helper1, T helper2, T helper17, regulatory T, and T follicular helper cells. Each of these subtypes has a specific gene expression program, which in turn is regulated by specific cytokines, transcription factors and epigenetic mechanisms (6).

T helper1 (Th1) cells act against intracellular pathogens, through producing cytokines including IFN- γ (interferon gamma). IFN- γ can activate macrophages and upregulated iNOS (the inducible isoform of Nitric oxide synthases) which directly leads to killing intracellular pathogens. The IFN- γ production is induced by expression of transcription factors such as STAT4 (Signal transducer and activator of transcription 4) and TBX21 (T-box protein 21 or T-bet), and the latter is the key transcription factor in Th1 differentiation. Following the cell response to interlucin-2 (IL-2) and the activation of mTOR (mammalian target of rapamycin)/Akt signaling, T-bet is expressed which led to the differentiation of the Th1 cells (7). In addition, through producing factors such as IL-2, IFN- γ and TNF- β (Tumor necrosis factor-beta), Th1 cells activate cytotoxic T-cells (8).

T helper2 (Th2) cells have a role in the humoral immune system and host defense against extracellular pathogens. These cells are also involved in asthma and other allergic diseases (9, 10). The differentiation of Th2 cells is induced by IL-4/IL-4R-mediated signaling, which leads to activation of STAT6 (Signal transducer and activator of transcription 6), and in turn it induces GATA3 (GATA binding protein 3) expression. GATA3 is the master regulator of Th2 cell differentiation, which operates by inducing the expression of IL-4, IL-5 and IL-13 (11-13).

T helper17 (Th17) cells can perform host defense against extracellular bacteria and fungi mainly at mucosal surface. These cells are also associated with autoimmune and inflammatory diseases. Th17 cells differentiation is induced by IL-6 and TGF- β (Transforming growth factor-beta) cytokines, followed by expression of the STAT3 transcription factor. This transcription factor induces expression of ROR γ t (Retinoic acid receptor-related orphan receptor gamma t), the master regulator of Th17 cell differentiation (14, 15).

Regulatory T (Treg) cells are in charge for regulating immune responses; maintaining tolerance to self-antigens, and preventing autoimmune diseases and cancer. Treg cells exist in many forms and the well-studied forms express markers such as CD4, CD25 and FOXP3 (forkhead box P3). By producing immunosuppressive cytokines such as TGF- β and IL-10, Treg cells mediate immune responses through contact-dependent and contact-independent mechanisms (16-19). T follicular helper (Tfh) cells are another subset of CD4+ T-cells which induce the activation and differentiation of B-cells into immunoglobulin producing cells. In activated form, they reside within and in proximity of germinal centers (GCs) of secondary lymphoid organs, while memory Tfh cells circulate in the blood. Similar to the other CD4+ T-cell lineages (Th1, Th2, Th17 and Treg cells), the development and differentiation of Tfh cells require signaling pathways activated by cytokines and subsequent launch of transcription factors (20). The master regulator of Tfh differentiation is BCL6 (B-cell lymphoma 6). The early differentiation process is induced by the presence of cytokines including TGF- β (21, 22), IL-6, IL-12 (23), IL-21 and IL-23 in T-cell zone (nascent stage of a germinal center reaction). This leads to the formation of pre-Tfh cells that exhibit a specific secretory profile (expression of IL-21 and CXCL13 (CXC chemokine ligand 13) chemokines, critical for B-cell recruitment into GCs and activation) and a specific cell surface receptor including CXCR5 (receptor of CXCL13, essential to localization of Tfh cells to GCs) and co-stimulatory molecules such as ICOS (inducible T-cell costimulator), PD1 (programmed cell death-1), CD28, and CD40L. These events prepare for a strong interaction of Tfh cells with B-cells, causing the differentiation of pre-Tfh into mature Tfh cells and entrance into GC along with B-cells (24-27). Tfh cells present in GC (referred to GC Tfh cells) are characterized by high level of markers like BCL-6, CXCR5, ICOS, PD-1 and IL-21, which assist in activation, differentiation into the immunoglobulin-producing cells, and B-cell survival (23, 24, 27).

On the other hand, CD8+ cells, known as Cytotoxic T (Tc) cells or CTL, are involved in destroying intracellular pathogens like bacteria and viruses and also tumor cells. This is achieved through production of cytolytic molecules such as Perforin and the granule enzymes (granzymes). Furthermore, they can induce apoptosis of target cells by secretion of some pro-inflammatory cytokines such as IFN- γ and TNF- α (28, 29). The cytotoxic function is triggered via Perforin which punctures holes in the membrane of a target cell. In the next step, TIA-1 (T-cell-restricted intracellular antigen), a cytotoxic granule-associated protein

along with granzyme B, enter in the cytoplasm through the formed holes and activate some target proteins which in turn induce apoptosis. Of note, TIA-1 is expressed irrespective of the activation state of cytotoxic T-cells, whereas Perforin and granzyme B are only expressed upon activation of these cells (28). An overview of T-cell variants discussed is depicted in Figure 1.1.

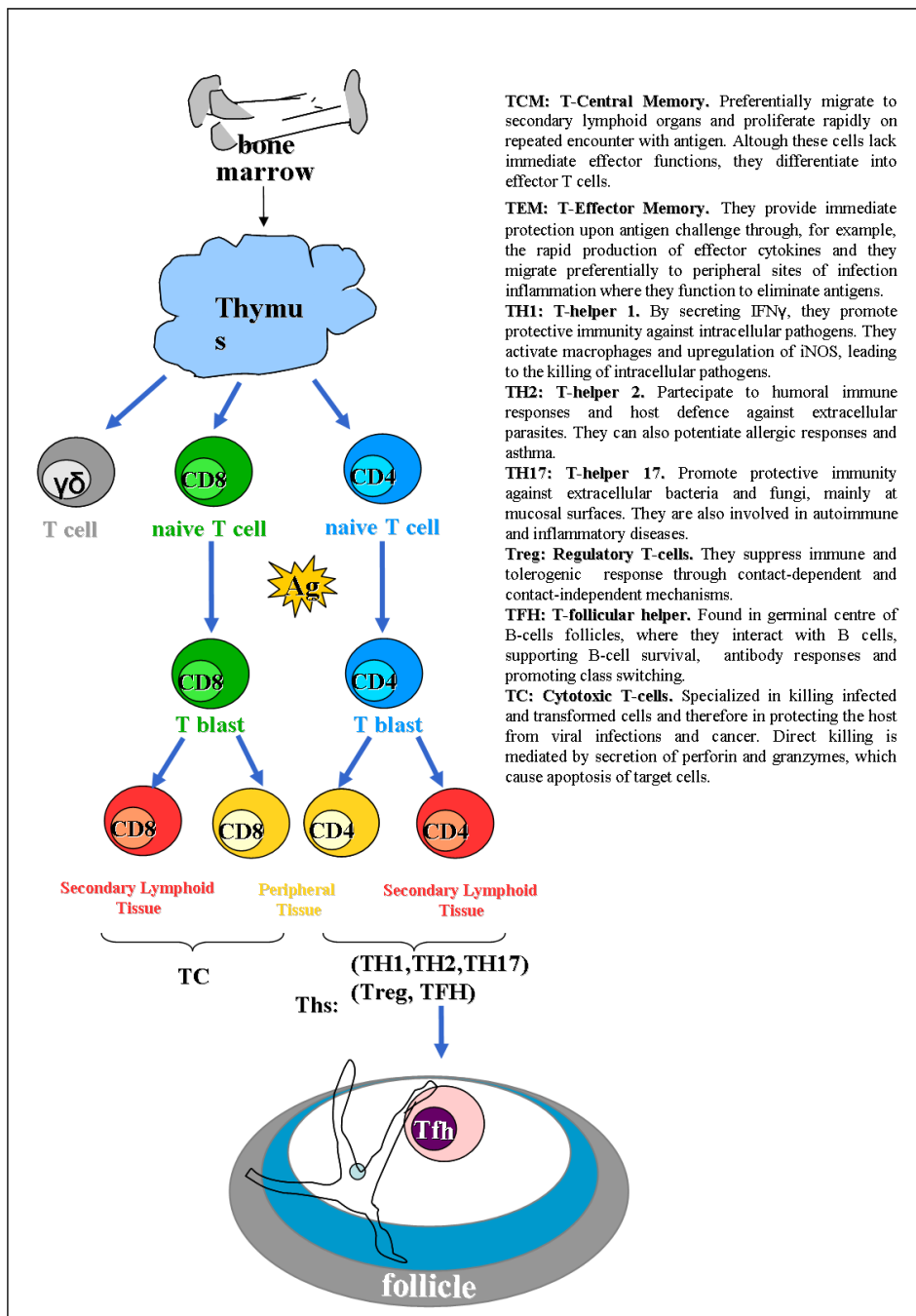


Figure 1.1. T-lymphocyte subpopulations including: TH, TC, TH1, TH2, TH17, TFH, and Treg.

1.3. The World Health Organization classification of nodal Peripheral T-cell lymphomas

The transition of a normal to a neoplastic T-cell is partially due to accumulation of genetic or epigenetic alterations (30) which leads to uncontrollable growth of neoplastic cells. Cancerous lymphocytes can travel to many parts of the body, including the lymph nodes, spleen, bone marrow, blood, or other organs, and form tumor masses.

There are many different forms of T-cell lymphomas, but here we describe the main topic of this thesis, i.e. nodal Peripheral T-cell lymphomas.

Peripheral T-cell lymphomas (PTCLs) are a rare heterogeneous group of non-Hodgkin lymphomas (NHL), which account for 10–15 % in Western countries and 20–25% in Asia (31). PTCLs are derived from mature T-lymphocytes or Natural killer cells and exhibit great versatility in their clinical, morphological, immunophenotypic, cytogenetic, and molecular features (32).

Clinically, most PTCLs are aggressive, generally non-response to conventional chemotherapy, and have a poor prognosis (33). According to The (2008) World Health Organization (WHO) classification of Haematopoietic and Lymphoid Tissues, based on the morphological, immunophenotypic, genetic, and clinical features, PTCLs are classified into nodal, extranodal, cutaneous, and leukemic forms (34). Some entities are fairly well-defined, while others are more heterogeneous. The most common type of PTCLs have nodal origin including Anaplastic large cell lymphoma (ALCL), Angioimmunoblastic T-cell lymphoma (AITL), and Peripheral T-cell lymphoma-not otherwise specified (PTCL/NOS). The latter accounts for more than a third of the PTCLs (30–50% of the cases), but cannot be further classified into any more specific entity (31, 35).

The majority of tumor cells in PTCLs are CD4+, a large proportion of which appears to be related to Tfh cells. There are also minor subtypes that seem to arise from the Th1, Th2, Th17 and Treg subsets (36). There are a number of increasing evidences suggesting that the cell of origin is a major determinant of the biology of PTCLs, and a substantial factor for further classification of PTCLs. Nevertheless, the cellular origin of many PTCLs (except for AITL and a follicular variant of PTCL/NOS, F-PTCL) remains controversial, probably due to the related heterogeneity (37).

Nowadays, genome-wide techniques such as microarray-based gene and microRNA (miRNA) expression profiling and massive parallel sequencing are becoming substantial in research and diagnosis, mainly because of lowered prices concomitant advances in bioinformatic methods (38). As concerned with PTCLs, just like any other class of tumors, these technologies have equipped us with novel information at genome and transcriptome level, and improved our comprehension regarding molecular diagnosis and prognosis, besides identification of novel molecular subtypes that could not be recognized by conventional methods (37, 39-42).

Recently, integration of massive parallel sequencing methods and gene expression profiling has discovered master genetic alterations in most common subtypes of PTCL which are responsible for activation of oncogenic pathways. As a result, genes altered in specific disease subtypes can be potentially be used for more tailored therapies, even with treatments already approved by FDA. Some examples of such targets include IDH2, NF-κB, JAK/STAT, or mTOR pathways, and they have illustrated the value of genome-wide techniques in spotting new targets in PTCL therapy (38).

It should be mentioned, however, that despite all the advances, there is a proportional lack of understanding of the biology of PTCLs, caused by their rarity and diversity and lack of appropriate cell lines and animal models.

1.3.1. Anaplastic large cell lymphoma (ALCL)

ALCL, characterized by large cells and consistent CD30 expression, is an aggressive tumor which responds well to therapy (43). Based on presence of a translocation involving a tyrosine kinase named anaplastic lymphoma kinase (ALK) gene, it is subdivided into 2 distinct entities as including ALK-positive (ALK+) and ALK-negative (ALK-) ALCL (43-45). The translocation is found in different varieties and the most common form involves nucleophosmin gene (NPM1). The overexpression of ALK causes the activation of several signaling pathways, including JAK/STAT3 and PI3K/AKT/mTOR, which result in cell growth and resistance to apoptosis. It has been shown that ALK protein is necessary and sufficient for inducing ALCL development *in vivo*, and STAT3 also displays a substantial role in ALCL

tumorigenesis. As a result, several therapies targeting ALK and the STAT3 are currently in clinical trials for ALK+ALCL patients (46).

Phenotypically, both ALK+ and ALK- ALCL express cytotoxic markers including TIA-1, perforin and/or granzyme B (47). Furthermore, they might share some signature which is independent of ALK that could be used for classifying them from other PTCLs (48). This includes, for example, the dependence of both subtypes upon IRF (Interferon regulatory factor) and MYC (v-myc avian myelocytomatisis viral oncogene homolog) signaling, and MTOR gene signature (49). In addition, a low expression of TCR signaling-related genes has been reported (40, 50).

However, distinct signatures have been described and used for molecular classification of ALCLs subtypes (40, 48, 51, 52). A combination of gene expression profiling along with proteomics and disease models indicate that signaling pathways significant in ALK-positive ALCL include ALK/STAT3, RAS/ERK, and PI3K/AKT/mTOR pathways (48, 53-55). Furthermore, gene expression profiling analysis indicated enrichment of several pathways like IL-10, H-Ras/K-Ras, and HIF1-alpha (hypoxia inducible factor 1 alpha subunit) in ALK-positive ALCL (40, 48, 51).

On the other hand, overexpression of several key genes such as *TNFRSF8* (tumor necrosis factor receptor superfamily member 8), *BATF3* (basic leucine zipper ATF-like transcription factor 3), and *TMOD1* (tropomodulin 1) is reported in ALK-negative ALCL (40). Interestingly, the same 3 genes could be used to distinguishing ALK-negative ALCL from CD30+ PTCL-NOS (56), previously achieved using gene expression profiling (52). Furthermore, another study found inactivation of PRDM1 (PR domain 1)/BLIMP1 in 52% of ALK-negative ALCL, and proposed its correlation with a more aggressive course (57). Although not carrying the major translocation, recent studies showed the presence of 2 specific recurrent rearrangements in ALK-negative ALCL. These include DUSP22-IRF4 rearrangement observed in 30% of cases which resulted in lowered expression of DUSP22 (at protein level), and TP63 (tumor protein p63, homolog of TP53) in 8% of cases. Of note, these two rearrangements seemed to have prognostic relevance, and were mutually exclusive (58, 59).

1.3.2. Angioimmunoblastic T-cell lymphoma (AITL)

As the second most common subtype of PTCL, AITL accounts for almost 20% of PTCLs. AITL has some unique clinical features and morphologic characteristics such as proliferation of high endothelial venules (HEV) and follicular dendritic cells (FDCs), and infiltration of tumors by inflammatory cells, including Epstein-Barr virus-positive B-cells, which are very useful in distinguishing it from other PTCLs (60). This lymphoma rarely responds to the currently used chemotherapy and the 5-year overall survival is less than 30% (60, 61). Tfh markers such as BCL6, PD-1, ICOS, CXCR5 and CXCL13 are expressed in AITL malignant cells, and there are other documents supporting Tfh cells as the cell of origin of AITL (62-66).

Gene expression profiling identified a dominance of microenvironmental signature (i.e., high expression of B cell and FDC-related genes) in AITL. Several major oncogenic signaling pathways were found to be highly active in AITL, including NF- κ B, IL-6, TGF β , and angiogenesis (represented mainly by VEGF) (38, 63-67). Of note, VEGF is produced by malignant cells as well, and besides promoting angiogenesis could induce tumor growth in an autocrine/paracrine loop (67).

Frequent mutations of some important genes like IDH2, TET2, DNMT3A and RHOA have been reported in AITL. Very importantly, besides DNMT3A which has substantial role in regulating epigenetic status of the cell, IDH2, TET2 participate in this process as well, emphasizing how epigenetic regulation might participate in AITL pathogenesis (41, 42, 68-71). A recent study by Wang et al reported the presence of TET2 and DNMT3A mutations in other subtypes of PTCL. This, however, did not apply to IDH2 mutations, suggesting a unique role for these mutations in the pathogenesis of AITL. This idea was supported by distinct gene expression signature of IDH2 mutated cases (71).

1.3.3. Peripheral T-cell lymphoma, not otherwise specified (PTCL/NOS)

PTCL/NOS, the most common T-cell-derived malignancy accounting for 26%-40% of all PTCLs, represent a heterogeneous group of tumors based on morphology and phenotype (34, 36, 72). At clinical ground, these tumors occur more frequently in adults with a median age of 60 years (73). Being mainly involved in lymph node, however, its distribution to extranodal sites has been observed, including bone marrow, liver, spleen, skin and lung (73,

74). PTCL/NOS responds poorly to the conventional chemotherapy, and 5-year overall survival (OS) is almost 32% (75).

The extreme heterogeneity in PTCL/NOS suggests it to include different diseases (34, 36, 72). At least at morphological level, it has been indicated the presence of three specific variants in PTCL/NOS including Lymphoepithelioid, follicular and T-zone variants (34). However, more molecular studies are needed in order to understand biological characteristics of PTCL/NOS category, aiming to achieve an accurate classification.

According to the immunophenotype, PTCL/NOS are mostly referred as central memory T-lymphocytes (TCM). Global gene expression profiling analysis has allowed tumors corresponding to T-lymphocytes related to T-helper (TH) or T-cytotoxic (TC) lineages to be distinguished (52, 62, 64, 76, 77). Because of frequent aberrant antigen expression by the neoplastic cells, gene expression profiling turned out to be more efficient at distinguishing these tumors than was immunophenotyping. This phenomenon, confirmed in large studies (64, 75, 78), was shown to be relevant for the distinction between TH and TC PTCL/NOS, which could not be reliably recognized on the basis of CD4/CD8 immunohistochemical expression (62, 79). Remarkably, the distinction between TH and TC cases is suggested to have prognostic relevance (64). Furthermore a subset of PTCL/NOS with Tfh phenotype (Tfh-PTCL/NOS) frequently shows some biological and clinicopathological features of AITL, questioning if the spectrum of AITL might be broader than is currently thought (41, 63, 80).

More recently, further evidences of the relevance of cellular derivation for PTCL/NOS has been provided at the molecular level. In particular, it has been shown that the expression of specific transcription factors, TBX21 (master regulator of Th1) and GATA3 (master regulator of Th2), involved in the specification of T-cell fate was associated with clinical outcome. On note, there was a difference in the oncogenic pathways activated in the two groups, with constitutive activation of the NF- κ B and STAT3 in the TBX21 subgroup, and constitutive activation of mTOR and PI3K in GATA3 subgroup (40, 81). Subsequently, using immunohistochemistry, an independent study identified high expression of GATA-3 in almost half of the cases of PTCL/NOS, which was also associated with inferior survival. On the other hand, the TBX21 group was found to be more heterogeneous, comprising a subset of cases with a cytotoxic profile (82).

These studies further strengthen the necessity for a deeper understanding of the potential cellular derivations of PTCL/NOS. Despite these advances in the understanding of PTCL pathobiology, systematic characterization of PTCLs/NOS neoplastic clones with respect to their potential recapitulation of different functional T-cell statuses is still lacking.

1.3.3.1. Lennert Lymphoma

Lennert lymphoma (LL) was first described by Karl Lennert in 1952, and later in 1968, by Lennert and Mestdagh (83). Although at first, the disease was classified as "lymphoepithelioid cellular lymphoma", it took some time for it to be recognized as a T-cell lymphoma (84). Since its discovery, the term LL has been used to describe a wide range of malignant lymphomas, all of which are characterized by the high level of epithelioid cells, although those lymphomas might actually correspond to different categories (34). In the fifth edition of the World Health Organization (WHO) classification, LL is classified as a morphological variant of PTCL/NOS characterized by the high level of epithelioid cells, clear cell cytology and, generally, cytotoxic immunophenotype. So far, few publications have dealt with the biological nature of LL, most probably because of the very low incidence level and lack of well-described diagnosis criteria. By means of immunohistochemistry, recent studies have discovered the prevalent expression of cytotoxic T-cell markers, e.g. CD8, Granzyme B, and T-cell Intracellular Antigen-1 (TIA-1), in LL, and have suggested the CD8+ T-cells as the cell of origin of most cases of LL (75, 85-87). Furthermore, LL was found to present different morphological and phonotypical features, when compared to the other epithelioid-rich subtypes of PTCL (88-91). These findings suggest the necessity of further studies on LL.

Nowadays Lennert Lymphoma is diagnosed by a combination of morphological and immunophenotyping features and some of them contained: 1) Predominantly proliferation of small lymphoid cells, 2) Dense clusters of epithelioid histocytes, 3) cytotoxic immunophenotype in the majority of cases (CD3+, CD8+, TIA-1+ and Granzyme B-), 4) low proliferation rate (lower Ki-67) respect to other PTCL subtypes (75, 86, 87, 92-94).

Based on cytogenetic studies Lennert Lymphoma differs morphologically and phenotypically from other epithelioid-rich PTCL subtypes and it is often derived from CD8+ cytotoxic T-cells

and as well as has a survival superior to other CD8+ PTCLs (75, 85, 86). These findings suggest that this special variant of PTCL/NOS should be further studied by precise molecular technologies to understand its accurate position among other PTCL subtypes and possibly could be separated as a distinctive entity in the future lymphoma classifications.

1.3.3.2. Follicular variant of Peripheral T-cell lymphoma, not otherwise specified

Follicular variant of Peripheral T-cell lymphoma, not otherwise specified (F-PTCL) is a rare morphological variant of PTCL/NOS (20–41%) which show a follicular growth pattern. The neoplastic cells are CD4+ αβ T-cells that express Tfh markers (PD1, ICOS, CXCL13 and BCL6) (64, 80, 95-97). In the fourth version of World Health Organization (WHO) classification F-PTCL is not considered a subtype of AITL because a) it shows no proliferating of follicular dendritic cell (FDCs) or high endothelial venules (HEVs) which are hallmark feature of AITL (34) and b) the presence of t(5;9) ITK-SYK translocation in 20% of F-PTCL cases, which was considered a genetic abnormality specific to F-PTCL (96). However, recent research identified t(5;9) in very small percentage of AITL as well, though it is still relatively specific to F-PTCL (98-100). SYK is a non-receptor protein tyrosine kinase which functions as regulator of multiple signal transduction pathways. Its overexpression has been reported in PTCL/NOS cases independently of ITK-SYK, suggesting that the SYK pathway is important in this condition (101). Since F-PTCL may present some biological and clinicopathological features overlapping with those of AITL (96, 102), hence, it has raised the controversy if F-PTCL might actually belong to the spectrum of AITL (96, 103).

1.3.3.3. T-zone variant of Peripheral T-cell lymphoma, not otherwise specified

T-zone variant is named for its involvement in a specific area of the lymph node that consists of a dense accumulation of T-cells and has been characterized by prominent high endothelial venules and numerous reactive cells, including plasma cells, eosinophils, and epithelioid histiocytes and also shows an interfollicular growth pattern with small or medium-sized cells without pronounced nuclear pleomorphism (34).

1.4. Aim of the thesis

This thesis follows three main aims including:

1. Reshaping the PTCL/NOS sub-classification based on the correspondence between their molecular features and those of different functional T-cell subsets, as well as assessing the clinical impact of such an approach.
2. Clarifying the accurate position of Lennert lymphoma among other PTCL/NOS based on its molecular expression signature.
3. Investigating the molecular correlation of F-PTCL and AITL based on their global gene expression profiles.

(2)

Material and Methods

2.1. Case selection

We studied 186 PTCLs/NOS including 106 cases from which GEPs (Gene expression profiling) had been determined using fresh/frozen tissues (52, 62, 64, 65, 104) (77 previously included in GEO data sets GSE6338 and GSE19069) and 80 cases for which GEP was performed on formalin-fixed-paraffin-embedded (FFPE) specimens. All of the cases were reviewed by at least two expert hematopathologists and diagnosed according to the WHO Classification (34); furthermore, the diagnosis was refined by applying a molecular classifier recently developed by our group (52). The detailed clinico-pathological characteristics of these cases were previously reported (104). We also studied the molecular profiles of normal T-cell subpopulations (CD4⁺, CD8⁺, TH1, TH2, TH17, Treg, and TFH) from which the GEPs were previously generated (62, 105).

2.2. Ethics statements

The study was conducted according to the principles of the Helsinki Declaration after obtaining approval from the local Ethical Committee. Written informed consent was obtained from all patients for the tissue analysis. All cases were studied by both GEP and extensive IHC.

2.3. Gene and microRNA expression profile generation

RecoverAll™ Total Nucleic Acid Isolation Kit was used to extract total RNA from FFPE samples. Up to five 10 µm-thick sections were processed per reaction. The samples were rehydrated using a series of xylene and ethanol washes. Next, they were subjected to a rigorous protease digestion with an incubation time tailored for recovery of total RNA. RNA was purified using a rapid glass-fiber filter methodology that includes an on-filter DNase treatment and were eluted into the low salt buffer provided. RNA was quantified using NanoDrop spectrophotometer.

In order to generate gene expression profiles, RNA was processed as for manufacturer's instructions to produce biotinylated cDNA (106, 107). Briefly, biotinylated -cDNA was then annealed to the DASL Assay Pool (DAP) probe groups that contain oligonucleotides specifically designed to interrogate each target sequence in the transcripts. Following this,

the correctly annealed, assay-specific, oligos were extended and ligated to generate amplifiable products. These templates were labeled during PCR amplification by including fluorescent primers in the reaction. The resulting PCR products were hybridized on the Illumina HumanHT-12 WG-DASL V4.0 R2 expression beadchip and scanned using the BeadArray Reader or iScan System to determine the presence or absence of specific genes.

MicroRNA expression profiles were generated using the TaqMan Array Human MicroRNA Cards A v.2.0 (Life Technologies, Carlsbad, CA USA) according to the manufacturer's instruction, as described previously (108). Of note, this qRT-PCR-based array enables accurate quantitation of 377 human microRNAs.

2.4. Gene and microRNA expression analysis

Gene and miRNA expression analysis was carried on as previously reported (62, 109, 110). Statistical Analysis was performed using GeneSpring version GX 12 (Agilent, MI, Italy). The expression value of each probe was normalized to have a zero mean value and unit standard deviation. Principal Component Analysis (PCA) was used to discriminate the different biological samples on the basis of the distances of a reduced set of new variables (Principal Components). Only the top 3 principal components were used for depicting the results. The distance between two individual samples was calculated by Pearson correlation with the normalized expression values. Unsupervised clustering was generated using a hierarchical algorithm based on the average-linkage method. Differentially expressed genes among sample groups were identified using ANOVA method, with adjusted p-value based on the case. Differentially expressed genes and miRNAs between any two groups of samples were identified with a two-tailed T-test with Welch approximation for different variance among groups and with different stringency criteria for false discovery rate (Benjamini correction, adjusted Bonferroni correction, or no correction). Based on the stringency criteria, the results of the test were further filtered based on a fold change in absolute value [fold change = mean (group A) – mean (group B)], which was chosen on a case-based method. The resulting genes/miRNAs were used to produce hierarchical clustering analysis based on the average-linkage method.

Different approaches were used for identifying the cellular counterparts of PTCLs. First, we generated the molecular signatures specific of CD4⁺, CD8⁺, TCM, TEM, TH1, and TH2. Secondly, we used a Support Vector Machine (SVM) algorithm as well as Broad Institute Gene Set Enrichment Analysis (GSEA) software (111, 112) to classify cell type correlating a given PTCL/NOS sample with either one of two possible molecular phenotypes (i.e. CD4 vs. CD8, TH1 vs. TH2, and TCM vs. TEM), based on the expression of genes characteristic of the different normal subpopulations (52, 62, 109, 110). This analysis was carried on 77 PTCL/NOS cases, for which frozen tissue was available. In brief, the classifier is a confidence measure scoring function based on the values of a set of genes (gene cluster), which are differentially expressed in two sets of cell types, and thus, can be used for cell type classification. The higher the score, the more likely it is that a cell type is related to the phenotype set. Samples with confidence measure score minor than 0.05 were not assigned to a particular cellular counterpart and flagged as unclassified. For GSEA, in case of nominal P values and False Discovery Rate (FDR) for enrichment scores minor than 0.01, a significant enrichments in single signatures was defined.

Third, GSEA was adopted to evaluate the possible enrichment in Treg, TH17, and TFH signatures, which were designed according to literature data (see Supplementary Table 1), being not available the cellular populations isolated *in vivo* from humans (nor deposited raw GEP).

Finally, stepwise discriminant analysis was performed using IBM SPSS Statistics 20.0 (IBM, Armonk, USA) to identify the minimal number of genes able to correctly classify a given sample in different molecular subtypes. To run this analysis, a training set was created selecting a random permutation of about one third of cases of PTCL/NOS (N=28), using the shuf function in UNIX Bash shell. The remaining cases constituted the test set (N=49). For every step of the analysis the gene that minimize Wilks' lambda test probability distribution was selected to enter in the discriminant model and included in the list of discriminant genes if its probability associated to F exact test was minor than 0.05. Otherwise, the genes with probability associated to F exact test greater than 0.10 were excluded from the list. Stepwise method was run until no further genes could be added or excluded to reduce Wilks' lambda probability distribution. A discriminant score was calculated for each sample and for each classification step. Each case from the validation set was then assigned to a

specific cellular counterpart or another according to the distance between its discriminant score and a cut-off value calculated for each predicted group.

As further validation, the discriminant function was then applied to a series of lymphomas for which the cellular counterpart was already recognized (namely AITL, corresponding to TFH (N=34); adult T-cell lymphoma/leukemia, ATLL, corresponding to Treg (N=13); and anaplastic large cell lymphoma ALCL, sometimes matching TH17 (N=33)) (34, 63-65, 113) (GEO data sets: GSE6338 and GSE19069). Finally, we applied it to FFPE for which GEP were generated using the Illumina DASL assay (106, 107). Gene expression studies were conducted according to MIAMI guidelines. The data discussed in this publication have been deposited in NCBI's Gene Expression Omnibus (114) and are accessible through GEO Series

accession	number	GSE45712
-----------	--------	----------

(<http://www.ncbi.nlm.nih.gov/geo/query/acc.cgi?acc=GSE45712>).

Broad Institute GSEA was used to identify KEGG pathways significantly enriched for genes mutated in every PTCL/NOS subgroup. DAVID Functional Annotation Bioinformatics Microarray Analysis (<http://david.abcc.ncifcrf.gov/>) was also used to establish whether specific biological processes defined according to Gene Ontology were significantly represented among different PTCL/NOS subgroups.

Ingenuity Pathway Analysis, (IPA, IPA®, QIAGEN Redwood City, www.qiagen.com/ingenuity) software was used for creating signal transduction networks in the samples.

2.5. High throughput massive parallel sequencing

Total DNA was extracted from 29 PTCL/NOS frozen samples with QIAamp DNA mini kit Qiagen according to manufacturer's procedure (Qiagen, Italy). 1 µg of DNA were sheared using Covaris instrument into 100–500 bp fragments and quality control of fragmentation was assessed using a DNA-7500 kit (Agilent, USA). Pre-enrichment DNA libraries were constructed following Illumina's TruSeq DNA Sample Preparation v2 Guide. Briefly, after end repair, adenylate 3'ends and ligate adapters steps we performed a PCR reaction to selectively enrich those DNA fragments that had adapter molecules on both ends. PCR libraries products were purified by AmpureXP beads (BeckmanCoulter, CA, USA) and exome enrichment was performed according to Illumina's TruSeq Exome Enrichment Guide

(Illumina, San Diego, USA). Two 20-h biotinylated bait-based hybridizations were performed with each followed with Streptavidin Magnetic Beads binding, a washing step and an elution step. A 10-cycle PCR enrichment was performed after the second elution and the enriched libraries were subjected to quality control analysis using a DNA-1000 kit (Agilent, USA). The quantification was performed by Quant-it PicoGreen dsDNA Assay Kit according to manufacturer's protocol (Invitrogen, Life Technologies, USA).

The paired-end libraries (2x100 base pair) were sequenced on an Illumina HiScan SQ (Illumina, San Diego, USA) following the manufacturer's instructions, generating an average of about 51 million 100bp paired-ends raw reads, with theoretical coverage, calculated on hg19 RefSeq non redundant exome length, ranging from 35X to 108X. Quality control on raw reads was performed using FastQC V0.10.0 (<http://www.bioinformatics.babraham.ac.uk/projects/fastqc/>). Illumina reads were mapped to Human GRCh37 Genome Assembly using the Burrows-Wheeler Aligner version 0.6.1 (BWA) (115). Multiple mapped reads pairs with identical external coordinates were collapsed to remove potential PCR duplicates using samtools command rmdup (116). Mapping quality score recalibration and local realignment around insertions and deletions (indels) was performed using Genome Analysis Toolkit (GATK) (117). Single-nucleotide variants (SNVs) and small insertions and deletions (INDELS) were called separately using GATK Unified-Genotyper.

All the mutations detected were filtered using thresholds based on quality, coverage and strand of the mapped reads (118) and according to variants already present in public databases (Hapmap, dbSNP and 1000genome project (119)). To reduce the presence of germline mutations, variants already present in 25 WES samples from unaffected individuals were excluded.

Annovar tool 2013May20 update (<http://www.openbioinformatics.org/annovar/>) was used for functional annotation of variants, including exonic functions and amino acid changes and only non-synonymous variants, including stop-gain SNVs, splicings and frameshift indels were selected for further analysis.

All the mutations found were manually checked and explored using the Integrative Genomic Viewer 2.03 (120).

Chi-Squared test with p-value <0.05 was used for every gene to find significant relations between number of mutated samples and PTCL/NOS subgroups.

2.6. Tissue microarray construction and Immunohistochemical analysis

For tissue microarray (TMA) construction, a slide stained with hematoxylin and eosin was prepared from each available paraffin block, and representative tumor regions were morphologically identified and marked on each slide. Tissue cylinders with a diameter of 1.0 mm were punched from the marked areas of each block and brought into a recipient paraffin block using a precision instrument, as previously described (121). Four µm-thick sections were cut from each recipient block and used for Giemsa or immunohistochemical stains. Details of the antibodies used, antigen retrieval, and detection methods strategies were previously reported (72, 78, 122). Each section was evaluated by two experienced pathologists. Each observer estimated the number of positive cells according to the criteria used by Hans et al (123).

Specific antibodies representative of the diverse T-lymphocyte commitments were used including TEM-TCM (CD45RA and CCR7), TH (CD4), TC (CD8, TIA1, PERF, and GRZB), TH1 (TBET and IFNG), TH2 (GATA3 and IL4), TH17 (IL17A), TFH (CD10, BCL6, CXCL13, and PD1), and Treg (FOXP3). Based on immunohistochemistry, cases were assigned to a specific group if the phenotype was either completely consistent (i.e. positive for the specific lineage markers and negative for all the others) or positive for all but one specific lineage markers and negative for all the other (being accepted a defective phenotype). Conversely, cases were defined as “unclassifiable” if inconsistent results were observed (i.e. positivity for markers representative of multiple lineages). PD1 and FOXP3 were accepted as consistent for a cytotoxic profile if at least CD8 was positive among cytotoxic markers and all the other markers typical of TH were negative.

2.7. Survival analyses

Overall survival (OS) was calculated from the time of diagnosis to death or last follow-up. Statistical analyses were carried out by IBM SPSS Statistics 20.0. Survival data were analyzed

with the Kaplan–Meier estimator method (124). The limit of significance for all analyses was defined as $P<0.05$ for the log-rank Mantle–Cox test.

(3)

Results

(3.1)

**Molecular Profiling Of Peripheral T-Cell
Lymphomas-NOS Identifies Clinical Subgroups
Corresponding To Distinct T-Cell Populations**

PTCL/NOS correspond to different functional T-cell subsets

The overall study design is depicted in Figure 3.1.1. We studied 106 PTCL/NOS cases for genes that were differentially expressed in purified T-lymphocyte subpopulations (TH, TC, TH1, TH2, TH17, TFH, and Treg). A score was obtained for each PTCL/NOS sample based on a support vector machine method and gene set enrichment analysis (GSEA). Each sample was then assigned to a specific T-cell counterpart or another one according to the distance between the obtained score and a cut-off value calculated for each predicted group.

First, we classified the PTCL/NOS according to their similarity to helper or cytotoxic T-cells. We observed that most PTCL/NOS were more closely related to TH cells (83/106, 78.3%), a minority were closer to TC (21/106, 19.8%), and two cases remained unclassified (1.9%). Within the group of PTCL/NOS classified as TH, the expression of genes characteristic of different TH functional/differentiation statuses was evaluated. We found that 29/83 (34.9%) samples were classified as TH1 cells, 34/83 (41%) as TH2, 4/83 (4.8%) as TFH, 3/83 (3.6%) as TH17, and 5/83 (8.1%) as Treg and that 8/83 (9.6%) cases could not be clearly assigned to any TH subtype (Figures 3.1.2A-D; Figure 3.1.3; Supplementary Table 2).

Importantly, the subdivision in the above-detailed categories was not associated with specific presenting features, including age, performance status, extranodal involvement, and international prognostic index.

Taken together, these results indicated that the heterogeneity of PTCL/NOS finds correspondence in the spectrum of functional T-cell subsets.

Minimal gene sets are sufficient to identify the different PTCL/NOS subtypes

Within the 106 fresh/frozen cases, a training set was created selecting a random permutation of about 50% of cases using the shuf function in UNIX Bash shell. The remaining cases constituted the test set. A stepwise discriminant function was then applied to the test set (N=57) to identify the minimal gene set (MGS) able to efficiently discriminate between the different PTCL/NOS subgroups (i.e., TH vs. TC, and TH1 vs. TH2 vs. TFH vs. Treg vs. TH17). For each classification step, a discriminant function based on a linear combination

of the discriminant genes was created. To validate the efficacy of the obtained MGS, the test set comprising 49 PTCL/NOS was analyzed (Supplementary Tables 3-4).

Each case previously classified with a complete molecular signature was re-classified by the MGS with an accuracy of 92.68% and 83.33% for the TH and TC subtypes, respectively, of 100% for TH1 and Treg, 95.24% for TH2, and 75% for TFH and TH17 (Figure 3.1.4A-B; Supplementary Tables 5-10).

The molecular classification relies on robust pathobiological features

To assess whether the obtained classification was provided with a robust biological significance, we first looked for molecular pathways differentially regulated in the various groups. Interestingly, by GSEA we found that 3 main groups could be appreciated, corresponding to cytotoxic (group A), Th1/Th2/Th17 (group B), and Tf_h/Treg (group C) cases and relying on different master pathways. The latter included MTOR pathway ($p=0.000252$), STAT3 targets ($p<0.0001$), IFNA response genes ($p<0.0001$), and genes silenced by methylation ($p<0.0001$). Overall, this was in line with the notion that different effector or regulatory functions of helper T-cell phenotypes and the Th-cell differentiation hierarchy relies on specific signaling with TH1/TH2/TH17 subsets sharing mTORC1/mTORC2 dependency (Figure 3.1.5 and 3.1.6A; Supplementary Table 11).

Second, we investigated by whole exome sequencing whether different genetic lesions were associated with the molecular groups. The analysis was performed in a subset of 29 cases, for which genomic DNA was available. Indeed, we found a few lesions that were highly recurrent within each single group. Beside the already known *FYN*, *IDH2* and *TET2* mutations we identified several lesions previously not reported in PTCLs such as *ABCB1*, *BAHCC1*, *BTN2A2*, *CX3CR1*, *NDUFV3*, *PLCL2*, and the tumor suppressor *PRDM2* in the TH1/TH2/TH17 group, *SOGA2*, *A2ML1*, *CCPG1*, *CDC27*, *LRP3*, *MOCS2*, and *MTDH* in the TC group, and *ATXN3*, *C3*, *COG3*, *CRYGS*, *FAM198B*, *GPAT2*, *IDH1*, *PHKA1*, *RBMXL1*, *TMEM204*, *TRIM61*, *TRMT44*, and *VWA1* in the TFH/TREG group (Figure 3.1.6B; Supplementary Table 12).

Remarkably, we found that the different genetic lesions targeted specific pathways in the 3 groups that largely corresponded to the pathways highlighted by the GEP analysis as characteristic of the 3 groups. Specifically, cytotoxic cases presented with mutations mainly

occurring in T-acute lymphoblastic leukemia and targeting *KRAS*, *JAK2*, *NOTCH1*, *LEF1*, *BMI1*, *RB1*, *TP53*, *EZH2*, and *HOXA9* ($p<0.0001$). This finding was quite relevant being in line with a higher aggressiveness of the tumor and suggests sensitivity to more aggressive chemotherapeutic regimens as well as to specific inhibitors. The TH1/TH2/TH17 group presented a preferential occurrence of lesions interfering with the MTOR/AKT pathway ($p<0.0001$) in line with the GEP. Finally, TFH/TREG cases presented mutations affecting the epigenetic regulation of gene expression (*EZH2* and histone deacetylase targets) as well as the FOXP3 network ($p<0.0001$) (Supplementary Table 13).

Based on the emerging evidence of specific pathways involved as drivers of PTCL/NOS subclassification, we tried to verify whether the selective inhibition of a master pathway could exert antitumor activity in PTCL cells. To this end, we first applied the molecular classifier to some PTCL cell lines. The two cutaneous T-cell lymphoma (HH and MAC1) lines and the only available PTCL/NOS cell line (Fe-Pd) were classified as belonging to the TH1/TH2/TH17 group. We thus treated them with MTOR and PI3K inhibitors (Everolimus and LY-294002) alone and in combination. Notably, though the single agents were scarcely effective, the combination potently and synergistically induced PTCL cell death in a dose-dependent manner (Figure 3.1.6C).

Collectively, these data indicate that molecular subgroups of PTCL/NOS corresponding to different counterparts rely on different pathways largely affected by genetic events, and that selective targeted treatment may be a rationale approach in this setting.

The molecular sub-classification of PTCL/NOS has clinical implications

We then assessed whether the proposed PTCL/NOS sub-classifications had clinical significance. To this end, we evaluated the overall survival (OS) of patients belonging to the different subgroups. TC-related PTCL/NOS had a worse outcome than TH-related PTCL/NOS, which was consistent with previous observations (64). Specifically, after a median follow-up of 33.90 months, the former had a median OS of 8.84 months (95% CI 2.41-15.26), and the latter had a median OS of 20.05 months (95% CI 10.37-30.63) ($p=0.04$; Figure 3.1.7A).

When the five TH subtypes were considered, no significant differences were observed, although the cases classified as Treg and TFH generally fared better. However, when the 3

functional and genetic subgroups were considered, significant differences in terms of OS were recorded. Specifically, the median OS for TC (N= 9; 8.84 months, 95% CI, 2.41-15.26) was significantly worse than that for TH1-TH2-TH17 (N=30; 20.5 months; 95% CI, 10.98-30.02; p=0.05) and for TFH-Treg (N=6; 40.9 months; 95% CI, 0-85.79; p=0.02; Figure 3.1.7B). Notably, this difference was independent of the other main clinico-pathological parameters at presentation (IPI, PIT, and modified PIT).

The molecular classification of PTCL/NOS can be applied to FFPE routine samples

We next sought whether the developed classifier could be efficiently applied to FFPE tissues, in order to evaluate its potential impact on routine diagnostics.

We first applied the molecular signature discriminating the TH vs. TC subtypes, which identified two groups (Figure 3.1.8A). Consistent with this, the MGS (5 genes) correctly classified 69/80 (86.25%) samples (Figure 3.1.8B). Notably, such classification of the FFPE samples retained a significant correlation with prognosis (Figures 3.1.8C).

Based on this evidence, we further divided TH cases into TH1-TH2-TH17 and Treg-TFH, which were characterized by significantly different OS. Specifically, after a median follow-up of 54.18 months, the TC cases had the worst outcome (N=15; 8.838 months, 95% CI 1.391-16.284; p=0.037 vs. TH1/TH2; p=0.003 vs. Treg/TFH), the Treg/TFH (N=12) cases displayed a better outcome (40.903 months, 95% CI 17.338-64.469; p=0.033 vs. TH1/TH2), and the remaining TH subsets (N=34) showed an intermediate outcome (15.901 months, 95% CI 8.396-23.407) (Figure 3.1.8D).

Altogether, these results demonstrated that PTCL/NOS sub-grouping, based on an integrated diagnostic approach, is clinically relevant and feasible in routine samples.

Immunohistochemistry can only partially replicate the molecular profiling

Given that the molecular PTCL/NOS sub-grouping had both biological and clinical relevance and could be reliably applied to routine samples, we sought to assess whether it could be efficiently substituted by IHC analyses.

We studied 16 markers representative of T-cell commitment, the complete panel of antibodies being evaluable in 63/80 cases. We found that 33/63 (52%) cases had a phenotype consistent with TH cells and that 11/63 (17%) had a phenotype consistent with TC cells but that 19/63 (30%) could not be assigned to a phenotype, either for discordant CD4/CD8 expression (double-negative or double-positive) or inconsistent expression of additional molecules. Among TH, 8/63 (13%) had a phenotype consistent with TH1, 14/63 (22%), TH2; 7/63 (11%), TFH; and 4/63 (6%), Treg. None of the analyzed cases was characterized by IL-17A expression, which is characteristic of TH17 and was only observed in scattered reactive lymphoid and myeloid cells (Figure 3.1.9A; Supplementary Table 14). Accordingly, the IHC-based classification did not determine a clinically meaningful distinction (Figure 3.1.9B).

These data suggest a note of caution about the applicability of immunophenotyping to fully recapitulate the GEP categories. Consistent with this, survival analysis based on immunohistochemistry-derived categories failed to offer significant prognostic information, reflecting an overall discrepancy between immunohistochemistry and GEP. In fact, IHC was quite accurate almost exclusively for the identification of Treg and TFH cases, as confirmed by GSEA. Particularly, immunohistochemistry performance was poor in the crucial distinction between TH and TC, being consistent with GSEA in 46.03% of cases only. Similarly, immunohistochemistry failed to definitely identify other TH subsets.

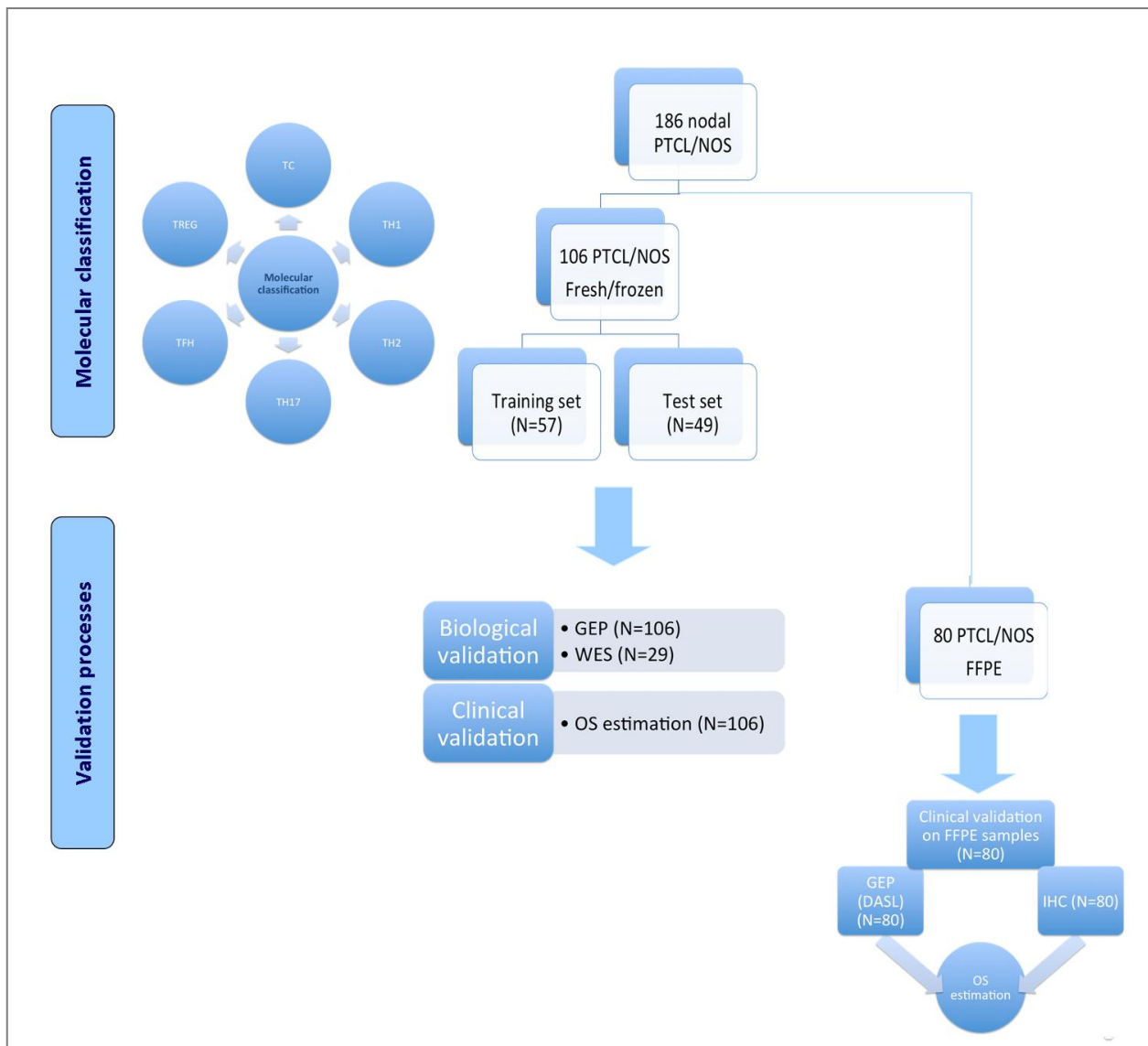


Figure 3.1.1. The overall study design.

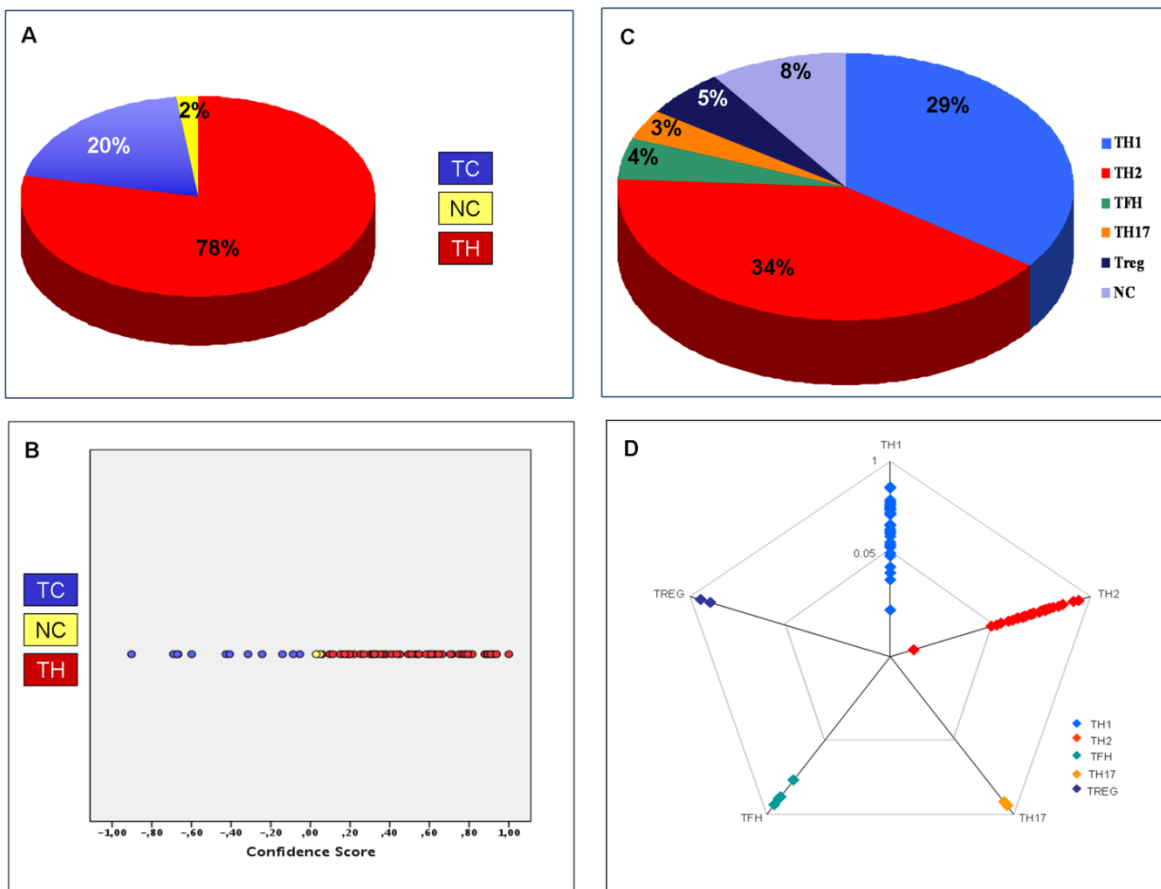


Figure 3.1.2. Molecular classification of peripheral T-cell lymphomas not otherwise specified according to their correspondence to different functional T-cell subsets. The pie charts and the scatter plots show the distribution of cases according to their molecular classification into the TH vs. TC (**A-B**), and TH1 vs. TH2 vs. TH17 vs. Treg vs. TFH (**C-D**) subgroups. The colors indicate different molecular subgroups. Cases with a confidence measure score less than 0.05 in absolute value fall within no classification area and are considered to be unclassified.

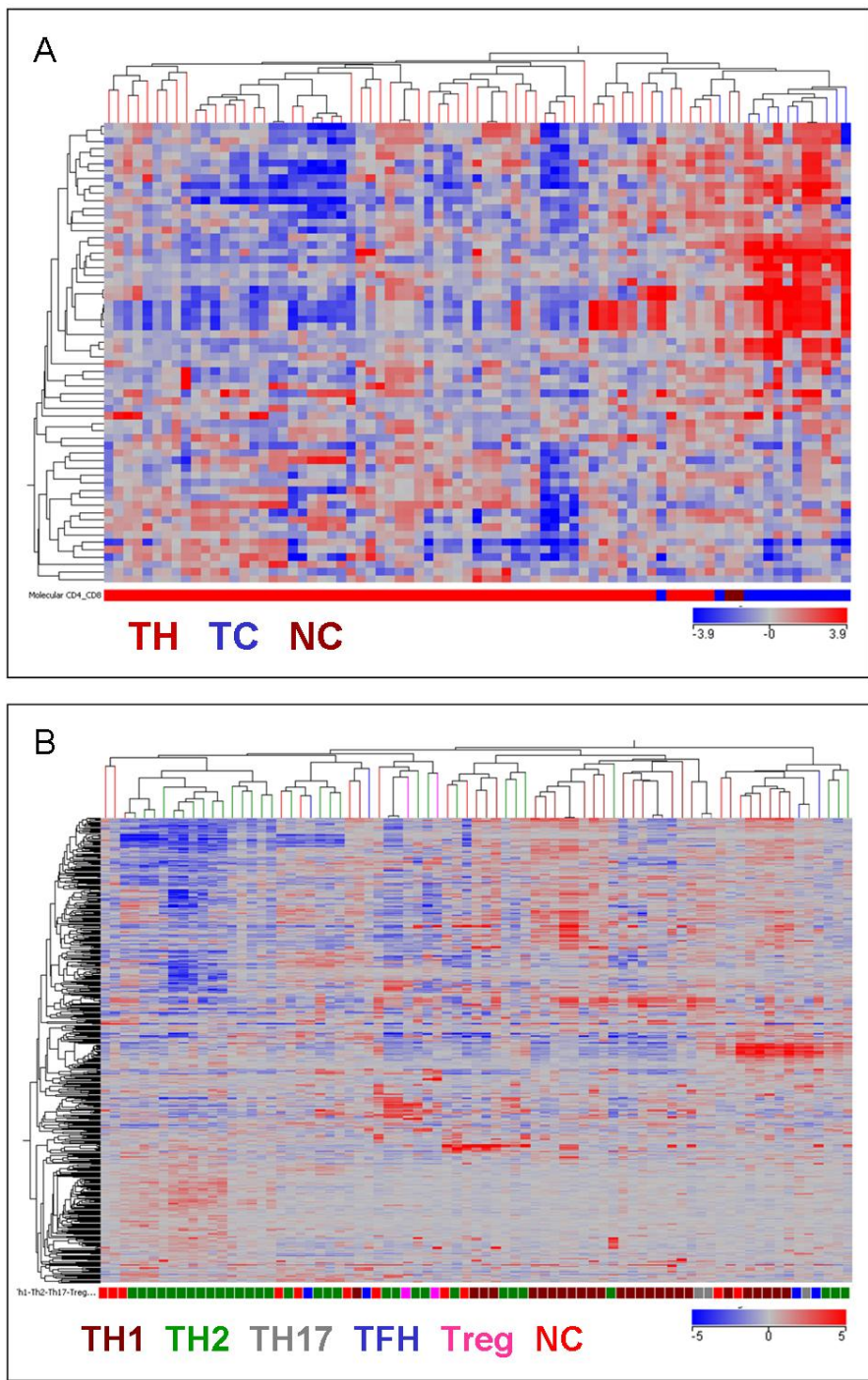


Figure 3.1.3. Molecular classification of PTCL/NOS according to T-cell subtype signature. **A)** Classification of PTCLs/NOS classified as helper or cytotoxic T-cells. **B)** Classification of PTCLs/NOS classified as TH in to TH subtypes. In the heat map, each column represents a sample, and each row represents a probeset (gene). The color scale bar shows the relative gene expression changes normalized to the standard deviation (0 is the mean expression level of a given gene).

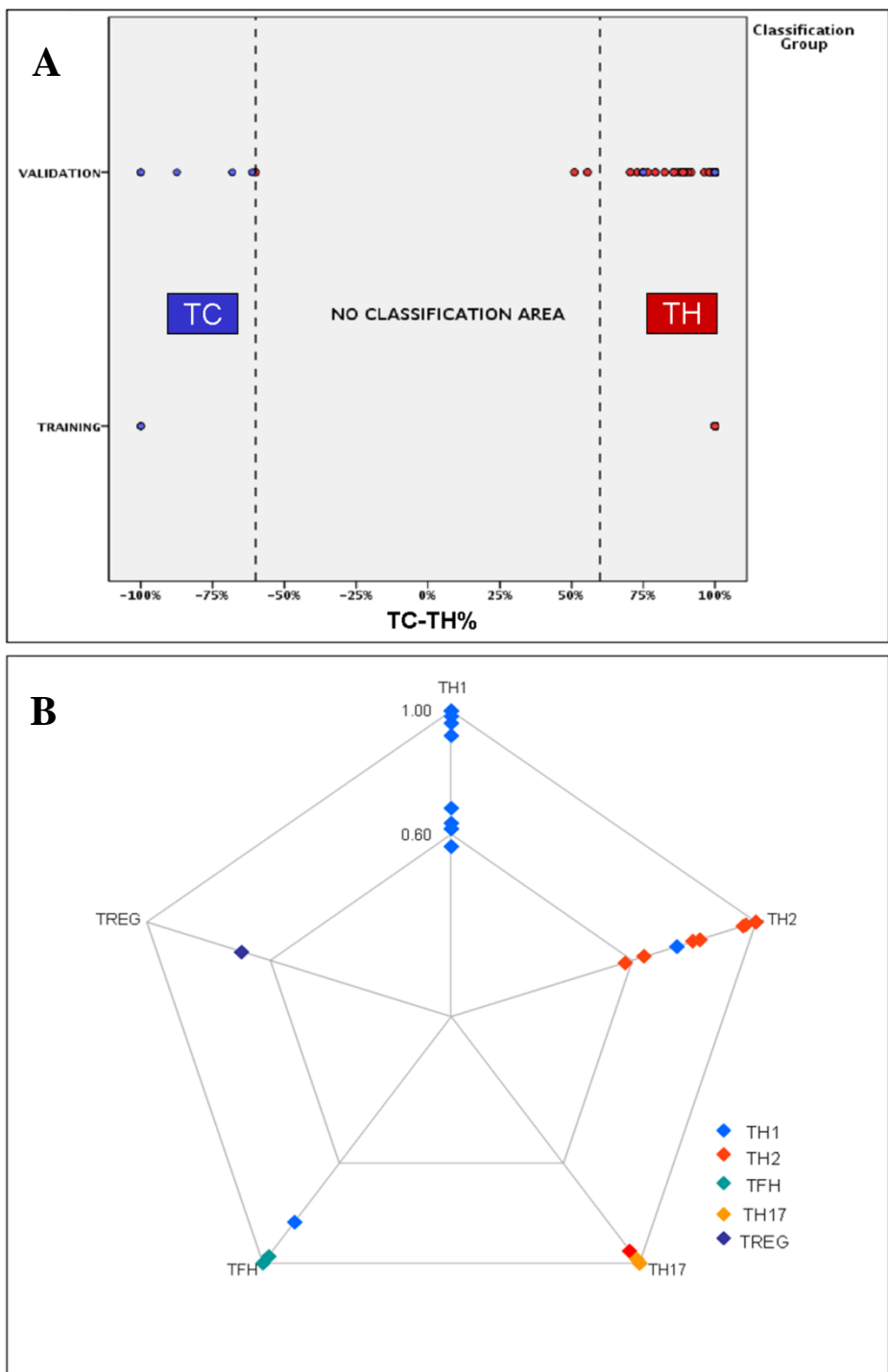


Figure 3.1.4. Linear discriminant analysis in the training and test sets of cases. The scatter plots show the distribution of the PTCL/NOS samples in the training and test sets according to their discriminant scores in the minimal gene sets classification step: TH vs. TC (**A**) and TH1 vs. TH2 vs. TH17 vs. Treg vs. TFH (**B**). The colors indicate different molecular subgroups. Cases with a discriminant score less than 0.6 in absolute value fall within no classification area and are considered to be unclassified.

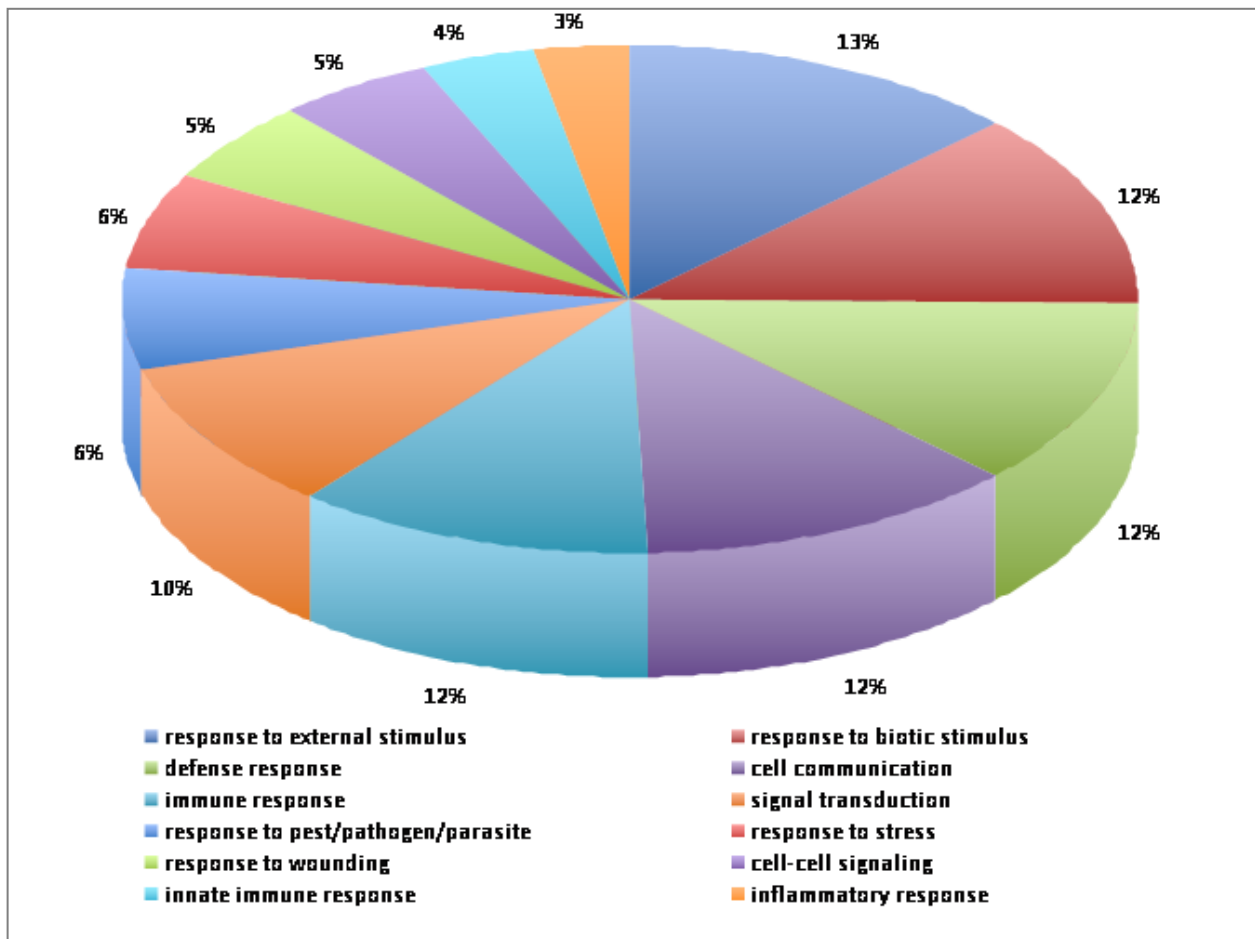


Figure 3.1.5: The molecular pathways differentially regulated in the various T cells groups.

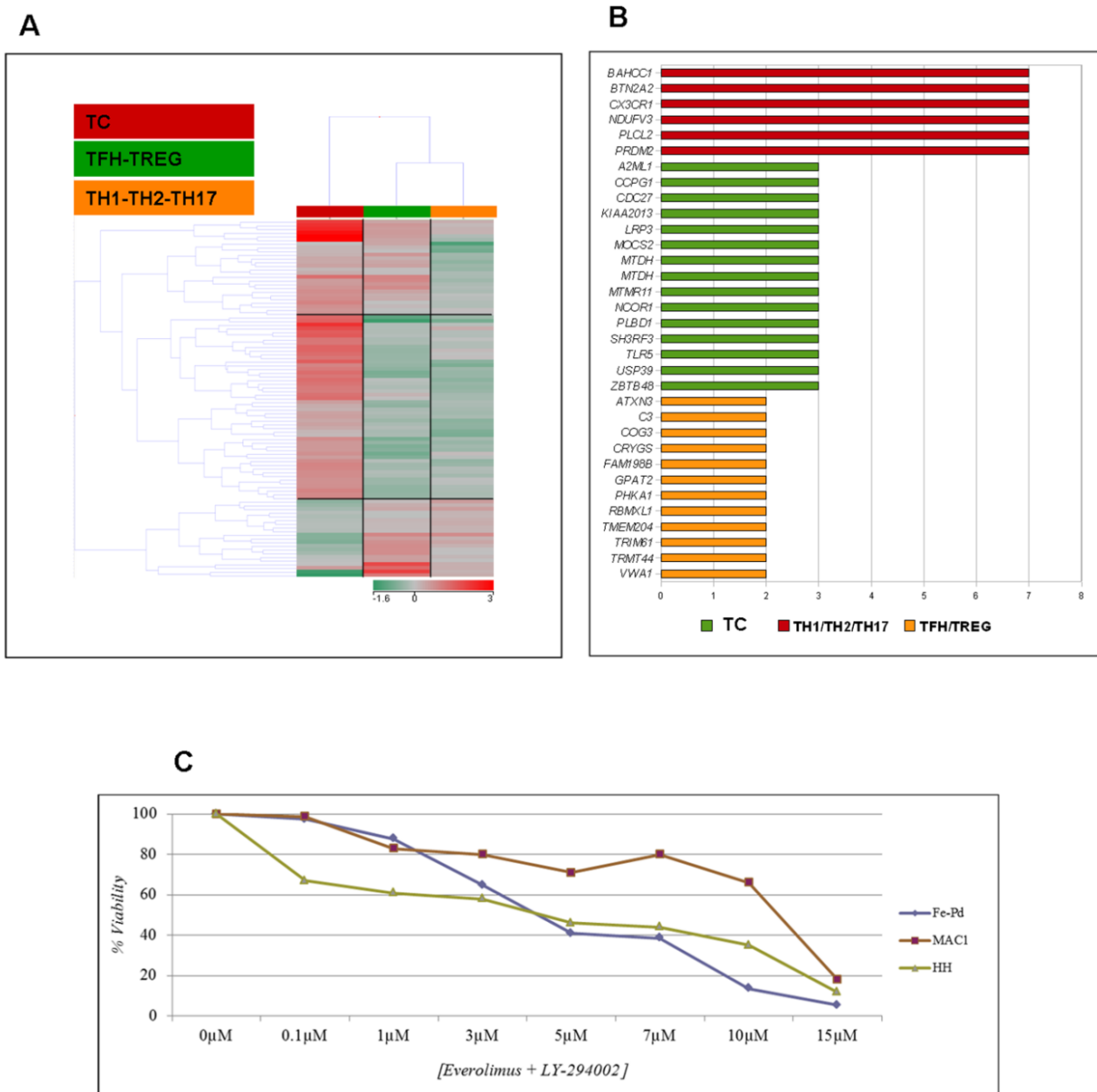


Figure 3.1.6. The PTCL/NOS molecular subgroups have distinct genetic and functional profiles. **A)** Hierarchical clustering of TC, TFH/TREG, and TH1/TH2/TH17 PTCLs/NOS based on the expression of differentially regulated genes (ANOVA, $p<0.05$; FC>2, Benjamini-Hockeberg FDR). Two main groups were generated, one corresponding to cytotoxic tumors (TC) and one to helper-related ones. The latter was further divided according the specific functions into TFH-TREG and TH1-TH2-TH17. **B)** Mutational landscape of PTCL/NOS subgroups: number of samples carrying somatic mutations (x axis) in a given gene (y axis) are represented by the histograms. Genes most significantly over-represented in each group

and mutated in only one of them are plotted. **C)** PTCL cell line viability upon treatment with Everolimus and LY-294002 in combination (IC₅₀ not reached with the single drugs, data not shown). The IC₅₀ values at 48 hours for the combination in the three cells lines were as follows: 4.8 μM (Fe-Pd), 10.3 μM (MAC1) and 3.15μM (HH), respectively.

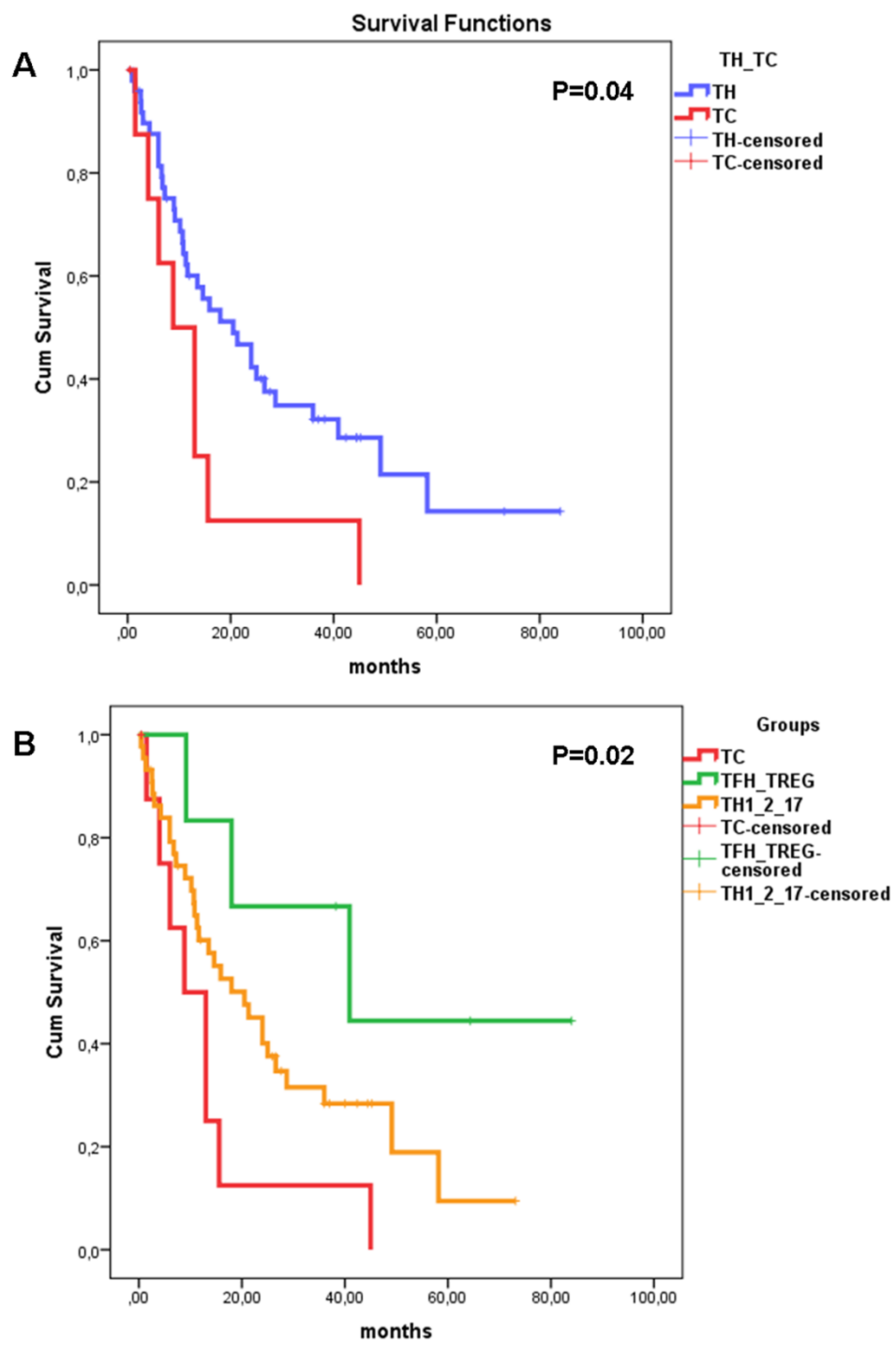


Figure 3.1.7. Survival analyses of PTCL/NOS patients divided according to the molecular classification steps: TH vs. TC (A), and TC vs. Treg and TFH vs. TH1, TH2 and TH17 (B). P-values less than 0.05 for the log rank Mantel-Cox test were considered statistically significant.

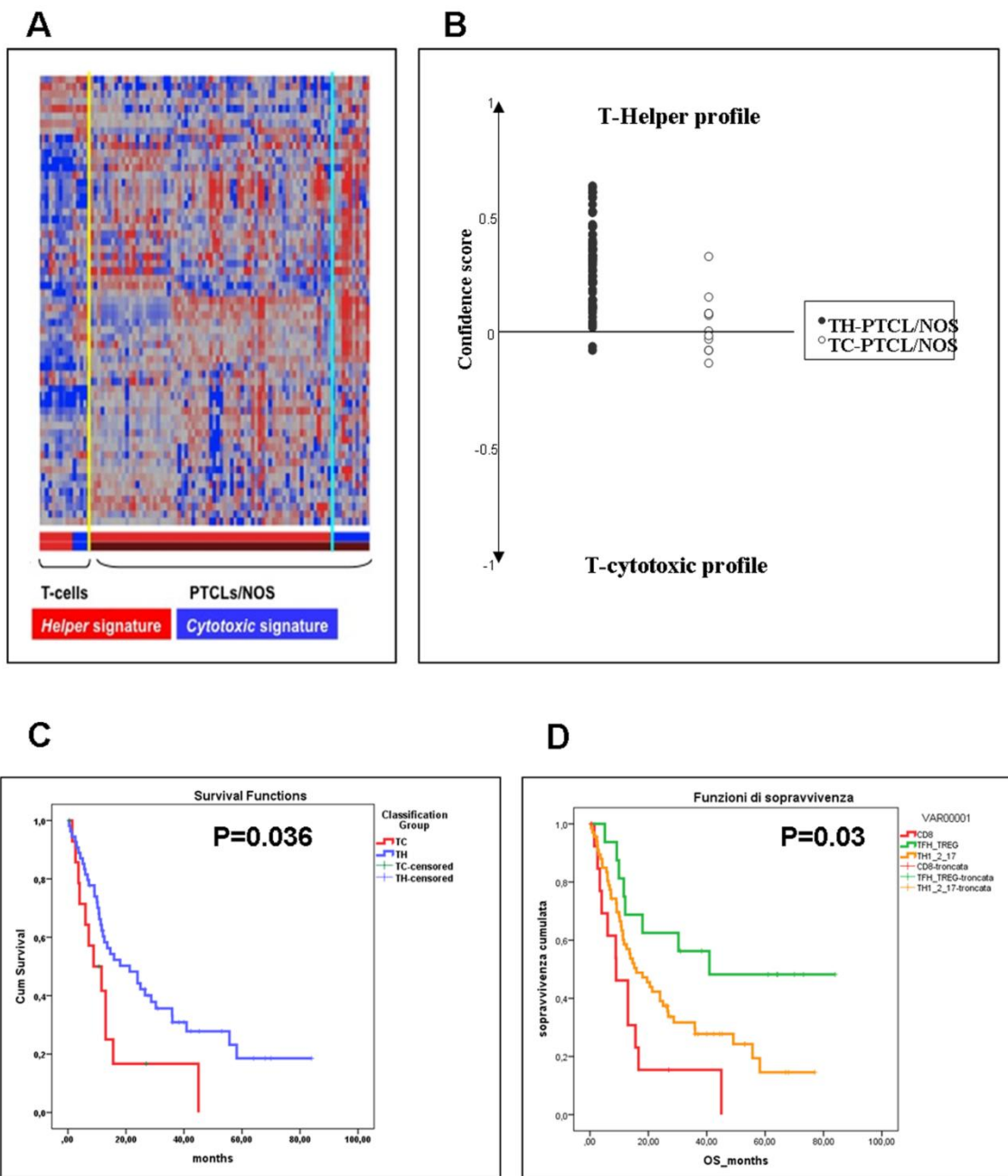


Figure 3.1.8. Molecular classification of FFPE PTCL/NOS cases. The heatmap of samples according to the signatures differentially expressed in TH vs. TC is plotted in panel A. In the matrix, each column represents a sample, and each row represents a gene. The color scale bar shows the relative gene expression changes normalized to the standard deviation (0 is the mean expression level of a given gene). In panel B the accuracy of the linear discriminant function was based on the 5-gene-based MGS (B). Survival analyses of PTCL/NOS patients studied on FFPE samples that served as validation set. TH vs. TC subgroups (C) and for TC vs. Treg and TFH vs. TH1, TH2 and TH17 (D). P-values less than 0.05 for the log rank Mantel-Cox test were considered statistically significant.

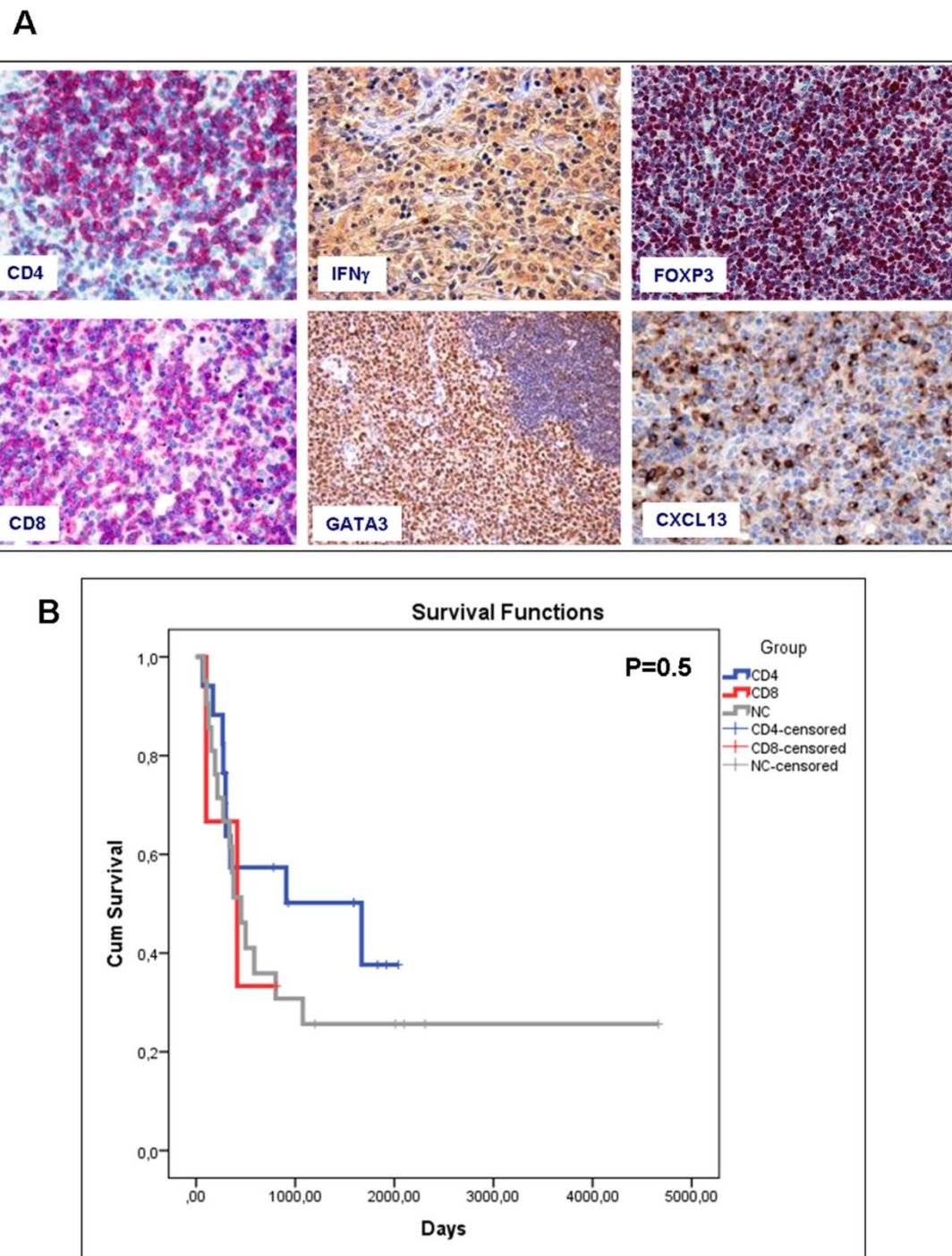


Figure 3.1.9. Immunohistochemical evaluation of T-cell specific markers. A) Examples of CD4, CD8, IFNg, nuclear GATA3, CXCL13, and FOXP3 staining are presented. **B)** Survival analyses of PTCL/NOS patients studied on FFPE samples by immunohistochemistry TH vs. TC subgroups **(B)**. P-values less than 0.05 for the log rank Mantel-Cox test were considered statistically significant.

(3.2)

**Gene and miRNA expression analysis of Lennert
lymphoma reveals a unique profile and identifies
novel therapeutic targets**

Unsupervised analysis suggests some shared molecular features between Lennert lymphoma, and other PTCL subtypes

In order to compare the molecular features of LL with other PTCL subtypes, we analyzed the global gene expression profiles of 12 LL and 90 PTCLs cases which included 10 AITL, 12 ALCL and 68 PTCL/NOS and also 10 T lymphocyte samples taken from normal donors. First, we exploited two widely used unsupervised approaches, namely principal component analysis (PCA) hierarchical clustering analysis (HCA). The results of PCA showed a homogeneous dispersion of almost all cases including LLs in the 3D space (Figure 3.2.1A), with cumulative variance equal to 34.4%. There were, however, two exceptions, including normal T-cells and AITLs, which constitute quite discrete subgroups in the analysis. The results of unsupervised HCA turned out to be very similar to PCA (Figure 3.2.1B).

We then focused on the comparison of LL cases with other PTCL/NOS, using the same two unsupervised methods mentioned above. Similarity, we were unable to discriminate the two groups based on their global gene expression profiles (Figure 3.2.1C-D).

Lennert lymphoma holds a unique gene expression signature which potentially can be used as a molecular diagnosis tool

To find the differentially expressed genes, we further proceeded with direct comparison of LL and other PTCL/NOS. First, the two groups of LL and other PTCL/NOS samples were randomly divided into two groups, namely training and test sets, corresponding to 6 LL and 31 PTCL/NOS samples for the former and 6 LL and 27 PTCL/NOS cases for the latter. Supervised analysis of the training set (Corrected p-value <0.05, FC<2) identified 90 genes differentially expressed between LL and other PTCL/NOS (Figure 3.2.2A, Supplementary Table 16). We then sought to assess whether the genes differentiating LL from other PTCLs/NOS cases might have a significant role in tumorigenesis. Interestingly, analysis of biological processes using GSEA MsigDB tool performed separately on the up- and downregulated genes in LL uncovered a significant enrichment in highly relevant processes, such as upregulation of cell communication, intracellular signaling cascade, and signal transduction for the former, and cell growth/maintenance and cell proliferation for the latter (Figure 3.2.2B). Furthermore, when applied in a supervised HCA, the resulted

signature emerged to be able to differentiate the two groups of the training set correctly, with a p-value equal to 0.0007, as judged by Fisher's exact test (Figure 3.2.2C).

Thereafter, we tried to decrease the number of the differentiating genes, with the intention of finding the most valuable ones which could be used as a diagnosis tool for classifying LL from other PTCL/NOS. In this regard, the 90 genes resulting from the training set were re-supervised in the test set (p-value <0.05, FC<2). A total number of 17 out of the initial 90 genes were achieved (Figure 3.2.3A, Supplementary Table 17), and used to classify all LL and other PTCL/NOS samples. The results showed a high accuracy of the classifier: 9 out of 12 LLs and 57 out of 68 PTCLs/NOS were correctly classified, resulting in an overall diagnostic accuracy (ODA) of 83% and negative predictive value (NPV) of 95%, clearly confirming the validity of the molecular signature as a diagnosis tool (Figure 3.2.3B, Table 3.2.1).

Gene signature of Lennert lymphoma demonstrates unique signature of cytotoxic function

We tried to examine the possible cytotoxic T-cell phenotype of LL cases using different approaches. A GSEA based on the cytotoxic molecular signature (Supplementary Table 1) was applied to compare LL with other PTCLS/NOS, and a significant enrichment was observed between the two groups (Figure 3.2.4A). A supervised analysis (p-value <0.05, FC<2) was then performed to explore the genes that would differentiate LL and other Cytotoxic-PTCL/NOS (Cy-PTCL/NOS), which resulted in 131 and 24 genes, up- and downregulated in LL, respectively (Supplementary Table 18). Intriguingly, this signature could clearly distinguish LL from other Cy-PTCL/NOS cases, when applied in a supervised HCA (p=0.0007) (Figure 3.2.4B). The resulting signature, when analyzed using GSEA, revealed a significant enrichment in the relevant biological processes such as defense response, regulation of apoptosis, cell development, intracellular signaling, gene regulation, regulation of transcription and translation (Figure 3.2.4C).

MicroRNA and gene expression signatures of Lennert lymphoma suggest PI3K/Akt/mTOR pathway as a candidate therapeutic target

To identify deregulated miRNAs in LL, we performed miRNA profiling using a TaqMan qPCR based assay on LL and PTCL/NOS cases. As before, a supervised analysis (p-value <0.05, fold

change>2) was carried out, which resulted in identification of 9 cellular miRNAs differentially expressed in LL, as compared to PTCL/NOS (Figure 3.2.5A, Supplementary Table 19). A HCA based on the expression of the deregulated miRNAs, resulted in the two diseases being clearly differentiated ($p\text{-value}=0.009$, Figure 3.2.5B). A similar approach was followed, comparing LL and normal T-lymphocyte samples, which identified 229 miRNAs differentially expressed (corrected $p\text{-value} <0.01$, fold change>2), most of which were underexpressed in LL (Figure 3.2.5C, Supplementary Table 20), and a clear classification of the normal and neoplastic samples was obtained in a HCA (Figure 3.2.5D).

We further proceeded with more detailed comparison of LL with normal T-lymphocyte. First, a supervised analysis was utilized in order to find the genes that distinguish the two set of samples. Totally 622 genes were found (corrected $p\text{-value} <0.005$, fold change>2) which were differentially expressed in the two categories, most of which were upregulated in LL (Figure 3.2.6A, Supplementary Table 21). Importantly, when we performed a supervised HCA based on the expression of those genes, normal and neoplastic samples were clearly differentiated (Figure 3.2.6B). Gene set enrichment analysis of the differentially expressed genes revealed a significant enrichment of biological processes highly relevant to malignant phenotype. Remarkably, most of such processes could be referred to two main categories or both: neoplastic clone (e.g. cell growth, angiogenesis and cell adhesion/cell-cell signaling) and microenvironment (e.g. response to wounding, collagen catabolism and extracellular matrix) (Figure 3.2.6C, Supplementary Table 22). As a confirmation, we evaluated the expression of CD68, a marker widely used for detection of tumor-associated macrophages in tumor microenvironment in LL samples, which turned out to be positive (Figure 3.2.6D).

Searching for the master cellular pathway(s) which could be mostly responsible for the malignant phenotype of LL, we analyzed its molecular signature, including both differentially expressed genes and predicted targets of differentially expressed miRNAs (as compared to normal T-cells) in Ingenuity Pathway Analysis (IPA) software. Very interestingly, PI3K/Akt/mTOR signaling axis, a well-described pathway in human malignancies, emerged to have a central role in molecular pathology of LL (Figure 3.2.7A). Very importantly, the tumor samples showed positivity for STAT5, as judged by IHC (Figure 3.2.7B). This is in line with the

above mentioned observation that PI3K/Akt/mTOR signaling axis inhibition could be a rationale therapeutic strategy in PTCLs.

Clinical features add more documents supporting Lennert lymphoma as a distinct entity

In addition, we analyzed different aspects of clinical information for LL patients and compared it to other PTCL/NOS, by means of Fisher's exact test or T-test for non-continuous and continuous variables, respectively. The data was available for 10 out of 12 LL and 68 of other PTCL/NOS patients. As described in Table 3.2.2, we found significant differences in some characteristics including male/female ratio (9 vs. 1, p-value=0.02) and B-symptoms (1 out of 10 patients, p-value=0.036). As concerns for treatment response and survival, a favorable trend was observed in LL, although the differences were not statistically meaningful (Table 3.2.2).

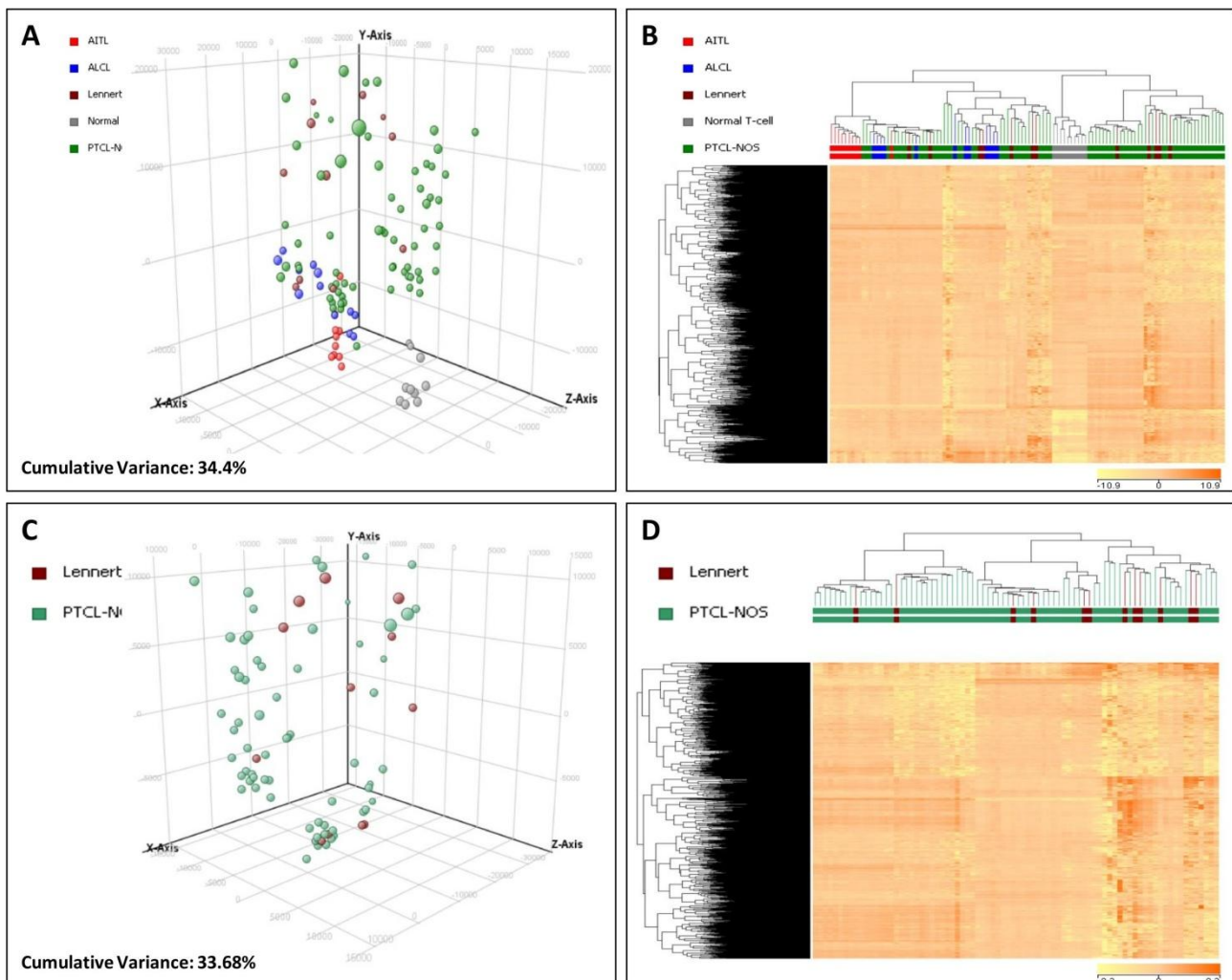


Figure 3.2.1. Unsupervised analysis hardly discriminates Lennert lymphoma from other PTCL subtypes with nodal origin. Principal component analysis (**A**) and unsupervised hierarchical clustering (**B**) performed on Lennert lymphoma, PTCL subtypes, and normal T-cells failed to discriminate them. There was, however, a distinct clustering of AITL and normal T-cell samples. Similarly, principal component analysis (**C**) and unsupervised hierarchical clustering (**D**) turned out to be incompetent in classifying LL from other PTCL/NOS cases. Each sphere in the three-dimensional space represents a single sample, and each dimension represents a principal component. In the heat map, each column represents a sample, and each row represents a probeset (gene). The color scale bar shows the relative gene expression changes normalized to the standard deviation (0 is the mean expression level of a given gene).

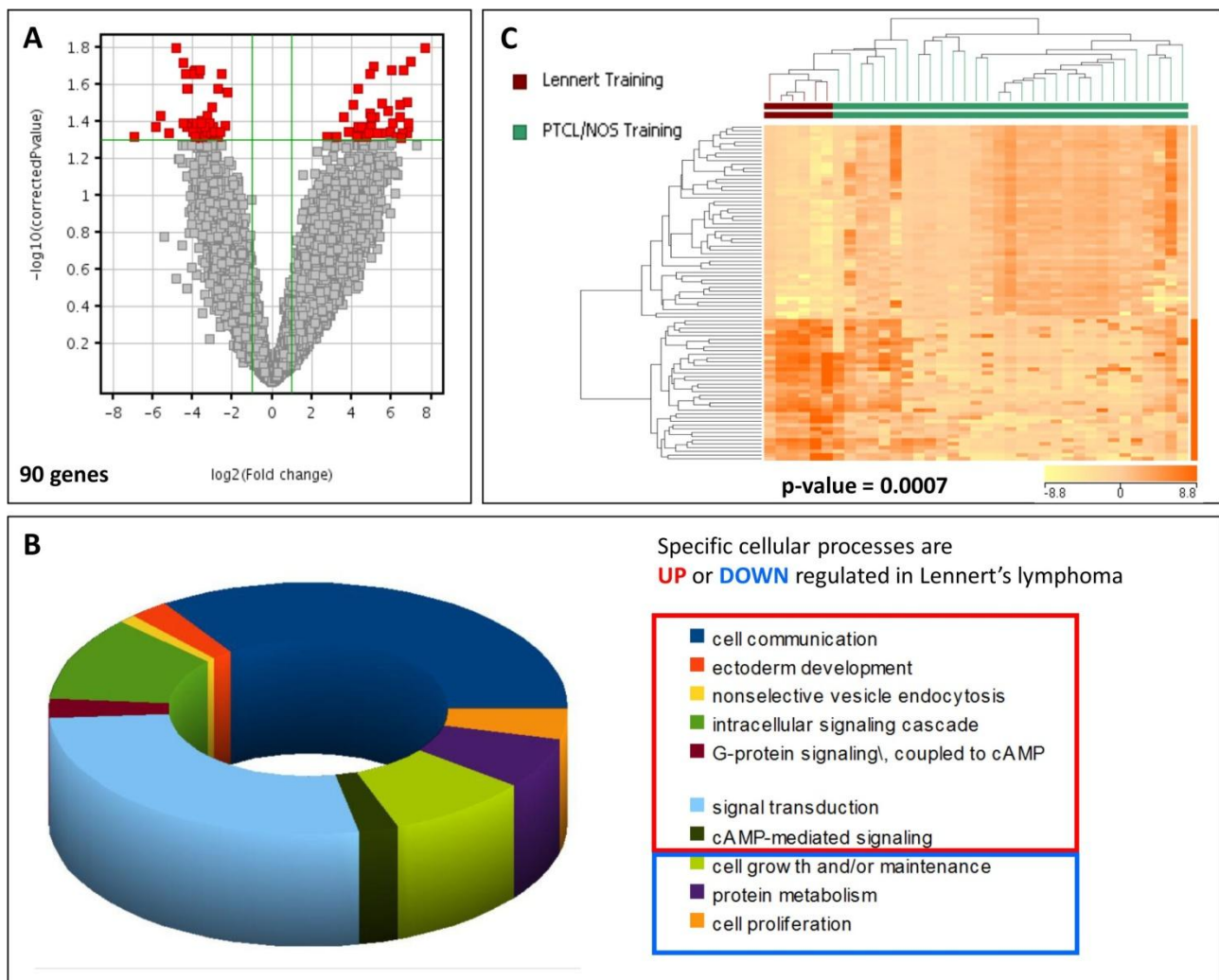


Figure 3.2.2. Supervised analysis identified genes distinguishing Lennert lymphoma from PTCL/NOS. A) Supervised HCA analysis identified 90 genes differentially expressed in Lennert lymphoma vs. PTCL/NOS in a training set of cases. In the volcano plot, each red square represents a gene. **B)** Based on the expression of the differentially expressed genes, the two diseases were clearly differentiated, when applied in a hierarchical clustering. In the heat map, each column represents a sample, and each row represents a probeset (gene). The color scale bar shows the relative gene expression changes normalized to the standard deviation (0 is the mean expression level of a given gene). **C)** GSEA showed a significant enrichment in specific biological processes which are UP or DOWN regulated in Lennert lymphoma.

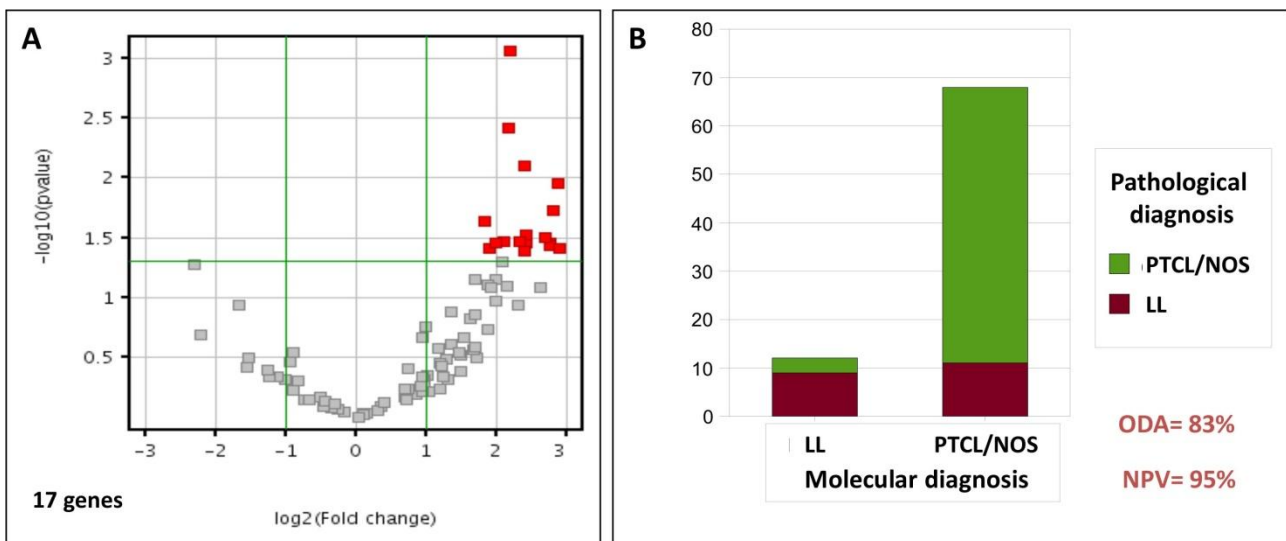


Figure 3.2.3. Validation of the molecular signature of Lennert lymphoma as a molecular diagnosis tool. **A)** A re-supervised analysis on the 90 genes differentially expressed of training set in a test set of cases resulted in 17 genes as the most valuable ones. In the volcano plot, each red square represents a gene. **B)** Based on the expression of the identified 19 genes in the test set, all the cases were efficiently diagnosed as Lennert lymphoma or other PTCL/NOS with an Overall Diagnostic Accuracy (ODA) of 83% and Negative Predictive Value (NPV) 95% and the pathological diagnosis graph was re-allocated to molecular diagnosis.

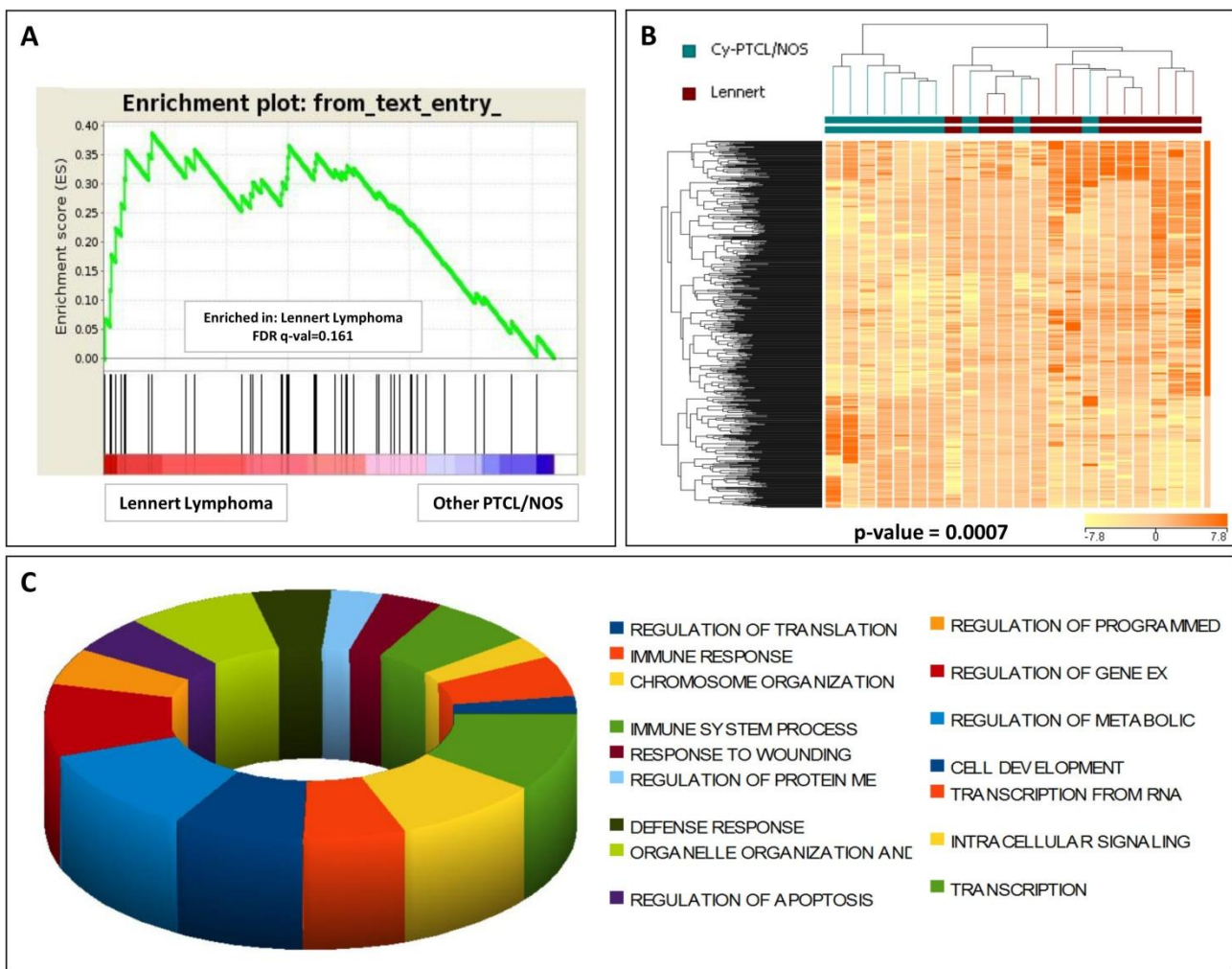


Figure 3.2.4. Lennert lymphoma signature is significantly enriched in genes belonging to the cytotoxic function. **A)** A gene set enrichment analysis of the cytotoxic T-cell signature distinguished Lennert lymphoma from other PTCL/NOS. **B)** A supervised analysis was performed to distinguish the genes differentially expressed between LL and other cytotoxic PTCL/NOS. A hierarchical clustering was followed based on the expression of such genes, and clearly distinguished LL from other cytotoxic PTCL/NOS cases ($p=0.0007$). In the heat map, each column represents a sample, and each row represents a probeset (gene). The color scale bar shows the relative gene expression changes normalized to the standard deviation (0 is the mean expression level of a given gene). **C)** A GSEA based on the differentially expressed genes from the previous step revealed a significant enrichment of tumor-related processes.

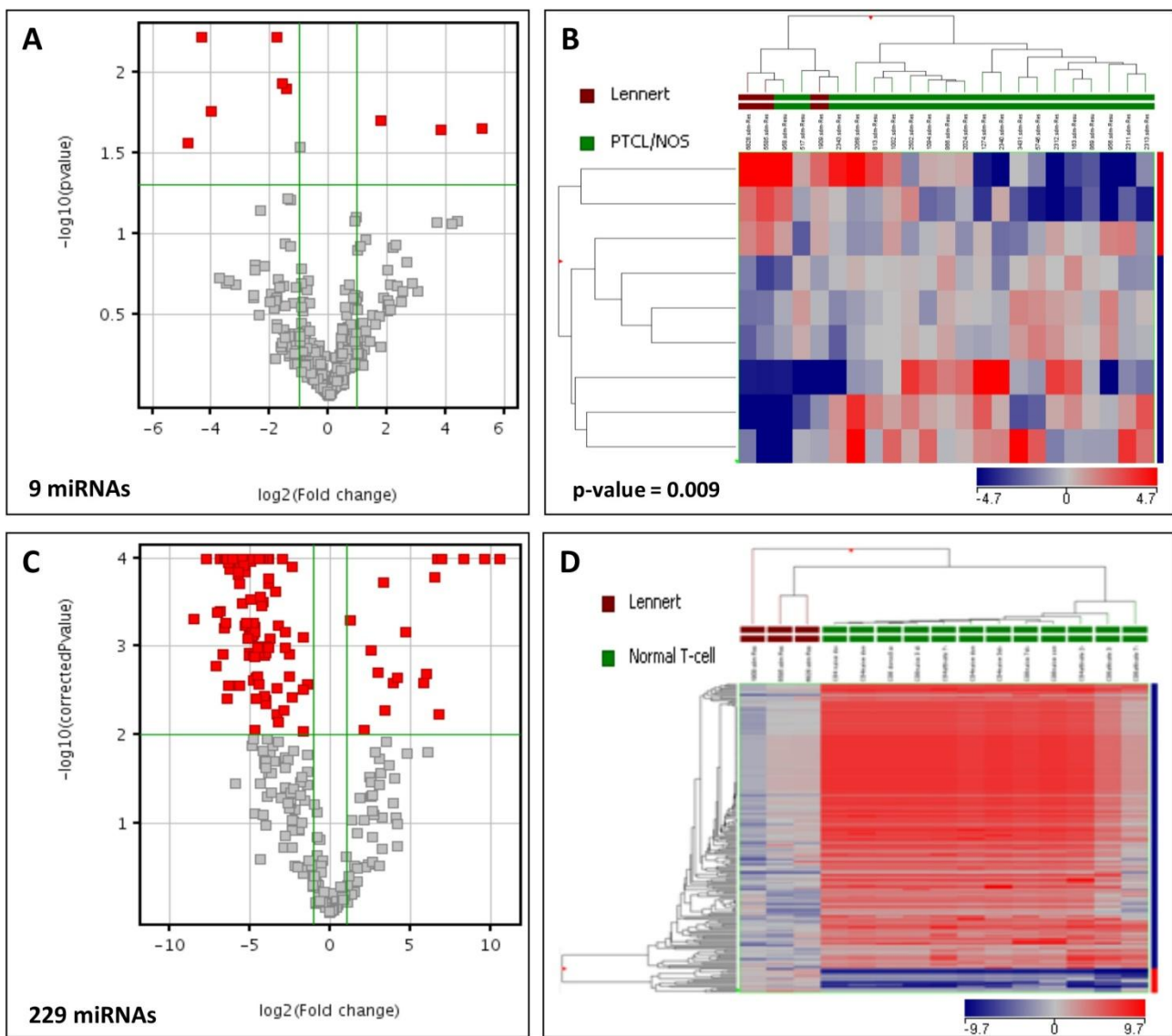


Figure 3.2.5. Lennert lymphoma represents a unique microRNA signature. **A)** Supervised analysis identified 9 miRNAs differentially expressed in Lennert lymphoma vs. other PTCL/NOS. **B)** Based on the expression levels of the found miRNAs, the two diseases were clearly classified in a hierarchical clustering analysis. **C)** Supervised analysis identified 229 miRNAs differentially expressed in LL as compared to normal T-lymphocytes. **D)** By a hierarchical clustering, normal and neoplastic samples were clearly differentiated based on the expression of such 229 miRNAs. In the volcano plot, each red square represents a miRNA. In the heat map, each column represents a sample, and each row represents a probeset (miRNA). The color scale bar shows the relative gene expression changes normalized to the standard deviation (0 is the mean expression level of a given miRNA).

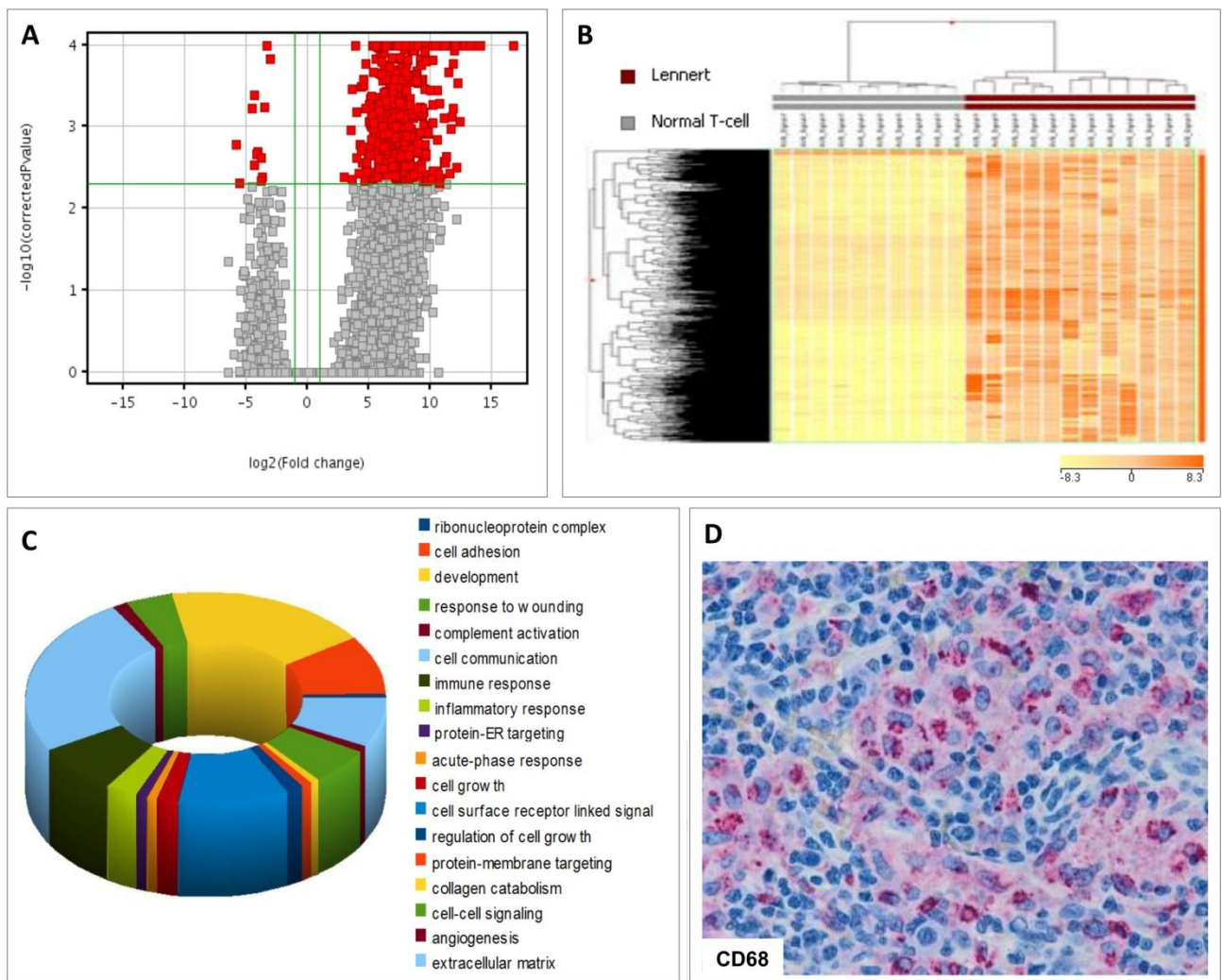


Figure 3.2.6. Genes distinguishing Lennert lymphoma from normal T-cells are involved in processes related to malignant phenotype. **A)** A supervised statistical investigation identified 622 genes differentially expressed in LL in comparison to normal T-lymphocytes. In the volcano plot, each red square represents a gene. **B)** The identified genes were used to classify normal and neoplastic samples, which turned out to be clearly differentiated in a hierarchical clustering analysis. In the heat map, each column represents a sample, and each row represents a probeset (gene). The color scale bar shows the relative gene expression changes normalized to the standard deviation (0 is the mean expression level of a given gene). **C)** Gene Set Enrichment Analysis of the differentially expressed genes identified significant enrichment referred to either the neoplastic clone or to the microenvironment or to both. **D)** Immunohistochemical staining of CD68, a marker used for analysis of microenvironment cells (tumor-associated macrophages), showed positivity in LL samples.

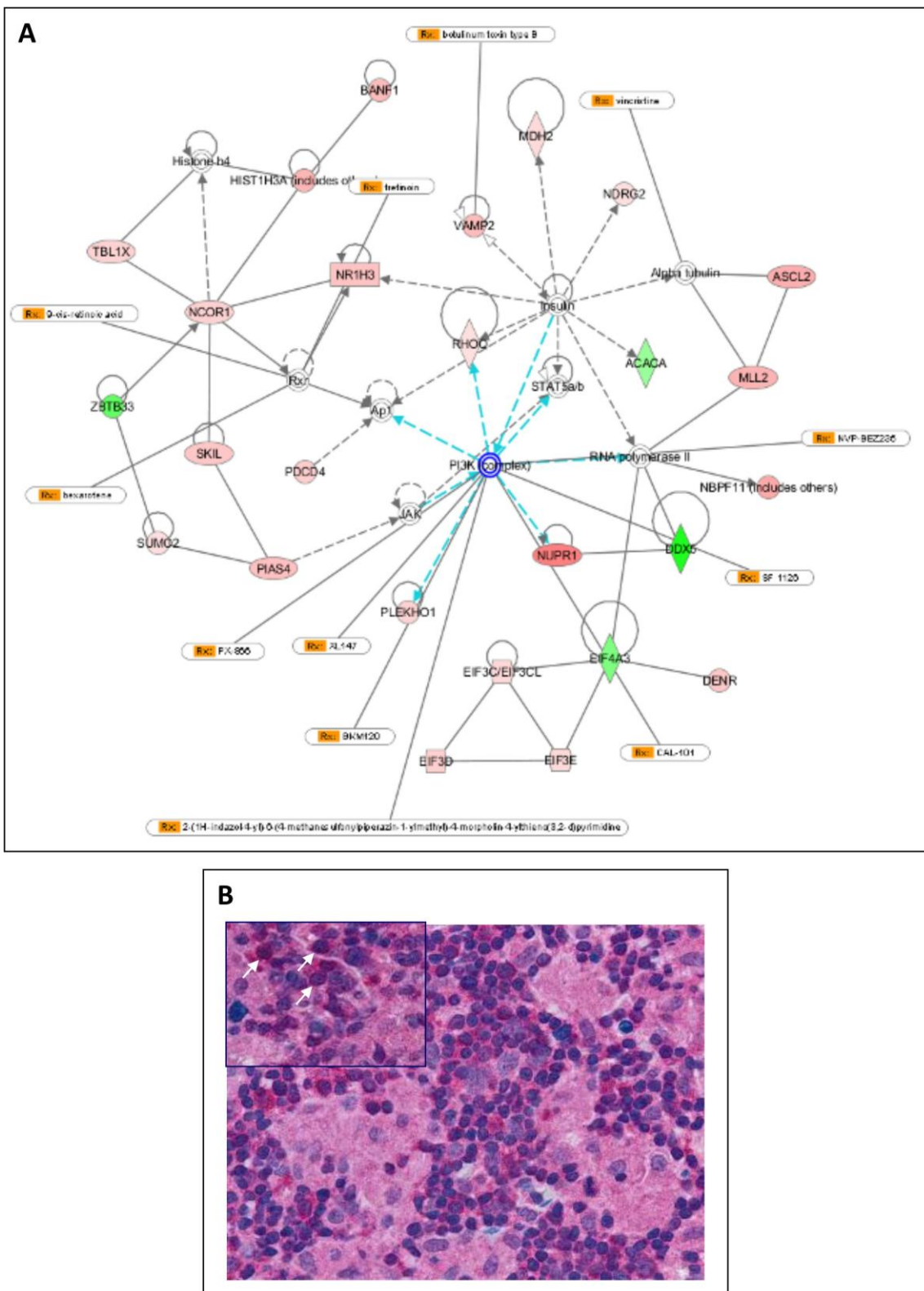


Figure 3.2.7. The MTOR/PI3K pathway is a candidate therapeutic target in LL. A) An analysis performed using Ingenuity Pathway Analysis (IPA) software using genes and (targets of) miRNAs deregulated in Lennert lymphoma identified PI3K/Akt/mTOR pathway as a

possible therapeutic target in Lennert lymphoma. **B)** Activity of PI3K/Akt/mTOR pathway in Lennert lymphoma was checked by Immunohistochemical staining of STAT5. The neoplastic cells showed the positive reactivity for STAT5 in the nucleus (white arrows in the inset).

Table 3.2.1. Accuracy evaluation of the 17 genes used to classify Lennert lymphoma vs. other PTCL/NOS.

Confusion Matrix				
Molecular	Pathological Diagnosis			Total
	LL	PTCL/NO S	LL	
	LL	9	11	20
	PTCL/NOS	3	57	60
	Total	12	68	80
Accuracy Calculations				
	Value	95% CI		
ST	75	51 to 100		
SP	84	75 to 93		
PtP	15	7 to 23		
PPV	45	23 to 67		
NPV	95	89 to 100		
LR+	4.64	2.46 to 8.72		
LR-	0.30	0.11 to 0.80		
Overall Diagnostic Accuracy: 83% (66 of 80)				

LL: Lennert Lymphoma; **PTCL/NOS:** Peripheral T-cell Lymphoma-Not otherwise specified; **ST:** SENSITIVITY; **SP:** SPECIFICITY; **PtP:** Pre-test Probability; **PPV:** Positive Predictive Value; **NPV:** Negative Predictive Value; **LR+:** LIKELIHOOD RATIO +; **LR-:** LIKELIHOOD RATIO -.

Table 3.2.2. Comparison of clinical features of Lennert lymphoma vs. other PTCL/NOS.

	Other PTCL/NOS	LL	p-value
Number of cases	68	10	NA
Male: Female	1:1	9:1	0.02
Mean age, years (range)	50.9 (7-80)	48.7 (22-67)	NS
Stage III-IV (%)	47/68 (69)	6/10 (60)	0.7
B-symptoms (%)	33/68 (49)	1/10 (10)	0.036
Bulky disease (%)	7/68 (10)	3/10 (30)	0.11
Mediastinal mass (%)	21/68 (31)	4/10 (40)	0.7
Bone marrow involvement (%)	21/68 (31)	1/10 (10)	0.26
Extra-nodal involvement (%)	26/68 (38)	2/10 (20)	0.32
Hemophagocytic syndrome (%)	3/68 (4)	0/10	1
Treatment response & Survival			
CR (%)	33/68 (49)	6/10 (60)	0.7
PR (%)	13/68 (19)	3/10 (30)	0.4
NR (%)	22/68 (32)	1/10 (10)	0.26
OR (%)	46/68 (67)	9/10 (90)	0.26
8-years OS (%)	29/68 (43)	6/10 (60)	0.3

LL: Lennert Lymphoma; **PTCL/NOS:** Peripheral T-cell Lymphoma-Not otherwise specified;

CR: Complete Response; **PR:** Partial Response; **NR:** Not Response; **OR:** Objective Response;

OS: Overall Survival.

(3.3)

**Molecular Signature of Follicular Variant of
Peripheral T-Cell Lymphoma Not Otherwise
Specified Implies Distinction from
Angioimmunoblastic T-cell Lymphoma**

Unsupervised approaches barely distinguish F-PTCL from other nodal PTCL subtypes

We analyzed the global gene expression profiles of 82 PTCL cases which included 10 AITL, 10 F-PTCL, 50 PTCL/NOS, 10 ALK-negative and 10 ALK-positive ALCLs. The most widely used unsupervised methods including principal component analysis (PCA) and hierarchical clustering analysis (HCA) were first utilized to compare the global profile of all the groups included. The results of PCA showed a dispersion of all cases, and a faint grouping of all categories (except for the major part of PTCL/NOS) gathering around Y-axis (Figure 3.3.1A). We found similar results when used HCA (Figure 3.3.1B).

We followed our analysis with comparison of Tfh-related nodal PTCLs (i.e. F-PTCL, AITL and Tfh-PTCL/NOS) using the same methods. Again we found a major proportional grouping around Y-axis, and notably, both Tfh-positive and negative cases of PTCL/NOs showed similarity with F-PTCL and AITL (Figure 3.3.1C). Once more, unsupervised HCA confirmed the results obtained from PCA (Figure 3.3.1D).

F-PTCL exhibits a global molecular profile more similar to PTCL/NOS rather than AITL

As concerned with the molecular correlation of F-PTCL, we aimed to analyze the closeness of F-PTCL to AITL or PTCL/NOS, in terms of molecular profiles. As a control, Tfh-PTCL/NOS cases were treated using the same approach. We used a classifier in GeneSpring software, and it was found that F-PTCL tumors exhibit a molecular profile much more similar to PTCL/NOS, rather than to AITL (Figure 3.3.2A). Of note, all the cases grouped very closely together, and none happened to be in the grey zone. Similarly, Tfh-PTCL/NOS cases were clustered close to the molecular profile of PTCL/NOS.

A supervised HCA based on the expression of genes differentially expressed between AITL and PTCL/NOS was then followed, which verified the previous results (Figure 3.3.2B). Here, F-PTCL samples categorized with PTCL/NOS cases, rather than AITL ones. However, unlike the previous analysis, Tfh-PTCL/NOS cases were dispersed in the classification tree (Figure 3.3.2B).

The gene expression profile of F-PTCL is distinct from AITL and Tfh-PTCL/NOS

Concerned with the possible molecular distinction among PTCLs with nodal origin, especially F-PTCL and other two categories, namely AITL and Tfh-PTCL/NOS, we used supervised approaches to find the genes that would distinguish them. First, by means of an ANOVA (corrected p-value<0.01 and fold change>2) analysis, we compared all the three groups. Collectively, we found 881 genes differentiating them, most of which seemed to be up-regulated in F-PTCL (Supplementary Table 23). These genes were able to cluster the groups accurately, when used in a HCA (Figure 3.3.3A). Of note, there was one single sample belonging to Tfh-PTCL/NOS happened to cluster with AITL samples (Figure 3.3.3A, red arrow).

A paired supervised analysis of the three sets was then performed, using student's T-test. Comparison of F-PTCL with AITL (corrected p-value<0.01 and fold change>2) resulted in identification of 581 genes, 248 up- and 333 downregulated in F-PTCL, respectively (Supplementary Table 24), which resulted in a precise classification of the two diseases (Figure 3.3.3B). As concerned with comparison of F-PTCL and Tfh-PTCL/NOS (corrected p-value<0.05 and fold change>2), we found 272 genes induced in F-PTCL and 22 genes suppressed in F-PTCL (Supplementary Table 25). Once again, a precise categorization was achieved using these genes (Figure 3.3.3C). The last pair of samples compared, i.e. AITL and Tfh-PTCL/NOS produced 43 and 75 genes over- and under-expressed in AITL (corrected p-value<0.05 and fold change>2, Supplementary Table 26). Although a clear distinction of the two sets was achieved using HCA, as in Figure 3.3.3A, the same sample of Tfh-PTCL/NOS was classified with AITL cases (Figure 3.3.3D).

Different master transcription regulators might operate in F-PTCL and AITL

We continued with examining the correlation of F-PTCL and AITL in terms of the regulatory molecules. Specifically, we used the gene signature distinguishing the two groups in a GSEA, aiming to recognize the transcription regulators that would be (at least in some extent) responsible for the different molecular profiles of the two cancers. Of note, the obtained data suggests involvement of several such molecules (Figure 3.3.4A). Among them, we analyzed the expression of two master regulators widely recognized in human cancers,

including *LEF1* (Lymphoid enhancer-binding factor 1) and *SP1* (specificity protein 1). Both genes were differentially expressed between F-PTCL and AITL (Figure 3.3.4B), being *LEF1* over-expressed in AITL (p-value = 0.04) and *SP1* upregulated in F-PTCL (p-value = 0.03).

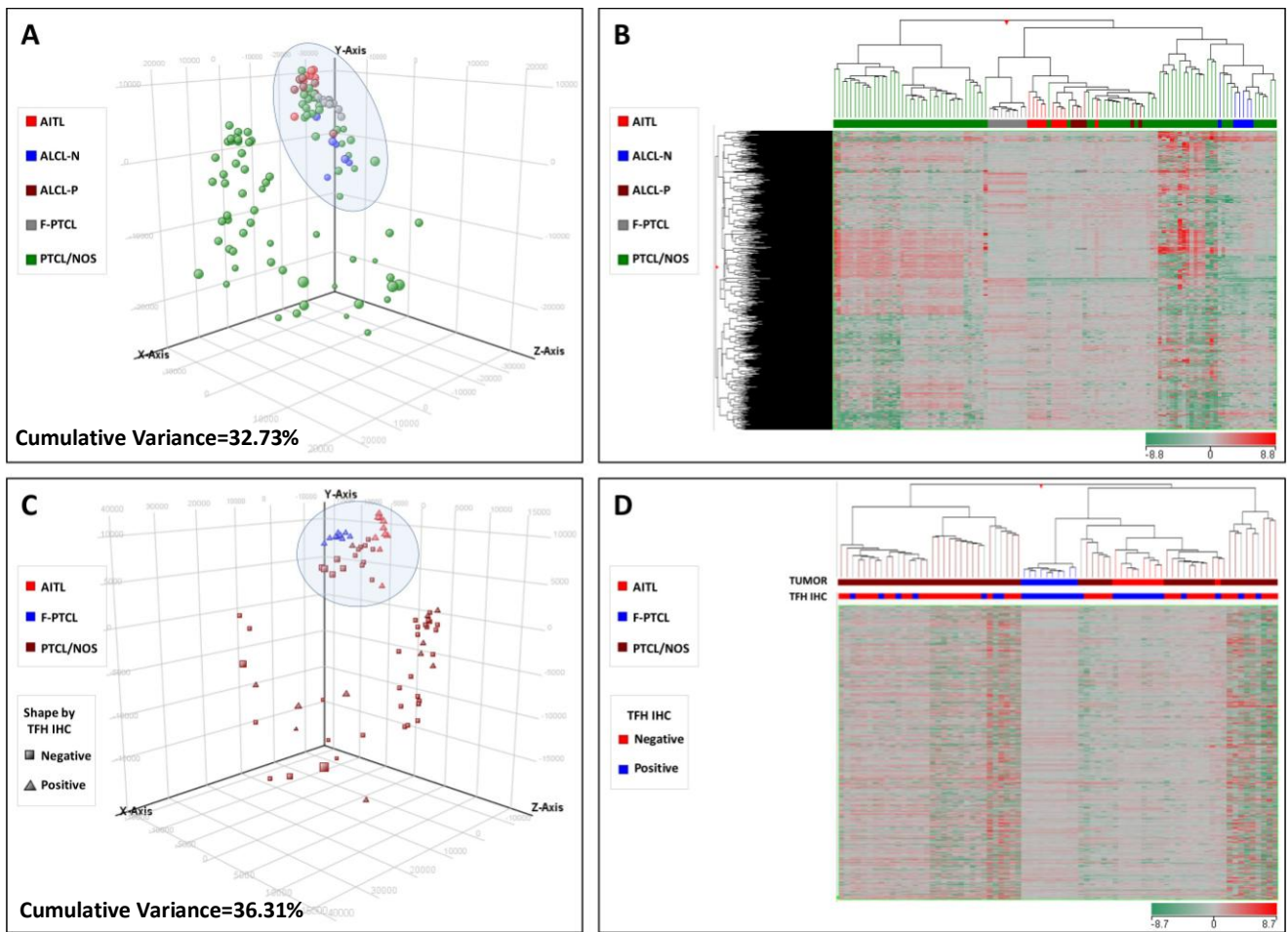


Figure 3.3.1. Unsupervised approaches barely distinguish F-PTCL from other nodal PTCL subtypes. Principal component analysis (**A**) and unsupervised hierarchical clustering (**B**) performed on PTCL subtypes including AITL, ALK-positive and ALK-negative ALCL, PTCL/NOS, and F-PTCL failed to discriminate them. Similarly, principal component analysis (**C**) and unsupervised hierarchical clustering (**D**) performed on Tfh-related nodal PTCLs including F-PTCL, AITL and Tfh-PTCL/NOS which did not result in clear grouping of the samples. Each sphere in the three-dimensional space represents a single sample, and each dimension represents a principal component. In the heat map, each column represents a sample, and each row represents a probeset (gene). The color scale bar shows the relative gene expression changes normalized to the standard deviation (0 is the mean expression level of a given gene).

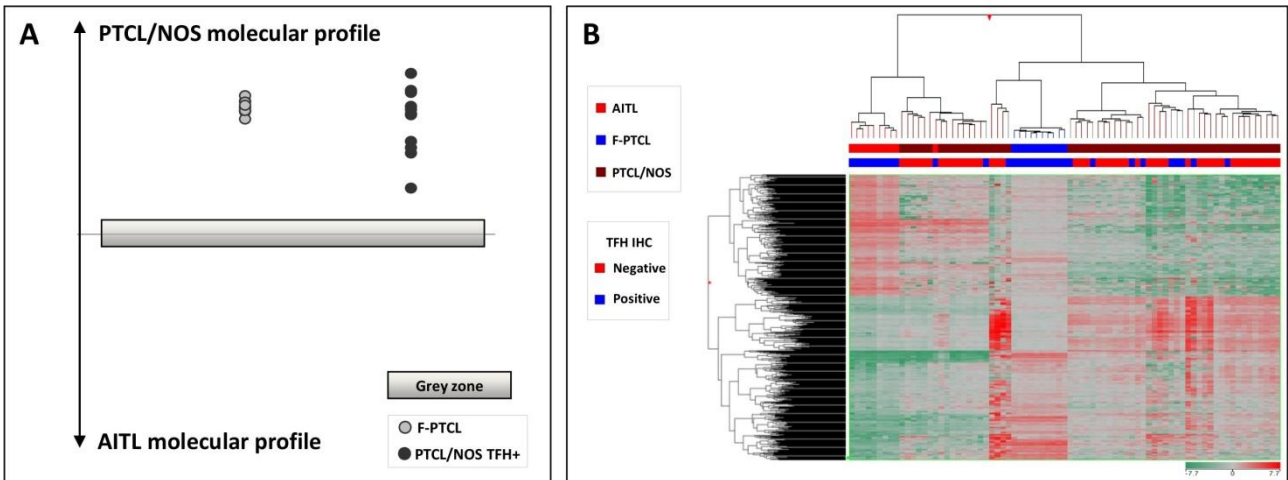


Figure 3.3.2. F-PTCL exhibits a global molecular profile more similar to PTCL/NOS rather than AITL. **A)** Using a classifier based on global gene expression profiles, F-PTCL samples exhibited molecular profiles more similar to PTCL/NOS, as compared to AITL. Similar as well as, Tfh-PTCL/NOS cases were clustered close to the molecular profile of PTCL/NOS. **B)** Similarly, a supervised HCA based on the genes differentially expressed between AITL and PTCL/NOS verified F-PTCL samples to categorize more closely with PTCL/NOS cases. In the heat map, each column represents a sample, and each row represents a probeset (gene). The color scale bar shows the relative gene expression changes normalized to the standard deviation (0 is the mean expression level of a given gene).

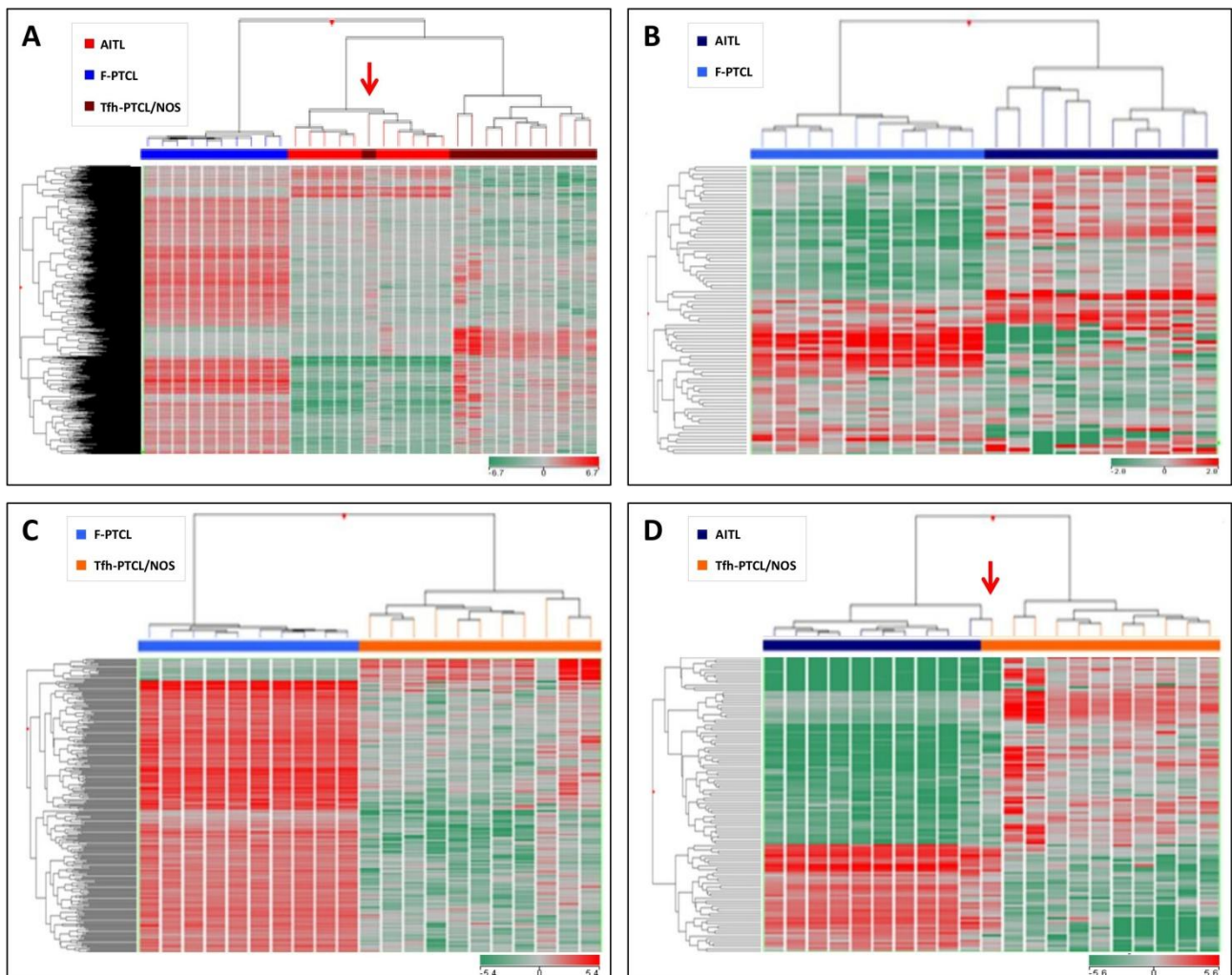


Figure 3.3.3. The gene expression profile of F-PTCL is distinct from AITL and Tfh-PTCL/NOS. A) Using ANNOVA analysis three groups of F-PTCL, AITL and Tfh-PTCL/NOS were clustered based on the genes differentially expressed among them. Paired supervised analysis followed by HCA performed between F-PTCL vs. AITL (B), F-PTCL vs. Tfh-PTCL/NOS (C), and AITL vs. Tfh-PTCL/NOS (D) resulted in precise classification of these three groups. The sample belonging to Tfh-PTCL/NOS which classified with AITL samples is indicated with red arrow. In the heat map, each column represents a sample, and each row represents a probeset (gene). The color scale bar shows the relative gene expression changes normalized to the standard deviation (0 is the mean expression level of a given gene).

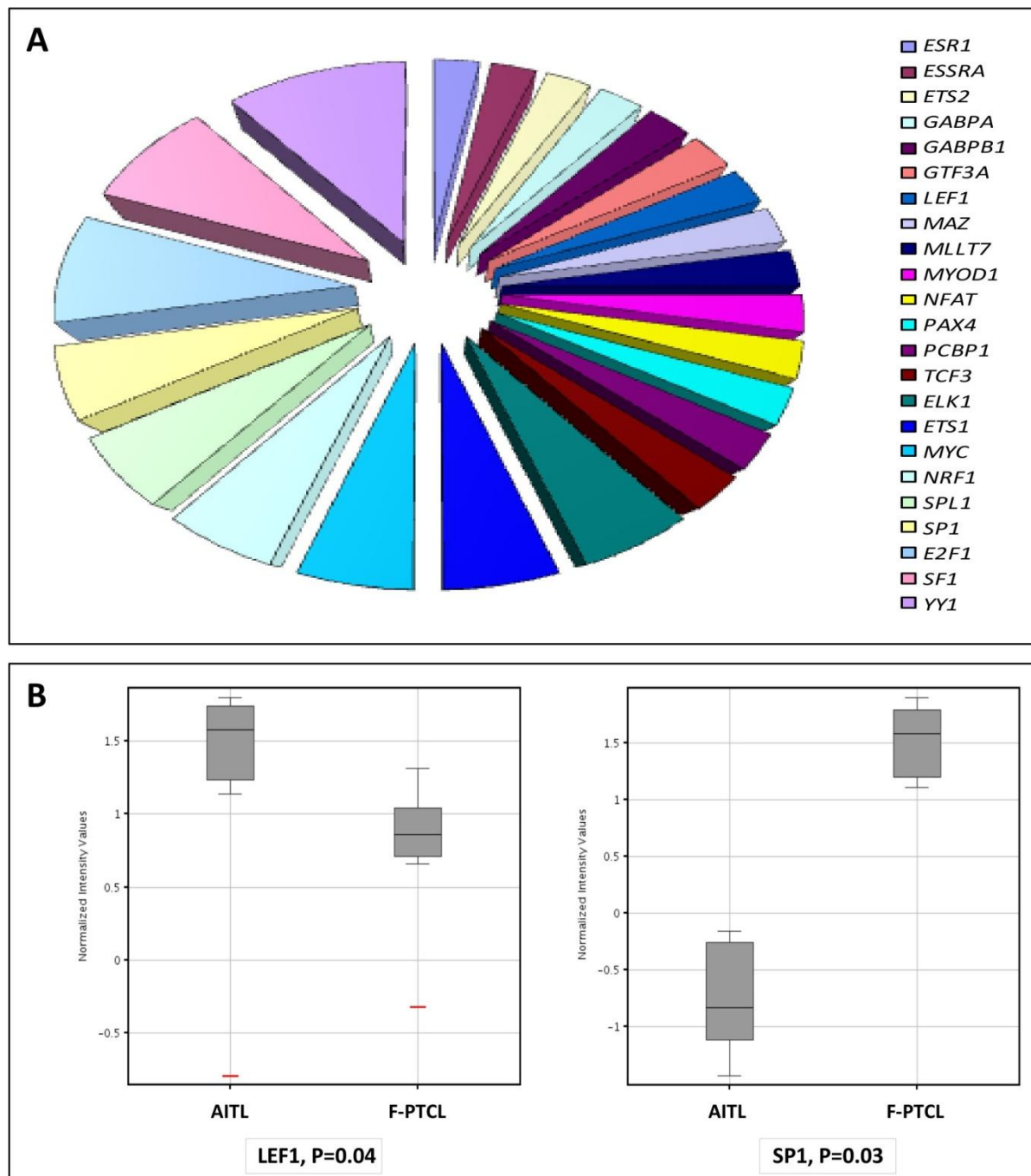


Figure 3.3.4. Different master transcription regulators might operate in F-PTCL and AITL.

A) The gene set enrichment analysis (GSEA) identified regulatory molecules responsible for the different molecular profiles of the F-PTCL and AITL. **B)** Among the identified molecules, two master regulators widely including LEF1 (Lymphoid enhancer-binding factor 1) and SP1 (specificity protein 1) were differentially expressed between F-PTCL and AITL.

(4)

Discussion and Conclusion

The sub-classification of PTCL/NOS based on their relation with different functional T-cell subsets provides new insights into the pathogenesis of PTCL/NOS and, at the same time, offers the opportunity to identify patient groups with diverse clinical behaviors to be evaluated in specific clinical trials.

PTCL/NOS have previously been shown to consist of activated TC or TH clones (34, 36, 62, 64, 78), which had different prognoses (64, 78), and GEP was the only approach able to clearly distinguish the two groups (62, 64).

Importantly, the identification of a very complex scenario further stressed a crucial issue in PTCL/NOS biology, i.e., whether these clones actually derive from different cell types or instead differentiate toward diverse lineages in response to microenvironmental stimuli or as a consequence of their individual characteristics. Indeed, T-cell priming conditions may deeply influence the relative prevalence of polarizing signals through the modulation of master transcription factors. A notable example is the transcription factor GATA-3, whose expression can be modulated by environmental signals through Notch signaling and whose activity in T-cell clones may go beyond the stabilization of TH2 commitment by affecting mature T-cell chromatin remodeling and proliferation in both the CD4+ TH and CD8+ TC subsets (125-127). This fact is not trivial because it might indicate a maintained sensitivity (or even a dependency) to the reactive *milieu*, which could, in turn, determine the functional properties of the neoplastic cells and consequently influence tumor development and progression. In this regard, our group recently demonstrated that non-neoplastic cells are associated with the clinical syndrome in AITL (128). However, a different histogenesis may be associated with different etiologic stimuli and/or with specific genetic events (41, 42, 80, 96, 129, 130). In this regard, we found that specific mutation patterns characterized the main PTCL/NOS subgroups in terms of both single lesions and pathways. Some of them, including those affecting JAK2 and NOTCH1 signaling in TC, epigenetic regulation of gene expression in TREG/TFH, and MTOR/AKT in other TH might represent suitable therapeutic targets. Indeed, we found that MTOR/PI3K inhibition was effective ex vivo for TH PTCL cells.

Our results formally demonstrate that PTCL/NOS is indeed a Pandora's box that contains biologically different T-cell neoplasms, which is differently reflected by genetic, transcriptional and phenotypic profiles. The gene signatures used proved to be successful in

the specification of PTCL/NOS, even when applying an MGS. Conflicting signature enrichment (i.e., the expression of overlapping signatures) resulted in few unclassified cases that likely reflect both the establishment of aberrant T-cell clones and the puzzling effect of the microenvironmental pressure. Conversely, we exclude, *bona fide*, major artifacts due to the reactive components as in all cases the percentage of tumor cells exceeded 60-70%. Therefore, the tumor component was responsible for the main signals in GEP.

One major limitation to the extensive usage of GEP in routine diagnostic practice is the limited availability of fresh/frozen samples in contrast to FFPE samples. We showed that reliable GEP analysis could be performed on FFPE samples, as we also recently demonstrated for improving nodal PTCLs diagnosis (104). Herein, we applied the cellular classifiers to FFPE PTCL/NOS cases with a high degree of success, even when limiting the number of discriminatory genes, thus enabling a simple diagnostic assay. Importantly, this method will allow the application of a focused custom-array if the whole genome profile is not requested. In fact, we identified an MGS that is able to classify PTCL/NOS cases both in frozen and FFPE samples.

When applied to the PTCL/NOS classification, IHC was unable to discriminate among most of the subtypes, including the relevant TH vs. TC dichotomy, but proved to be quite effective at identifying the Treg/TFH-related cases, which are characterized by a better outcome. Therefore, the combination of molecular techniques and conventional immunophenotyping may enable an integrated diagnostic algorithm limiting the costs of extensive molecular analyses (Supplementary Figure 1). On the other hand, the expression of single master transcription factors such as TBX1 and GATA3 was not sufficient to recapitulate the entire classification and was not confirmed to be enough to discriminate different clinical subgroups. This fact could be possibly related to the actual heterogeneity and complexity of the disease and/or to the promiscuity of certain molecules across T-cell types (i.e. GATA3 in both TH2 and T-cytotoxic; Supplementary Figure 2).

We also sought to investigate the molecular profile of two morphological variants of PTCL/NOS, namely Lennert lymphoma and PTCL/NOS follicular variant. In general, being rare diseases, there is scarce amount of information on the biological nature of LL and F-PTCL (34). Concerning LL, it is currently diagnosed only based on morphology and

immunohistochemical characteristics, misdiagnosis being quite frequent (75, 86, 87, 92-94). Some researchers, however, have suggested that LL might actually be a distinct entity, although there are few evidences supporting this hypothesis (75, 86). Here, for the first time, we present our results obtained from studying the molecular profile of LL concerning both gene and microRNA expression signatures indicating that LL is distinct from other PTCLs/NOS and might be regarded as distinct entity.

We started with comparison of global gene signatures of all PTCL subtypes, along with normal T-cells, trying to define the general position of LL. However, the unsupervised methods failed a clear discrimination of LL and other PTCL/NOS. Of note, however, we found a sharp clustering for normal T-cell, which was somehow expected. In fact, a similar pattern was previously observed in previous studies on PTCLs (48, 62, 64, 65). A comparison of LL with other PTCL/NOS using the same approach was then carried out, but again we were unsuccessful in achieving significant results.

However, a more stringent comparison of LL and other PTCL/NOS, accomplished using supervised methods, supported the existence of different molecular signatures at some level. The differentially expressed genes turned out to be engaged in malignancy-related processes, probably pointing at some different tumorigenesis mechanisms in the two groups. The gained signature could potentially classify the two categories correctly.

In addition, in order to prove the validity of such signature, we further processed it in a separate set of samples (test set) and ended up with a limited number of genes which could strongly differentiate LL samples from other PTCL/NOS. This strengthened our hypothesis of LL being a distinct.

There are some evidences which suggest that the major part of LL could be originated from cytotoxic T-cells. For example, Geissinger et al. (85) performed IHC on 101 PTCL/NOS cases which include 18 LL and represented LL is mainly derived from CD8+ cytotoxic cells. Furthermore, Hartmann et al. (86) studied on 97 epithelioid cell-rich lymphomas which include 17 LL and they showed that the most LL cases extremely express cytotoxic T cell markers and are different from other epithelioid cell-rich lymphomas. Therefore, cytotoxic t-cell markers might be used as diagnostic criteria for LL (75, 87, 94, 131, 132).

Inspired by the results obtained so far, we decided to expand our analysis to the miRNA signature of LL as compared to other PTCL/NOS. We could find some miRNAs differentiating the two, but again the number was limited, which once more made the similar nature of the two diseases standing out. The resulted miRNAs, furthermore, were capable of separating the two set of samples in a HCA. Of note, we have previously reported the usage of miRNAs profiling in classifying PTCL subtypes (108).

Next, we compared miRNA signature of LL with normal T-cells, with the intention of discovering the underlying pathological mechanism of LL. Compared to what observed in the case of LL vs. other PTCL/NOS, here we found a much higher number of differentially regulated miRNAs, which could be a result of comparison of tumor vs. normal cells, as compared to tumor vs. tumor in the previous case. Importantly, few of the miRNAs seemed to be overexpressed in LL, which corresponds to the previous reports regarding a global lowered expression of human miRNAs in the tumors (133, 134). Very interestingly, when a similar approach was carried out on the gene expression profiles of LL and normal T-cells, we found the major part of deregulated genes to have increased expression level in LL. This, would reflect the linkage between gene and miRNA expression, and suggest at least some of those genes might be direct or indirect targets of the downregulated miRNAs in LL. Again, the number of the differentially expressed genes was higher compared to LL vs. other PTCL/NOS, and the deregulated genes, as anticipated, were involved in relevant tumorigenesis processes, most notably microenvironment as well as neoplastic clone. Analysis of CD68 expression using IHC confirmed the validity of our results, and promoted the inflammation induced by tumor-associated macrophage as an underlying tumorigenesis mechanism in this cancer (135). Conversely, PDCD4 was identified for the first time as aberrantly expressed in LL cells (136) (Supplementary Figure 3).

Since our results of both miRNA and gene expression profiles of LL seemed to be correlated with its pathogenesis, we used them to create a functional network of correlated cell signaling pathways using IPA, which resulted in the discovery of PI3K/Akt/mTOR axis as the most relevant pathway. Although using an *in silico* approach, Martin-Sanchez et al. recognized this pathway to be activated in PTCL (137), this is for the first time that this hypothesis is suggested for LL.

Since by far we found molecular evidences supporting LL as a distinct entity, we tried to analyze the clinical data, as a complementary approach. We observed a significant difference of male:female ratio and B-symptoms in LL, as compared to other PTCL/NOS. Furthermore, although a trend of better treatment response and survival rate was found for LL in comparison with other PTCL/NOS, our results were not statistically significant. This might be due to the limited number of the patients analyzed by us, since Wiesenberger et al. reported a better overall survival in LL as compared to other PTCL/NOS (75).

As far as F-PTCL is concerned, the recent recognition of its relatedness to FTH-lymphocytes raised the hypothesis that it could represent an early stage of AITL; the prototype of TFH related lymphoma (138-140). Our data, however, seem to indicate that F-PTCL and AITL are quite distinct. In fact, GEP analysis showed that F-PTCL is possibly closer to other PTCLs/NOS rather than to AITL. The major limitation of this study, beside the limited number of F-PTCL cases included, is represented by the lack of genetic analysis. In fact, it should be acknowledged that recurrent genetic lesions have been recently recognized in AITL, including those affecting TET2, IDH2, and RHOA (41, 42, 68-71). Therefore, it would be definitely warranted to test them in F-PTCLs to assess a possible genetic similarity. Of interest, in this regard, the commonest lesion recorded in F-PTCL, the t(5;9) leading to ITK/SYK fusion gene, has been described in a unique case of AITL, thus confirming their diversity rather than a real similarity (98). However, only a comprehensive genomic profile will refine this information supporting one or the other hypothesis. Indeed, as the presence of some of the above mentioned mutations might be associated with a preferential sensitivity to some novel anti-lymphoma agents including demethylating ones, the comprehension of the genetic profile of the tumor would have relevant consequences not only for PTCL classification but also for future treatment selection.

In terms of classification, our data currently support the inclusion of F-PTCL in a broad category of FTH-related PTCLs, together with AITL, a fraction of PTCL/NOS and some cutaneous lymphomas. This concept will be probably sustained in the upcoming edition of the WHO classification that is expected to be released in late 2016 (38).

In conclusion, our study showed for the first time that 1) PTCL/NOS can be divided into subgroups corresponding to different cellular counterparts and characterized by different

genetic patterns and possibly sensitivity to specific therapeutic approaches; 2) Lennert lymphoma is distinct from other PTCLs/NOS based not only on morphology and clinical features but also on gene and miRNA expression, this finally supporting its recognition as distinct entity; 3) F-PTCL cannot be included among AITLs at least based on GEP, genetic studies being required for a more refined classification. Overall, these results may impact on PTCL classification as well as on future studies aimed to define the more appropriate therapeutic strategy for each identified subgroup/entity.

References

1. Koch U, Radtke F. Mechanisms of T cell development and transformation. *Annu Rev Cell Dev Biol.* 2011;27:539-62.
2. Gaulard P, de Leval L. Pathology of peripheral T-cell lymphomas: where do we stand? *Semin Hematol.* 2014 Jan;51(1):5-16.
3. Sallusto F, Geginat J, Lanzavecchia A. Central memory and effector memory T cell subsets: function, generation, and maintenance. *Annu Rev Immunol.* 2004;22:745-63.
4. Mueller SN, Gebhardt T, Carbone FR, Heath WR. Memory T cell subsets, migration patterns, and tissue residence. *Annu Rev Immunol.* 2013;31:137-61.
5. Sallusto F, Lenig D, Forster R, Lipp M, Lanzavecchia A. Two subsets of memory T lymphocytes with distinct homing potentials and effector functions. *Nature.* 1999 Oct 14;401(6754):708-12.
6. O'Shea JJ, Paul WE. Mechanisms underlying lineage commitment and plasticity of helper CD4+ T cells. *Science.* 2010 Feb 26;327(5969):1098-102.
7. Ray JP, Staron MM, Shyer JA, Ho PC, Marshall HD, Gray SM, et al. The Interleukin-2-mTORc1 Kinase Axis Defines the Signaling, Differentiation, and Metabolism of T Helper 1 and Follicular B Helper T Cells. *Immunity.* 2015 Oct 20;43(4):690-702.
8. Luckheeram RV, Zhou R, Verma AD, Xia B. CD4(+)T cells: differentiation and functions. *Clin Dev Immunol.* 2012;2012:925135.
9. Mowen KA, Glimcher LH. Signaling pathways in Th2 development. *Immunol Rev.* 2004 Dec;202:203-22.
10. Okoye IS, Wilson MS. CD4+ T helper 2 cells--microbial triggers, differentiation requirements and effector functions. *Immunology.* 2011 Dec;134(4):368-77.
11. Kaplan MH, Schindler U, Smiley ST, Grusby MJ. Stat6 is required for mediating responses to IL-4 and for development of Th2 cells. *Immunity.* 1996 Mar;4(3):313-9.
12. Takeda K, Tanaka T, Shi W, Matsumoto M, Minami M, Kashiwamura S, et al. Essential role of Stat6 in IL-4 signalling. *Nature.* 1996 Apr 18;380(6575):627-30.
13. Scheinman EJ, Avni O. Transcriptional regulation of GATA3 in T helper cells by the integrated activities of transcription factors downstream of the interleukin-4 receptor and T cell receptor. *J Biol Chem.* 2009 Jan 30;284(5):3037-48.
14. Korn T, Bettelli E, Oukka M, Kuchroo VK. IL-17 and Th17 Cells. *Annu Rev Immunol.* 2009;27:485-517.
15. Ciofani M, Madar A, Galan C, Sellars M, Mace K, Pauli F, et al. A validated regulatory network for Th17 cell specification. *Cell.* 2012 Oct 12;151(2):289-303.
16. Jonuleit H, Schmitt E, Stassen M, Tuettenberg A, Knop J, Enk AH. Identification and functional characterization of human CD4(+)CD25(+) T cells with regulatory properties isolated from peripheral blood. *J Exp Med.* 2001 Jun 4;193(11):1285-94.

17. Taylor PA, Noelle RJ, Blazar BR. CD4(+)CD25(+) immune regulatory cells are required for induction of tolerance to alloantigen via costimulatory blockade. *J Exp Med.* 2001 Jun 4;193(11):1311-8.
18. Hori S, Nomura T, Sakaguchi S. Control of regulatory T cell development by the transcription factor Foxp3. *Science.* 2003 Feb 14;299(5609):1057-61.
19. Fontenot JD, Gavin MA, Rudensky AY. Foxp3 programs the development and function of CD4+CD25+ regulatory T cells. *Nat Immunol.* 2003 Apr;4(4):330-6.
20. Chtanova T, Tangye SG, Newton R, Frank N, Hodge MR, Rolph MS, et al. T follicular helper cells express a distinctive transcriptional profile, reflecting their role as non-Th1/Th2 effector cells that provide help for B cells. *J Immunol.* 2004 Jul 1;173(1):68-78.
21. Schmitt N, Liu Y, Bentebibel SE, Munagala I, Bourdery L, Venuprasad K, et al. The cytokine TGF-beta co-opts signaling via STAT3-STAT4 to promote the differentiation of human TFH cells. *Nat Immunol.* 2014 Sep;15(9):856-65.
22. Kobayashi S, Watanabe T, Suzuki R, Furu M, Ito H, Ito J, et al. TGF-beta induces the differentiation of human CXCL13-producing CD4 T cells. *Eur J Immunol.* 2015 Nov 6.
23. Ma CS, Suryani S, Avery DT, Chan A, Nanan R, Santner-Nanan B, et al. Early commitment of naive human CD4(+) T cells to the T follicular helper (T(FH)) cell lineage is induced by IL-12. *Immunol Cell Biol.* 2009 Nov-Dec;87(8):590-600.
24. Rasheed AU, Rahn HP, Sallusto F, Lipp M, Muller G. Follicular B helper T cell activity is confined to CXCR5(hi)ICOS(hi) CD4 T cells and is independent of CD57 expression. *Eur J Immunol.* 2006 Jul;36(7):1892-903.
25. Breitfeld D, Ohl L, Kremmer E, Ellwart J, Sallusto F, Lipp M, et al. Follicular B helper T cells express CXC chemokine receptor 5, localize to B cell follicles, and support immunoglobulin production. *J Exp Med.* 2000 Dec 4;192(11):1545-52.
26. Schaerli P, Willimann K, Lang AB, Lipp M, Loetscher P, Moser B. CXC chemokine receptor 5 expression defines follicular homing T cells with B cell helper function. *J Exp Med.* 2000 Dec 4;192(11):1553-62.
27. Bentebibel SE, Schmitt N, Banchereau J, Ueno H. Human tonsil B-cell lymphoma 6 (BCL6)-expressing CD4+ T-cell subset specialized for B-cell help outside germinal centers. *Proc Natl Acad Sci U S A.* 2011 Aug 16;108(33):E488-97.
28. Peters PJ, Borst J, Oorschot V, Fukuda M, Krahenbuhl O, Tschopp J, et al. Cytotoxic T lymphocyte granules are secretory lysosomes, containing both perforin and granzymes. *J Exp Med.* 1991 May 1;173(5):1099-109.
29. Bolitho P, Voskoboinik I, Trapani JA, Smyth MJ. Apoptosis induced by the lymphocyte effector molecule perforin. *Curr Opin Immunol.* 2007 Jun;19(3):339-47.
30. Pearson PL, Van der Luijt RB. The genetic analysis of cancer. *J Intern Med.* 1998 Jun;243(6):413-7.

31. Jaffe ES, Nicolae A, Pittaluga S. Peripheral T-cell and NK-cell lymphomas in the WHO classification: pearls and pitfalls. *Mod Pathol.* 2013 Jan;26 Suppl 1:S71-87.
32. Rudiger T, Gascoyne RD, Jaffe ES, de Jong D, Delabie J, De Wolf-Peeters C, et al. Workshop on the relationship between nodular lymphocyte predominant Hodgkin's lymphoma and T cell/histiocytic-rich B cell lymphoma. *Ann Oncol.* 2002;13 Suppl 1:44-51.
33. Briski R, Feldman AL, Bailey NG, Lim MS, Ristow K, Habermann TM, et al. The role of front-line anthracycline-containing chemotherapy regimens in peripheral T-cell lymphomas. *Blood Cancer J.* 2014;4:e214.
34. Swerdlow S, Campo E, Harris N, al. e. *WHO Classification of Tumours of Haematopoietic and Lymphoid Tissues*. Geneva, Switzerland: WHO Press; 2008.
35. Jaffe ES. Pathobiology of peripheral T-cell lymphomas. *Hematology Am Soc Hematol Educ Program.* 2006:317-22.
36. Pileri SA, Piccaluga PP. New molecular insights into peripheral T cell lymphomas. *J Clin Invest.* 2012 Oct;122(10):3448-55.
37. Inghirami G, Chan WC, Pileri S. Peripheral T-cell and NK cell lymphoproliferative disorders: cell of origin, clinical and pathological implications. *Immunol Rev.* 2015 Jan;263(1):124-59.
38. Iqbal J, Wilcox R, Naushad H, Rohr J, Heavican TB, Wang C, et al. Genomic signatures in T-cell lymphoma: How can these improve precision in diagnosis and inform prognosis? *Blood Rev.* 2015 Aug 18.
39. Crescenzo R, Abate F, Lasorsa E, Tabbo F, Gaudiano M, Chiesa N, et al. Convergent mutations and kinase fusions lead to oncogenic STAT3 activation in anaplastic large cell lymphoma. *Cancer Cell.* 2015 Apr 13;27(4):516-32.
40. Iqbal J, Wright G, Wang C, Rosenwald A, Gascoyne RD, Weisenburger DD, et al. Gene expression signatures delineate biological and prognostic subgroups in peripheral T-cell lymphoma. *Blood.* 2014 May 8;123(19):2915-23.
41. Palomero T, Couronne L, Khiabanian H, Kim MY, Ambesi-Impiombato A, Perez-Garcia A, et al. Recurrent mutations in epigenetic regulators, RHOA and FYN kinase in peripheral T cell lymphomas. *Nat Genet.* 2014 Feb;46(2):166-70.
42. Sakata-Yanagimoto M, Enami T, Yoshida K, Shiraishi Y, Ishii R, Miyake Y, et al. Somatic RHOA mutation in angioimmunoblastic T cell lymphoma. *Nat Genet.* 2014 Feb;46(2):171-5.
43. Morris SW, Kirstein MN, Valentine MB, Dittmer KG, Shapiro DN, Saltman DL, et al. Fusion of a kinase gene, ALK, to a nucleolar protein gene, NPM, in non-Hodgkin's lymphoma. *Science.* 1994 Mar 4;263(5151):1281-4.
44. Mason DY, Bastard C, Rimokh R, Dastugue N, Huret JL, Kristoffersson U, et al. CD30-positive large cell lymphomas ('Ki-1 lymphoma') are associated with a chromosomal translocation involving 5q35. *Br J Haematol.* 1990 Feb;74(2):161-8.

45. Rimokh R, Magaud JP, Berger F, Samarut J, Coiffier B, Germain D, et al. A translocation involving a specific breakpoint (q35) on chromosome 5 is characteristic of anaplastic large cell lymphoma ('Ki-1 lymphoma'). *Br J Haematol.* 1989 Jan;71(1):31-6.
46. Iragavarapu C, Mustafa M, Akinleye A, Furqan M, Mittal V, Cang S, et al. Novel ALK inhibitors in clinical use and development. *J Hematol Oncol.* 2015;8:17.
47. Chiarle R, Voena C, Ambrogio C, Piva R, Inghirami G. The anaplastic lymphoma kinase in the pathogenesis of cancer. *Nat Rev Cancer.* 2008 Jan;8(1):11-23.
48. Piva R, Agnelli L, Pellegrino E, Todoerti K, Grosso V, Tamagno I, et al. Gene expression profiling uncovers molecular classifiers for the recognition of anaplastic large-cell lymphoma within peripheral T-cell neoplasms. *J Clin Oncol.* 2010 Mar 20;28(9):1583-90.
49. Weilemann A, Grau M, Erdmann T, Merkel O, Sobhiafshar U, Anagnostopoulos I, et al. Essential role of IRF4 and MYC signaling for survival of anaplastic large cell lymphoma. *Blood.* 2015 Jan 1;125(1):124-32.
50. Bonzheim I, Geissinger E, Roth S, Zettl A, Marx A, Rosenwald A, et al. Anaplastic large cell lymphomas lack the expression of T-cell receptor molecules or molecules of proximal T-cell receptor signaling. *Blood.* 2004 Nov 15;104(10):3358-60.
51. Lamant L, de Reynies A, Duplantier MM, Rickman DS, Sabourdy F, Giuriato S, et al. Gene-expression profiling of systemic anaplastic large-cell lymphoma reveals differences based on ALK status and two distinct morphologic ALK+ subtypes. *Blood.* 2007 Mar 1;109(5):2156-64.
52. Piccaluga PP, Fuligni F, De Leo A, Bertuzzi C, Rossi M, Bacci F, et al. Molecular profiling improves classification and prognostication of nodal peripheral T-cell lymphomas: results of a phase III diagnostic accuracy study. *J Clin Oncol.* 2013 Aug 20;31(24):3019-25.
53. Lim MS, Carlson ML, Crockett DK, Fillmore GC, Abbott DR, Elenitoba-Johnson OF, et al. The proteomic signature of NPM/ALK reveals deregulation of multiple cellular pathways. *Blood.* 2009 Aug 20;114(8):1585-95.
54. Chiarle R, Simmons WJ, Cai H, Dhall G, Zamo A, Raz R, et al. Stat3 is required for ALK-mediated lymphomagenesis and provides a possible therapeutic target. *Nat Med.* 2005 Jun;11(6):623-9.
55. Marzec M, Kasprzycka M, Liu X, El-Salem M, Halasa K, Raghunath PN, et al. Oncogenic tyrosine kinase NPM/ALK induces activation of the rapamycin-sensitive mTOR signaling pathway. *Oncogene.* 2007 Aug 16;26(38):5606-14.
56. Agnelli L, Mereu E, Pellegrino E, Limongi T, Kwee I, Bergaggio E, et al. Identification of a 3-gene model as a powerful diagnostic tool for the recognition of ALK-negative anaplastic large-cell lymphoma. *Blood.* 2012 Aug 9;120(6):1274-81.
57. Boi M, Rinaldi A, Kwee I, Bonetti P, Todaro M, Tabbo F, et al. PRDM1/BLIMP1 is commonly inactivated in anaplastic large T-cell lymphoma. *Blood.* 2013 Oct 10;122(15):2683-93.

58. Feldman AL, Dogan A, Smith DI, Law ME, Ansell SM, Johnson SH, et al. Discovery of recurrent t(6;7)(p25.3;q32.3) translocations in ALK-negative anaplastic large cell lymphomas by massively parallel genomic sequencing. *Blood*. 2011 Jan 20;117(3):915-9.
59. Vassatzis G, Johnson SH, Knudson RA, Ketterling RP, Braggio E, Fonseca R, et al. Genome-wide analysis reveals recurrent structural abnormalities of TP63 and other p53-related genes in peripheral T-cell lymphomas. *Blood*. 2012 Sep 13;120(11):2280-9.
60. de Leval L, Gisselbrecht C, Gaulard P. Advances in the understanding and management of angioimmunoblastic T-cell lymphoma. *Br J Haematol*. 2010 Mar;148(5):673-89.
61. Vose J, Armitage J, Weisenburger D. International peripheral T-cell and natural killer/T-cell lymphoma study: pathology findings and clinical outcomes. *J Clin Oncol*. 2008 Sep 1;26(25):4124-30.
62. Piccaluga PP, Agostinelli C, Califano A, Rossi M, Basso K, Zupo S, et al. Gene expression analysis of peripheral T cell lymphoma, unspecified, reveals distinct profiles and new potential therapeutic targets. *J Clin Invest*. 2007 Mar;117(3):823-34.
63. de Leval L, Rickman DS, Thielen C, Reynies A, Huang YL, Delsol G, et al. The gene expression profile of nodal peripheral T-cell lymphoma demonstrates a molecular link between angioimmunoblastic T-cell lymphoma (AITL) and follicular helper T (TFH) cells. *Blood*. 2007 Jun 1;109(11):4952-63.
64. Iqbal J, Weisenburger DD, Greiner TC, Vose JM, McKeithan T, Kucuk C, et al. Molecular signatures to improve diagnosis in peripheral T-cell lymphoma and prognostication in angioimmunoblastic T-cell lymphoma. *Blood*. 2010 Feb 4;115(5):1026-36.
65. Piccaluga PP, Agostinelli C, Califano A, Carbone A, Fantoni L, Ferrari S, et al. Gene expression analysis of angioimmunoblastic lymphoma indicates derivation from T follicular helper cells and vascular endothelial growth factor deregulation. *Cancer Res*. 2007 Nov 15;67(22):10703-10.
66. Grogg KL, Attygalle AD, Macon WR, Remstein ED, Kurtin PJ, Dogan A. Angioimmunoblastic T-cell lymphoma: a neoplasm of germinal-center T-helper cells? *Blood*. 2005 Aug 15;106(4):1501-2.
67. Zhao WL, Mourah S, Mounier N, Leboeuf C, Daneshpouy ME, Legres L, et al. Vascular endothelial growth factor-A is expressed both on lymphoma cells and endothelial cells in angioimmunoblastic T-cell lymphoma and related to lymphoma progression. *Lab Invest*. 2004 Nov;84(11):1512-9.
68. Cairns RA, Iqbal J, Lemonnier F, Kucuk C, de Leval L, Jais JP, et al. IDH2 mutations are frequent in angioimmunoblastic T-cell lymphoma. *Blood*. 2012 Feb 23;119(8):1901-3.
69. Odejide O, Weigert O, Lane AA, Toscano D, Lunning MA, Kopp N, et al. A targeted mutational landscape of angioimmunoblastic T-cell lymphoma. *Blood*. 2014 Feb 27;123(9):1293-6.

70. Couronne L, Bastard C, Bernard OA. TET2 and DNMT3A mutations in human T-cell lymphoma. *N Engl J Med.* 2012 Jan 5;366(1):95-6.
71. Wang C, McKeithan TW, Gong Q, Zhang W, Bouska A, Rosenwald A, et al. IDH2R172 mutations define a unique subgroup of patients with angioimmunoblastic T-cell lymphoma. *Blood.* 2015 Oct 8;126(15):1741-52.
72. Agostinelli C, Hartmann S, Klapper W, Korkolopoulou P, Righi S, Marafioti T, et al. Peripheral T cell lymphomas with follicular T helper phenotype: a new basket or a distinct entity? Revising Karl Lennert's personal archive. *Histopathology.* 2011 Oct;59(4):679-91.
73. Tang T, Tay K, Quek R, Tao M, Tan SY, Tan L, et al. Peripheral T-cell lymphoma: review and updates of current management strategies. *Adv Hematol.* 2010;2010:624040.
74. Rizvi MA, Evens AM, Tallman MS, Nelson BP, Rosen ST. T-cell non-Hodgkin lymphoma. *Blood.* 2006 Feb 15;107(4):1255-64.
75. Weisenburger DD, Savage KJ, Harris NL, Gascoyne RD, Jaffe ES, MacLennan KA, et al. Peripheral T-cell lymphoma, not otherwise specified: a report of 340 cases from the International Peripheral T-cell Lymphoma Project. *Blood.* 2011 Mar 24;117(12):3402-8.
76. Ballester B, Ramuz O, Gisselbrecht C, Doucet G, Loi L, Loriod B, et al. Gene expression profiling identifies molecular subgroups among nodal peripheral T-cell lymphomas. *Oncogene.* 2006 Mar 9;25(10):1560-70.
77. Tsuchiya T, Ohshima K, Karube K, Yamaguchi T, Suefuji H, Hamasaki M, et al. Th1, Th2, and activated T-cell marker and clinical prognosis in peripheral T-cell lymphoma, unspecified: comparison with AILD, ALCL, lymphoblastic lymphoma, and ATLL. *Blood.* 2004 Jan 1;103(1):236-41.
78. Went P, Agostinelli C, Gallamini A, Piccaluga PP, Ascani S, Sabattini E, et al. Marker expression in peripheral T-cell lymphoma: a proposed clinical-pathologic prognostic score. *J Clin Oncol.* 2006 Jun 1;24(16):2472-9.
79. Piccaluga PP, Agostinelli C, Tripodo C, Gazzola A, Bacci F, Sabattini E, et al. Peripheral T-cell lymphoma classification: the matter of cellular derivation. *Expert Rev Hematol.* 2011 Aug;4(4):415-25.
80. Lemonnier F, Couronne L, Parrens M, Jais JP, Travert M, Lamant L, et al. Recurrent TET2 mutations in peripheral T-cell lymphomas correlate with TFH-like features and adverse clinical parameters. *Blood.* 2012 Aug 16;120(7):1466-9.
81. Amsen D, Spilianakis CG, Flavell RA. How are T(H)1 and T(H)2 effector cells made? *Curr Opin Immunol.* 2009 Apr;21(2):153-60.
82. Wang T, Feldman AL, Wada DA, Lu Y, Polk A, Briski R, et al. GATA-3 expression identifies a high-risk subset of PTCL, NOS with distinct molecular and clinical features. *Blood.* 2014 May 8;123(19):3007-15.
83. Lennert K, Mestdagh J. [Hodgkin's disease with constantly high content of epithelioid cells]. *Virchows Arch A Pathol Pathol Anat.* 1968;344(1):1-20.

84. Lennert K, Stein H, Kaiserling E. Cytological and functional criteria for the classification of malignant lymphomata. *Br J Cancer Suppl.* 1975 Mar;2:29-43.
85. Geissinger E, Odenwald T, Lee SS, Bonzheim I, Roth S, Reimer P, et al. Nodal peripheral T-cell lymphomas and, in particular, their lymphoepithelioid (Lennert's) variant are often derived from CD8(+) cytotoxic T-cells. *Virchows Arch.* 2004 Oct;445(4):334-43.
86. Hartmann S, Agostinelli C, Klapper W, Korkolopoulou P, Koch K, Marafioti T, et al. Revising the historical collection of epithelioid cell-rich lymphomas of the Kiel Lymph Node Registry: what is Lennert's lymphoma nowadays? *Histopathology.* 2011 Dec;59(6):1173-82.
87. Parimal S, Pai R, Manipadam MT, Nair S. Lennert's lymphoma: clinicopathological profile of five cases. *Indian J Pathol Microbiol.* 2013 Jul-Sep;56(3):248-51.
88. Rudiger T, Weisenburger DD, Anderson JR, Armitage JO, Diebold J, MacLennan KA, et al. Peripheral T-cell lymphoma (excluding anaplastic large-cell lymphoma): results from the Non-Hodgkin's Lymphoma Classification Project. *Ann Oncol.* 2002 Jan;13(1):140-9.
89. Kojima H, Hasegawa Y, Suzukawa K, Mukai HY, Kaneko S, Kobayashi T, et al. Clinicopathological features and prognostic factors of Japanese patients with "peripheral T-cell lymphoma, unspecified" diagnosed according to the WHO classification. *Leuk Res.* 2004 Dec;28(12):1287-92.
90. Gallamini A, Stelitano C, Calvi R, Bellei M, Mattei D, Vitolo U, et al. Peripheral T-cell lymphoma unspecified (PTCL-U): a new prognostic model from a retrospective multicentric clinical study. *Blood.* 2004 Apr 1;103(7):2474-9.
91. Ascani S, Zinzani PL, Gherlinzoni F, Sabattini E, Briskomatis A, de Vivo A, et al. Peripheral T-cell lymphomas. Clinico-pathologic study of 168 cases diagnosed according to the R.E.A.L. Classification. *Ann Oncol.* 1997 Jun;8(6):583-92.
92. Rysenga E, Linden MD, Carey JL, Ross CW, Schnitzer B, Sawdyk M, et al. Peripheral T-cell non-Hodgkin's lymphoma following treatment of nodular lymphocyte predominance Hodgkin's disease. *Arch Pathol Lab Med.* 1995 Jan;119(1):88-91.
93. Suchi T, Lennert K, Tu LY, Kikuchi M, Sato E, Stansfeld AG, et al. Histopathology and immunohistochemistry of peripheral T cell lymphomas: a proposal for their classification. *J Clin Pathol.* 1987 Sep;40(9):995-1015.
94. Summers TA, Jr., Rush W, Aguilera N, Lupton G. Cutaneous involvement in the lymphoepithelioid variant of peripheral T-cell lymphoma, unspecified (Lennert lymphoma). Report of a case and review of the literature. *J Cutan Pathol.* 2009 Oct;36 Suppl 1:25-30.
95. Rodriguez-Pinilla SM, Atienza L, Murillo C, Perez-Rodriguez A, Montes-Moreno S, Roncador G, et al. Peripheral T-cell lymphoma with follicular T-cell markers. *Am J Surg Pathol.* 2008 Dec;32(12):1787-99.
96. Huang Y, Moreau A, Dupuis J, Streubel B, Petit B, Le Gouill S, et al. Peripheral T-cell lymphomas with a follicular growth pattern are derived from follicular helper T cells (TFH) and may show overlapping features with angioimmunoblastic T-cell lymphomas. *Am J Surg Pathol.* 2009 May;33(5):682-90.

97. de Leval L, Savilo E, Longtine J, Ferry JA, Harris NL. Peripheral T-cell lymphoma with follicular involvement and a CD4+/bcl-6+ phenotype. *Am J Surg Pathol*. 2001 Mar;25(3):395-400.
98. Attygalle AD, Feldman AL, Dogan A. ITK/SYK translocation in angioimmunoblastic T-cell lymphoma. *Am J Surg Pathol*. 2013 Sep;37(9):1456-7.
99. Federico M, Rudiger T, Bellei M, Nathwani BN, Luminari S, Coiffier B, et al. Clinicopathologic characteristics of angioimmunoblastic T-cell lymphoma: analysis of the international peripheral T-cell lymphoma project. *J Clin Oncol*. 2013 Jan 10;31(2):240-6.
100. Delas A, Gaulard P, Plat G, Brousset P, Laurent C. Follicular variant of peripheral T cell lymphoma with mediastinal involvement in a child: a case report. *Virchows Arch*. 2015 Mar;466(3):351-5.
101. Feldman AL, Sun DX, Law ME, Novak AJ, Attygalle AD, Thorland EC, et al. Overexpression of Syk tyrosine kinase in peripheral T-cell lymphomas. *Leukemia*. 2008 Jun;22(6):1139-43.
102. Moroch J, Copie-Bergman C, de Leval L, Plonquet A, Martin-Garcia N, Delfau-Larue MH, et al. Follicular peripheral T-cell lymphoma expands the spectrum of classical Hodgkin lymphoma mimics. *Am J Surg Pathol*. 2012 Nov;36(11):1636-46.
103. Bacon CM, Paterson JC, Liu H, Payne K, Munson P, Du MQ, et al. Peripheral T-cell lymphoma with a follicular growth pattern: derivation from follicular helper T cells and relationship to angioimmunoblastic T-cell lymphoma. *Br J Haematol*. 2008 Nov;143(3):439-41.
104. Piccaluga PP, Agostinelli C, Zinzani PL, Baccarani M, Dalla Favera R, Pileri SA. Expression of platelet-derived growth factor receptor alpha in peripheral T-cell lymphoma not otherwise specified. *Lancet Oncol*. 2005 Jun;6(6):440.
105. Chtanova T, Newton R, Liu SM, Weininger L, Young TR, Silva DG, et al. Identification of T cell-restricted genes, and signatures for different T cell responses, using a comprehensive collection of microarray datasets. *J Immunol*. 2005 Dec 15;175(12):7837-47.
106. Piccaluga PP, Navari M, De Falco G, Ambrosio MR, Lazzi S, Fuligni F, et al. Virus-encoded microRNA contributes to the molecular profile of EBV-positive Burkitt lymphomas. *Oncotarget*. 2016 Jan 5;7(1):224-40.
107. Navari M, Etebari M, De Falco G, Ambrosio MR, Gibellini D, Leoncini L, et al. The presence of Epstein-Barr virus significantly impacts the transcriptional profile in immunodeficiency-associated Burkitt lymphoma. *Front Microbiol*. 2015;6:556.
108. Laginestra MA, Piccaluga PP, Fuligni F, Rossi M, Agostinelli C, Righi S, et al. Pathogenetic and diagnostic significance of microRNA deregulation in peripheral T-cell lymphoma not otherwise specified. *Blood Cancer J*. 2014;4:259.
109. Piccaluga PP, Califano A, Klein U, Agostinelli C, Bellosillo B, Gimeno E, et al. Gene expression analysis provides a potential rationale for revising the histological grading of follicular lymphomas. *Haematologica*. 2008 Jul;93(7):1033-8.

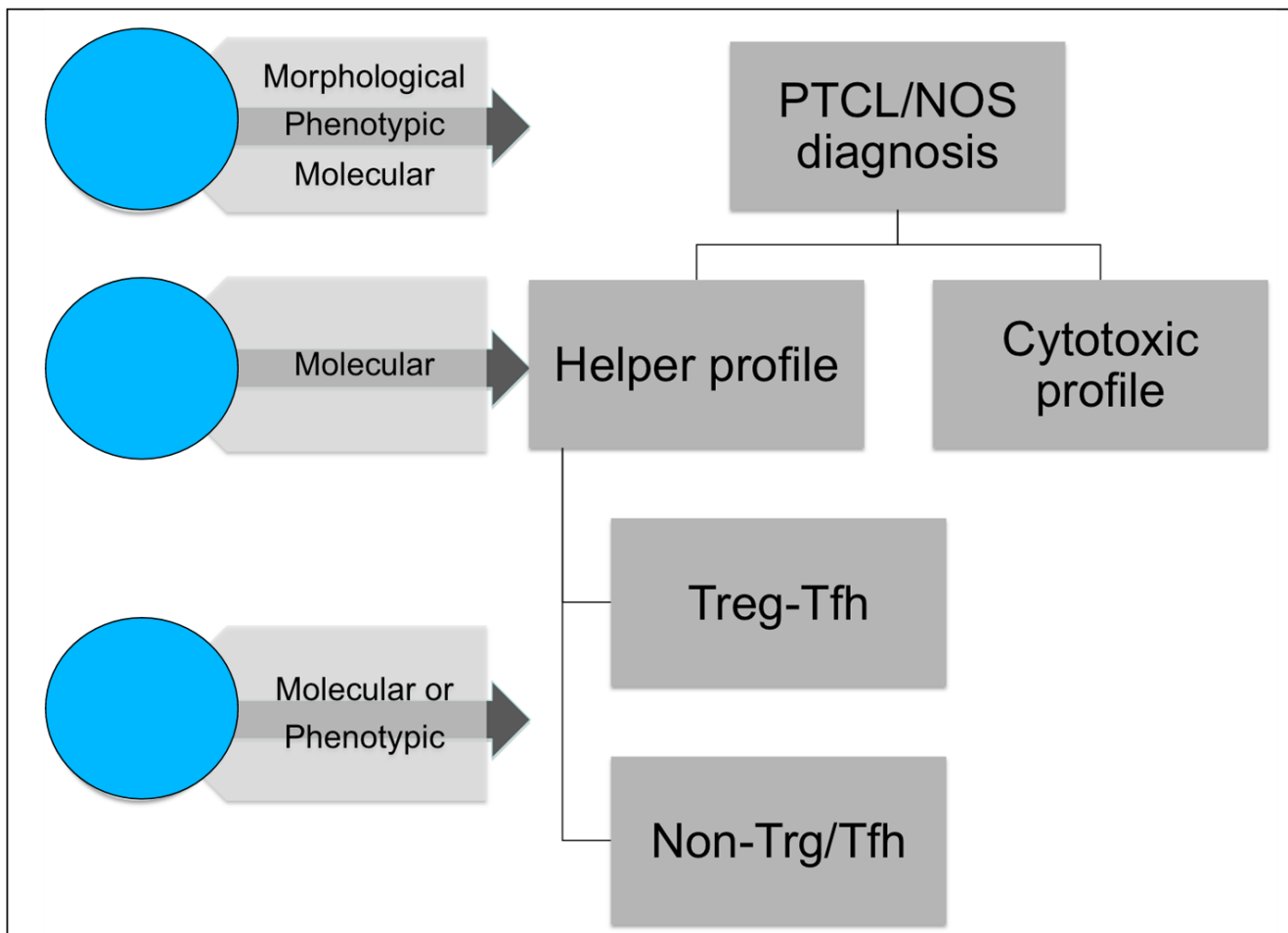
110. Piccaluga PP, De Falco G, Kustagi M, Gazzola A, Agostinelli C, Tripodo C, et al. Gene expression analysis uncovers similarity and differences among Burkitt lymphoma subtypes. *Blood*. 2011 Mar 31;117(13):3596-608.
111. Subramanian A, Tamayo P, Mootha VK, Mukherjee S, Ebert BL, Gillette MA, et al. Gene set enrichment analysis: a knowledge-based approach for interpreting genome-wide expression profiles. *Proc Natl Acad Sci U S A*. 2005 Oct 25;102(43):15545-50.
112. Mootha VK, Lindgren CM, Eriksson KF, Subramanian A, Sihag S, Lehar J, et al. PGC-1alpha-responsive genes involved in oxidative phosphorylation are coordinately downregulated in human diabetes. *Nat Genet*. 2003 Jul;34(3):267-73.
113. Ohshima K, Karube K, Kawano R, Tsuchiya T, Suefuji H, Yamaguchi T, et al. Classification of distinct subtypes of peripheral T-cell lymphoma unspecified, identified by chemokine and chemokine receptor expression: Analysis of prognosis. *Int J Oncol*. 2004 Sep;25(3):605-13.
114. Edgar R, Domrachev M, Lash AE. Gene Expression Omnibus: NCBI gene expression and hybridization array data repository. *Nucleic Acids Res*. 2002 Jan 1;30(1):207-10.
115. Li H, Durbin R. Fast and accurate short read alignment with Burrows-Wheeler transform. *Bioinformatics*. 2009 Jul 15;25(14):1754-60.
116. Li H, Handsaker B, Wysoker A, Fennell T, Ruan J, Homer N, et al. The Sequence Alignment/Map format and SAMtools. *Bioinformatics*. 2009 Aug 15;25(16):2078-9.
117. McKenna N, Hanna M, Banks E, Sivachenko A, Cibulskis K, Kernytsky A, et al. The Genome Analysis Toolkit: a MapReduce framework for analyzing next-generation DNA sequencing data. *Genome Res*. 2010 Sep;20(9):1297-303.
118. Piccaluga PP, Rossi M, Agostinelli C, Ricci F, Gazzola A, Righi S, et al. Platelet-derived growth factor alpha mediates the proliferation of peripheral T-cell lymphoma cells via an autocrine regulatory pathway. *Leukemia*. 2014 Aug;28(8):1687-97.
119. A map of human genome variation from population-scale sequencing. *Nature*. [10.1038/nature09534]. 2010;467(7319):1061-73.
120. Robinson JT, Thorvaldsdottir H, Winckler W, Guttman M, Lander ES, Getz G, et al. Integrative genomics viewer. *Nat Biotechnol*. 2011 Jan;29(1):24-6.
121. Bubendorf L, Nocito A, Moch H, Sauter G. Tissue microarray (TMA) technology: miniaturized pathology archives for high-throughput *in situ* studies. *J Pathol*. 2001 Sep;195(1):72-9.
122. Agostinelli C, Sabattini E, Gjorret JO, Righi S, Rossi M, Mancini M, et al. Characterization of a new monoclonal antibody against PAX5/BASP in 1525 paraffin-embedded human and animal tissue samples. *Appl Immunohistochem Mol Morphol*. 2010 Dec;18(6):561-72.

123. Hans CP, Weisenburger DD, Greiner TC, Gascoyne RD, Delabie J, Ott G, et al. Confirmation of the molecular classification of diffuse large B-cell lymphoma by immunohistochemistry using a tissue microarray. *Blood*. 2004 Jan 1;103(1):275-82.
124. Kaplan EL, Meier P. Nonparametric Estimation from Incomplete Observations. *Journal of the American Statistical Association*. 1958;53(282):457-81.
125. Amsen D, Antov A, Jankovic D, Sher A, Radtke F, Souabni A, et al. Direct regulation of Gata3 expression determines the T helper differentiation potential of Notch. *Immunity*. 2007 Jul;27(1):89-99.
126. Fang TC, Yashiro-Ohtani Y, Del Bianco C, Knoblock DM, Blacklow SC, Pear WS. Notch directly regulates Gata3 expression during T helper 2 cell differentiation. *Immunity*. 2007 Jul;27(1):100-10.
127. Wang Y, Huang G, Zeng H, Chi H. Metabolic control of dendritic cell development and function (P4490). *The Journal of Immunology*. 2013;190(Meeting Abstracts 1):52.62.
128. Tripodo C, Gri G, Piccaluga PP, Frossi B, Guarnotta C, Piconese S, et al. Mast cells and Th17 cells contribute to the lymphoma-associated pro-inflammatory microenvironment of angioimmunoblastic T-cell lymphoma. *Am J Pathol*. 2010 Aug;177(2):792-802.
129. Streubel B, Vinatzer U, Willheim M, Raderer M, Chott A. Novel t(5;9)(q33;q22) fuses ITK to SYK in unspecified peripheral T-cell lymphoma. *Leukemia*. 2006 Feb;20(2):313-8.
130. Yoo HY, Sung MK, Lee SH, Kim S, Lee H, Park S, et al. A recurrent inactivating mutation in RHOA GTPase in angioimmunoblastic T cell lymphoma. *Nat Genet*. 2014 Apr;46(4):371-5.
131. Norval EJ, Raubenheimer EJ. Second malignancies in Hodgkin's disease: A review of the literature and report of a case with a secondary Lennert's lymphoma. *J Oral Maxillofac Pathol*. 2014 Sep;18(Suppl 1):S90-5.
132. Kapoor A, Beniwal S, Purohit R, Kumar V, Kumar HS. Lennert's lymphoma-a diagnostic dilemma: a case report and pathologic review of literature. *International Journal*. 2015;2(1):47.
133. Gaur A, Jewell DA, Liang Y, Ridzon D, Moore JH, Chen C, et al. Characterization of microRNA expression levels and their biological correlates in human cancer cell lines. *Cancer Res*. 2007 Mar 15;67(6):2456-68.
134. Lu J, Getz G, Miska EA, Alvarez-Saavedra E, Lamb J, Peck D, et al. MicroRNA expression profiles classify human cancers. *Nature*. 2005 Jun 9;435(7043):834-8.
135. Greaves P, Clear A, Coutinho R, Wilson A, Matthews J, Owen A, et al. Expression of FOXP3, CD68, and CD20 at diagnosis in the microenvironment of classical Hodgkin lymphoma is predictive of outcome. *J Clin Oncol*. 2013 Jan 10;31(2):256-62.
136. Yamanaka Y, Tagawa H, Takahashi N, Watanabe A, Guo YM, Iwamoto K, et al. Aberrant overexpression of microRNAs activate AKT signaling via down-regulation of tumor suppressors in natural killer-cell lymphoma/leukemia. *Blood*. 2009 Oct 8;114(15):3265-75.

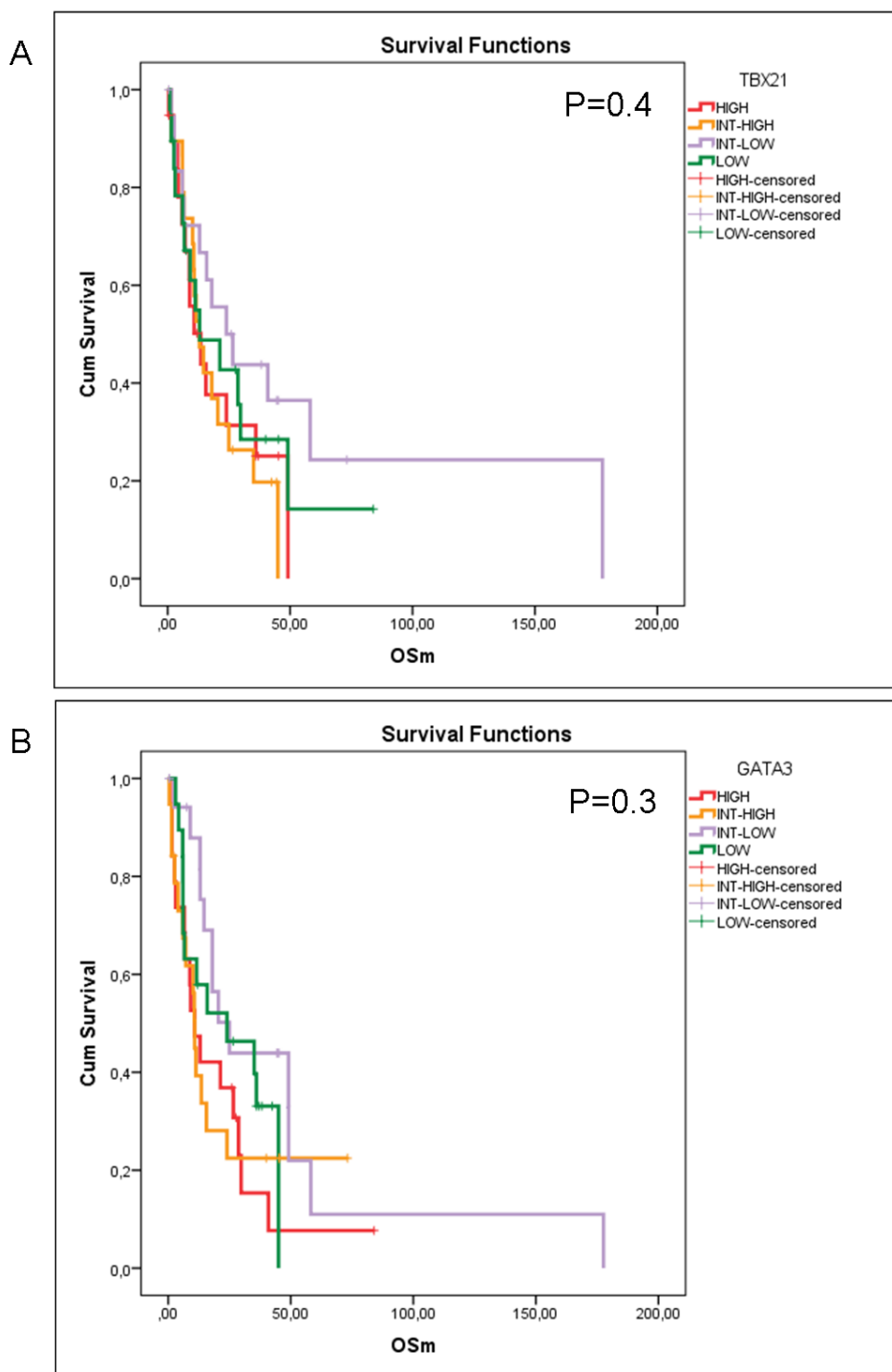
137. Martin-Sanchez E, Rodriguez-Pinilla SM, Sanchez-Beato M, Lombardia L, Dominguez-Gonzalez B, Romero D, et al. Simultaneous inhibition of pan-phosphatidylinositol-3-kinases and MEK as a potential therapeutic strategy in peripheral T-cell lymphomas. *Haematologica*. 2013 Jan;98(1):57-64.
138. Pileri SA. Follicular helper T-cell-related lymphomas. *Blood*. 2015 Oct 8;126(15):1733-4.
139. Gaulard P, de Leval L. The microenvironment in T-cell lymphomas: emerging themes. *Semin Cancer Biol*. 2014 Feb;24:49-60.
140. Miyoshi H, Sato K, Niino D, Arakawa F, Kimura Y, Kiyasu J, et al. Clinicopathologic analysis of peripheral T-cell lymphoma, follicular variant, and comparison with angioimmunoblastic T-cell lymphoma: Bcl-6 expression might affect progression between these disorders. *Am J Clin Pathol*. 2012 Jun;137(6):879-89.

Appendix

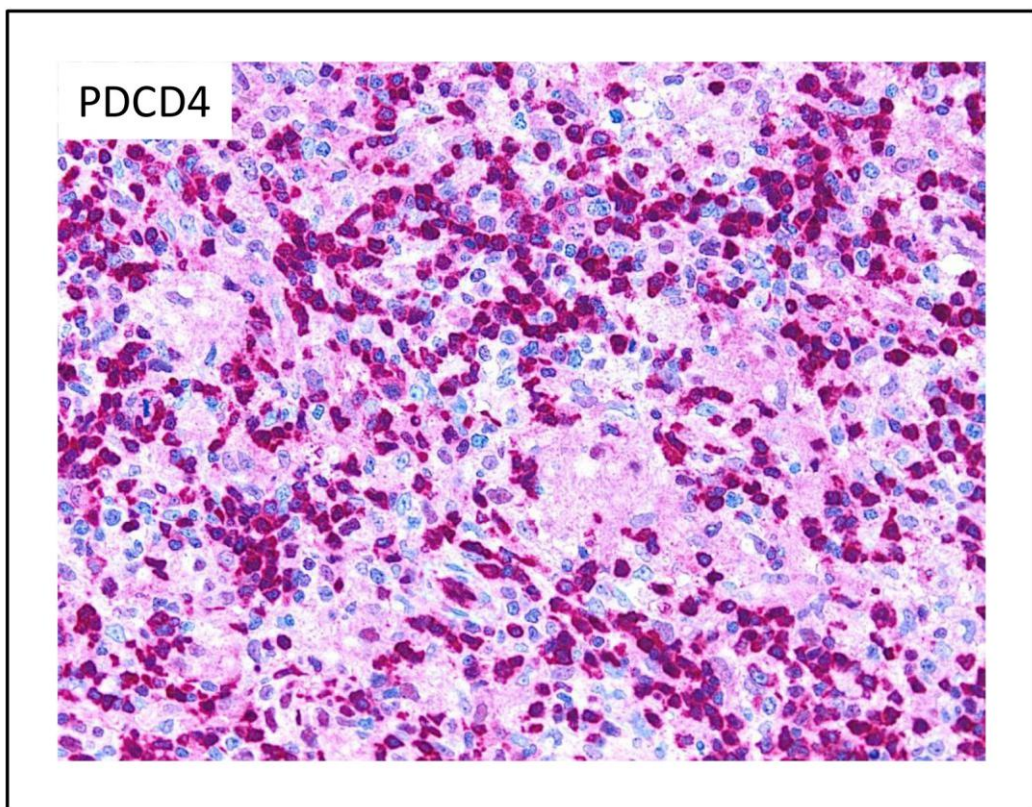
(Supplementary Material)



Supplementary Figure 1. The combination of molecular techniques and conventional immunophenotyping may enable an integrated diagnostic algorithm limiting the costs of extensive molecular analyses.



Supplementary Figure 2. The expression of single master transcription factors (TBX1 and GATA3) was not sufficient to reiterate the entire classification and was not confirmed to be enough to discriminate different clinical subgroups



Supplementary Figure 3. Immunostaining of PDCD4 in Lennert Lymphoma samples shows aberrant positivity.

Supplementary Table 1. Gene signatures representative of normal T-cell subsets

Cell type	Probe ID	Gene Symbol
Tcm	202440_s_at	<i>ST5</i>
	202478_at	<i>TRIB2</i>
	203386_at	<i>TBC1D4</i>
	203387_s_at	<i>TBC1D4</i>
	203413_at	<i>NELL2</i>
	204067_at	<i>SUOX</i>
	204563_at	<i>SELL</i>
	204777_s_at	<i>MAL</i>
	205210_at	<i>TGFBRAP1</i>
	205544_s_at	<i>CR2</i>
	205666_at	<i>FMO1</i>
	205945_at	<i>IL6R</i>
	205977_s_at	<i>EPHA1</i>
	206110_at	
	206126_at	<i>CXCR5</i>
	206150_at	<i>CD27</i>
	206337_at	<i>CCR7</i>
	206828_at	<i>TXK</i>
	208636_at	<i>ACTN1</i>
	210268_at	<i>NFX1</i>
	210711_at	<i>C1orf217</i>
	210715_s_at	<i>SPINT2</i>
	211160_x_at	<i>ACTN1</i>
	211300_s_at	<i>TP53</i>
	212442_s_at	<i>LASS6</i>
	212561_at	<i>DENND5A</i>
	213534_s_at	<i>PASK</i>
	213652_at	<i>PCSK5</i>
	215198_s_at	<i>CALD1</i>
	215949_x_at	<i>IGHM /// LOC652494</i>
	216682_s_at	<i>FAM48A</i>
	216945_x_at	<i>PASK</i>
	217489_s_at	<i>IL6R</i>
	217594_at	<i>ZCCHC11</i>
	218678_at	<i>NES</i>
	218793_s_at	<i>SCML1</i>
	220454_s_at	<i>SEMA6A</i>
	220581_at	<i>C6orf97</i>
	220636_at	<i>DNAI2</i>
	221042_s_at	<i>CLMN</i>
	221266_s_at	<i>TM7SF4</i>
	221558_s_at	<i>LEF1</i>
	221747_at	<i>TNS1</i>
	45714_at	<i>HCFC1R1</i>
Tem	200897_s_at	<i>PALLD</i>
	200907_s_at	<i>PALLD</i>
	200931_s_at	<i>VCL</i>
	201105_at	<i>LGALS1</i>
	201137_s_at	<i>HLA-DPB1</i>
	201301_s_at	<i>ANXA4</i>
	201487_at	<i>CTSC</i>
	201590_x_at	<i>ANXA2</i>
	202192_s_at	<i>GAS7</i>
	202458_at	<i>PRSS23</i>
	203186_s_at	<i>S100A4</i>
	203470_s_at	<i>PLEK</i>
	204103_at	<i>CCL4</i>
	204205_at	<i>APOBEC3G</i>
	204266_s_at	<i>CHKA</i>
	204655_at	<i>CCL5</i>
	204731_at	<i>TGFBR3</i>
	204896_s_at	<i>PTGER4</i>
	205425_at	<i>HIP1</i>

	205488_at	GZMA
	205495_s_at	GNLY
	205639_at	AOAH
	205663_at	PCBP3
	205786_s_at	ITGAM
	205821_at	KLRK1
	205870_at	BDKRB2
	205898_at	CX3CR1
	206267_s_at	MATK
	206589_at	GFI1
	206999_at	IL12RB2
	207072_at	IL18RAP
	207173_x_at	CDH11
	207861_at	CCL22
	208306_x_at	
	208438_s_at	FGR
	208456_s_at	RRAS2
	208523_x_at	HIST1H2BI
	208868_s_at	GABARAPL1
	208937_s_at	ID1
	209160_at	AKR1C3
	210140_at	CST7
	210164_at	GZMB
	210288_at	KLRG1
	210321_at	GZMH
	210660_at	LILRA1
	210764_s_at	CYR61
	210982_s_at	HLA-DRA
	211110_s_at	AR
	211144_x_at	TARP /// TRGC2
	211469_s_at	CXCR6
	211597_s_at	HOPX
	211748_x_at	PTGDS
	212070_at	GPR56
	212509_s_at	MXRA7
	212671_s_at	HLA-DQA1 /// HLA-DQA2
	213524_s_at	GOS2
	213737_x_at	GOLGA9P
	213915_at	NKG7
	214326_x_at	JUND
	214450_at	CTSW
	214470_at	KLRB1
	214567_s_at	XCL1 /// XCL2
	214591_at	KLHL4
	214617_at	PRF1
	215806_x_at	TARP /// TRGC2
	216915_s_at	PTPN12
	216920_s_at	TARP /// TRGC2
	217078_s_at	CD300A
	217395_at	MT4
	218272_at	TTC38
	219142_at	RASL11B
	219159_s_at	SLAMF7
	219197_s_at	SCUBE2
	219402_s_at	DERL1
	219978_s_at	NUSAP1
	37145_at	GNLY
Th	201506_at	TGFBI
	205336_at	PVALB
	213975_s_at	LYZ
	219666_at	MS4A6A
	39402_at	IL1B
	223280_x_at	MS4A6A
	226694_at	AKAP2 /// PALM2 /// PALM2-AKAP2
Tc	1405_i_at	CCL5
	201160_s_at	CSDA
	201161_s_at	CSDA
	202196_s_at	DKK3

	202806_at	DBN1
	203413_at	NELL2
	204011_at	SPRY2
	204655_at	CCL5
	205495_s_at	GNLY
	205758_at	CD8A
	205821_at	KLRK1
	206118_at	STAT4
	206267_s_at	MATK
	206365_at	XCL1
	206366_x_at	XCL1
	206666_at	GZMK
	206785_s_at	KLRC1 /// KLRC2
	206914_at	CRTAM
	207001_x_at	TSC22D3
	207314_x_at	KIR3DL2 /// LOC727787
	207723_s_at	KLRC3
	207795_s_at	KLRD1
	207840_at	CD160
	207979_s_at	CD8B
	208982_at	PECAM1
	208983_s_at	PECAM1
	209813_x_at	TARP
	209993_at	ABCB1
	210140_at	CST7
	210354_at	IFNG
	210606_x_at	KLRD1
	210690_at	KLRC4
	211144_x_at	TARP /// TRGC2
	212240_s_at	PIK3R1
	213385_at	CHN2
	213915_at	NKG7
	214247_s_at	DKK3
	214450_at	CTSW
	214567_s_at	XCL1 /// XCL2
	214660_at	PELO
	215806_x_at	TARP /// TRGC2
	215894_at	PTGDR
	216191_s_at	TRA@ /// TRD@
	216676_x_at	KIR3DL3
	216920_s_at	TARP /// TRGC2
	219013_at	GALNT11
	219033_at	PARP8
	220307_at	CD244
	220646_s_at	KLRF1
	221127_s_at	DKK3
	36711_at	MAFF
	37145_at	GNLY
	225496_s_at	SYTL2
	226731_at	PELO
	229309_at	ADRB1
	230508_at	DKK3
	231093_at	FCRL3
	231776_at	EOMES
	236782_at	SAMD3
	242385_at	RORB
	1555691_a_at	KLRK1
	1555759_a_at	CCL5
	1555938_x_at	VIM
TH1	1405_i_at	CCL5
	200748_s_at	FTH1
	200887_s_at	STAT1
	200923_at	LGALS3BP /// LOC100133842
	200983_x_at	CD59
	200984_s_at	CD59
	200985_s_at	CD59
	201124_at	ITGB5
	201125_s_at	ITGB5

	201392_s_at	<i>IGF2R</i>
	201393_s_at	<i>IGF2R</i>
	201489_at	<i>PPIF</i>
	201490_s_at	<i>PPIF</i>
	201502_s_at	<i>NFKBIA</i>
	201525_at	<i>APOD</i>
	201641_at	<i>BST2</i>
	202086_at	<i>MX1</i>
	202191_s_at	<i>GAS7</i>
	202192_s_at	<i>GAS7</i>
	202269_x_at	<i>GBP1</i>
	202270_at	<i>GBP1</i>
	202307_s_at	<i>TAP1</i>
	202403_s_at	<i>COL1A2</i>
	202404_s_at	<i>COL1A2</i>
	202430_s_at	<i>PLSCR1</i>
	202446_s_at	<i>PLSCR1</i>
	202855_s_at	<i>SLC16A3</i>
	202856_s_at	<i>SLC16A3</i>
	202859_x_at	<i>IL8</i>
	202869_at	<i>OAS1</i>
	203044_at	<i>CHSY1</i>
	203131_at	<i>PDGFRA</i>
	203167_at	<i>TIMP2</i>
	203290_at	<i>HLA-DQA1</i>
	203535_at	<i>S100A9</i>
	203562_at	<i>FEZ1</i>
	203595_s_at	<i>IFIT5</i>
	203596_s_at	<i>IFIT5</i>
	203620_s_at	<i>FCHSD2</i>
	203708_at	<i>PDE4B</i>
	203716_s_at	<i>DPP4</i>
	203717_at	<i>DPP4</i>
	203747_at	<i>AQP3</i>
	203973_s_at	<i>CEBDP</i>
	204103_at	<i>CCL4</i>
	204205_at	<i>APOBEC3G</i>
	204224_s_at	<i>GCH1</i>
	204655_at	<i>CCL5</i>
	204720_s_at	<i>DNAJC6</i>
	204721_s_at	<i>DNAJC6</i>
	204972_at	<i>OAS2</i>
	205027_s_at	<i>MAP3K8</i>
	205098_at	<i>CCR1</i>
	205099_s_at	<i>CCR1</i>
	205114_s_at	<i>CCL3</i> /// <i>CCL3L1</i> /// <i>CCL3L3</i> /// <i>LOC728830</i>
	205396_at	<i>SMAD3</i>
	205397_x_at	<i>SMAD3</i>
	205398_s_at	<i>SMAD3</i>
	205404_at	<i>HSD11B1</i>
	205495_s_at	<i>GNLY</i>
	205552_s_at	<i>OAS1</i>
	205660_at	<i>OASL</i>
	205798_at	<i>IL7R</i>
	205801_s_at	<i>RASGRP3</i>
	205872_x_at	<i>PDE4DIP</i>
	205936_s_at	<i>HK3</i>
	205973_at	<i>FEZ1</i>
	205992_s_at	<i>IL15</i>
	206155_at	<i>ABCC2</i>
	206553_at	<i>OAS2</i>
	206666_at	<i>GZMK</i>
	206806_at	<i>DGKI</i>
	206975_at	<i>LTA</i>
	206999_at	<i>IL12RB2</i>
	207113_s_at	<i>TNF</i>
	207313_x_at	<i>KIR3DL2</i> /// <i>LOC727787</i>
	207314_x_at	<i>KIR3DL1</i> /// <i>LOC727787</i>

	207334_s_at	TGFBR2
	207616_s_at	TANK
	207691_x_at	ENTPD1
	207704_s_at	GAS7
	208200_at	IL1A
	208309_s_at	MALT1
	208426_x_at	KIR2DL4
	208436_s_at	IRF7
	208944_at	TGFBR2
	208999_at	SEPT8
	209000_s_at	SEPT8
	209182_s_at	C10orf10
	209183_s_at	C10orf10
	209369_at	ANXA3
	209374_s_at	IGHM
	209392_at	ENPP2
	209451_at	TANK
	209457_at	DUSP5
	209473_at	ENTPD1
	209474_s_at	ENTPD1
	209514_s_at	RAB27A
	209515_s_at	RAB27A
	209676_at	TFPI
	209700_x_at	PDE4DIP
	209969_s_at	STAT1
	210017_at	MALT1
	210018_x_at	MALT1
	210094_s_at	PARD3
	210118_s_at	IL1A
	210228_at	CSF2
	210229_s_at	CSF2
	210305_at	PDE4DIP
	210354_at	IFNG
	210426_x_at	RORA
	210448_s_at	P2RX5
	210458_s_at	TANK
	210479_s_at	RORA
	210495_x_at	FN1
	210664_s_at	TFPI
	210665_at	TFPI
	210797_s_at	OASL
	210839_s_at	ENPP2
	210845_s_at	PLAUR
	210872_x_at	GAS7
	210874_s_at	NAT6
	210951_x_at	RAB27A
	211067_s_at	GAS7
	211242_x_at	KIR2DL4
	211245_x_at	KIR2DL4
	211302_s_at	PDE4B
	211430_s_at	IGH@///IGHG1///IGHG2///IGHM///IGHV4-31
	211478_s_at	DPP4
	211506_s_at	IL8
	211533_at	PDGFRA
	211632_at	IGHD///IGHM///LOC652128///VSIG6
	211634_x_at	IGHM///LOC100133862
	211635_x_at	IGH@///IGHA1///IGHA2///IGHG1///IGHG3///IGHM///IGHV10R15-5///IGHV4-31///IGHV7-81///LOC642131
	211636_at	IGH@///IGHA1///IGHA2///IGHG1///IGHM///LOC100126583///LOC652128///VSIG6
	211637_x_at	IGH@///IGHA1///IGHA2///IGHD///IGHG1///IGHG3///IGHG4///IGHM///IGHV3-23///IGHV4-31///LOC100126583///LOC642131///LOC652128///VSIG6
	211638_at	IGH@///IGHA1///IGHA2///IGHD///IGHG1///IGHG3///IGHG4///IGHM///IGHV4-31///LOC100126583///LOC652128///VSIG6
	211639_x_at	IGH@///IGHA1///IGHA2///IGHD///IGHG1///IGHG3///IGHG4///IGHM///IGHV4-31///LOC100126583///LOC642131///LOC652128///VSIG6
	211640_x_at	IGHA1///IGHG1///LOC100133862
	211641_x_at	IGH@///IGHA1///IGHA2///IGHG1///IGHG3///IGHM///IGHV3-23///IGHV4-31
	211646_at	IGH@///IGHA1///IGHG1///IGHG2///IGHG3///IGHM///LOC100126583///LOC652494

	211647_x_at	IGHA1 /// IGHG1 /// LOC100133862
	211648_at	IGHA1 /// IGHG1 /// LOC100133862
	211649_x_at	IGH@///IGHA1///IGHA2///IGHG1///IGHM///LOC642131
	211650_x_at	IGHA1 /// IGHG1 /// IGHG3 /// IGHM /// IGHV3-23 /// IGHV4-31 /// LOC100126583
	211685_s_at	NCALD
	211688_x_at	KIR3DL2 /// LOC727787
	211719_x_at	FN1
	211751_at	PDE4DIP
	211868_x_at	IGH@///IGHA1///IGHG1///IGHG3///IGHM///IGHV3-23///IGHV4-31
	211924_s_at	PLAUR
	212262_at	QKI
	212263_at	QKI
	212265_at	QKI
	212390_at	LOC727893 /// PDE4DIP
	212392_s_at	LOC652526 /// PDE4DIP
	212463_at	CD59
	212464_s_at	FN1
	212501_at	CEBPB
	212599_at	AUTS2
	212614_at	ARID5B
	212636_at	QKI
	212671_s_at	HLA-DQA1 /// HLA-DQA2
	212827_at	IGHM
	212841_s_at	PPFIBP2
	212970_at	APBB2
	212972_x_at	APBB2
	212985_at	APBB2
	213003_s_at	CEBD
	213006_at	CEBD
	213258_at	TFPI
	213388_at	PDE4DIP
	213419_at	APBB2
	213522_s_at	SLC16A3
	213524_s_at	GOS2
	213716_s_at	SECTM1
	213831_at	HLA-DQA1
	214020_x_at	ITGB5
	214021_x_at	ITGB5
	214059_at	IFI44
	214099_s_at	PDE4DIP
	214129_at	PDE4DIP
	214130_s_at	PDE4DIP
	214211_at	FTH1
	214378_at	TFPI
	214453_s_at	IFI44
	214541_s_at	QKI
	214543_x_at	QKI
	214617_at	PRF1
	214701_s_at	FN1
	214702_at	FN1
	214844_s_at	DOK5
	214866_at	PLAUR
	214916_x_at	IGH@///IGHA1///IGHA2///IGHD///IGHG1///IGHG2///IGHG3///IGHM///IGHV3-23///IGHV4-31 ///LOC100126583
	214995_s_at	APOBEC3F /// APOBEC3G
	215305_at	PDGFRA
	215575_at	PDE4DIP
	215579_at	APOBEC3G
	215671_at	PDE4B
	215949_x_at	IGHM /// LOC652494
	215959_at	
	216442_x_at	FN1
	216491_x_at	IGHM
	216510_x_at	IGHA1 /// IGHG1 /// IGHM /// IGHV3-23 /// IGHV4-31
	216541_x_at	IGHA1 /// IGHG1 /// LOC100133862
	216542_x_at	IGHA1 /// IGHG1 /// IGHV3-23
	216557_x_at	IGH@///IGHA1///IGHG1///IGHG3///IGHM///IGHV3-23///IGHV4-31
	216558_x_at	IGHA1 /// IGHG1 /// IGHG2 /// IGHG3 /// IGHM /// IGHV4-31 /// LOC652494

	216747_at	APBB2
	216750_at	APBB2
	216907_x_at	KIR3DL2 /// LOC727787
	217084_at	IGHA1 /// IGHG1 /// IGHM /// IGHV3-23 /// IGHV4-31
	217169_at	IGHA1
	217217_at	IGH@ /// IGH@1 /// IGH@2 /// IGH@D /// IGHG1 /// IGHG3 /// IGHG4 /// IGHM /// IGHV4-31 /// LOC100126583 /// LOC642131 /// LOC652128 /// VSIG6
	217236_x_at	IGH@ /// IGH@1 /// IGH@2 /// IGH@D /// IGHG1 /// IGHG3 /// IGHG4 /// IGHM /// IGHV4-31 /// LOC100126583 /// LOC642131 /// LOC652128 /// VSIG6
	217281_x_at	IGH@ /// IGH@1 /// IGH@2 /// IGHG1 /// IGHG2 /// IGHG3 /// IGHM /// IGHV4-31 /// LOC100126583 /// LOC652494
	217360_x_at	IGHA1 /// IGHG1 /// IGHG3 /// IGHM /// LOC652494
	217371_s_at	IL15
	217685_at	SLC16A3
	217691_x_at	SLC16A3
	217933_s_at	LAP3
	218284_at	SMAD3
	218400_at	OAS3
	218888_s_at	NETO2
	218964_at	ARID3B
	219102_at	RCN3
	219159_s_at	SLAMF7
	219211_at	USP18
	219454_at	EGFL6
	219656_at	PCDH12
	219716_at	APOL6
	220684_at	TBX21
	220941_s_at	C21orf91
	221271_at	IL21
	221280_s_at	PARD3
	221526_x_at	PARD3
	221527_s_at	PARD3
	37145_at	GNLY
	39248_at	AQP3
	39249_at	AQP3
	40148_at	APBB2
	61734_at	RCN3
	222774_s_at	NETO2
	222838_at	SLAMF7
	224560_at	TIMP2
	226109_at	C21orf91
	226218_at	IL7R
	226627_at	SEPT8
	226682_at	RORA
	228518_at	IGH@ /// IGHG1 /// IGHM
	228540_at	QKI
	228585_at	ENTPD1
	228607_at	OAS2
	228748_at	CD59
	229218_at	COL1A2
	231577_s_at	GBP1
	231578_at	GBP1
	231579_s_at	TIMP2
	232509_at	PDE4DIP
	232666_at	OAS3
	234306_s_at	SLAMF7
	234419_x_at	IGH@ /// IGH@1 /// IGH@D /// IGHG1 /// IGHG3 /// IGHM /// IGHV3-23 /// IGHV4-31
	235404_at	ARID5B
	235421_at	MAP3K8
	235567_at	RORA
	236154_at	QKI
	236203_at	HLA-DQA1
	236266_at	RORA
	239550_at	RORA
	240163_at	RORA
	240951_at	RORA
	241760_x_at	RORA
	241869_at	APOL6

	241938_at	<i>QKI</i>
	241969_at	<i>ARID5B</i>
	243111_at	
	243364_at	<i>AUTS2</i>
	243365_s_at	<i>AUTS2</i>
	244315_at	<i>PLSCR1</i>
	244526_at	<i>RASGRP3</i>
	1553681_a_at	<i>PRF1</i>
	1554360_at	<i>FCHSD2</i>
	1554828_at	<i>PDGFRA</i>
	1554863_s_at	<i>DOK5</i>
	1555154_a_at	<i>QKI</i>
	1555759_a_at	<i>CCL5</i>
	1557116_at	<i>APOL6</i>
	1557236_at	<i>APOL6</i>
	1558000_at	<i>ARID5B</i>
	1558001_s_at	<i>ARID5B</i>
	1558199_at	<i>FN1</i>
	1562682_at	<i>RORA</i>
	1562790_at	<i>NCALD</i>
TH2	200715_x_at	<i>RPL13A</i>
TH2	200716_x_at	<i>RPL13A</i>
TH2	200878_at	<i>EPAS1</i>
TH2	200879_s_at	<i>EPAS1</i>
TH2	201309_x_at	<i>C5orf13</i>
TH2	201310_s_at	<i>C5orf13</i>
TH2	201416_at	<i>SOX4</i>
TH2	201417_at	<i>SOX4</i>
TH2	201418_s_at	<i>SOX4</i>
TH2	201438_at	<i>COL6A3</i>
TH2	201642_at	<i>IFNGR2</i>
TH2	201693_s_at	<i>EGR1</i>
TH2	201694_s_at	<i>EGR1</i>
TH2	202718_at	<i>IGFBP2</i>
TH2	202741_at	<i>PRKACB</i>
TH2	202742_s_at	<i>PRKACB</i>
TH2	202769_at	<i>CCNG2</i>
TH2	202770_s_at	<i>CCNG2</i>
TH2	203075_at	<i>SMAD2</i>
TH2	203076_s_at	<i>SMAD2</i>
TH2	203077_s_at	<i>SMAD2</i>
TH2	203139_at	<i>DAPK1</i>
TH2	203608_at	<i>ALDH5A1</i>
TH2	203609_s_at	<i>ALDH5A1</i>
TH2	203675_at	<i>NUCB2</i>
TH2	204032_at	<i>BCAR3</i>
TH2	204041_at	<i>MAOB</i>
TH2	204179_at	<i>MB</i>
TH2	204388_s_at	<i>MAOA</i>
TH2	204389_at	<i>MAOA</i>
TH2	204612_at	<i>PKIA</i>
TH2	204748_at	<i>PTGS2</i>
TH2	204753_s_at	<i>HLF</i>
TH2	204754_at	<i>HLF</i>
TH2	204755_x_at	<i>HLF</i>
TH2	205249_at	<i>EGR2</i>
TH2	205376_at	<i>INPP4B</i>
TH2	205389_s_at	<i>ANK1</i>
TH2	205390_s_at	<i>ANK1</i>
TH2	205391_x_at	<i>ANK1</i>
TH2	205639_at	<i>AOAH</i>
TH2	205668_at	<i>LY75</i>
TH2	206035_at	<i>REL</i>
TH2	206036_s_at	<i>REL</i>
TH2	206115_at	<i>EGR3</i>
TH2	206275_s_at	<i>MICAL2</i>
TH2	206527_at	<i>ABAT</i>
TH2	206809_s_at	<i>HNRNPA3 // HNRNPA3P1</i>

206914_at	CRTAM
206942_s_at	PMCH
206974_at	CXCR6
207087_x_at	ANK1
207907_at	TNFSF14
208129_x_at	RUNX1
208131_s_at	PTGIS
208164_s_at	IL9R /// IL9RP3
208193_at	IL9
208352_x_at	ANK1
208353_x_at	ANK1
208605_s_at	NTRK1
208768_x_at	RPL22
208891_at	DUSP6
208892_s_at	DUSP6
208893_s_at	DUSP6
209359_x_at	RUNX1
209360_s_at	RUNX1
209459_s_at	ABAT
209460_at	ABAT
209602_s_at	GATA3
209603_at	GATA3
209604_s_at	GATA3
210145_at	PLA2G4A
210279_at	GPR18
210365_at	RUNX1
210517_s_at	AKAP12
210646_x_at	RPL13A
210702_s_at	PTGIS
210715_s_at	SPINT2
210805_x_at	RUNX1
211179_at	RUNX1
211180_x_at	RUNX1
211181_x_at	RUNX1
211182_x_at	RUNX1
211214_s_at	DAPK1
211469_s_at	CXCR6
211559_s_at	CCNG2
211620_x_at	RUNX1 /// SH3D19
211892_s_at	PTGIS
211929_at	HNRNPA3
211930_at	HNRNPA3
211931_s_at	HNRNPA3 /// HNRNPA3P1
211932_at	HNRNPA3
211933_s_at	HNRNPA3 /// HNRNPA3P1
211942_x_at	RPL13A /// RPL13AP25 /// RPL13AP5 /// RPL13AP6
212085_at	SLC25A6
212110_at	SLC39A14
212472_at	MICAL2
212473_s_at	MICAL2
212741_at	MAOA
212790_x_at	RPL13A
212826_s_at	SLC25A6
213665_at	SOX4
213668_s_at	SOX4
214042_s_at	RPL22
217080_s_at	HOMER2
217123_x_at	PMCHL1
217212_s_at	IL9R /// IL9RP3
217263_x_at	RUNX1
218313_s_at	GALNT7
219255_x_at	IL17RB
219683_at	FZD3
220212_s_at	THADA
220365_at	ALLC
220418_at	UBASH3A
220841_s_at	AHI1
220842_at	AHI1

	220960_x_at	RPL22
	221111_at	IL26
	221328_at	CLDN17
	221569_at	AHI1
	221726_at	RPL22
	221775_x_at	RPL22
	54632_at	THADA
	222587_s_at	GALNT7
	223878_at	INPP4B
	224156_x_at	IL17RB
	224361_s_at	IL17RB
	224418_x_at	PMCHL1
	224419_x_at	PMCHL1
	224421_x_at	PMCHL1
	226563_at	SMAD2
	226864_at	PKIA
	227404_s_at	EGR1
	227499_at	
	227524_at	
	227529_s_at	AKAP12
	227530_at	AKAP12
	228081_at	CCNG2
	229838_at	NUCB2
	230424_at	C5orf13
	231067_s_at	
	232461_at	AHI1
	235598_at	SMAD2
	235780_at	PRKACB
	236475_at	MICAL2
	238411_x_at	C5orf13
	239271_at	SMAD2
	240363_at	ANK1
	241055_at	EPAS1
	244699_at	AHI1
	1554492_at	THADA
	1554493_s_at	THADA
	1554997_a_at	PTGS2
	1555056_at	CCNG2
	1555395_at	AKAP12
	1555433_at	SLC39A14
	1555434_a_at	SLC39A14
	1555653_at	HNRNPA3
	1558306_at	THADA
	1561009_at	MAOB
	1561010_a_at	MAOB
	1566889_at	THADA
	1567906_at	SOX4
TH17	204562_at	IRF4
	205067_at	IL1B
	205965_at	BATF
	206419_at	RORC
	208129_x_at	RUNX1
	208402_at	IL17A
	208991_at	STAT3
	208992_s_at	STAT3
	209359_x_at	RUNX1
	209360_s_at	RUNX1
	210365_at	RUNX1
	210426_x_at	RORA
	210479_s_at	RORA
	210805_x_at	RUNX1
	211179_at	RUNX1
	211180_x_at	RUNX1
	211181_x_at	RUNX1
	211182_x_at	RUNX1
	211620_x_at	RUNX1 /// SH3D19
	214470_at	KLRB1
	216857_at	

	216876_s_at	<i>IL17A</i>
	216986_s_at	<i>IRF4</i>
	216987_at	<i>IRF4</i>
	217263_x_at	<i>RUNX1</i>
	217326_x_at	<i>TRBC1</i> /// <i>TRBC2</i> /// <i>TRBV7-4</i> /// <i>TRBV7-6</i> /// <i>TRBV7-7</i> /// <i>TRBV7-8</i>
	220054_at	<i>IL23A</i>
	221165_s_at	<i>IL22</i>
	221271_at	<i>IL21</i>
	39402_at	<i>IL1B</i>
	222974_at	<i>IL22</i>
	223217_s_at	<i>NFKBIZ</i>
	223218_s_at	<i>NFKBIZ</i>
	225289_at	<i>STAT3</i>
	226682_at	<i>RORA</i>
	228806_at	<i>RORC</i>
	234408_at	<i>IL17F</i>
	235567_at	<i>RORA</i>
	236266_at	<i>RORA</i>
	239550_at	<i>RORA</i>
	240163_at	<i>RORA</i>
	240951_at	<i>RORA</i>
	241760_x_at	<i>RORA</i>
	243213_at	<i>STAT3</i>
	1562682_at	<i>RORA</i>
Treg	203084_at	<i>TGFB1</i>
	203085_s_at	<i>TGFB1</i>
	203939_at	<i>NTSE</i>
	205291_at	<i>IL2RB</i>
	206341_at	<i>IL2RA</i>
	206486_at	<i>LAG3</i>
	207433_at	<i>IL10</i>
	207691_x_at	<i>ENTPD1</i>
	208023_at	<i>TNFRSF4</i>
	209473_at	<i>ENTPD1</i>
	209474_s_at	<i>ENTPD1</i>
	210439_at	<i>ICOS</i>
	211269_s_at	<i>IL2RA</i>
	214228_x_at	<i>TNFRSF4</i>
	221331_x_at	<i>CTLA4</i>
	221333_at	<i>FOXP3</i>
	221334_s_at	<i>FOXP3</i>
	224211_at	<i>FOXP3</i>
	227486_at	<i>NTSE</i>
	228585_at	<i>ENTPD1</i>
	229354_at	<i>AHRR</i>
	231794_at	<i>CTLA4</i>
	234362_s_at	<i>CTLA4</i>
	234895_at	<i>CTLA4</i>
	236341_at	<i>CTLA4</i>
	243111_at	
	1553994_at	<i>NTSE</i>
	1553995_a_at	<i>NTSE</i>
Tfh	203639_s_at	<i>FGFR2</i>
	204002_s_at	<i>ICA1</i>
	204995_at	<i>CDK5R1</i>
	204996_s_at	<i>CDK5R1</i>
	205242_at	<i>CXCL13</i>
	205945_at	<i>IL6R</i>
	206126_at	<i>BLR1</i>
	207607_at	<i>ASCL2</i>
	207949_s_at	<i>ICA1</i>
	208189_s_at	<i>MYO7A</i>
	208225_at	<i>FGFR2</i>
	208228_s_at	<i>FGFR2</i>
	208229_at	<i>FGFR2</i>
	208234_x_at	<i>FGFR2</i>
	209160_at	<i>AKR1C3</i>
	209189_at	<i>FOS</i>

	210055_at	<i>TSHR</i>
	210073_at	<i>SIAT8A</i>
	210547_x_at	<i>ICA1</i>
	211103_at	<i>MYO7A</i>
	211104_s_at	<i>MYO7A</i>
	211398_at	<i>FGFR2</i>
	211399_at	<i>FGFR2</i>
	211400_at	<i>FGFR2</i>
	211401_s_at	<i>FGFR2</i>
	211740_at	<i>ICA1</i>
	214191_at	<i>ICA1</i>
	215442_s_at	<i>TSHR</i>
	215443_at	<i>TSHR</i>
	216734_s_at	<i>BLR1</i>
	217489_s_at	<i>IL6R</i>
	218559_s_at	<i>MAFB</i>
	218839_at	<i>HEY1</i>
	222670_s_at	<i>MAFB</i>
	226333_at	<i>IL6R</i>
	229215_at	<i>ASCL2</i>
	230378_at	<i>SCGB3A1</i>
	230842_at	<i>FGFR2</i>
	237349_at	<i>TSHR</i>
	240913_at	<i>FGFR2</i>
	33197_at	<i>MYO7A</i>
	44783_s_at	<i>HEY1</i>

Supplementary Table 2. Molecular classification of PTCLs according to their correspondence to the different counterparts

Identifier	T-helper vs. T-cytotoxic		Tem vs. Tcm		TH1 vs. TH2 vs. TH17 vs. Treg vs. TFH	
	Prediction	Confidence Measure	Prediction	Confidence Measure	Prediction	Confidence Measure
GSM472034	CD4	0.05483767	TEM	0.5397353	TH1	0.22225842
GSM472035	CD4	0.8792574	TCM	0.43320644	TH2	0.20155877
GSM472036	CD4	0.92096376	TCM	0.39508796	TH2	0.24746904
GSM472037	CD4	0.16107923	TEM	0.47575614	TH1	0.05058226
GSM472041	CD4	0.18602279	NC	0.007362604	TH17	0.64963453
GSM472042	CD4	0.22059606	NC	0.037550926	TH17	0.74263566
GSM472044	CD4	0.32339743	NC	0.046786785	TH2	0.092894405
GSM472045	CD8	0.24375308	TEM	0.62550867	TH1	0.1050137
GSM472046	CD4	0.4934061	TCM	0.2388232	TFH	0.64894566
GSM472048	CD8	0.053890225	TEM	0.64435995	TH2	0.108162545
GSM472051	CD4	0.5314873	TCM	0.23975971	NC	0.02408194
GSM472052	CD4	0.32253292	NC	0.01305475	TH2	0.081010215
GSM472053	CD4	0.14957592	TEM	0.1767476	TH1	0.18692046
GSM472055	CD4	0.32781687	TCM	0.14525402	TH2	0.12380959
GSM472057	CD4	0.3055477	TEM	0.26023036	TH1	0.18063259
GSM472060	CD4	0.6237464	TCM	0.09437314	TH1	0.05671855
GSM472061	CD4	1	TCM	0.093601584	TH2	0.19806242
GSM472067	CD8	0.31454957	TEM	0.5730862	NC	0.002197931
GSM472068	CD4	0.8921284	NC	0.045115566	TH2	0.13576272
GSM472069	CD8	0.42570004	TEM	0.40469006	TH1	0.1950911
GSM472070	CD4	0.4507805	TEM	0.15644054	TH1	0.08173423
GSM472071	CD4	0.3802928	TEM	0.22600344	TH1	0.15021868
GSM472072	CD4	0.89513415	TCM	0.38177902	TH2	0.23805884
GSM472073	CD4	0.38029218	TCM	0.26621363	TH2	0.098294474
GSM472078	CD4	0.8012558	NC	0.028153956	TH2	0.17126118
GSM472087	CD4	0.71471405	TCM	0.29026657	NC	0.038981684
GSM472088	CD4	0.78601414	NC	0.036012568	TH2	0.27195293
GSM472090	CD8	0.66783565	TEM	0.8560791	TH1	0.39705765
GSM472091	CD8	0.66949964	TEM	0.8472239	TH1	0.3944276
GSM472092	CD4	0.19665727	TEM	0.07922295	TH17	0.72848392
GSM472093	CD4	0.25312403	TEM	0.11955827	TFH	0.22324567
GSM472094	CD4	0.3007129	TEM	0.12920836	TH1	0.08821334
GSM472095	CD4	0.75019044	TCM	0.38723052	TH2	0.06832034
GSM472097	CD4	0.91148233	TCM	0.29818636	TH2	0.106093585
GSM472098	CD4	0.9095245	TCM	0.33320656	TH2	0.17650221
GSM472100	CD4	0.9380916	TCM	0.23010881	TH2	0.54802024
GSM472101	CD4	0.6088621	TCM	0.16218323	TH2	0.32242948
GSM472102	CD8	0.90215635	TEM	1	TH1	0.2035213
GSM472106	CD4	0.81567633	TCM	0.17600505	TH2	0.37949967

GSM472109	CD4	0.31734893	TEM	0.1280496	TH1	0.0695476
GSM472128	CD4	0.7677358	TCM	0.2256378	TH2	0.647312
GSM472129	CD4	0.597095	TEM	0.14994349	NC	4.48E-04
GSM472133	CD4	0.54355496	NC	0.002528623	TH2	0.21704476
GSM472146	CD4	0.096931174	TCM	0.18343353	TH2	0.13977978
GSM472148	CD8	0.69063264	TEM	0.5687444	TH2	0.10587785
GSM472149	CD4	0.7057298	TEM	0.21633327	TH2	0.058564898
GSM472155	CD4	0.40983316	TCM	0.22943091	TREG	0.495486584
GSM472156	CD4	0.19678819	TEM	0.18853916	TH1	0.15605317
GSM472157	CD4	0.36318445	TEM	0.22466786	NC	0.047692917
PTCL_021	CD4	0.31689897	TEM	0.06063488	TH1	0.077397525
PTCL_025	CD4	0.5982696	TCM	0.17823666	TH2	0.08225937
PTCL_026	CD4	0.43547502	TCM	0.06707667	NC	0.019214673
PTCL_027	CD4	0.62213516	TCM	0.43253648	TH2	0.13232735
PTCL_028	CD4	0.60790086	TCM	0.28131053	TH2	0.07729836
PTCL_AV_019	CD4	0.31722522	TCM	0.29094213	TH2	0.1298176
PTCL_AV_020	CD4	0.11305948	TEM	0.33042276	TH1	0.16004606
PTCL_AV_022	CD4	0.6636183	TCM	0.2853693	NC	0.015093046
PTCL_AV_023	CD4	0.78092754	TCM	0.33951902	NC	0.038951445
PTCL_AV_024	CD4	0.5475377	TCM	0.46628696	TH2	0.20561633
PTCL_AV_029	CD4	0.7794126	TCM	0.31514302	TFH	0.48642345
PTCL_BO_01	CD8	0.40744558	TEM	0.6591986	TH1	0.17789663
PTCL_BO_013	NC	0.048709106	TEM	0.45440286	TH1	0.0533007
PTCL_BO_012	CD8	0.5987399	TCM	0.1048778	TH1	0.21674937
PTCL_BO_02	CD4	0.5083611	TEM	0.110364504	NC	0.033066668
PTCL_BO_03	CD8	0.14107165	TEM	0.5281591	TH1	0.106095314
PTCL_BO_04	CD4	0.35076547	TCM	0.13343695	TH2	0.09655729
PTCL_BO_05	CD4	0.7929655	NC	0.024722062	TH2	0.10501019
PTCL_BO_06	CD4	0.64544487	TCM	0.11693561	TH2	0.10596316
PTCL_BO_08	CD4	0.5823569	TCM	0.07019313	TFH	0.45756786
PTCL_BO_09	CD8	0.087207325	TEM	0.43265566	TH1	0.25613612
PTCL_BO_10	CD8	0.67040133	TEM	0.59567535	NC	0.044250138
PTCL_BO_11	NC	0.02855229	NC	0.019826481	NC	0.035181366
PTCL_PG_14	CD4	0.059059896	TEM	0.27745417	TH1	0.16193448
PTCL_PG_15	CD4	0.32255587	TEM	0.0872888	TH1	0.08911885
PTCL_PG_16	CD4	0.60982984	TCM	0.27298284	TREG	0.69023434
PTCL_PG_17	CD4	0.17219996	TEM	0.32021385	TH1	0.2364545
PTCL_PG_18	CD4	0.2693943	TEM	0.5092342	TH1	0.23905414

Supplementary Table 3. Minimal gene sets identified by linear discriminant analysis

Classification step	Minimal gene set
TH vs. TC	<i>DBN1</i>
	<i>NELL2</i>
	<i>CRTAM</i>
	<i>KLRD1</i>
	<i>EOMES</i>
TCM vs. TEM	<i>GAS7</i>
	<i>SELL</i>
	<i>MAL</i>
	<i>PTGER4</i>
	<i>TGFBRAP1</i>
	<i>AOAH</i>
	<i>EPHA1</i>
	<i>ACTN1</i>
	<i>AKR1C3</i>
	<i>GZMB</i>
	<i>NFX1</i>
	<i>SPINT2</i>
	<i>ACTN1</i>
	<i>MXRA7</i>
	<i>NKG7</i>
	<i>KLHL4</i>
	<i>NUSAP1</i>
TH1 vs. TH2 vs. TH17 vs. TFH vs. Treg	<i>CD59</i>
	<i>IL8</i>
	<i>DPP4</i>
	<i>MAOA</i>
	<i>CCL5</i>
	<i>RASGRP3</i>
	<i>GZMK</i>
	<i>SEPT8</i>
	<i>DPP4</i>
	<i>CD59</i>
	<i>CTLA4</i>
	<i>IL17A</i>
	<i>IL17F</i>
	<i>CDK5R1</i>
	<i>CXCL13</i>
	<i>FGFR2</i>
	<i>AKR1C3</i>
	<i>ST8SIA1</i>
	<i>ICA1</i>
	<i>IL6R</i>
	<i>HEY1</i>
	<i>FGFR2</i>

Supplementary Table 4. Molecular classification of PTCLs according to their correspondence to the different counterparts (test set, according to the discriminant functions based on minimal gene sets)

Sample ID	Classification steps														
	Th vs. Tc	%Th	%Tc	Predicted subtype	Tem vs. Tcm	%Tem	%Tcm	Predicted subtype	Th1 vs. Th2 vs. Th17 vs. Treg vs. TfH	%Th1	%Th2	%TfH	%Th17	%Treg	Predicted subtype
GSM472034	CD4	72.90	27.10	CD4	TEM	100	0	TEM	TH1	100					TH1
GSM472035	CD4	100	0	CD4	TCM	0	100	TCM	TH2		100				TH2
GSM472036	CD4	100	0	CD4	TCM	0	100	TCM	TH2		100				TH2
GSM472037	CD4	87.31	12.69	CD4	TEM	89.20	10.80	TEM	TH1		95.32				TH2
GSM472041	CD4	39.91	60.09	CD8	NC	47.10	52.90	NC	TH17			100			TH17
GSM472042	CD4	51.01	48.99	NC	NC	44.13	55.87	NC	TH17			94.59			TH17
GSM472044	CD4	76.53	23.47	CD4	NC	33.29	66.71	TCM	TH2		63.03				TH2
GSM472045	CD8	100	0	CD4	TEM	100	0	TEM							
GSM472046	CD4	91.74	8.26	CD4	TCM	0	100	TCM	TFH			100			TFH
GSM472048	CD8	38.71	61.29	CD8	TEM	73.88	26.12	TEM							
GSM472051	CD4	96.31	3.69	CD4	TCM	30.06	69.94	TCM		NC		73.94			TH2
GSM472052	CD4	79.19	20.81	CD4	NC	0	100	TCM	TH2			81.75			TH2
GSM472053	CD4	55.57	44.43	NC	TEM	54.15	45.85	NC	TH1		68.15				TH1
GSM472055	CD4	99.57	0.43	CD4	TCM	21.05	78.95	TCM	TH2			79.35			TH2
GSM472057	CD4	85.73	14.27	CD4	TEM	85.79	14.21	TEM	TH1		100				TH1
GSM472060	CD4	100	0	CD4	TCM	37.26	62.74	TCM	TH1		98.04				TH1
GSM472061	CD4	100	0	CD4	TCM	0	100	TCM	TH2			100			TH2
GSM472067	CD8	100	0	CD4	TEM	100	0	TEM							
GSM472068	CD4	100	0	CD4	NC	57.87	42.13	NC	TH2			97.01			TH2
GSM472069	CD8	31.88	68.12	CD8	TEM	100	0	TEM							
GSM472070	CD4	100	0	CD4	TEM	50.30	49.70	NC	TH1		55.46				NC
GSM472071	CD4	89.12	10.88	CD4	TEM	83.65	16.35	TEM	TH1		92.12				TH1
GSM472072	CD4	100	0	CD4	TCM	30.67	69.33	TCM	TH2			100			TH2
GSM472073	CD4	82.46	17.54	CD4	TCM	0	100	TCM	TH2			100			TH2
GSM472078	CD4	74.85	25.15	CD4	NC	65.42	34.58	TEM	TH2			100			TH2
GSM472087	CD4	98.10	1.90	CD4	TCM	18.72	81.28	TCM		NC		100			TH2
GSM472088	CD4	100	0	CD4	NC	0	100	TCM	TH2			100			TH2
GSM472090	CD8	0	100	CD8	TEM	100	0	TEM							
GSM472091	CD8	0	100	CD8	TEM	100	0	TEM							
GSM472092	CD4	98.58	1.42	CD4	TEM	0	100	TCM	TH17				100		TH17
GSM472093	CD4	88.66	11.34	CD4	TEM	7.47	92.53	TCM	TFH			82.99			TFH
GSM472094	CD4	100	0	CD4	TEM	87.39	12.61	TEM	TH1		61.37				TH1
GSM472095	CD4	90.58	9.42	CD4	TCM	2.85	97.15	TCM	TH2			100			TH2
GSM472097	CD4	100	0	CD4	TCM	6.17	93.83	TCM	TH2			100			TH2
GSM472098	CD4	100	0	CD4	TCM	54.63	45.37	NC	TH2			100			TH2
GSM472100	CD4	100	0	CD4	TCM	0	100	TCM	TH2			100			TH2

GSM472101	CD4	85.65	14.35	CD4	TCM	0	100	TCM	TH2		100				TH2
GSM472102	CD8	12.51	9	CD8	TEM	100	0	TEM							
GSM472106	CD4	89.39	10.61	CD4	TCM	0	100	TCM	TH2		100				TH2
GSM472109	CD4	100	0	CD4	TEM	100	0	TEM	TH1	63.18					TH1
GSM472128	CD4	100	0	CD4	TCM	0	100	TCM	TH2		100				TH2
GSM472129	CD4	98.04	1.96	CD4	TEM	0	100	TCM	NC		100				TH2
GSM472133	CD4	100	0	CD4	NC	8.88	91.12	TCM	TH2		100				TH2
GSM472146	CD4	88.81	11.19	CD4	TCM	19.67	80.33	TCM	TH2		100				TH2
GSM472148	CD8	74.99	25.01	CD4	TEM	88.07	11.93	TEM							
GSM472149	CD4	100	0	CD4	TEM	17.58	82.42	TCM	TH2	57.10					NC
GSM472155	CD4	100	0	CD4	TCM	25.62	74.38	TCM	TREG				68.57		TREG
GSM472156	CD4	70.48	29.52	CD4	TEM	35.49	64.51	TCM	TH1	96.11					TH1
GSM472157	CD4	100	0	CD4	TEM	28.35	71.65	TCM	NC		65.29				TH2

Supplementary Table 5. Diagnostic accuracy of the TEM vs. TCM molecular classifier (linear discriminant function) evaluated in the test set using the minimal gene set

	T-effector memory molecular phenotype*		
	Present	Absent	Likelihood Ratios
Positive	14	0	24.38 (3.27 to 181.52)
Negative	6	18	0.30 (0.15 to 0.59)
Sensitivity	70%; CI: 50 to 90		
Specificity	100%; CI: 100 to 100		
Prevalence	53%; CI: 37 to 69		
Positive Predictive Value	100%; CI: 100 to 100		
Negative Predictive Value	75%; CI: 58 to 92		

*Calculated vs. T-central memory molecular phenotype

Supplementary Table 6. Diagnostic accuracy of the TH vs. TC molecular classifier (linear discriminant function) evaluated in the test set using the minimal gene set

	T-cytotoxic molecular phenotype*		
	Present	Absent	Likelihood Ratios
Positive	5	1	24.38 (3.27 to 181.52)
Negative	3	38	0.38 (0.16 to 0.94)
Sensitivity	63%; CI: 29 to 96		
Specificity	97%; CI: 92 to 100		
Prevalence	17%; CI: 6 to 28		
Positive Predictive Value	83%; CI: 54 to 100		
Negative Predictive Value	93%; CI: 85 to 100		

*Calculated vs. T-helper molecular phenotype

Supplementary Table 7. Diagnostic accuracy of the TH1 molecular classifier (linear discriminant function) evaluated in the test set using the minimal gene set

	TH1 molecular phenotype*		
	Present	Absent	
<i>Positive</i>	8	1	Likelihood Ratios
<i>Negative</i>	2	28	23.20 (3.30 to 163.18) 0.21 (0.06 to 0.72)
Sensitivity	80%; CI: 55 to 100		
Specificity	97%; CI: 90 to 100		
Prevalence	26%; CI: 12 to 39		
Positive Predictive Value	89%; CI: 68 to 100		
Negative Predictive Value	93%; CI: 84 to 100		

* Calculated vs. Th2-Th17-Treg-Tfh molecular phenotypes

Supplementary Table 8. Diagnostic accuracy of the TH2 molecular classifier (linear discriminant function) evaluated in the test set using the minimal gene set

	TH2 molecular phenotype*		
	Present	Absent	
<i>Positive</i>	20	2	Likelihood Ratios
<i>Negative</i>	1	16	8.57 (2.31 to 31.77) 0.05 (0.01 to 0.37)
Sensitivity	95%; CI: 86 to 100		
Specificity	89%; CI: 74 to 100		
Prevalence	54%; CI: 38 to 69		
Positive Predictive Value	91%; CI: 79 to 100		
Negative Predictive Value	94%; CI: 83 to 100		

* Calculated vs. Th1-Th17-Treg-Tfh molecular phenotypes

Supplementary Table 9. Diagnostic accuracy of the TH17 molecular classifier (linear discriminant function) evaluated in the test set using the minimal gene set

	TH17 molecular phenotype*		
	Present	Absent	Likelihood Ratios
<i>Positive</i>	3	0	12.00 (4.06 to 35.46)
<i>Negative</i>	0	33	0.05 (0.01 to 0.37)
Sensitivity	100%; CI: 100 to 100		
Specificity	100%; CI: 100 to 100		
Prevalence	8%; CI: -1 to 17		
Positive Predictive Value	100%; CI: 100 to 100		
Negative Predictive Value	100%; CI: 100 to 100		

* Calculated vs. Th1-Th2-Treg-Tfh molecular phenotypes

Supplementary Table 10. Diagnostic accuracy of the TFH molecular classifier (linear discriminant function) evaluated in the test set using the minimal gene set

	TFH molecular phenotype*		
	Present	Absent	Likelihood Ratios
<i>Positive</i>	3	0	12.00 (4.06 to 35.46)
<i>Negative</i>	0	33	0.05 (0.01 to 0.37)
Sensitivity	100%; CI: 100 to 100		
Specificity	100%; CI: 100 to 100		
Prevalence	8%; CI: -1 to 17		
Positive Predictive Value	100%; CI: 100 to 100		
Negative Predictive Value	100%; CI: 100 to 100		

* Calculated vs. Th1-Th2-Th17-Treg molecular phenotypes

Supplementary Table 11. Diagnostic accuracy of the Treg molecular classifier (linear discriminant function) evaluated in the test set using the minimal gene set

	Treg molecular phenotype*		
	Present	Absent	Likelihood Ratios
<i>Positive</i>	2	0	12.00 (4.06 to 35.46)
<i>Negative</i>	0	34	0.05 (0.01 to 0.37)
Sensitivity	100%; CI: 100 to 100		
Specificity	100%; CI: 100 to 100		
Prevalence	6%; CI: -2 to 13		
Positive Predictive Value	100%; CI: 100 to 100		
Negative Predictive Value	100%; CI: 100 to 100		

* Calculated vs. Th1-Th2-Th17-Tfh molecular phenotypes

Supplementary Table 12. Gene set enrichment analysis shows significant enrichment in selected pathways in genes differentially expressed in the molecular subgroups of PTCL/NOS.

Gene Set Name	Description	FDR q-value
<u>HELLER SILENCED BY METHYLATION UP</u>	Genes up-regulated in at least one of three multiple myeloma (MM) cell lines treated with the DNA hypomethylating agent decitabine (5-aza-2'-deoxycytidine) [PubChem=451668].	0.00E+00
<u>WALLACE PROSTATE CANCER RACE UP</u>	Genes up-regulated in prostate cancer samples from African-American patients compared to those from the European-American patients.	0.00E+00
<u>ALTEMEIER RESPONSE TO LPS WITH MECHANICAL VENTILATION</u>	Genes up-regulated in lung tissue upon LPS aspiration with mechanical ventilation (MV) compared to control (PBS aspiration without MV).	0.00E+00
<u>BROWNE INTERFERON RESPONSIVE GENES</u>	Genes up-regulated in primary fibroblast culture after treatment with interferon alpha for 6 h.	0.00E+00
<u>NUYTEN EZH2 TARGETS UP</u>	Genes up-regulated in PC3 cells (prostate cancer) after knockdown of EZH2 [GeneID=2146] by RNAi.	1.57E-12
<u>KEGG CYTOKINE CYTOKINE RECEPTOR INTERACTION</u>	Cytokine-cytokine receptor interaction	1.57E-12
<u>REACTOME IMMUNE SYSTEM</u>	Genes involved in Immune System	2.32E-12
<u>KEGG GRAFT VERSUS HOST DISEASE</u>	Graft-versus-host disease	4.78E-12
<u>BOSCO INTERFERON INDUCED ANTIVIRAL MODULE</u>	Genes representing interferon-induced antiviral module in sputum during asthma exacerbations.	1.01E-11
<u>TAKEDA TARGETS OF NUP98 HOXA9 FUSION 3D UP</u>	Genes up-regulated in CD34+ [GeneID=947] hematopoietic cells by expression of NUP98-HOXA9 fusion [GeneID=4928;3205] off a retroviral vector at 3 days after transduction.	1.44E-11
<u>DAUER STAT3 TARGETS DN</u>	Top 50 genes down-regulated in A549 cells (lung cancer) expressing STAT3 [GeneID=6774] off an adenovirus vector.	1.57E-11
<u>TAKEDA TARGETS OF NUP98 HOXA9 FUSION 10D UP</u>	Genes up-regulated in CD34+ [GeneID=947] hematopoietic cells by expression of NUP98-HOXA9 fusion [GeneID=4928;3205] off a retroviral vector at 10 days after transduction.	2.22E-11
<u>GRAESSMANN APOPTOSIS BY SERUM DEPRIVATION UP</u>	Genes up-regulated in ME-A cells (breast cancer) undergoing apoptosis upon serum starvation (5% to 0% FCS) for 22 hr.	2.22E-11
<u>KEGG ANTIGEN PROCESSING AND PRESENTATION</u>	Antigen processing and presentation	2.22E-11
<u>FULCHER INFLAMMATORY RESPONSE LECTIN VS LPS DN</u>	Genes down-regulated in monocyte-derived dendritic cells (MDDC) after stimulation with galectin-1 (lectin, LGALS1) [GeneID=3956] compared to that with bacterial lipopolysaccharide (LPS).	3.32E-11
<u>MOSERLE IFNA RESPONSE</u>	Top 50 genes up-regulated in ovarian cancer progenitor cells (also known as side population, SP, cells) in response to interferon alpha (IFNA).	3.32E-11
<u>WONG ADULT TISSUE STEM MODULE</u>	The 'adult tissue stem' module: genes coordinately up-regulated in a compendium of adult tissue stem cells.	5.08E-11
<u>DER IFN BETA RESPONSE UP</u>	Genes up-regulated in HT1080 (fibrosarcoma) cells by treatment with interferon beta for 6 h.	6.12E-11
<u>REACTOME INTERFERON GAMMA SIGNALING</u>	Genes involved in Interferon gamma signaling	6.43E-11
<u>TAKEDA TARGETS OF NUP98 HOXA9 FUSION 8D UP</u>	Genes up-regulated in CD34+ [GeneID=947] hematopoietic cells by expression of NUP98-HOXA9 fusion [GeneID=4928;3205] off a retroviral vector at 8 days	6.63E-11

<u>JAATINEN HEMATOPOIETIC STEM CELL DN</u>	<u>after transduction.</u> <u>Genes down-regulated in CD133+ [GeneID=8842] cells (hematopoietic stem cells, HSC) compared to the CD133- cells.</u>	<u>7.38E-11</u>
<u>DEURIG T CELL PROLYMPHOCYTIC LEUKEMIA DN</u>	<u>Genes down-regulated in T-PLL cells (T-cell prolymphocytic leukemia) bearing the inv(14)/t(14;14) chromosomal aberration.</u>	<u>1.22E-10</u>
<u>HAHTOLA SEZARY SYNDROM DN</u>	<u>Genes down-regulated in monocytes isolated from peripheral blood samples of Sezary syndrom patients compared to those from healthy normal donors.</u>	<u>2.33E-10</u>
<u>FARMER BREAST CANCER CLUSTER 1</u>	<u>Cluster 1: interferon, T and B lymphocyte genes clustered together across breast cancer samples.</u>	<u>3.17E-10</u>
<u>REACTOME CYTOKINE SIGNALING IN IMMUNE SYSTEM</u>	<u>Genes involved in Cytokine Signaling in Immune system</u>	<u>4.29E-10</u>
<u>TAVOR CEBPA TARGETS UP</u>	<u>Genes up-regulated in KCL22 cells (chronic myelogenous leukemia, CML, with BCR-ABL1 [GeneID=613;25] fusion) by expression of CEBPA [GeneID=1050].</u>	<u>5.58E-10</u>

Supplementary Table 13. Somatic mutations occurring in the main PTCL/NOS subgroups. Genes affected by lesions significantly over-represented in each group are listed. For each group, the number of samples carrying mutations in a given gene is indicated.

Gene	TC mutated samples	TH1/TH2/TH17 mutated samples	TFH/TREG mutated samples
<i>A2ML1</i>	3	0	0
<i>ABCB1</i>	1	9	0
<i>ANKRD18A</i>	3	0	1
<i>ARHGAP33</i>	1	0	2
<i>ARHGAP4</i>	0	1	2
<i>ATXN3</i>	0	0	2
<i>BAHCC1</i>	0	7	0
<i>BTD</i>	2	0	1
<i>BTN2A2</i>	0	7	0
<i>C3</i>	0	0	2
<i>C3orf17</i>	0	8	1
<i>CCPG1</i>	3	0	0
<i>CDC27</i>	3	0	0
<i>CDRT4</i>	0	1	2
<i>CHD2</i>	1	0	2
<i>COG3</i>	0	0	2
<i>CRYGS</i>	0	0	2
<i>CX3CR1</i>	0	7	0
<i>DBR1</i>	0	1	2
<i>DCP1A</i>	1	1	2
<i>FAM115C</i>	0	1	2
<i>FAM198B</i>	0	0	2

<i>FAM207A</i>	0	2	2
<i>GPAT2</i>	0	0	2
<i>HLA_C</i>	4	2	0
<i>HLA_DQB2</i>	2	0	2
<i>HLA_DRB5</i>	4	1	1
<i>IGFLR1</i>	2	0	2
<i>IL4R</i>	0	1	2
<i>IL9R</i>	1	1	2
<i>KIAA0040</i>	0	1	2
<i>KIAA1107</i>	2	0	1
<i>KIAA2013</i>	3	0	0
<i>LMF1</i>	0	2	2
<i>LRP3</i>	3	0	0
<i>LRRC37A3</i>	0	1	2
<i>LSG1</i>	0	2	2
<i>MICAL3</i>	2	0	1
<i>MOCS2</i>	3	0	0
<i>MORN2</i>	3	1	1
<i>MTDH</i>	3	0	0
<i>MTDH</i>	3	0	0
<i>MTMR11</i>	3	0	0
<i>MUC20</i>	2	4	3
<i>MUM1</i>	2	0	1
<i>NCOR1</i>	3	0	0
<i>NDUFA10</i>	0	1	2
<i>NDUFV3</i>	0	7	0
<i>NPC1</i>	3	0	1
<i>PABPC1L</i>	0	1	2
<i>PARG</i>	1	1	2
<i>PHKA1</i>	0	0	2
<i>PKD1</i>	3	5	3
<i>PKD1L3</i>	2	0	1
<i>PLBD1</i>	3	0	0
<i>PLCL2</i>	0	7	0
<i>PRDM2</i>	0	7	0
<i>PTDSS2</i>	1	1	2
<i>RBMXL1</i>	0	0	2
<i>SECTM1</i>	1	1	2
<i>SETD1B</i>	0	1	2
<i>SH3RF3</i>	3	0	0
<i>SMG1</i>	2	3	3
<i>SOGA2</i>	4	2	0
<i>SSB</i>	2	0	1
<i>TLR5</i>	3	0	0
<i>TMEM204</i>	0	0	2
<i>TNS3</i>	1	1	2

TRIM61	0	0	2
TRMT44	0	0	2
TSHR	2	0	1
TXK	0	2	2
USP39	3	0	0
VWA1	0	0	2
ZBTB32	2	0	2
ZBTB48	3	0	0
ZNFS86	0	1	2
ZNF708	2	0	1
ZNF831	0	1	2
ZSWIM8	2	0	1

Supplementary Table 14. Gene set enrichment analysis was performed on genes target by mutations in PTCL/NOS subgroups. Top 30 significantly enriched pathways in each group are listed.

Subgroup	Gene Set Name	Description	FDR q-value
TC	RELA_DN.V1_DN	Genes down-regulated in HEK293 cells (kidney fibroblasts) upon knockdown of RELA [Gene ID=5970] gene by RNAi.	1.56E-6
	LTE2_UP.V1_UP	Genes up-regulated in MCF-7 cells (breast cancer) positive for ESR1 [Gene ID=2099] MCF-7 cells (breast cancer) and long-term adapted for estrogen-independent growth.	1.25E-5
	CYCLIN_D1_UP.V1_UP	Genes up-regulated in MCF-7 cells (breast cancer) over-expressing CCND1 [Gene ID=595] gene.	2.21E-5
	ESC_J1_UP_LATE.V1_UP	Genes up-regulated during late stages of differentiation of embryoid bodies from J1 embryonic stem cells.	2.21E-5
	RAPA_EARLY_UP.V1_DN	Genes down-regulated in BJAB (lymphoma) cells by everolimus [PubChem = 6442177].	2.21E-5
	E2F1_UP.V1_DN	Genes down-regulated in mouse fibroblasts over-expressing E2F1 [Gene ID=1869] gene.	2.21E-5
	NFE2L2.V2	Genes up-regulated in MEF cells (embryonic fibroblasts) with knockout of NFE2L2 [Gene ID=4780] gene.	3.85E-5
	KRAS.LUNG_UP.V1_UP	Genes up-regulated in epithelial lung cancer cell lines over-expressing an oncogenic form of KRAS [Gene ID=3845] gene.	3.85E-5
	JAK2_DN.V1_UP	Genes up-regulated in HEL cells (erythroleukemia) after knockdown of JAK2 [Gene ID=3717] gene by RNAi.	4.94E-5
	NOTCH_DN.V1_DN	Genes down-regulated in MOLT4 cells (T-ALL) by DAPT [PubChem=16219261], an inhibitor of NOTCH signaling pathway.	4.94E-5
	VEGF_A_UP.V1_DN	Genes down-regulated in HUVEC cells (endothelium) by treatment with VEGFA [Gene ID=7422].	5.85E-5
	KRAS.600_UP.V1_DN	Genes down-regulated in four lineages of epithelial cell lines over-expressing an oncogenic form of KRAS [Gene ID=3845] gene.	5.85E-5
	RAF_UP.V1_UP	Genes up-regulated in MCF-7 cells (breast cancer) positive for ESR1 [Gene ID=2099] MCF-7 cells (breast cancer) stably over-expressing constitutively active RAF1 [Gene ID=5894] gene.	6.21E-5
	IL21_UP.V1_DN	Genes down-regulated in Sez-4 cells (T lymphocyte) that were first starved of IL2 [Gene ID=3558] and then stimulated with IL21 [Gene ID=59067].	1.21E-4
	KRAS.600_UP.V1_UP	Genes up-regulated in four lineages of epithelial cell lines over-expressing an oncogenic form of KRAS [Gene ID=3845] gene.	1.21E-4
	CYCLIN_D1_KE_.V1_UP	Genes up-regulated in MCF-7 cells (breast cancer) over-expressing a mutant K112E form of CCND1 [Gene ID=595] gene.	1.21E-4
	LEF1_UP.V1_DN	Genes down-regulated in DLD1 cells (colon carcinoma) over-expressing LEF1 [Gene ID=51176].	1.21E-4
	KRAS.600.LUNG.BREAST_UP.V1_UP	Genes up-regulated in epithelial lung and breast cancer cell lines over-expressing an oncogenic form of KRAS [Gene ID=3845] gene.	1.21E-4
	STK33_SKM_DN	Genes down-regulated in SKM-1 cells (AML) after knockdown of STK33 [Gene ID=65975] by RNAi.	1.21E-4
	ERB2_UP.V1_UP	Genes up-regulated in MCF-7 cells (breast cancer) positive for ESR1 [Gene ID=2099] and engineered to express ligand-activatable	1.21E-4

		ERBB2 [Gene ID=2064].	
	TBK1.DF_UP	Genes up-regulated in epithelial lung cancer cell lines upon over-expression of an oncogenic form of KRAS [Gene ID=3845] gene and knockdown of TBK1 [Gene ID=29110] gene by RNAi.	1.21E-4
	IL21_UP.V1_UP	Genes up-regulated in Sez-4 cells (T lymphocyte) that were first starved of IL2 [Gene ID=3558] and then stimulated with IL21 [Gene ID=59067].	1.23E-4
	MEK_UP.V1_DN	Genes down-regulated in MCF-7 cells (breast cancer) positive for ESR1 [Gene ID=2099] MCF-7 cells (breast cancer) stably over-expressing constitutively active MAP2K1 [Gene ID=5604] gene.	1.42E-4
	RB_DN.V1_UP	Genes up-regulated in primary keratinocytes from RB1 [Gene ID=5925] skin specific knockout mice.	2.45E-4
	ESC_V6.5_UP_LATE.V1_UP	Genes up-regulated during late stages of differentiation of embryoid bodies from V6.5 embryonic stem cells.	3.74E-4
	BMI1_DN_MEL18_DN.V1_UP	Genes up-regulated in DAOY cells (medulloblastoma) upon knockdown of BMI1 and PCGF2 [Gene ID=648, 7703] genes by RNAi.	3.77E-4
	CYCLIN_D1_KE_.V1_DN	Genes down-regulated in MCF-7 cells (breast cancer) over-expressing a mutant K112E form of CCND1 [Gene ID=595] gene.	3.77E-4
	HOXA9_DN.V1_UP	Genes up-regulated in MOLM-14 cells (AML) with knockdown of HOXA9 [Gene ID=3205] gene by RNAi vs. controls.	3.77E-4
	P53_DN.V1_UP	Genes up-regulated in NCI-60 panel of cell lines with mutated TP53 [Gene ID=7157].	3.77E-4
	PRC2_EZH2_UP.V1_DN	Genes down-regulated in TIG3 cells (fibroblasts) upon knockdown of EZH2 [Gene ID=2146] gene.	3.77E-4
TH1/TH2/TH 17	JAK2_DN.V1_UP	Genes up-regulated in HEL cells (erythroleukemia) after knockdown of JAK2 [Gene ID=3717] gene by RNAi.	1.35E-7
	JNK_DN.V1_UP	Genes up-regulated in JNK inhibitor-treated (SP600125[PubChem=8515]) keratinocytes.	1.35E-7
	ATF2_S_UP.V1_UP	Genes up-regulated in myometrial cells over-expressing a shortened splice form of ATF2 [Gene ID=1386] gene.	1.35E-7
	MTOR_UP.N4.V1_UP	Genes up-regulated in CEM-C1 cells (T-CLL) by everolimus [PubChem = 6442177], an mTOR pathway inhibitor.	7.05E-7
	CYCLIN_D1_UP.V1_DN	Genes down-regulated in MCF-7 cells (breast cancer) over-expressing CCND1 [Gene ID=595] gene.	1.82E-6
	LTE2_UP.V1_DN	Genes down-regulated in MCF-7 cells (breast cancer) positive for ESR1 [Gene ID=2099] MCF-7 cells (breast cancer) and long-term adapted for estrogen-independent growth.	2.27E-6
	KRAS.AMP.LUNG_UP.V1_UP	Genes up-regulated in epithelial lung cancer cell lines over-expressing KRAS [Gene ID=3845] gene.	2.27E-6
	NFE2L2.V2	Genes up-regulated in MEF cells (embryonic fibroblasts) with knockout of NFE2L2 [Gene ID=4780] gene.	2.39E-6
	BMI1_DN.V1_UP	Genes up-regulated in DAOY cells (medulloblastoma) upon knockdown of BMI1 [Gene ID=648] gene by RNAi.	2.39E-6
	AKT_UP_MTOR_DN.V1_UP	Genes up-regulated by everolimus [PubChem = 6442177] in mouse prostate tissue transgenically expressing human AKT1 gene [Gene ID=207] vs. untreated controls.	2.44E-6
	KRAS.600.LUNG.BREAST_UP.V1_UP	Genes up-regulated in epithelial lung and breast cancer cell lines over-expressing an oncogenic form of KRAS [Gene ID=3845] gene.	3.17E-6
	RAPA_EARLY_UP.V1_DN	Genes down-regulated in BJAB (lymphoma) cells by everolimus [PubChem = 6442177].	3.65E-6
	CTIP_DN.V1_DN	Genes down-regulated in MCF10A cells (breast cancer) upon knockdown of RBBP8 [Gene ID=RBBP8] gene by RNAi.	4.68E-6
	VEGF_A_UP.V1_UP	Genes up-regulated in HUVEC cells (endothelium) by treatment with VEGFA [Gene ID=7422].	4.68E-6
	TBK1.DF_DN	Genes down-regulated in epithelial lung cancer cell lines upon over-expression of an oncogenic form of KRAS [Gene ID=3845] gene and knockdown of TBK1 [Gene ID=29110] gene by RNAi.	8.25E-6
	KRAS.600.LUNG.BREAST_UP.V1_DN	Genes down-regulated in epithelial lung and breast cancer cell lines over-expressing an oncogenic form of KRAS [Gene ID=3845] gene.	8.64E-6
	AKT_UP.V1_DN	Genes down-regulated in mouse prostate by transgenic expression of human AKT1 gene [Gene ID=207] vs. controls.	8.64E-6
	ESC_V6.5_UP_LATE.V1_UP	Genes up-regulated during late stages of differentiation of embryoid bodies from V6.5 embryonic stem cells.	1.03E-5
	ATF2_UP.V1_UP	Genes up-regulated in myometrial cells over-expressing ATF2 [Gene ID=1386] gene.	1.14E-5
	CYCLIN_D1_KE_.V1_DN	Genes down-regulated in MCF-7 cells (breast cancer) over-expressing a mutant K112E form of CCND1 [Gene ID=595] gene.	1.25E-5
	AKT_UP_MTOR_DN.V1_DN	Genes down-regulated by everolimus [PubChem = 6442177] in mouse prostate tissue transgenically expressing human AKT1 gene [Gene ID=207] vs. untreated controls.	2.23E-5
	BMI1_DN_MEL18_DN.V1_UP	Genes up-regulated in DAOY cells (medulloblastoma) upon knockdown of BMI1 and PCGF2 [Gene ID=648, 7703] genes by RNAi.	2.23E-5
	ATM_DN.V1_UP	Genes up-regulated in HEK293 cells (kidney fibroblasts) upon knockdown of ATM [Gene ID=472] gene by RNAi.	2.32E-5
	ATM_DN.V1_DN	Genes down-regulated in HEK293 cells (kidney fibroblasts) upon knockdown of ATM [Gene ID=472] gene by RNAi.	2.87E-5
	PKCA_DN.V1_UP	Genes up-regulated in small intestine in PRKCA [Gene ID=5578] knockout mice.	3.18E-5

	JNK_DN.V1_DN	Genes down-regulated in JNK inhibitor-treated (SP600125[PubChem=8515]) keratinocytes.	3.31E-5
	P53_DN.V1_DN	Genes down-regulated in NCI-60 panel of cell lines with mutated TP53 [Gene ID=7157].	3.41E-5
	DCA_UP.V1_DN	Genes down-regulated in A549 lung carcinoma and M059K glioblastoma cells treated with dichloroacetate [PubChem=6597].	3.41E-5
	VEGF_A_UP.V1_DN	Genes down-regulated in HUVEC cells (endothelium) by treatment with VEGFA [Gene ID=7422].	3.41E-5
	NRL_DN.V1_UP	Genes up-regulated in retina cells from NRL [Gene ID=4901] knockout mice.	3.55E-5
<hr/>			
TFH/TREG	BLALOCK_ALZHEIMERS_DISEASE_UP	Genes up-regulated in brain from patients with Alzheimer's disease.	1.22E-5
	NUYTEN_EZH2_TARGETS_UP	Genes up-regulated in PC3 cells (prostate cancer) after knockdown of EZH2 [GeneID=2146] by RNAi.	1.44E-5
	BILD_HRAS_ONCOGENIC_SIGNATURE	Genes selected in supervised analyses to discriminate cells expressing activated HRAS [GeneID=3265] oncogene from control cells expressing GFP.	9.2E-5
	SMID_BREAST_CANCER_BASAL_UP	Genes up-regulated in basal subtype of breast cancer samples.	1.23E-4
	HELLER_HDAC_TARGETS_DN	Genes down-regulated in at least one of three multiple myeloma (MM) cell lines by TSA [PubChem=5562].	1.33E-4
	PURBEY_TARGETS_OF_CTBP1_AND_SATB1_DN	Genes down-regulated in HEK-293 cells (fibroblast) upon knockdown of both CTBP1 and SATB1 [GeneID=1487, 6304] by RNAi.	1.33E-4
	DELYS_THYROID_CANCER_UP	Genes up-regulated in papillary thyroid carcinoma (PTC) compared to normal tissue.	1.33E-4
	KRIGE_RESPONSE_TO_TOSEDOSTAT_24HR_UP	Genes up-regulated in HL-60 cells (acute promyelocytic leukemia, APL) after treatment with the aminopeptidase inhibitor tosedostat (CHR-2797) [PubChem=15547703] for 24 h.	1.33E-4
	ONKEN_UVEAL_MELANOMA_UP	Genes up-regulated in uveal melanoma: class 2 vs class 1 tumors.	1.33E-4
	SMID_BREAST_CANCER_BASAL_DN	Genes down-regulated in basal subtype of breast cancer samples.	1.41E-4
	BUYTAERT_PHOTO_DYNAMIC_THERAPY_STRESS_UP	Genes up-regulated in T24 (bladder cancer) cells in response to the photodynamic therapy (PDT) stress.	1.77E-4
	PUJANA_ATM_PCC_NETWORK	Genes constituting the ATM-PCC network of transcripts whose expression positively correlated (Pearson correlation coefficient, PCC >= 0.4) with that of ATM [GeneID=472] across a compendium of normal tissues.	1.81E-4
	GRAESSMANN_APOPTOSIS_BY_DOXORUBICIN_UP	Genes up-regulated in ME-A cells (breast cancer) undergoing apoptosis in response to doxorubicin [PubChem=31703].	2.36E-4
	ACEVEDO_LIVER_CANCER_UP	Genes up-regulated in hepatocellular carcinoma (HCC) compared to normal liver samples.	3.75E-4
	WHITFIELD_CELL_CYCLE_S	Genes periodically expressed in synchronized HeLa cells (cervical carcinoma), with peak during the S phase of cell cycle.	3.75E-4
	KOINUMA_TARGETS_OF_SMAD2_OR_SMAD3	Genes with promoters occupied by SMAD2 or SMAD3 [GeneID=4087, 4088] in HaCaT cells (keratinocyte) according to a ChIP-chip analysis.	7.19E-4
	DODD_NASOPHARYNGEAL_CARCINOMA_DN	Genes down-regulated in nasopharyngeal carcinoma (NPC) compared to the normal tissue.	8.16E-4
	ZHENG_BOUND_BY_FOXP3	Genes whose promoters are bound by FOXP3 [GeneID=50943] based on a ChIP-chip analysis.	1.23E-3
	JOHNSTONE_PARVB_TARGETS_2_DN	Genes down-regulated upon overexpression of PARVB [GeneID=29780] in MDA-MB-231 cells (breast cancer) cultured in 3D collagen I and 3D Matrigel only.	1.34E-3
	BENPORATH_NANOG_TARGETS	Set 'Nanog targets': genes upregulated and identified by ChIP on chip as Nanog [GeneID=79923] transcription factor targets in human embryonic stem cells.	1.38E-3
	GEORGES_TARGETS_OF_MIR192_AND_MIR215	Genes down-regulated in HCT116 cells (colon cancer) by expression of MIR192 or MIR215 [GeneID=406967;406997] at 24 h.	1.51E-3
	MARSON_BOUND_BY_FOXP3_UNSTIMULATED	Genes with promoters bound by FOXP3 [GeneID=50943] in unstimulated hybridoma cells.	1.58E-3
	LASTOWSKA_NEUROBLASTOMA_COPY_NUMBER_DN	Genes with copy number losses in primary neuroblastoma tumors.	1.58E-3
	RODRIGUES_THYROID_CARCINOMA_POORLY_DIFFERENTIATED_DN	Genes down-regulated in poorly differentiated thyroid carcinoma (PDTC) compared to normal thyroid tissue.	1.63E-3
	MARSON_BOUND_BY_FOXP3_STIMULATED	Genes with promoters bound by FOXP3 [GeneID=50943] in hybridoma cells stimulated by PMA [PubChem=4792] and ionomycin [PubChem=3733].	1.71E-3
	DORN_ADENOVIRUS_INFECTION_12HR_UP	Genes up-regulated in HeLa cells (cervical carcinoma) 12 h after infection with adenovirus Ad12.	1.94E-3

	ZWANG_DOWN_BY_2ND_EGF_PULSE	Genes down-regulated by second pulse of EGF [GeneID =1950] in 184A1 cells (mammary epithelium).	2.1E-3
	BENPORATH_SOX2_TARGETS	Set 'Sox2 targets': genes upregulated and identified by ChIP on chip as SOX2 [GeneID=6657] transcription factor targets in human embryonic stem cells.	2.1E-3
	KINSEY_TARGETS_OF_EWSR1_FLII_FUSION_UP	Genes up-regulated in TC71 and EWS502 cells (Ewing's sarcoma) by EWSR1-FLI1 [GeneID=2130;2314] as inferred from RNAi knockdown of this fusion protein.	2.1E-3
	GRAESSMANN_APOPTOSIS_BY_SERUM_DEPRIVATION_UP	Genes up-regulated in ME-A cells (breast cancer) undergoing apoptosis upon serum starvation (5% to 0% FCS) for 22 hr.	2.3E-3

Supplementary Table 15. Classification of PTCLs/NOS according to immunohistochemistry

Sample_ID	T-helper	T-cytotoxic				T-follicular helper				T-regulatory	T-effector and central memory		T-helper 1, T-helper 2, and T-helper 17				IHC classification	Molecular classification
		CD4	CD8	TIA	GB	Perforin	CXCL13	PD1	CD10		FOXP3	CD45RA	CCR7	IF gamma	GATA3	IL17	Tbet	
PTCL_002	NEG	NEG	NEG	NEG	NEG	NEG	POS	NEG	ne	NEG	POS	NEG	POS	POS	NEG	ne	Th1	Ths
PTCL_003	POS	ne	NEG	NEG	ne	ne	NEG	ne	ne	ne	ne	ne	ne	ne	NEG	ne	NC	Ths
PTCL_004	POS	NEG	POS	POS	NEG	NEG	NEG	NEG	NEG	POS	NEG	POS	NEG	NEG	NEG	NEG	Treg	TFH_TREG
PTCL_005	POS	NEG	NEG	NEG	NEG	POS	NEG	NEG	NEG	NEG	NEG	NEG	NEG	POS	NEG	NEG	Th2	Ths
PTCL_006	ne	ne	NEG	NEG	NEG	POS	POS	POS	POS	NEG	NEG	POS	POS	NEG	NEG	ne	TFH	TFH_TREG
PTCL_007	ne	NEG	NEG	NEG	NEG	NEG	NEG	NEG	NEG	NEG	NEG	NEG	NEG	POS	NEG	NEG	Th2	Ths
PTCL_008	NEG	NEG	NEG	NEG	ne	ne	ne	NEG	ne	ne	ne	ne	ne	POS	NEG	ne	NC	Ths
PTCL_009	POS	NEG	NEG	ne	ne	ne	ne	NEG	ne	ne	ne	ne	ne	ne	NEG	ne	NC	Ths
PTCL_010	POS	NEG	POS	NEG	NEG	NEG	POS	NEG	POS	NEG	NEG	POS	NEG	POS	NEG	NEG	Th2	Ths
PTCL_012	NEG	NEG	POS	NEG	POS	NEG	NEG	NEG	NEG	NEG	NEG	POS	NEG	NEG	NEG	NEG	TC	Ths
PTCL_013	POS	NEG	POS	NEG	ne	ne	ne	NEG	ne	ne	ne	ne	ne	ne	NEG	ne	TC	Ths
PTCL_015	NEG	NEG	NEG	NEG	NEG	NEG	NEG	NEG	NEG	NEG	NEG	POS	POS	POS	NEG	NEG	Th1	Ths
PTCL_018	POS	POS	POS	NEG	NEG	NEG	NEG	NEG	NEG	NEG	NEG	NEG	NEG	NEG	NEG	NEG	TC	Ths
PTCL_019	ne	NEG	NEG	NEG	NEG	NEG	NEG	NEG	NEG	NEG	NEG	POS	NEG	NEG	NEG	NEG	NC	Ths
PTCL_020	NEG	NEG	NEG	NEG	NEG	NEG	NEG	NEG	NEG	NEG	NEG	POS	POS	NEG	NEG	NEG	NC	Ths
PTCL_021	NEG	NEG	NEG	NEG	NEG	NEG	NEG	NEG	NEG	NEG	NEG	POS	NEG	NEG	NEG	NEG	Th1	Ths
PTCL_022	NEG	NEG	POS	NEG	NEG	NEG	POS	POS	NEG	NEG	NEG	POS	NEG	NEG	NEG	NEG	NC	TFH_TREG
PTCL_024	POS	NEG	NEG	NEG	NEG	NEG	POS	NEG	NEG	NEG	NEG	POS	NEG	POS	NEG	NEG	Th2	Ths
PTCL_025	POS	NEG	NEG	NEG	NEG	NEG	NEG	NEG	NEG	NEG	NEG	NEG	NEG	NEG	NEG	ne	NC	Ths*
PTCL_026	POS	NEG	NEG	NEG	NEG	POS	POS	NEG	ne	NEG	NEG	ne	POS	POS	NEG	NEG	NC	TC
PTCL_027	POS	NEG	NEG	NEG	NEG	NEG	POS	POS	NEG	NEG	POS	NEG	POS	NEG	NEG	TFH	TFH_TREG	
PTCL_028	POS	POS	NEG	partial POS	POS	NEG	NEG	NEG	NEG	NEG	NEG	POS	NEG	POS	NEG	NEG	NC	TC
PTCL_029	POS	NEG	NEG	NEG	NEG	POS	POS	NEG	POS	NEG	POS	POS	NEG	POS	NEG	ne	TFH	TFH_TREG
PTCL_030	NEG	NEG	NEG	NEG	NEG	NEG	NEG	NEG	NEG	POS	NEG	NEG	NEG	POS	NEG	NEG	Treg	TFH_TREG
PTCL_031	NEG	NEG	NEG	NEG	NEG	NEG	POS	ne	NEG	POS	NEG	POS	NEG	POS	NEG	NEG	Treg	TFH_TREG
PTCL_032	POS	NEG	NEG	NEG	NEG	partial POS	POS	NEG	NEG	partial POS	NEG	NEG	NEG	NEG	NEG	ne	NC	TC*
PTCL_034	POS	NEG	NEG	NEG	NEG	NEG	NEG	NEG	NEG	NEG	NEG	NEG	POS	NEG	NEG	Th2		Ths

PTCL_035	POS	NEG	NEG	NEG	NEG	NEG	NEG	NEG	NEG	ne	POS	POS	NEG	NEG	NEG	Th1	Ths
PTCL_036	POS	NEG	NEG	NEG	NEG	NEG	NEG	NEG	NEG	ne	POS	POS	NEG	NEG	ne	Th1	Ths
PTCL_037	POS	NEG	NEG	NEG	NEG	NEG	POS	NEG	NEG	NEG	POS	NEG	POS	NEG	NEG	Th2	Ths
PTCL_038	NEG	POS	ne	ne	ne	ne	ne	ne	ne	ne	NEG	NEG	POS	NEG	NEG	TC	Ths
PTCL_039	NEG	POS	POS	POS	POS	NEG	POS	NEG	TC	Ths							
PTCL_040	POS	NEG	NEG	NEG	NEG	POS	POS	NEG	NEG	NEG	NEG	POS	POS	POS	ne	NC	TFH_TREG*
PTCL_041	POS	NEG	NEG	NEG	NEG	NEG	POS	NEG	NEG	NEG	NEG	POS	POS	NEG	NEG	Th1	Ths
PTCL_042	POS	NEG	POS	POS	POS	ne	POS	NEG	TC	TC							
PTCL_043	POS	NEG	NEG	NEG	NEG	POS	NEG	NEG	NEG	NEG	NEG	POS	POS	NEG	NEG	Th1	TC
PTCL_044	POS	NEG	NEG	NEG	NEG	POS	POS	POS	POS	NEG	NEG	POS	NEG	POS	NEG	TFH	TFH_TREG
PTCL_045	POS	NEG	NEG	NEG	NEG	NEG	NEG	NEG	NEG	NEG	NEG	POS	NEG	NEG	Th2	Ths	
PTCL_046	POS	NEG	NEG	NEG	NEG	NEG	NEG	POS	POS	NEG	POS	NEG	POS	NEG	ne	Treg	TFH_TREG
PTCL_047	NEG	NEG	NEG	NEG	NEG	NEG	NEG	NEG	NEG	NEG	POS	NEG	POS	NEG	NEG	Th2	Ths
PTCL_048	POS	NEG	NEG	NEG	NEG	partial POS	partial POS	NEG	NEG	NEG	POS	NEG	POS	NEG	NEG	Th2	Ths
PTCL_049	POS	NEG	NEG	NEG	NEG	POS	NEG	NEG	NEG	NEG	NEG	NEG	POS	NEG	NEG	Th2	Ths
PTCL_050	POS	NEG	NEG	NEG	NEG	POS	POS	NEG	POS	NEG	NEG	NEG	POS	NEG	NEG	TFH	TC
PTCL_051		NEG	NEG	NEG	NEG	NEG	NEG	NEG	NEG	NEG	NEG	NEG	POS	NEG	NEG	Th1	TC
PTCL_052	POS	NEG	POS	NEG	NEG	POS	NEG	NEG	NEG	NEG	NEG	NEG	POS	NEG	NEG	NC	Ths
PTCL_053	POS	NEG	NEG	NEG	POS	POS	NEG	POS	NEG	NEG	POS	NEG	POS	NEG	NEG	Th2	Ths
PTCL_054	POS	POS	POS	NEG	NEG	NEG	NEG	NEG	NEG	NEG	NEG	NEG	NEG	NEG	NEG	TC	TC*
PTCL_055	POS	NEG	NEG	NEG	NEG	NEG	NEG	NEG	NEG	NEG	NEG	POS	POS	NEG	NEG	NC	Ths*
PTCL_056	NEG	POS	NEG	NEG	NEG	POS	NEG	NEG	NEG	NEG	POS	NEG	POS	NEG	ne	TC	Ths
PTCL_057	POS	NEG	NEG	NEG	POS	POS	NEG	POS	NEG	NEG	NEG	ne	POS	NEG	NEG	TFH	TFH_TREG
PTCL_058	POS	NEG	NEG	NEG	NEG	NEG	NEG	NEG	NEG	NEG	POS	POS	POS	NEG	ne	NC	TC
PTCL_059	POS	POS	ne	ne	ne	POS	POS	POS	POS	ne	ne	ne	ne	NEG	ne	NC	TFH_TREG
PTCL_061		NEG	NEG	NEG	NEG	POS	NEG	NEG	NEG	NEG	NEG	NEG	NEG	NEG	NEG	NC	TFH_TREG
PTCL_062	POS	NEG	NEG	NEG	NEG	POS	NEG	NEG	NEG	POS	POS	NEG	POS	NEG	NEG	Th2	Ths
PTCL_063	POS	NEG	NEG	NEG	NEG	partial POS	partial POS	POS	NEG	NEG	POS	NEG	POS	NEG	NEG	TFH	TFH_TREG
PTCL_064	NEG	POS	POS	POS	ne	NEG	NEG	NEG	NEG	NEG	POS	NEG	NEG	NEG	NEG	TC	TC
PTCL_065	POS	NEG	NEG	NEG	NEG	NEG	NEG	NEG	NEG	NEG	POS	NEG	POS	NEG	NEG	Th2	Ths
PTCL_066	NEG	NEG	POS	POS	POS	POS	POS	NEG	POS	NEG	NEG	POS	NEG	POS	NEG	ne	NC
PTCL_067	NEG	POS	NEG	NEG	NEG	POS	NEG	POS	NEG	NEG	POS	NEG	NEG	NEG	NEG	TC	TC*
PTCL_068	POS	NEG	POS	POS	POS	NEG	POS	NEG	NEG	NEG	NEG	POS	NEG	NEG	ne	TC	Ths
PTCL_069	POS	NEG	NEG	NEG	ne	ne	NEG	NEG	NEG	NEG	ne	POS	POS	ne	NEG	ne	TC
PTCL_070	NEG	NEG	NEG	partial POS	NEG	partial POS	NEG	NEG	NEG	ne	POS	NEG	POS	NEG	NEG	Th2	Ths
PTCL_071	POS	NEG	NEG	NEG	NEG	POS	NEG	NEG	NEG	NEG	NEG	POS	NEG	NEG	ne	NC	TFH_TREG

Ne=not evaluable, Ths= Th1/Th2/Th17, *the confidence measure score was <0.0.

Supplementary Table 16. Genes differentially expressed between LL and other PTCL/NOS

Gene ID	Corrected p-value	Fold Change Absolute	Regulation in Lennert lymphoma
AARS	0.048042	8.328094	down
ANOS	0.048042	23.54169	up
ANP32B	0.019203	22.0195	down
AP1M1	0.040698	15.8283	down
ARL6IP5	0.040698	11.42905	down
ATP5J2	0.033406	8.247275	down
ATP6V1F	0.040698	14.39947	down
BEST3	0.045729	109.1387	up
BTAF1	0.04847	12.26237	down
BTN1A1	0.018851	122.2571	up
C16ORF58	0.015787	28.50922	down
C16ORF82	0.045119	59.71398	up
C1ORF116	0.042085	31.26302	up
C1ORF21	0.045332	14.17014	up
C1ORF212	0.04489	7.245252	down
CBX6	0.026254	19.07741	down
CCDC28A	0.042085	19.54007	down
CCNA1	0.045555	37.51136	up
CD247	0.040698	22.6524	down
CIDECP	0.042085	19.74863	up
CMTM8	0.048042	121.642	down
CNDP2	0.048042	14.431	down
CRYBA1	0.035962	29.78777	up
CSF1R	0.020946	14.67107	down
CST2	0.042085	113.6776	up
DND1	0.019929	33.64642	up
ELMO2	0.048042	6.763801	up
ERCC2	0.042085	58.39888	down
EXOSC8	0.042085	7.755707	down
FAM19A5	0.045555	45.43218	up
FBN3	0.034616	56.76897	up
FEM1A	0.021777	13.19775	down
FSCN1	0.04489	13.49049	down
GADL1	0.020946	96.16802	up
GIMAP4	0.021254	15.27739	down
GLOD4	0.036741	49.1977	down
GNS	0.026254	6.788456	down
GRTP1	0.020946	63.88782	up
GSTT2	0.037735	12.12487	up
HDAC1	0.045119	15.8912	down
HDDC2	0.040698	11.27747	down
HOXC5	0.042085	22.62152	up
HSPB7	0.045555	93.09251	up
IFNA14	0.026254	19.9188	up
IGSF3	0.031962	16.43183	up
KLF16	0.040698	112.0658	up
KLF2	0.039421	12.15451	down
KRTAP21-2	0.045555	38.046	up
KRTAP5-2	0.040698	67.19664	up
METAP2	0.048042	13.55544	down
NACAP1	0.048042	74.54222	up
NDUFS3	0.04847	14.75795	down
NUP62	0.021867	5.891832	down
OR2J3	0.031306	107.6506	up
OR51S1	0.015787	203.3402	up
P15RS	0.045555	8.513782	down
PCP4	0.031761	46.26405	up
PGLYRP3	0.031962	83.86409	up
PNLIPRP3	0.048042	26.46125	up
PPP1R14A	0.048042	14.64327	down
PPP1R14C	0.037638	84.77431	up
PPP1R15A	0.045555	36.12256	down
PRDM16	0.021777	29.96874	up
PSMB3	0.021777	20.77113	down
PSMC5	0.04847	10.18691	down

QARS	0.048042	10.3333	down
RARS	0.045119	8.669651	down
RFX2	0.037735	34.91593	up
RNF123	0.041762	5.112667	down
RPL11	0.048042	7.517418	down
RPL5	0.037118	9.529422	down
RPS27A	0.021777	15.52451	down
RPUSD4	0.04489	9.614982	down
SCGB1C1	0.04847	89.68658	up
SEPHS2	0.045555	8.611829	down
SFRS5	0.048042	6.598389	down
SH3YL1	0.020946	12.46181	down
SHANK1	0.037735	31.68711	up
SLC13A2	0.048042	18.91503	up
SLC25A42	0.045555	7.602004	down
SLC38A2	0.026254	19.79868	down
SPRY4	0.048042	9.27606	up
SUGT1	0.040698	9.070003	down
TAS1R2	0.045555	29.14978	up
TIMM8B	0.04489	7.428672	down
TMEM218	0.042085	10.55598	down
TOMM7	0.040698	12.19069	down
UBB	0.04489	6.179905	down
VDAC3	0.048042	14.51976	down
YWHAZ	0.027551	4.736977	down

Supplementary Table 17. Minimum number of genes used to classify Lennert Lymphoma vs. Other PTCL/NOS

Gene ID	p-value	Fold Change Absolute	Regulation in Lennert Lymphoma
AARS	0.034643	5.351144	up
ANP32B	0.040764	5.276015	up
C16ORF58	0.034774	6.782455	up
CBX6	0.038325	3.728618	up
FEM1A	0.03344	4.312741	up
GRTP1	0.029674	5.317543	up
HDDC2	0.034736	3.994825	up
KLF2	0.007834	5.288072	up
QARS	0.036329	6.758295	up
RPL11	0.033991	5.052949	up
RPUSD4	0.003753	4.535713	up
SFRS5	0.011129	7.316927	up
SLC38A2	0.038574	7.406537	up
SUGT1	0.018644	7.025328	up
TMEM218	0.031185	6.44771	up
VDAC3	0.022675	3.537255	up
YWHAZ	8.46E-04	4.561161	up

Supplementary Table 18. Genes differentially expressed between Lennert Lymphoma and other Cytotoxic-PTCL/NOS.

Gene ID	Absolute fold change	Regulation in Lennert lymphoma
ACADVL	3.116902	Up
ACRC	3.6132402	Up
ADAMDEC1	10.209334	Up
AP2S1	3.441176	Up
ATP2A2	3.1684623	Up
ATP6V0E1	12.777383	Up
BBC3	4.3282285	Up
BCAS2	3.981759	Up
C10ORF46	11.763814	Up

C17ORF70	4.614214	Up
C22ORF28	6.6235423	Up
C4ORF7	17.456026	Up
C6ORF108	7.160199	Up
CAB39	6.009047	Up
CALCOCO1	6.2506027	Up
CAPS	6.525078	Up
CARS	6.383906	Up
CD276	4.9524817	Up
CD68	4.7363253	Up
CIRH1A	4.2664757	Up
CNIH3	8.399947	Up
COTL1	6.9181404	Up
COX19	4.1591444	Up
CPNE9	8.810795	Up
CTSS	15.798656	Up
DBT	3.7400055	Up
DCXR	4.6417174	Up
DGKQ	6.7778916	Up
DOK3	14.490645	Up
DPYD	6.0663257	Up
EDNRA	13.539241	Up
EIF3C	4.836497	Up
ERAL1	3.9320552	Up
ERH	4.4225154	Up
FAIM3	8.564781	Up
FAM53C	5.5226445	Up
FAM98C	5.3446026	Up
FKBP1A	3.443761	Up
FKSG30	13.01743	Up
FLJ46309	4.7801	Up
FNDC8	14.6923685	Up
FOXRED2	3.4148333	Up
FTL	6.4756722	Up
G0S2	4.957224	Up
GATAD2B	7.516201	Up
GNB2	5.666305	Up
GPR153	8.613095	Up
GPR4	8.417191	Up
GPR50	7.3658705	Up
GSDMB	4.5593534	Up
GZMK	7.9394627	Up
HDHD2	4.0754285	Up
HERC2P2	49.46249	Up
HERPUD1	7.6170588	Up
HGS	7.9817104	Up
HIST1H3F	10.317671	Up
HLA-DRB1	16.504635	Up
HOXB5	7.9177694	Up
HTRA4	5.0577416	Up
IFRD2	23.346718	Up
IL21R	5.0096636	Up
IL33	23.124323	Up
KRT19	6.1300125	Up
LDB2	7.787828	Up
LOC440157	3.615458	Up
LOC442582	8.34117	Up
LTA	5.4489226	Up
LY6E	5.0762987	Up
MDM2	5.1392217	Up
MED16	5.011195	Up
MKRN1	3.026339	Up
MLL2	6.0631843	Up
MRPS16	4.670593	Up
MVD	16.966854	Up
NFKBIZ	4.431783	Up
NR1H3	4.855749	Up
NUPR1	8.693555	Up
OAT	5.4859695	Up

OLFML3	9.461977	Up
P2RXL1	8.162519	Up
PHCA	4.3148108	Up
PLA2G7	4.0816355	Up
PLDN	15.32583	Up
PNPLA7	5.2977753	Up
PRDX5	5.9678206	Up
PSMC4	4.659525	Up
QRICH1	3.1744618	Up
RGS12	3.7804742	Up
RPL30	4.3365235	Up
RPL39	10.139755	Up
RPL41	5.6382694	Up
RPS3	4.404897	Up
RTN1	3.8055818	Up
RTN4RL1	5.751417	Up
RYR1	5.3531823	Up
SBDSP	29.219948	Up
SDK1	8.426482	Up
SDK2	4.841416	Up
SERPINA1	3.071698	Up
SFXN3	6.677094	Up
SKIL	5.9285398	Up
SLC30A4	3.9101827	Up
SLFN13	4.6696396	Up
SNORA25	8.169617	Up
SNRPD3	10.983438	Up
SNX27	5.1733003	Up
STT3A	11.5508795	Up
SUMO2	3.3813713	Up
TBC1D9	3.5861583	Up
TBL1X	3.9607947	Up
TDH	22.116198	Up
TGM7	6.306344	Up
TMEM141	4.822222	Up
TMEM156	4.507389	Up
TMEM176B	11.173895	Up
TMEM189 -UBE2V1	6.4012413	Up
TNFRSF4	6.17836	Up
TRAK1	3.7911801	Up
TSNARE1	14.135962	Up
TSPAN33	5.745453	Up
TSPYL4	12.93785	Up
UBXN2A	3.5488248	Up
UNKL	8.83826	Up
VAMP2	9.436797	Up
VRK2	6.4054008	Up
ZCCHC6	5.852641	Up
ZNF100	5.673135	Up
ZNF148	3.759338	Up
ZNF385A	8.265473	Up
ZNF75D	9.818688	Up
ZSWIM4	4.0180464	Up
ACACA	6.219462	Down
ANAPC1	9.536929	Down
APBB3	4.7698927	Down
ATG2A	10.330487	Down
CSE1L	4.666507	Down
CYP2J2	17.303497	Down
DDX5	11.32598	Down
DNAJA3	12.485661	Down
DOPEY1	19.042269	Down
EIF4A3	7.640334	Down
ERP27	5.11796	Down
GTF3C4	14.742162	Down
KIF15	6.880068	Down
LCMT2	22.541142	Down
MSI2	6.35985	Down

PPFIA4	21.600674	Down
QSOX2	10.239131	Down
RABGAP1	9.783725	Down
RFWD3	11.9629755	Down
SFRS9	6.4106755	Down
TACSTD2	10.699939	Down
TUSC4	4.3865237	Down
ZDHHC7	6.3109584	Down
ZW10	6.3244047	Down

Supplementary Table 19. MicroRNAs differentially expressed between Lennert Lymphoma and other PTCL/NOS.

MicroRNA ID	p-value	Absolute fold change	Regulation in Lennert lymphoma
hsa-let-7d-4395394	0.012553142	2.7276673	down
hsa-let-7e-4395517	0.011690697	3.0097759	down
hsa-miR-146a-4373132	0.019856786	3.381771	up
hsa-miR-147b-4395373	0.022377128	37.29126	up
hsa-miR-199b-5p-4373100	0.005994446	20.567883	down
hsa-miR-23a-4373074	0.027455721	28.169153	down
hsa-miR-337-5p-4395267	0.017264001	16.229063	down
hsa-miR-361-5p-4373035	0.006049584	3.3813345	down
hsa-miR-503-4373228	0.022841154	14.025469	up

Supplementary Table 20. MicroRNAs differentially expressed between Lennert Lymphoma and normal T-lymphocytes.

MicroRNA ID	Corrected p-value	Absolute fold change	Regulation in Lennert lymphoma
hsa-let-7a-4373169	3.61E-08	80.45558	down
hsa-let-7b-4395446	1.11E-04	58.60917	down
hsa-let-7c-4373167	8.43E-05	54.11149	down
hsa-let-7d-4395394	2.99E-07	60.116455	down
hsa-let-7e-4395517	3.84E-06	58.55097	down
hsa-let-7g-4395393	2.68E-06	35.678413	down
hsa-miR-103-4373158	2.04E-07	18.852873	down
hsa-miR-105-4395278	8.00E-05	66.7315	down
hsa-miR-106a-4395280	0.007125661	9.885492	down
hsa-miR-107-4373154	0.001655065	143.55693	down
hsa-miR-10b-4395329	1.64E-04	88.91393	up
hsa-miR-122-4395356	7.20E-04	28.72273	down
hsa-miR-124-4373295	0.002220829	25.887716	down
hsa-miR-125a-5p-4395309	1.95E-04	14.433721	down
hsa-miR-126-4395339	6.82E-05	101.86429	up
hsa-miR-127-5p-4395340	7.30E-05	68.620255	down
hsa-miR-128-4395327	3.40E-05	22.22271	down
hsa-miR-129-3p-4373297	0.00121894	104.67908	down
hsa-miR-129-5p-4373171	6.82E-05	71.09103	down
hsa-miR-133b-4395358	6.82E-05	84.198875	down
hsa-miR-136-4373173	1.42E-04	56.22069	down
hsa-miR-137-4373301	0.003990321	17.002647	down
hsa-miR-139-5p-4395400	5.77E-04	9.9506855	down
hsa-miR-140-3p-4395345	6.82E-05	21.325573	down
hsa-miR-141-4373137	1.87E-04	9.826057	up
hsa-miR-143-4395360	1.20E-06	1468.8832	up
hsa-miR-145-4395389	0.002026504	60.935905	up
hsa-miR-146b-3p-4395472	1.20E-06	95.16415	down
hsa-miR-146b-5p-4373178	0.00122144	6.0564437	down
hsa-miR-150-4373127	7.27E-05	77.75678	down
hsa-miR-154-4373270	6.82E-05	71.09107	down
hsa-miR-15b-4373122	5.40E-09	106.267975	down

hsa-miR-17-4395419	0.005749429	10.5224285	down
hsa-miR-181a-4373117	3.40E-05	46.79759	down
hsa-miR-181c-4373115	1.05E-04	45.563152	down
hsa-miR-188-3p-4395217	6.22E-04	100.71986	down
hsa-miR-191-4395410	1.72E-04	15.18671	down
hsa-miR-192-4373108	7.67E-04	3.3630126	down
hsa-miR-193a-5p-4395392	0.001162334	16.482971	down
hsa-miR-193b-4395478	3.51E-04	20.11634	down
hsa-miR-197-4373102	6.52E-05	77.87767	down
hsa-miR-198-4395384	5.99E-04	27.235113	down
hsa-miR-199a-3p-4395415	0.005749429	106.92413	up
hsa-miR-19b-4373098	0.002631858	2.7876596	down
hsa-miR-200b-4395362	9.85E-04	17.039028	down
hsa-miR-200c-4395411	3.61E-08	40.910633	down
hsa-miR-202-4395474	6.82E-05	62.797626	down
hsa-miR-208-4373091	6.82E-05	88.85641	down
hsa-miR-20a-4373286	3.09E-04	18.68084	down
hsa-miR-210-4373089	6.82E-05	18.533596	down
hsa-miR-21-4373090	5.06E-04	2.316405	up
hsa-miR-215-4373084	0.00292297	10.27159	down
hsa-miR-216a-4395331	9.60E-05	49.347176	down
hsa-miR-216b-4395437	3.23E-04	45.986214	down
hsa-miR-217-4395448	6.82E-05	71.09103	down
hsa-miR-218-4373081	0.002565206	56.033585	up
hsa-miR-219-1-3p-4395206	6.82E-05	214.05992	down
hsa-miR-219-2-3p-4395501	6.82E-05	71.09107	down
hsa-miR-219-5p-4373080	6.82E-05	71.09105	down
hsa-miR-220-4373078	1.19E-04	44.10578	down
hsa-miR-220b-4395317	6.82E-05	71.09103	down
hsa-miR-220c-4395322	6.82E-05	71.09103	down
hsa-miR-222-4395387	0.001010677	7.1059165	down
hsa-miR-223-4395406	6.82E-05	74.272804	down
hsa-miR-22-4373079	1.83E-06	745.4907	up
hsa-miR-224-4395210	0.002565206	14.793198	up
hsa-miR-23a-4373074	1.59E-05	102.82014	down
hsa-miR-24-4373072	0.002967551	3.402679	down
hsa-miR-25-4373071	3.53E-06	19.841572	down
hsa-miR-26a-4395166	6.82E-05	37.50873	down
hsa-miR-26b-4395167	6.70E-06	31.565748	down
hsa-miR-27a-4373287	0.009016768	3.271165	down
hsa-miR-28-3p-4395557	3.40E-05	14.475548	down
hsa-miR-296-3p-4395212	7.60E-04	33.311626	down
hsa-miR-296-5p-4373066	1.88E-05	91.032715	down
hsa-miR-298-4395301	0.00387515	25.720179	down
hsa-miR-299-3p-4373189	6.82E-05	71.09103	down
hsa-miR-299-5p-4373188	6.82E-05	71.09107	down
hsa-miR-29a-4395223	1.24E-04	5.3029532	down
hsa-miR-302a-4378070	3.98E-04	116.27155	down
hsa-miR-302b-4378071	0.004433442	17.031845	down
hsa-miR-30b-4373290	2.38E-06	27.244072	down
hsa-miR-30c-4373060	3.92E-06	33.961716	down
hsa-miR-31-4395390	1.50E-05	65.14107	down
hsa-miR-320-4395388	5.51E-05	64.36276	down
hsa-miR-323-3p-4395338	7.11E-05	73.57172	down
hsa-miR-324-3p-4395272	2.01E-05	15.925911	down
hsa-miR-324-5p-4373052	0.003657605	5.4264016	down
hsa-miR-325-4373051	6.82E-05	71.09107	down
hsa-miR-326-4373050	3.61E-08	74.51434	down
hsa-miR-328-4373049	8.24E-05	75.37232	down
hsa-miR-329-4373191	1.93E-04	51.829296	down
hsa-miR-330-3p-4373047	1.14E-04	51.447227	down
hsa-miR-331-3p-4373046	2.47E-05	18.872269	down
hsa-miR-339-5p-4395368	6.82E-05	88.839	down
hsa-miR-33b-4395196	6.82E-05	71.09105	down
hsa-miR-342-3p-4395371	1.26E-06	61.85865	down
hsa-miR-342-5p-4395258	6.82E-05	79.59399	down
hsa-miR-346-4373038	1.42E-04	56.123333	down
hsa-miR-361-5p-4373035	3.70E-05	21.182549	down
hsa-miR-363-4378090	6.28E-09	83.19141	down

hsa-miR-365-4373194	2.41E-04	10.666114	down
hsa-miR-369-3p-4373032	6.82E-05	71.09103	down
hsa-miR-369-5p-4373195	6.82E-05	71.09105	down
hsa-miR-371-3p-4395235	6.82E-05	71.09105	down
hsa-miR-375-4373027	1.08E-04	32.883205	down
hsa-miR-376b-4373196	6.82E-05	71.09107	down
hsa-miR-377-4373025	6.82E-05	71.09107	down
hsa-miR-380-4373022	6.82E-05	71.09103	down
hsa-miR-382-4373019	0.002342956	28.989588	down
hsa-miR-384-4373017	6.82E-05	71.09107	down
hsa-miR-409-5p-4395442	6.82E-05	71.09107	down
hsa-miR-423-5p-4395451	1.09E-05	97.37894	down
hsa-miR-424-4373201	0.001077875	5.71487	up
hsa-miR-429-4373203	0.003591576	17.881916	down
hsa-miR-431-4395173	6.82E-05	71.09105	down
hsa-miR-448-4373206	6.82E-05	71.09105	down
hsa-miR-450b-3p-4395319	8.00E-05	66.6514	down
hsa-miR-450b-5p-4395318	5.72E-04	39.88836	down
hsa-miR-452-4395440	6.86E-04	24.758244	up
hsa-miR-453-4395429	6.82E-05	71.09107	down
hsa-miR-455-5p-4378098	1.26E-06	122.35287	up
hsa-miR-483-5p-4395449	9.69E-05	42.259033	down
hsa-miR-484-4381032	0.001010677	14.543935	down
hsa-miR-485-5p-4373212	6.82E-05	71.09103	down
hsa-miR-486-3p-4395204	0.002686553	81.4469	down
hsa-miR-486-5p-4378096	4.91E-04	369.4228	down
hsa-miR-487a-4378097	2.91E-04	32.83046	down
hsa-miR-487b-4378102	6.05E-04	30.510933	down
hsa-miR-489-4395469	0.005155399	7.8477526	down
hsa-miR-490-3p-4373215	6.82E-05	71.09103	down
hsa-miR-491-3p-4395471	6.82E-05	71.09107	down
hsa-miR-491-5p-4381053	9.34E-06	32.163155	down
hsa-miR-492-4373217	6.82E-05	71.09103	down
hsa-miR-496-4386771	6.87E-05	72.03769	down
hsa-miR-499-3p-4395538	6.82E-05	71.09107	down
hsa-miR-499-5p-4381047	6.82E-05	71.09105	down
hsa-miR-501-3p-4395546	5.31E-04	93.96086	down
hsa-miR-502-3p-4395194	6.89E-04	7.164897	down
hsa-miR-502-5p-4373227	0.001968731	7.4537277	up
hsa-miR-503-4373228	0.008556373	4.0969133	up
hsa-miR-504-4395195	6.82E-05	71.09105	down
hsa-miR-506-4373231	6.82E-05	71.09105	down
hsa-miR-507-4373232	6.82E-05	75.08985	down
hsa-miR-508-3p-4373233	5.28E-04	28.161697	down
hsa-miR-508-5p-4395203	6.82E-05	71.09105	down
hsa-miR-509-3-5p-4395266	6.82E-05	71.09107	down
hsa-miR-510-4395352	6.82E-05	71.09107	down
hsa-miR-512-5p-4373238	6.82E-05	71.09103	down
hsa-miR-513-5p-4395201	6.82E-05	71.687325	down
hsa-miR-515-3p-4395480	7.61E-04	29.642006	down
hsa-miR-515-5p-4373242	6.82E-05	71.09107	down
hsa-miR-516a-5p-4395527	6.82E-05	71.09107	down
hsa-miR-516b-4395172	6.77E-04	26.417011	down
hsa-miR-518a-5p-4395507	6.82E-05	71.09107	down
hsa-miR-518b-4373246	0.008556373	26.09354	down
hsa-miR-518c-4395512	1.42E-04	40.977566	down
hsa-miR-518d-3p-4373248	6.82E-05	71.09107	down
hsa-miR-518d-5p-4395500	6.82E-05	71.09107	down
hsa-miR-518e-4395506	0.002126356	24.25924	down
hsa-miR-518f-4395499	0.001182622	22.145823	down
hsa-miR-519c-3p-4373251	6.82E-05	71.09105	down
hsa-miR-520a-3p-4373268	6.82E-05	71.09105	down
hsa-miR-520a-5p-4378085	6.82E-05	71.09103	down
hsa-miR-520d-5p-4395504	6.82E-05	71.09107	down
hsa-miR-520e-4373255	6.82E-05	71.09103	down
hsa-miR-520g-4373257	8.07E-05	75.066	down
hsa-miR-521-4373259	6.51E-05	83.90615	down
hsa-miR-522-4395524	9.60E-05	66.788185	down
hsa-miR-524-5p-4395174	6.82E-05	71.09107	down

hsa-miR-525-5p-4378088	6.82E-05	71.09103	down
hsa-miR-526b-4395493	6.82E-05	71.09103	down
hsa-miR-532-3p-4395466	4.99E-07	92.18991	down
hsa-miR-539-4378103	0.002230879	17.837038	up
hsa-miR-541-4395312	0.001162334	33.642113	down
hsa-miR-544-4395376	6.82E-05	71.09103	down
hsa-miR-548a-3p-4380948	0.001253028	34.723244	down
hsa-miR-548a-5p-4395523	6.82E-05	71.09107	down
hsa-miR-548b-3p-4380951	6.82E-05	71.09105	down
hsa-miR-548c-3p-4380993	4.13E-04	131.35822	down
hsa-miR-548c-5p-4395540	0.001253028	28.382477	down
hsa-miR-548d-3p-4381008	4.45E-06	81.80428	down
hsa-miR-548d-5p-4395348	0.001314656	26.69374	down
hsa-miR-551b-4380945	9.85E-04	24.099463	down
hsa-miR-556-3p-4395456	6.82E-05	71.09103	down
hsa-miR-556-5p-4395455	6.82E-05	71.09107	down
hsa-miR-561-4380938	1.44E-04	55.7872	down
hsa-miR-576-5p-4395461	6.82E-05	69.40356	down
hsa-miR-579-4395509	0.005155399	10.072881	up
hsa-miR-582-3p-4395510	6.82E-05	71.09107	down
hsa-miR-582-5p-4395175	6.82E-05	71.09105	down
hsa-miR-597-4380960	4.06E-05	45.87345	down
hsa-miR-615-3p-4386777	6.82E-05	71.09107	down
hsa-miR-615-5p-4395464	6.82E-05	71.09105	down
hsa-miR-616-4395525	0.002686553	50.96274	down
hsa-miR-618-4380996	0.002672494	21.818733	down
hsa-miR-624-4395541	6.82E-05	71.09107	down
hsa-miR-625-4395542	6.82E-05	42.055714	down
hsa-miR-629-4395547	6.82E-05	22.818056	down
hsa-miR-636-4395199	2.76E-04	21.04169	down
hsa-miR-642-4380995	1.15E-08	73.859146	down
hsa-miR-651-4381007	1.35E-04	80.48955	down
hsa-miR-652-4395463	7.05E-06	8.060042	down
hsa-miR-654-5p-4381014	6.82E-05	71.09107	down
hsa-miR-660-4380925	3.40E-05	305.576	up
hsa-miR-671-3p-4395433	2.38E-06	81.73437	down
hsa-miR-672-4395438	5.28E-04	38.153137	down
hsa-miR-674-4395193	6.82E-05	72.1159	down
hsa-miR-744-4395435	2.63E-07	46.19919	down
hsa-miR-758-4395180	6.82E-05	71.416595	down
hsa-miR-871-4395465	6.82E-05	71.09107	down
hsa-miR-872-4395375	6.82E-05	71.09107	down
hsa-miR-874-4395379	1.11E-04	82.106316	down
hsa-miR-875-3p-4395315	6.82E-05	71.45992	down
hsa-miR-876-3p-4395336	6.82E-05	71.09103	down
hsa-miR-876-5p-4395316	6.82E-05	71.09107	down
hsa-miR-885-3p-4395483	0.003815113	86.37674	down
hsa-miR-887-4395485	1.51E-04	54.713673	down
hsa-miR-889-4395313	0.00100865	23.954018	down
hsa-miR-890-4395320	6.82E-05	71.09107	down
hsa-miR-891a-4395302	7.96E-04	37.14928	down
hsa-miR-891b-4395321	6.82E-05	71.09107	down
hsa-miR-892a-4395306	6.82E-05	71.09107	down
hsa-miR-92a-4395169	1.26E-06	121.121605	down
hsa-miR-93-4373302	7.96E-04	14.133492	down
hsa-miR-95-4373011	0.001244283	17.408205	down
hsa-miR-96-4373372	6.82E-05	71.09105	down
hsa-miR-98-4373009	6.82E-05	66.1558	down
hsa-miR-99b-4373007	0.002137616	6.099767	down

Supplementary Table 21. Genes differentially expressed between Lennert Lymphoma and normal T-lymphocytes.

Gene ID	Corrected p-value	Absolute fold change	Regulation in Lennert lymphoma
CCDC107	0.004824301	47.71441	down
EAF1	0.002051818	16.950863	down
EFHA1	0.004074807	12.785063	down
MAGOH	0.001658394	56.60359	down
MAPBPIP	0.002178571	18.467093	down
MRPL1	4.12E-04	20.259808	down
PPIH	6.16E-06	9.901969	down
RPP38	5.91E-04	23.624487	down
SIGIRR	5.75E-04	11.742586	down
TAPT1	0.004604011	14.049687	down
TERF2IP	1.48E-04	8.229083	down
TMEM60	0.002367497	13.576537	down
UQCRCQ	0.002908249	21.078123	down
A1CF	2.48E-04	148.90007	up
A2M	0.004109861	919.30115	up
A4GALT	5.30E-05	238.38931	up
ABCA6	0.002588788	60.411644	up
ABCA8	7.76E-05	562.2567	up
ABCC3	0.003477665	192.81596	up
ABCC8	7.91E-05	94.09664	up
ABHD12B	0.004047907	70.868416	up
ABI3BP	1.96E-05	494.4472	up
ABL2	0.00411369	7.981921	up
ABP1	5.19E-04	56.52589	up
ACMSD	3.20E-04	103.09564	up
ACVRL1	0.004335573	1838.7761	up
ADAMTS14	4.28E-04	71.91135	up
ADAMTS18	1.03E-04	289.33682	up
ADAMTS5	5.48E-06	275.51382	up
ADCY2	1.56E-05	311.60263	up
ADCY6	0.001586153	70.971016	up
ADCYAP1	3.70E-04	163.7449	up
ADRA1B	3.23E-04	261.2697	up
AIRE	0.001705347	58.04078	up
AKR1C4	0.004229457	110.69178	up
ALDH1A1	0.004618076	837.84015	up
ALDH3A1	2.25E-04	78.19763	up
ALK	4.61E-04	34.806988	up
ALPL	0.00263254	2267.68	up
ANG	0.001113428	11.674992	up
ANGPT2	2.48E-05	2365.0767	up
ANKRD29	0.002515058	328.54285	up
ANKRD45	0.001436541	71.605865	up
ANKS1B	7.62E-05	150.37242	up
ANO5	2.00E-04	111.99926	up
ANTXR1	1.16E-08	63.353504	up
APBB2	0.003382847	149.02454	up
APCDD1L	0.003074952	480.98248	up
APLNR	1.14E-05	3473.3835	up
APOC1	1.15E-04	344.844	up
APOE	7.77E-04	2233.9165	up
ARL15	0.00270423	22.049297	up
ASB10	0.003141448	52.688026	up
ASCL2	0.001964778	118.28999	up
ASGR2	2.21E-04	57.568855	up
ASPA	1.14E-05	3224.0264	up
ATOH8	2.92E-05	1082.949	up
BAZ1B	0.001176386	97.57641	up
BGN	3.64E-06	1629.443	up
BHLHB3	2.16E-04	2960.5522	up
BNC2	0.001104544	150.11607	up

C10ORF11	9.26E-04	172.50426	up
C10ORF65	4.60E-05	212.2882	up
C11ORF40	0.004347653	132.00244	up
C11ORF41	6.09E-04	198.70433	up
C12ORF64	5.15E-06	94.457596	up
C13ORF30	6.64E-05	1291.303	up
C14ORF73	2.81E-04	329.22418	up
C15ORF38	1.09E-05	395.89264	up
C16ORF3	0.002115656	489.15015	up
C17ORF77	2.66E-04	648.3065	up
C17ORF82	0.001596325	281.1157	up
C18ORF34	1.18E-04	429.263	up
C1ORF110	0.003764643	3111.9236	up
C1ORF95	0.003836555	67.09627	up
C1QA	9.33E-08	625.223	up
C1QB	1.11E-05	3583.602	up
C1QL2	7.90E-04	384.19763	up
C1QTNF5	0.001791736	311.08853	up
C1QTNF7	8.58E-04	73.58816	up
C1S	4.80E-04	197.54514	up
C20ORF186	7.82E-04	147.35855	up
C2ORF65	0.002478448	328.45575	up
C3	5.30E-05	412.74664	up
C3ORF24	0.004375497	150.04103	up
C4ORF18	5.02E-08	258.1374	up
C4ORF37	3.93E-05	203.60419	up
C4ORF45	0.003388995	93.93394	up
C4ORF7	5.02E-09	108460.086	up
C5ORF20	2.25E-04	117.61034	up
C6ORF138	4.44E-04	46.523273	up
C7	7.39E-04	454.45554	up
C8ORF4	1.04E-05	7308.287	up
C8ORF42	2.46E-04	247.81018	up
C9	0.001948395	356.19333	up
C9ORF61	0.002686916	106.81605	up
CA4	8.57E-04	153.8369	up
CACNA1E	1.57E-05	195.48915	up
CACNA2D3	2.63E-04	623.852	up
CALB1	0.002006047	48.680122	up
CALML3	9.52E-04	143.59138	up
CART1	0.00131751	303.34482	up
CARTPT	9.14E-04	34.514526	up
CAV1	0.001473657	71.21753	up
CBFA2T3	2.73E-04	67.96304	up
CCDC80	2.61E-05	332.15182	up
CCL11	0.002176097	149.17578	up
CCL21	3.89E-06	17100.742	up
CD14	0.001810738	51.036827	up
CD180	0.001892739	144.80896	up
CD1E	3.11E-09	121.20033	up
CD209	3.94E-05	175.3683	up
CD300LG	0.002122958	67.6576	up
CD36	0.0011447	64.84553	up
CDC42EP1	8.56E-06	111.05538	up
CDC42EP5	2.81E-08	2126.6475	up
CDCA8	3.43E-04	11.861703	up
CDH10	3.03E-05	8959.266	up
CDH11	3.49E-06	135.86707	up
CDH13	0.004550356	124.89088	up
CDH5	2.75E-07	411.45947	up
CDX1	5.96E-07	723.2297	up
CEACAM20	0.002311474	329.75888	up
CELSR1	0.00406698	144.05043	up
CGB2	0.001487034	83.452705	up
CGNL1	1.05E-04	322.99033	up
CHRD	2.91E-04	129.61572	up
CHRDL1	0.001507737	457.46326	up

CHRDL2	0.004037772	124.771515	up
CLDN2	0.0017472	141.44775	up
CLDN3	0.001003348	35.39689	up
CLEC14A	7.80E-06	420.6127	up
CLEC4G	4.62E-04	195.2623	up
CLEC4M	6.81E-05	231.7394	up
CLU	0.001613511	51.188614	up
CMKLR1	0.002228843	660.51776	up
COL16A1	7.20E-05	61.017914	up
COL1A1	6.42E-04	219.96974	up
COL1A2	0.003206673	290.22144	up
COL3A1	8.44E-05	674.1037	up
COL4A2	5.40E-05	840.0196	up
COL4A4	2.47E-05	1123.8839	up
COMP	6.65E-04	693.0022	up
CP	7.60E-06	1791.0645	up
CPVL	7.20E-04	671.02625	up
CRIM1	0.004679355	90.89279	up
CRYBA1	9.60E-04	127.26573	up
CRYBB1	3.87E-04	259.5617	up
CSDC2	1.39E-05	457.7034	up
CSMD2	0.00103971	44.628788	up
CSN3	0.003536882	1489.3837	up
CSPG4	6.52E-05	1001.82794	up
CST9	2.67E-04	128.37216	up
CTGF	0.003019353	68.822426	up
CUEDC1	6.18E-05	118.245	up
CX3CL1	0.003605685	226.8698	up
CXCL12	1.43E-07	285.7934	up
CXCL14	3.89E-09	4735.3433	up
CYP2C19	0.004225662	970.40063	up
CYP4F11	0.004890965	64.39434	up
CYP8B1	0.002256816	120.34287	up
CYR61	0.001668595	739.83136	up
DAAM2	0.00149221	41.989517	up
DACT2	1.89E-05	131.11925	up
DAPL1	6.93E-04	132.9525	up
DCLK1	1.65E-06	324.77914	up
DCN	2.11E-07	1564.5222	up
DEFB122	2.25E-06	570.08154	up
DEFB125	0.002905576	304.0734	up
DEFB129	2.04E-06	376.678	up
DES	0.003394246	157.65027	up
DIO2	2.09E-04	79.228035	up
DLL4	2.87E-04	153.34657	up
DLX1	2.82E-05	56.58711	up
DLX5	0.001596655	98.3629	up
DMRT3	8.56E-05	204.13988	up
DNALI1	0.001791371	29.736288	up
DOK3	0.003878779	752.33435	up
DPPA2	0.001257183	55.031273	up
DPT	1.53E-05	61.211666	up
DSC2	4.92E-05	170.65591	up
DSCR10	6.47E-04	51.88543	up
DSE	0.001671509	19.59557	up
DTNA	5.35E-07	630.1794	up
DUX3	6.47E-05	6843.355	up
DZIP1	0.004565985	96.16974	up
EBF3	1.04E-04	54.036602	up
EDNRA	1.42E-05	11640.301	up
EFEMP1	1.26E-08	230.84818	up
EFS	4.39E-05	105.1983	up
EGFLAM	3.60E-07	282.19333	up
ELA3A	0.002186013	147.34988	up
EMILIN1	0.004873649	318.553	up
EPHA2	9.97E-04	175.6159	up
EPHA3	6.99E-06	135.0204	up

ERC2	6.84E-04	104.00445	up
ERVWE1	0.001722565	106.04717	up
ETV1	9.44E-04	82.34332	up
EVI1	8.89E-04	89.03203	up
EYA4	0.003720977	65.86412	up
F10	7.08E-04	637.6613	up
F8	0.001630355	35.73296	up
FA2H	0.002530525	181.99431	up
FAM107A	4.75E-07	159.64517	up
FAM123A	1.43E-06	376.09506	up
FAM155A	3.49E-04	133.82468	up
FAM19A5	0.003436749	236.76608	up
FAM20A	0.001061105	164.18413	up
FAM3D	5.84E-05	278.88446	up
FAM43B	7.48E-04	83.4497	up
FAM70A	5.16E-06	442.61203	up
FAM70B	2.84E-04	246.27187	up
FARP1	1.47E-04	47.40466	up
FBLN1	4.78E-12	99.17179	up
FBN1	1.49E-07	794.04956	up
FBN2	3.95E-05	269.9577	up
FBXO22OS	0.004076702	72.679924	up
FCN3	9.55E-05	119.374756	up
FCRL2	7.45E-04	50.109898	up
FGFR3	5.38E-04	31.377474	up
FHL2	3.21E-04	19.971106	up
FIGN	8.53E-05	1105.1294	up
FILIP1	6.61E-04	187.55183	up
FILIP1L	0.003159087	26.868729	up
FLJ25996	5.43E-04	1166.0594	up
FLJ35409	0.001648607	103.118675	up
FLJ44653	0.001286436	298.49823	up
FLJ45445	3.51E-05	206.28146	up
FLNC	0.004016951	540.0853	up
FLRT2	8.55E-04	31.151913	up
FMO2	8.72E-05	333.3134	up
FMO3	0.003437823	71.283516	up
FN1	2.75E-06	332.47342	up
FOXP2	0.004162769	33.952377	up
FPR3	0.00462868	504.4062	up
FREM2	0.001817113	39.243195	up
FRK	0.003582864	167.15329	up
FRRS1	0.001788051	23.334436	up
FXYD2	1.67E-04	25.653507	up
FXYD6	2.11E-04	489.31894	up
FZD7	3.17E-04	23.441677	up
GAB1	2.22E-04	61.992752	up
GABRB1	1.70E-04	3799.038	up
GABRR1	0.001085003	193.58792	up
GAGE12I	1.99E-04	122.79657	up
GAGE6	4.45E-04	105.42413	up
GALNTL1	5.48E-06	239.00746	up
GAS7	5.14E-06	95.60258	up
GCNT3	5.42E-04	167.22176	up
GEM	4.40E-04	112.1868	up
GGTA1	0.001489612	130.66629	up
GHR	0.003255331	398.58572	up
GHSR	3.19E-06	163.89807	up
GKN2	2.58E-04	109.851036	up
GLI2	0.003188962	204.99214	up
GLIS1	0.001440324	188.22276	up
GLT8D2	0.002366317	15.790633	up
GLUL	1.04E-04	51.363754	up
GNG12	1.31E-05	1042.1455	up
GNRHR	0.00456848	69.804306	up
GOLM1	5.02E-07	38.82523	up
GPC6	5.86E-04	50.608315	up

GPR162	0.003690091	34.816776	up
GPR176	0.002935388	28.542063	up
GPR4	1.43E-06	1400.7784	up
GREM1	2.11E-06	73.58937	up
GRM3	8.53E-04	5340.1646	up
GRRP1	1.20E-04	61.554356	up
GSN	0.002156649	30.12112	up
GUCY1A2	4.35E-05	1178.7905	up
H19	0.00429109	1557.6794	up
HAND1	1.54E-05	1110.7249	up
HLA-DQA2	5.15E-04	1708.3074	up
HLA-DQB2	3.53E-04	1482.4127	up
HOXA13	2.94E-04	504.62964	up
HOXA6	0.003629437	28.177776	up
HOXA7	5.58E-05	105.590675	up
HOXB13	1.33E-05	424.14804	up
HOXC10	2.32E-04	413.47003	up
HOXC4	7.05E-04	113.471085	up
HOXC5	9.01E-04	92.594894	up
HOXC9	4.41E-04	162.44164	up
HOXD13	9.98E-05	1413.4087	up
HS3ST3A1	4.25E-04	37.257675	up
HTR2A	0.001071974	3164.6924	up
HTR2B	5.00E-06	70.07199	up
HTR3D	1.76E-04	74.046936	up
HTRA1	1.46E-04	137.02522	up
HTRA4	1.88E-04	200.73428	up
HYAL1	2.02E-05	50.469807	up
IGFBP5	1.58E-05	1914.119	up
IGFBP7	3.93E-05	172.29695	up
IGFL1	0.001366323	337.98065	up
IGFL3	2.89E-04	4854.438	up
IL18	0.001198142	145.2589	up
IL1RAPL1	0.002290845	2546.491	up
IL1RAPL2	0.002276349	89.73773	up
IL31RA	2.06E-04	96.76271	up
INHBC	2.29E-04	165.13293	up
IRX3	2.37E-04	435.91623	up
IRX6	4.75E-06	1632.3883	up
ISLR	2.39E-04	279.7606	up
ISLR2	5.65E-04	254.10277	up
ITGA11	0.002167827	92.08847	up
ITGA8	5.22E-06	2191.2146	up
ITIH5	8.33E-08	165.04219	up
KCNB1	2.05E-05	150.76038	up
KCNE4	0.001919829	117.4119	up
KCNF1	1.49E-05	622.38104	up
KCNJ10	1.22E-05	338.96042	up
KCNJ5	3.27E-04	155.1142	up
KCNJ6	8.47E-04	217.86787	up
KCNJ8	0.001589894	162.59445	up
KCNMA1	5.94E-07	192.40115	up
KCNN2	0.001898851	321.46735	up
KCNN3	0.001136565	42.375698	up
KCNT1	6.29E-05	366.20413	up
KIAA0319	1.01E-05	721.6995	up
KIAA1409	0.001660763	106.65528	up
KIF17	0.002893751	613.18823	up
KIRREL	1.15E-05	431.3474	up
KLK2	2.98E-05	88.02464	up
KPRP	1.48E-07	482.98526	up
KRT23	0.00431706	181.0255	up
KRT6A	0.001132019	144.53497	up
KRT6B	0.001925398	86.53376	up
KRTAP10-10	0.002214061	804.22845	up
KRTAP10-3	0.003796856	124.36412	up
KRTAP12-4	0.002336789	59.83807	up

KRTAP1-3	1.43E-04	198.16115	up
KRTAP17-1	0.001237259	150.86696	up
KRTAP19-6	0.003120377	62.078194	up
KRTAP4-4	4.78E-05	215.9409	up
KRTDAP	6.79E-04	98.9798	up
L3MBTL4	0.001976545	20.367863	up
LAMA4	3.20E-05	2262.7773	up
LAMB2	4.47E-04	332.431	up
LDB2	0.001651511	86.49941	up
LEPREL1	0.004015781	119.51305	up
LGALS13	0.001188021	123.39415	up
LGI2	3.95E-05	58.88168	up
LHFP	5.85E-04	580.59863	up
LHX1	5.52E-04	144.22237	up
LHX6	8.63E-04	64.01631	up
LIFR	6.10E-06	55.019253	up
LILRB5	1.81E-04	101.5764	up
LIPG	7.79E-04	59.91872	up
LMNA	9.00E-04	35.6897	up
LMOD1	4.68E-05	1776.0135	up
LOC285016	0.001765019	46.21854	up
LOC348174	7.42E-06	237.7254	up
LOC392196	0.00379843	327.80914	up
LOC440157	6.07E-04	206.01009	up
LOC731102	8.06E-04	229.54295	up
LONRF2	0.001787801	43.235313	up
LOR	0.004821098	1685.4519	up
LOX	4.08E-05	666.38574	up
LOXL4	0.003532113	1134.1008	up
LPAR1	5.02E-07	361.0595	up
LPAR4	3.52E-04	769.57965	up
LRFN5	2.04E-05	3432.411	up
LRIG3	9.56E-04	710.72015	up
LRRK2	0.001896128	56.143425	up
LRRTM4	0.001217455	102.53022	up
LSAMP	1.60E-06	77.765114	up
LUZP4	0.00219027	140.69855	up
LY6H	2.67E-06	254.0602	up
MADCAM1	0.002480526	177.32721	up
MAGEA10	6.55E-04	550.77234	up
MAP1LC3A	0.001904424	36.111324	up
MAP1LC3C	1.67E-05	73.540504	up
MAPK4	2.21E-04	146.72054	up
MEFV	0.001605888	72.865616	up
MEOX2	1.93E-05	275.5825	up
MFAP4	0.00234179	723.2828	up
MFAP5	4.81E-05	47.543274	up
MGC27121	5.14E-05	168.04108	up
MMP12	5.05E-09	2709.5725	up
MMP13	5.84E-04	68.96292	up
MMP2	5.28E-06	61.831566	up
MMP3	8.51E-04	87.47894	up
MOSC1	5.81E-06	263.11017	up
MPDZ	5.09E-04	64.34496	up
MRAP	5.32E-04	60.589733	up
MRAS	3.58E-04	272.27283	up
MSI1	7.03E-04	255.04903	up
MSRB3	5.52E-05	44.87327	up
MTNR1B	0.004329397	40.839153	up
MTTP	5.17E-05	3380.7405	up
MUSK	1.39E-06	516.88776	up
MYH11	7.60E-06	750.68353	up
MYO5B	0.001162439	60.44324	up
MYOCD	1.72E-05	467.8155	up
NANOS2	0.003863444	196.19159	up
NAT8	9.45E-04	214.28177	up
NAV2	3.68E-06	53.121204	up

NEK5	0.001448384	113.17294	up
NFATC4	1.21E-06	202.98984	up
NFIB	3.61E-04	1049.692	up
NID1	1.57E-05	346.5735	up
NKX2-1	0.002989617	317.29813	up
NME5	5.88E-04	644.3234	up
NOTCH3	8.94E-04	1185.1599	up
NOX4	0.001169555	227.9215	up
NPSR1	4.82E-04	154.71399	up
NPY6R	0.001174096	241.03683	up
NR2E3	0.001526152	95.86641	up
NR2F1	1.46E-05	1087.3461	up
NRP2	0.001072524	42.229126	up
NRSN1	5.81E-05	793.55634	up
NRXN2	0.004514083	205.9631	up
NT5C1B	9.69E-05	273.5819	up
NUPR1	0.002202877	793.7373	up
NXPH2	0.003517729	67.41285	up
ODAM	0.001466551	117.64898	up
OLFML1	2.34E-05	1543.4946	up
OR10K2	4.87E-05	129.11392	up
OR10V1	0.00111295	213.17496	up
OR14J1	0.001548844	167.61324	up
OR1C1	9.25E-06	472.94186	up
OR1K1	1.32E-05	214.81801	up
OR1L1	0.00128794	99.23074	up
OR2B11	5.97E-04	3598.4714	up
OR2B2	0.002063465	43.159	up
OR2G3	8.86E-04	129.04976	up
OR2J3	0.001619971	493.38773	up
OR2T11	7.04E-04	100.30433	up
OR3A3	0.001021731	197.63304	up
OR4M1	4.07E-06	231.60004	up
OR51B5	0.003494288	66.16081	up
OR51G1	0.002982765	143.17113	up
OR56B4	1.71E-04	262.6104	up
OR5F1	6.39E-04	148.26363	up
OR5H14	5.54E-04	112.95109	up
OR6B1	8.09E-04	128.85097	up
OR6C65	1.42E-04	116.61705	up
OR6T1	3.12E-06	686.43414	up
OR8D1	8.88E-05	196.64044	up
OR8G1	2.57E-06	124.24818	up
OR911	0.004601611	835.7051	up
ORM2	4.73E-05	190.63899	up
P8	7.14E-04	378.74487	up
PALM	7.04E-06	56.240726	up
PANX3	0.004079317	360.93683	up
PCDH17	2.59E-06	9980.728	up
PCDHB9	0.003241059	187.77606	up
PCDHGC4	1.26E-04	72.09526	up
PDPN	6.57E-08	1008.50433	up
PDZK3	3.32E-05	99.90719	up
PEBP4	6.96E-05	112.78131	up
PEX5L	9.34E-04	174.05534	up
PGM5	0.001382236	225.2195	up
PGM5P2	2.60E-04	84.71546	up
PHACTR3	9.86E-05	192.2646	up
PIWIL3	0.002950644	140.30675	up
PKD1L2	0.001477617	57.44774	up
PKLR	0.003794031	48.050297	up
PLA2G2D	7.89E-04	230.62663	up
PLA2G7	2.37E-05	125.715775	up
PLAC9	8.54E-06	2086.843	up
PLB1	0.00359402	44.618774	up
PLCXD3	2.73E-09	160.30923	up
PLD5	0.001055989	229.84026	up

PLOD2	4.95E-04	181.44655	up
PLTP	0.003465322	51.93781	up
PNLIPRP3	0.003493602	234.86588	up
PON3	0.003802454	1631.0358	up
POU4F2	6.09E-04	359.31378	up
PPAP2B	9.79E-05	206.34972	up
PPARGC1A	0.002412457	198.6367	up
PPFIA2	8.06E-05	3782.9546	up
PPIC	0.001913146	235.22502	up
PPP1R1B	7.08E-04	37.030556	up
PRICKLE1	0.004674999	307.3969	up
PRKD1	3.67E-04	82.32182	up
PRM2	0.004219161	156.84526	up
PRODH2	0.003957356	90.40628	up
PROL1	0.001222166	888.17	up
PRRT2	9.77E-04	68.4832	up
PRRX1	5.55E-07	368.77744	up
PTGDS	7.10E-04	143.50684	up
PTPN21	0.00327386	607.1209	up
RAB39	4.01E-05	171.18495	up
RAG2	3.17E-05	213.9133	up
RALGDS	9.19E-05	14.426056	up
RAMP2	2.54E-04	452.15808	up
RAMP3	0.00446462	1118.2327	up
RARRES1	3.23E-04	124.77976	up
RASL12	3.84E-04	73.79914	up
RBP5	0.004485567	12.2856455	up
REG1B	7.30E-07	418.95358	up
REM1	0.003050858	249.94296	up
RERG	5.46E-04	327.1301	up
RET	5.39E-04	82.4246	up
RGMA	5.91E-04	26.182306	up
RGS17	0.001259865	199.95795	up
RHOJ	1.86E-05	134.22394	up
RNASE4	0.002249527	35.068375	up
RNF126P1	0.004019871	137.05261	up
RNF150	1.18E-04	3844.842	up
ROR2	1.61E-04	65.22503	up
RORB	0.003360013	136.6301	up
RPESP	1.75E-05	572.2533	up
RSPO1	0.001233968	720.04456	up
RSPO3	1.97E-05	372.38776	up
RTN1	6.31E-07	214.88795	up
S100A1	0.002133442	198.5234	up
S100A3	1.08E-06	696.359	up
S100A7A	0.001056142	339.94147	up
SCARA3	9.48E-09	270.27948	up
SCARA5	1.12E-04	232.99756	up
SCGB1A1	0.001438105	1483.2852	up
SCN2A	3.00E-05	155.35559	up
SCRG1	0.003827123	157.83875	up
SDC3	8.79E-05	825.1376	up
SDS	0.004168576	316.6017	up
SEBOX	9.36E-04	122.36459	up
SERPINA1	1.07E-04	58.425026	up
SERPINA3	1.46E-06	173.20938	up
SHANK1	6.65E-04	127.22191	up
SHANK3	1.85E-04	102.214836	up
SHE	7.45E-05	261.58145	up
SIGLEC15	5.88E-04	465.40466	up
SIGLEC16	1.62E-04	572.7653	up
SIGLEC8	6.38E-05	252.1981	up
SLC13A4	0.002034852	510.63922	up
SLC13A5	1.76E-05	169.95865	up
SLC18A1	3.95E-04	126.1464	up
SLC1A3	0.004293684	145.53325	up
SLC22A11	0.001525222	237.51735	up

SLC22A8	0.00132263	151.87383	up
SLC26A3	2.55E-04	298.81332	up
SLC2A10	1.17E-04	380.36444	up
SLC30A4	8.06E-04	117.31016	up
SLC35D3	3.74E-06	110.1957	up
SLC36A2	2.80E-04	406.93173	up
SLC6A10P	0.001531576	47.97308	up
SLC6A11	7.50E-04	3513.751	up
SLC6A17	0.001758472	73.8967	up
SLC7A10	9.65E-04	151.2397	up
SLCO2A1	9.91E-07	163.38977	up
SLCO2B1	1.61E-09	830.4838	up
SLN	2.67E-04	204.70993	up
SMAD9	2.63E-06	214.02264	up
SMOC2	6.00E-07	259.05295	up
SNAI2	1.59E-05	42.37089	up
SNAP25	8.95E-04	41.470043	up
SNAP91	2.56E-07	1499.8495	up
SOD3	1.73E-05	730.4651	up
SORBS1	0.002527741	53.59134	up
SORCS1	6.79E-04	144.44037	up
SOX11	0.00315207	4497.8096	up
SPANXB1	0.002434531	134.49309	up
SPARCL1	7.23E-08	2456.402	up
SPATA12	4.61E-04	106.80242	up
SPATA3	0.001180969	125.55184	up
SPHKAP	0.002730298	89.17387	up
SPIC	0.001247437	72.561165	up
SPRR1A	0.001425172	36.418526	up
SPRR2F	0.002502649	52.818954	up
ST5	2.06E-05	52.736828	up
ST6GALNAC5	1.67E-05	146.01675	up
STARD13	1.71E-06	92.28207	up
STEAP3	6.83E-04	66.18517	up
STEAP4	2.51E-07	351.58655	up
STGC3	9.52E-06	56.281895	up
STK32B	2.36E-04	280.14255	up
STOX2	6.47E-05	1338.115	up
SULT1C3	0.002288653	198.22928	up
SULT2B1	1.05E-04	50.864433	up
SVEP1	1.23E-08	229.75906	up
SYNPO2	6.48E-04	57.020897	up
SYT15	2.65E-04	23.90129	up
SYTL4	2.74E-04	473.2943	up
TAS1R1	3.00E-06	191.2977	up
TEAD3	8.00E-04	139.49211	up
TFF3	9.16E-07	2068.8347	up
TGM2	1.42E-05	164.37233	up
TGM3	0.002707904	28.728588	up
THBS2	1.32E-06	4278.7144	up
THSD4	0.001163739	917.2173	up
THY1	1.15E-04	733.15814	up
TIMP3	9.99E-04	299.3404	up
TINAGL1	1.12E-06	2395.152	up
TJP1	1.26E-05	46.303905	up
TLR2	0.003287221	58.478287	up
TLR8	2.15E-04	41.789314	up
TM4SF1	0.001288201	274.4715	up
TMEM171	1.49E-04	594.2408	up
TMEM195	0.003266833	74.15769	up
TMEM26	0.001393076	113.79935	up
TMEM75	8.80E-05	168.10236	up
TMTC1	2.72E-06	85.9973	up
TNFAIP8L3	0.004190413	49.924923	up
TNS1	6.67E-04	15.689797	up
TRPM3	2.65E-04	142.75385	up
TUBA3E	7.54E-04	137.89758	up

UNC13A	0.003771088	17.918474	up
UNC13C	4.83E-04	84.42842	up
UNC5A	7.22E-04	186.22348	up
VNN1	1.51E-04	289.19934	up
VWA1	0.001006489	153.42297	up
VWA3B	0.002667479	116.05175	up
WFDC10A	2.17E-04	244.91806	up
WFIKKN2	0.00300101	123.60882	up
WIPF3	0.004153004	142.43684	up
WISP2	3.66E-05	249.52612	up
WNT5A	0.00223808	294.5755	up
WNT7B	7.20E-05	508.14038	up
XCR1	2.28E-04	63.998413	up
XIRP2	0.002705287	2361.8362	up
XKR4	0.001337646	130.1594	up
XKR5	0.003984506	142.36823	up
XLKD1	1.78E-04	602.039	up
ZCCHC13	1.52E-04	1167.9548	up
ZDHHC1	0.003813832	384.42322	up
ZNF205	8.94E-05	155.21086	up
ZNF280A	0.001214629	95.34848	up
ZNF385D	1.56E-04	818.25183	up
ZNF521	0.001165658	590.53326	up
ZNF793	0.004648638	24.574905	up
ZSCAN4	1.23E-04	749.0319	up

Supplementary Table 22. GSEA of genes differentially expressed between Lennert Lymphoma and normal T-lymphocytes. Malignant phenotype-related processes were enriched, especially those related to neoplastic clone and microenvironment.

Neoplastic clone
ribonucleoprotein complex
cell growth
cell surface receptor linked signal transduction
protein-membrane targeting
angiogenesis
cell adhesion/cell-cell signaling
Microenvironment
response to wounding
acute-phase response
collagen catabolism
extracellular matrix
Undefined
Immune response

Supplementary Table 23. ANOVA analysis uncovers genes differentially expressed among F-PTCL, AITL and Tfh-PTCL/NOS.

Gene ID	Corrected p-value	Absolute Fold Change: AITL Vs. F-PTCL	Regulation AITL Vs. F-PTCL	Absolute Fold Change: AITL Vs. PTCL	Regulation AITL Vs. PTCL	Absolute Fold Change: F-PTCL Vs. PTCL	Regulation F-PTCL Vs. PTCL
AADACL1	0.001246996	9.904725	down	2.175747	down	4.5523324	up
AAMP	0.009295695	3.4186523	down	1.5310509	down	2.2328796	up
AASDHPPPT	1.07E-04	13.124998	down	3.144928	up	41.277176	up
AASS	4.74E-07	71.739685	down	13.6204605	down	5.267051	up
ABAT	0.004343298	11.01732	down	1.2647185	down	8.711282	up
ABCA10	1.15E-06	78.97764	down	14.27884	down	5.5310946	up
ABCD2	6.53E-05	30.074425	down	5.573287	down	5.3961735	up
ABCG1	5.14E-04	7.1144695	down	1.8464853	down	3.8529792	up
ACCN2	0.008303245	12.381062	down	1.832688	down	6.755684	up
ACN9	1.94E-05	21.397886	down	4.096282	down	5.2237315	up
ACSL5	6.54E-06	10.398006	down	1.3989923	down	7.4324985	up
ACSS2	2.66E-06	13.295097	down	2.1199014	down	6.2715645	up
ACTN1	0.00559174	2.795224	up	3.2780654	down	9.162927	down
ADD1	2.06E-07	39.967064	down	5.622322	down	7.10864	up
ADIPOR1	6.74E-04	10.277856	down	2.126429	down	4.8333874	up
AFAP1	2.46E-04	13.257741	down	1.689685	down	7.8462806	up
AFAP1L2	0.002347473	7.593563	down	1.7708074	down	4.288193	up
AFTP8	0.008122655	2.5097299	down	2.8622034	up	7.183357	up
AGL	6.68E-07	16.168526	down	1.1938038	down	13.543705	up
AGPAT1	0.002387813	4.1738486	down	1.2225398	up	5.102696	up
AHNAK	5.17E-07	8.019853	down	2.1932101	down	3.6566732	up
AIM2	6.94E-07	34.74169	down	23.48162	down	1.4795269	up
AKAP11	0.003588038	1.7516906	down	3.65986	up	6.4109416	up
ALAS1	6.07E-06	5.3228407	down	1.8349404	up	9.767095	up
ALDH1B1	1.25E-05	17.793158	down	2.9807088	down	5.9694376	up
ALDH6A1	2.14E-13	529.4471	down	48.15558	down	10.994508	up
ALG13	3.97E-05	24.527004	down	3.3062491	down	7.418378	up
ANGPTL4	1.79E-04	30.106907	down	10.276458	down	2.9296973	up
ANKRD32	6.97E-05	10.229765	down	1.6579145	down	6.1702604	up
ANKRD35	4.70E-10	286.24924	down	155.26956	down	1.8435636	up
ANKRD9	3.51E-05	3.8828113	up	21.909216	up	5.6426167	up
ANKS6	0.001738924	62.17433	down	7.7144723	down	8.059438	up
ANXA7	3.69E-08	37.629814	down	1.0734142	up	40.392372	up
AP2A1	0.002037566	2.4466686	down	4.1612477	up	10.181193	up
AP2B1	0.001094781	2.4232616	up	23.275143	up	9.604879	up
APLP1	7.62E-06	25.448235	down	5.720786	down	4.44838	up
APLP2	2.96E-07	197.61658	down	45.58968	down	4.334678	up
APOBEC3F	4.09E-05	4.235448	down	2.61094	down	1.6221929	up
APOBEC3G	9.90E-07	16.910416	down	22.663546	down	1.3402123	down
APOLD1	0.001122735	5.015797	up	61.081253	up	12.177776	up
AQR	3.64E-10	129.09029	down	24.508722	down	5.2671165	up
ARFGEF1	4.75E-08	63.772713	down	8.537048	down	7.4701123	up
ARID2	2.03E-05	37.394726	down	3.7664998	down	9.928244	up
ARL5A	1.48E-06	12.794352	down	1.4137621	down	9.049862	up
ARL6IP1	5.67E-05	13.101061	down	5.7216125	down	2.2897499	up
ARMET	0.003449182	3.5742214	up	2.9759593	down	10.636738	down
ARPC4	0.003511525	2.3130229	down	1.750456	up	4.048845	up
ARRB2	4.30E-06	5.1609178	down	1.1482829	down	4.4944654	up
ARSB	4.37E-04	8.794027	down	2.9599025	down	2.971053	up
ASB5	0.001178149	168.59918	down	45.047447	down	3.7427025	up
ASCC3	0.003937953	5.68304	down	1.7321751	down	3.280869	up
ATF5	0.003724473	1.7016205	down	9.788631	down	5.752536	down
ATM	1.76E-04	5.3131356	down	1.0619304	down	5.0032797	up
ATP11C	7.67E-08	6.114761	down	1.8620368	down	3.2839098	up
ATP2B1	4.41E-05	4.168872	down	1.1628553	up	4.847795	up
ATP5G2	0.005278971	5.0369673	down	1.4072149	down	3.579387	up
ATP5L	2.21E-08	48.565826	down	11.2997055	down	4.297974	up

ATP6V1G2	1.35E-04	5.6181703	down	1.9775796	up	11.110379	up
ATP8B2	0.009249712	1.3420045	down	4.074953	up	5.468606	up
ATPBD4	2.38E-05	23.61913	down	5.132805	down	4.601603	up
ATXN2	0.002202987	1.0571984	down	10.637157	down	10.061647	down
AUH	0.003189515	5.727949	up	1.3075429	down	7.489539	down
BAG5	2.63E-04	12.724475	down	1.2921387	down	9.847608	up
BAZ1B	2.13E-04	4.30323	up	23.257877	up	5.4047494	up
BBS7	1.64E-04	7.690821	down	1.2984395	down	5.923126	up
BCAP31	0.00796214	1.5180069	up	4.866111	down	7.386791	down
BCAS2	2.81E-04	17.096949	down	4.900972	down	3.4884803	up
BCCIP	3.24E-05	3.0433586	down	1.3689297	up	4.166144	up
BCL7B	6.95E-04	1.955827	up	1.5303007	down	2.9930036	down
BFAR	0.001193434	9.199177	down	2.8891294	up	26.577612	up
BRCA1	2.79E-04	13.979983	down	7.6151934	down	1.8358012	up
BRE	8.59E-05	3.7354674	down	1.4953438	up	5.585808	up
BRWD1	2.49E-06	9.2595	down	1.5731457	down	5.8859763	up
BTBD1	3.97E-04	5.191556	down	1.0548459	up	5.476292	up
C11ORF2	0.001575938	4.8104544	up	1.3838251	down	6.656827	down
C11ORF46	0.001723428	2.1481802	up	22.80408	up	10.615533	up
C11ORF57	0.00441437	10.6306095	down	2.7204897	down	3.9076092	up
C11ORF58	3.21E-12	203.9501	down	24.138603	down	8.449126	up
C12ORF10	0.003947689	1.7051575	down	9.361445	down	5.490077	down
C12ORF30	4.36E-06	22.89879	down	3.389835	down	6.755136	up
C12ORF35	8.80E-08	26.772688	down	2.7401166	down	9.77064	up
C14ORF118	2.49E-04	3.0249796	down	4.318876	up	13.064511	up
C14ORF135	0.00265581	10.2977915	down	2.067354	down	4.9811463	up
C14ORF138	2.58E-06	5.4421487	down	3.3879352	up	18.437647	up
C14ORF142	5.23E-04	9.858709	down	1.0932045	down	9.018175	up
C14ORF43	4.91E-05	2.159268	down	3.4558392	up	7.4620814	up
C14ORF80	0.007015869	1.0889019	up	7.9593167	down	8.666915	down
C14ORF85	1.13E-04	42.235912	down	149.10243	down	3.5302281	down
C15ORF5	9.99E-04	11.17792	down	18.255774	down	1.6331993	down
C17ORF70	0.004404484	1.1758431	down	13.4976225	down	11.4791	down
C17ORF81	4.96E-06	5.5671334	down	1.0218657	up	5.688863	up
C18ORF10	1.03E-04	30.550146	down	12.206318	down	2.5028143	up
C18ORF22	0.006550901	7.782738	up	1.7032353	down	13.255833	down
C18ORF54	9.54E-10	125.29043	down	10.372313	down	12.079316	up
C19ORF12	0.006464407	4.031581	down	2.1703336	down	1.8575857	up
C1D	1.22E-05	20.613302	down	1.2006072	down	17.16907	up
C1GALT1C1	6.17E-08	36.576504	down	3.448389	down	10.606838	up
C1ORF25	1.68E-05	14.3245325	down	4.4451237	down	3.2225273	up
C1ORF9	3.24E-04	14.680495	down	1.0514292	up	15.435501	up
C1QBP	6.90E-07	25.762548	up	12.265031	up	2.100488	down
C20ORF7	0.001573397	4.659437	down	1.5425037	up	7.187198	up
C20ORF94	4.34E-05	6.4175563	down	4.157234	down	1.543708	up
C20ORF96	1.08E-04	530.22955	down	128.80238	down	4.116612	up
C2ORF56	0.001005175	2.7590113	down	2.1958876	down	1.2564447	up
C2ORF63	1.86E-05	20.037655	down	5.762256	down	3.4773974	up
C3ORF17	4.37E-05	3.8582609	down	1.4391828	up	5.552743	up
C3ORF42	1.30E-05	3.4663858	down	5.351521	up	18.550438	up
C4ORF18	0.007799124	13.150004	down	1.3149791	down	10.000161	up
C4ORF43	0.004450902	9.963679	down	1.5402771	up	15.346827	up
C5ORF34	2.73E-05	171.51009	down	44.67423	down	3.8391283	up
C6ORF204	0.005850927	4.4938726	down	1.3733133	up	6.1714954	up
C7ORF54	0.004138387	1.2066888	up	8.320272	down	10.039979	down
C8ORF33	1.70E-09	8.610316	down	5.143032	down	1.6741713	up
C9ORF10OS	0.001592465	8.3046665	down	3.94565	up	32.76731	up
C9ORF142	9.11E-04	4.5617256	up	5.017203	down	22.887108	down
C9ORF41	0.002140351	3.3928452	up	4.449594	up	1.3114638	up
C9ORF5	0.007543863	2.5723488	down	4.9881954	up	12.83138	up
C9ORF6	1.07E-04	44.5116	down	6.7946615	down	6.550966	up
C9ORF72	1.27E-04	13.662694	down	1.5791752	down	8.651792	up
CA12	0.007189686	7.2197328	down	2.1882696	down	3.299288	up
CAMK1D	6.40E-04	8.236349	down	1.0860595	up	8.945166	up
CAMK2D	3.63E-05	5.6928477	down	1.0834448	down	5.254396	up
CAMK4	2.92E-06	110.37201	down	2.7331512	down	40.382694	up
CAMKK2	4.07E-06	16.935188	down	4.238069	down	3.9959671	up

CAND1	7.61E-06	15.086078	down	1.3366377	down	11.286586	up
CAPRIN1	7.79E-06	8.620933	down	1.4162129	up	12.209074	up
CAPZB	4.78E-06	93.08448	down	67.7006	down	1.3749435	up
CASP4	3.40E-07	15.640286	down	1.06344	down	14.70726	up
CASP6	0.004623504	2.143239	down	4.361602	up	9.347956	up
CASP8	0.00325764	1.6286442	up	4.077292	up	2.5034883	up
CBL	4.02E-06	7.169271	down	1.15638	down	6.199753	up
CCBL2	1.01E-04	2.6370053	down	2.5427816	up	6.705328	up
CCDC117	0.00306498	31.154354	down	4.23758	down	7.351923	up
CCDC132	1.73E-06	12.1627035	down	1.4434386	down	8.426201	up
CCDC28B	1.07E-04	21.085524	down	13.018768	down	1.6196252	up
CCDC34	3.87E-05	9.583994	down	1.2927667	down	7.4135528	up
CCDC75	0.004216792	6.0038686	down	1.8100219	up	10.867133	up
CCDC84	6.38E-05	52.152954	up	128.052	up	2.4553163	up
CCDC91	1.29E-05	22.582506	down	2.4538512	down	9.202882	up
CCNG1	2.55E-04	6.701451	down	4.106789	down	1.6317983	up
CCNT2	2.13E-08	9.104096	down	1.2217581	up	11.123002	up
CCNY	7.29E-04	11.202788	down	2.321396	down	4.825884	up
CD14	1.11E-04	13.002725	down	2.5200295	down	5.159751	up
CD302	1.25E-04	30.98856	down	2.5040636	down	12.375309	up
CD46	0.002449624	2.484371	up	11.242708	up	4.5253744	up
CD86	0.002879767	4.4291444	down	1.3726383	up	6.079613	up
CDC14A	1.31E-05	6.318688	down	2.1705766	up	13.715196	up
CDC2L5	2.20E-05	6.060674	down	1.6446925	up	9.967944	up
CDC42	5.42E-04	1.9608763	down	5.6598606	up	11.098288	up
CDC7	0.005795735	17.057585	down	1.7067695	down	9.994079	up
CDH6	4.76E-09	237.00363	down	48.682053	down	4.8683987	up
CDYL	7.34E-05	9.144621	down	1.5190665	up	13.891286	up
CENPH	0.002678235	9.034363	up	10.292864	up	1.1393018	up
CENTA1	0.008997127	1.5869792	up	5.0921755	down	8.081176	down
CENTB2	1.99E-08	28.440783	down	1.5682466	down	18.135399	up
CENTD1	9.01E-06	8.903371	down	2.6250186	up	23.371517	up
CEP170	0.003953619	1.3944284	up	8.709852	up	6.246181	up
CFD	0.008404002	2.1304965	down	12.296059	down	5.7714524	down
CGGBP1	0.001935814	2.5231285	down	2.2492425	up	5.675128	up
CHD6	9.24E-04	6.9827895	down	1.8124697	down	3.8526375	up
CHL1	1.06E-04	35.08638	down	2.9682133	down	11.820706	up
CHN1	3.51E-06	27.954819	down	1.0837982	up	30.29738	up
CHORDC1	4.64E-04	19.114462	down	1.0751766	down	17.777973	up
CHPT1	1.95E-04	5.700605	down	1.0872836	up	6.1981745	up
CICK0721Q,1	0.008639534	1.8583665	down	11.315681	up	21.028683	up
CLASP2	0.002288599	8.182097	up	80.66772	up	9.859052	up
CLEC2D	0.002764909	1.6594439	down	6.2119575	up	10.308395	up
CLIP1	0.003852108	1.8752615	down	2.679027	up	5.023876	up
CLTA	1.74E-05	6.8595667	down	1.7558178	up	12.044148	up
CMTM3	9.89E-06	4.514377	down	1.8920391	up	8.541378	up
CNNM2	0.002910974	10.870246	down	3.7469494	down	2.901092	up
CNOT1	4.99E-08	11.741206	down	1.1164685	up	13.108686	up
CNOT7	8.15E-07	7.1379547	down	1.029604	down	6.932718	up
CNPY3	2.73E-05	6.626014	up	38.411995	up	5.79715	up
COL5A1	5.09E-04	28.602577	down	4.3755636	down	6.5368896	up
COL6A3	0.008423174	5.66545	down	1.5018104	up	8.508432	up
COL8A1	8.47E-04	26.323908	down	3.871358	down	6.799658	up
COMM10	0.002490725	10.726184	down	1.0212939	up	10.954586	up
COMM6	3.72E-06	11.820783	down	1.0880262	up	12.861322	up
COMM8	3.42E-07	122.818245	down	9.94667	down	12.347673	up
COPS2	4.11E-06	69.262344	down	13.851325	down	5.000412	up
COPS8	0.006057812	3.4114227	down	2.048898	up	6.9896564	up
COQ2	3.34E-04	320.44833	down	31.02767	down	10.327825	up
COQ7	6.65E-06	7.584196	up	96.48538	up	12.721901	up
CPEB3	8.12E-08	80.90322	down	33.154354	down	2.440199	up
CPNE8	3.67E-04	21.38781	down	3.610503	down	5.923776	up
CRLF3	0.008547629	7.5367403	down	1.0050765	down	7.498674	up
CROP	0.003121943	8.063984	down	1.2076457	down	6.6774416	up
CSF3R	0.006368076	10.450152	down	2.969644	down	3.5189915	up
CSMD2	6.50E-04	48.579887	down	28.481722	down	1.7056515	up
CSTF3	0.002729614	1.429186	down	5.0671988	up	7.2419696	up

CTAGE5	3.57E-04	14.72133	down	1.5155886	down	9.713276	up
CTHRC1	6.39E-07	179.28728	down	20.111801	down	8.91453	up
CTPS2	1.26E-04	2.687841	down	6.2268977	up	16.736912	up
CUGBP1	2.78E-05	4.234678	down	1.3432223	up	5.6881137	up
CUL4A	8.63E-04	30.053667	down	4.3952765	down	6.8377194	up
CXCL11	1.45E-05	136.15999	down	11.336061	down	12.011225	up
CXORF40A	9.92E-07	4.845087	up	24.014153	up	4.9563923	up
CYP20A1	5.88E-05	8.071167	down	1.4811857	up	11.954899	up
CYP2U1	5.27E-04	53.00102	down	13.726109	down	3.8613293	up
CYP7B1	0.007764282	19.698	down	4.8605137	down	4.0526586	up
DAAM1	1.68E-04	42.180164	down	25.258785	down	1.6699207	up
DARS	0.001079141	1.0129716	up	4.2799354	down	4.335453	down
DBR1	1.59E-05	10.893142	down	4.095151	down	2.6600099	up
DBT	0.009230945	1.0450393	up	5.736111	down	5.994461	down
DCK	2.95E-04	7.9042015	down	1.6174058	up	12.784302	up
DCTN6	6.34E-07	44.22589	down	4.394694	down	10.063475	up
DDI2	1.73E-04	2.476255	up	9.440678	up	3.812482	up
DDT	0.007228914	1.0756946	up	5.741438	down	6.1760335	down
DDX21	0.001387818	1.3415962	down	16.138866	up	21.651844	up
DDX59	1.00E-04	7.1355295	down	1.0447564	up	7.4548907	up
DEPDC1B	0.003059834	30.601454	down	3.5997372	down	8.501024	up
DEPDC6	0.001671258	59.211323	down	9.433188	down	6.276916	up
DHRS13	0.0012034	3.529708	down	15.06404	down	4.267787	down
DIAPH3	2.62E-04	7.0934224	down	4.7782164	down	1.4845337	up
DIP2A	4.29E-04	1.6176693	up	6.7515445	up	4.1736245	up
DLEU2L	0.004851418	18.862309	down	1.9830962	down	9.511544	up
DNAJB14	0.003783139	2.6863444	down	1.0365125	up	2.7844293	up
DNAJB6	0.001588501	1.6615915	up	14.124414	up	8.500533	up
DNAJC21	5.42E-05	16.3427	down	6.1820235	down	2.643584	up
DNMT3A	5.09E-05	3.2664802	up	23.469175	up	7.1848526	up
DOK3	0.004626186	7.406154	up	4.551228	down	33.707104	down
DPH3	0.006211512	2.4159834	up	6.5938597	up	2.7292652	up
DPY30	1.63E-07	5.6862535	up	48.782364	up	8.5789995	up
DSCC1	6.53E-04	8.940125	down	9.444442	down	1.0564104	down
DSEL	1.57E-07	204.17982	down	20.554495	down	9.933589	up
DSP	1.86E-04	51.593758	down	8.99091	down	5.7384357	up
DST	1.51E-05	8.180347	down	1.568211	up	12.828513	up
DTWD1	2.02E-04	1.930194	down	3.8965423	up	7.521082	up
DUSP22	9.30E-04	9.075396	down	1.0903138	up	9.89503	up
DUSP3	0.001856833	5.175609	down	13.1385355	down	2.5385492	down
DYNC2LI1	0.001033654	8.683132	down	1.1889133	up	10.323492	up
DYNLT3	2.09E-06	17.349197	down	2.444413	down	7.09749	up
DYRK1A	7.99E-07	11.732118	down	1.2438458	down	9.43213	up
DYRK2	0.002471531	5.876634	down	1.0065339	up	5.9150314	up
EAF1	0.008829953	13.536249	down	1.8206338	down	7.4349113	up
EDEM3	2.87E-05	23.759974	down	6.2795315	down	3.7837174	up
EEF1D	0.003241727	1.7025343	up	6.969356	up	4.0935183	up
EEF1E1	7.69E-04	32.327827	down	6.9569054	down	4.646868	up
EFNA1	9.55E-07	8.454091	down	1.3131679	up	11.101642	up
EGFR	2.45E-06	28.686802	down	2.0741303	down	13.83076	up
EGLN2	6.36E-04	9.404717	down	5.6819205	down	1.6552004	up
EHD4	0.004176542	22.756878	up	37.869507	up	1.6640906	up
EID2B	2.95E-04	52.563522	down	69.699135	down	1.3259982	down
EIF1AX	2.57E-04	4.8611574	down	1.7993506	up	8.746927	up
EIF3J	0.003042212	5.180734	down	2.5675426	up	13.301756	up
EIF4A1	0.008876865	2.7072546	up	3.8327951	up	1.4157498	up
EIF5A2	2.14E-07	714.739	down	96.493546	down	7.4071174	up
EOMES	0.002033323	1.0102395	down	10.905686	down	10.795148	down
EPB41	7.74E-04	6.291788	down	1.3555015	up	8.528528	up
EPB41L2	1.90E-04	37.55555	down	2.9290788	down	12.821627	up
EPN1	0.00559278	1.2299707	down	9.616178	down	7.8182178	down
ERAL1	4.00E-04	2.4313023	down	10.915455	down	4.48955	down
ERC1	0.001633283	5.3521786	down	1.0153263	down	5.271388	up
ERMN	1.27E-05	18.369017	down	1.1965694	down	15.3513975	up
ETV6	0.001186558	2.4133296	down	15.039108	down	6.2316847	down
EVI2B	0.006932993	13.780733	down	1.4690162	down	9.380928	up
FABP5	0.009540696	4.996763	down	1.2458599	down	4.010694	up

FAHD1	0.004465252	9.26783	down	1.5594801	down	5.942898	up
FAIM	3.85E-04	7.07123	down	1.2608625	up	8.915849	up
FAM108B1	1.59E-05	4.585267	down	2.2000718	up	10.087914	up
FAM116A	5.07E-05	11.725	down	1.153098	down	10.168262	up
FAM122A	8.54E-07	95.91794	down	11.173426	down	8.584471	up
FAM126A	5.19E-06	136.32053	down	20.556187	down	6.6316056	up
FAM126B	1.64E-07	40.280502	down	2.846622	down	14.150282	up
FAM133B	0.00521203	5.605519	down	2.2008693	down	2.5469568	up
FAM134B	5.95E-04	1.3238282	up	9.194124	up	6.9451036	up
FAM135A	1.88E-10	473.1892	down	11.565421	down	40.914135	up
FAM158A	0.001960101	2.6322176	up	5.78529	down	15.228142	down
FAM177A1	3.28E-05	5.1595407	down	1.3700769	down	3.7658768	up
FAM38A	0.003196077	2.0549228	up	5.9086227	down	12.141764	down
FAM48A	1.25E-04	2.3725362	up	23.848028	up	10.051703	up
FAM49B	1.77E-06	14.621328	down	1.3007001	down	11.241121	up
FAM53B	2.25E-07	41.035698	down	23.678072	down	1.7330678	up
FAM98A	0.00166707	5.7734246	down	13.817567	down	2.393305	down
FAM98B	0.006262566	6.4610553	down	3.3611047	down	1.9223013	up
FANCC	0.009213107	10.501526	down	2.3458505	down	4.476639	up
FAS	0.008276012	9.734545	down	1.2582617	down	7.736503	up
FBXL10	1.03E-04	16.486692	down	2.3955095	down	6.882332	up
FBXL5	5.00E-06	6.700698	down	1.3204118	up	8.84768	up
FBXO11	2.00E-08	7.0109916	down	2.167934	down	3.2339509	up
FBXO3	2.61E-06	15.472262	down	1.0076846	down	15.354269	up
FBXO30	6.41E-07	6.3222632	down	1.7054402	up	10.782243	up
FBXO5	4.83E-09	157.02716	down	22.07946	down	7.111912	up
FBXW11	0.001750636	9.120728	down	1.0144235	down	8.991045	up
FBXW7	2.31E-04	4.76063	down	1.1840707	down	4.0205626	up
FEM1C	7.81E-09	40.470467	down	18.65839	down	2.1690226	up
FEN1	0.00178487	4.5905895	up	2.0807688	up	2.2061985	down
FGFR1OP2	0.002117208	8.191137	down	7.035421	down	1.1642711	up
FGR	4.54E-04	10.95887	down	10.045702	down	1.0909014	up
FKBP9	1.14E-04	31.178705	down	1.2519028	down	24.905056	up
FN3KRP	0.001284373	209.12703	down	30.18241	down	6.928772	up
FNTA	5.20E-05	3.246649	down	1.1845907	up	3.8459501	up
FOXK1	3.19E-05	6.9784207	down	3.311436	down	2.1073701	up
FOXN3	0.002008155	50.237125	down	7.7715883	down	6.464203	up
FOXO4	3.69E-04	13.497975	down	16.194887	down	1.1998012	down
FOXP1	0.003953058	6.2018867	down	1.4898136	down	4.1628613	up
FYB	2.03E-06	5.7482224	down	2.287686	up	13.150131	up
FYTTD1	6.49E-04	5.073023	down	2.5889766	down	1.9594704	up
GABARPL2	5.69E-10	14.737273	down	5.8641047	down	2.513133	up
GABPA	1.55E-09	1117.9828	down	20.69278	down	54.02769	up
GALNT1	1.23E-07	193.9958	down	13.533997	down	14.333962	up
GALNT7	5.63E-04	6.7276382	down	3.3531816	up	22.558992	up
GBP4	0.002967842	7.4265313	down	1.4224347	up	10.563755	up
GCLM	0.002786256	65.47651	down	38.46505	down	1.7022339	up
GCN1L1	0.008817226	2.2645416	down	9.124068	down	4.029101	down
GCNT1	4.69E-05	59.21103	down	44.644897	down	1.3262664	up
GFPT1	2.76E-10	234.82909	down	32.4352	down	7.2399464	up
GFRA1	1.69E-05	25.143847	down	2.5656877	down	9.800043	up
GGNBP2	7.94E-06	26.503847	up	149.64116	up	5.6460156	up
GIMAP2	0.001107436	13.35949	down	1.0795429	up	14.422142	up
GIMAP5	3.55E-04	163.69382	down	267.79944	down	1.6359779	down
GJC1	0.004110443	15.1259	down	7.302077	down	2.071452	up
GLB1L	0.006900696	29.799995	down	24.494576	down	1.2165959	up
GLMN	2.75E-04	10.229098	down	1.0611	up	10.854096	up
GMEB1	0.004739895	9.7296715	up	13.283859	up	1.3652939	up
GNAI1	2.75E-12	257.3373	down	69.33706	down	3.7113967	up
GNAQ	7.62E-05	2.193989	down	16.596046	up	36.411545	up
GNAS	2.94E-07	29.977169	down	1.7149321	down	17.480091	up
GNPTG	0.00609777	24.386105	up	14.094748	up	1.7301553	down
GOLT1B	0.006657008	25.09118	down	1.269323	up	31.848818	up
GOSR2	0.001350936	8.605287	down	1.6781911	up	14.441317	up
GPBP1L1	0.005646233	18.246496	down	4.8769503	down	3.7413747	up
GPR177	3.36E-04	11.310786	down	1.3638299	down	8.293401	up
GPR52	9.81E-05	6.914979	down	1.0448744	up	7.225284	up

GPR64	0.001883869	45.255013	down	5.175649	down	8.743833	up
GPX1	0.005916653	14.681089	down	1.3859973	down	10.592436	up
GRINL1A	0.001228461	1.0850697	down	11.419933	up	12.391422	up
GSDMD	0.009581806	1.0123322	down	6.7394004	down	6.657301	down
GSR	7.31E-04	2.078229	down	5.922943	down	2.849995	down
GTF2A1	0.006253314	10.044042	down	1.4753186	down	6.808049	up
GTF2F2	0.001569423	10.505913	down	2.0282261	down	5.1798525	up
GTF2H2	0.005379363	1.719688	down	10.466433	up	17.998997	up
GTF2H3	1.38E-04	32.12152	down	13.827334	down	2.3230453	up
GUCY1A3	6.07E-07	118.35761	down	19.728878	down	5.999207	up
H2AFY	0.002108078	9.820655	down	2.0233867	down	4.8535733	up
HBXIP	6.33E-08	4.93098	up	44.76022	up	9.077346	up
HDAC9	0.001077939	17.959415	down	1.8112288	down	9.915596	up
HDHD3	0.002759276	1.8215264	down	9.350478	down	5.13332	down
HEATR3	0.001358968	11.889785	down	1.0882158	down	10.925944	up
HECA	2.61E-09	10.711477	down	2.2539809	up	24.14347	up
HERPUD2	3.59E-05	10.391134	down	2.0004613	down	5.1943674	up
HHEX	1.21E-05	15.716794	down	1.9019333	down	8.263589	up
HIAT1	4.17E-08	12.991061	down	1.6441956	down	7.9011655	up
HINT2	0.004989176	4.24004	up	2.6247795	down	11.129169	down
HIPK1	5.81E-04	7.198212	down	1.0437564	down	6.8964486	up
HIPK2	0.002110592	1.7727716	down	11.906194	down	6.7161465	down
HIST1H1E	0.004333782	2.6260324	down	4.1076775	up	10.786895	up
HK1	1.43E-05	11.173793	down	1.5568973	down	7.176962	up
HLA-E	3.31E-06	36.091705	down	126.870316	down	3.5152214	down
HMGA1	3.47E-07	17.937365	down	2.8732607	down	6.2428613	up
HMGN1	0.009876753	1.0394559	up	18.312157	up	17.61706	up
HN1	0.00989945	7.129945	down	2.9131281	up	20.770443	up
HNRNPH2	0.001185441	10.414838	down	1.4630586	down	7.118539	up
HNRPC	0.002507886	6.3655343	up	12.152678	up	1.9091371	up
HNRPK	0.004013233	1.7446643	down	16.115274	up	28.115753	up
HOOK3	2.08E-05	9.218437	down	1.5258414	down	6.041543	up
HOXA2	3.86E-13	237.02618	down	53.005295	down	4.4717455	up
HOXC6	8.60E-04	9.550111	down	2.2786646	down	4.1911	up
HSPD1	2.21E-04	4.726075	down	2.4694428	up	11.670771	up
ICK	1.67E-06	55.393986	down	5.736879	down	9.65577	up
ID4	0.007065751	53.52036	down	5.87956	down	9.102783	up
IDH1	0.006324537	1.9263746	up	8.435468	up	4.378934	up
IGF1	5.01E-07	185.71706	down	16.044197	down	11.575339	up
IGF2BP2	0.003339899	1.1057867	down	10.079997	down	9.115681	down
IIP45	0.006701313	28.405573	up	108.87883	up	3.8330088	up
IKBKAP	0.003471525	14.781226	down	2.9808226	down	4.958774	up
IL33	5.95E-06	397.38214	down	12.628908	down	31.466072	up
IL7	1.11E-05	167.70605	down	17.384308	down	9.646979	up
IMPDH1	8.74E-06	15.215018	down	3.9641762	down	3.8381288	up
INCENP	0.002613781	3.1451616	up	14.045565	up	4.465769	up
INPP5F	0.002803432	6.945363	down	2.8211236	down	2.4619136	up
IPO8	0.003751391	2.0631042	down	8.538611	up	17.616047	up
IQCC	7.30E-04	7.0553875	down	11.905117	down	1.6873797	down
IRAK1	0.004043514	2.61604	up	4.170231	down	10.90949	down
IRF2	6.91E-06	19.785364	down	4.089206	down	4.8384356	up
ITFG1	2.09E-04	13.572194	down	1.5725269	down	8.630818	up
ITGB1	3.97E-13	10.69448	down	1.3682294	down	7.8162904	up
ITM2B	7.81E-06	134.46323	down	6.3441377	down	21.194881	up
JARID1A	8.96E-05	1123.0938	down	283.76633	down	3.9578133	up
JMY	0.001278945	2.9973602	up	17.05962	up	5.691548	up
KCNJ10	0.001460063	2.7032263	down	11.204566	down	4.144886	down
KCTD17	6.49E-04	9.5382185	down	5.702253	down	1.6727105	up
KHDRBS3	1.97E-10	200.35898	down	163.35817	down	1.226501	up
KIAA1128	5.51E-04	1.677084	up	9.3544445	up	5.577803	up
KIAA1143	0.005855662	13.462083	down	2.4121325	down	5.580987	up
KIAA1199	0.009992975	76.85203	down	2.6680794	down	28.80425	up
KIAA1274	0.005573234	7.813993	down	19.980244	down	2.556982	down
KIAA1333	3.01E-07	157.43074	down	34.416027	down	4.574344	up
KIAA1370	2.20E-07	22.017706	down	1.4862624	down	14.814141	up
KIAA1704	1.97E-05	41.120255	down	4.1744547	down	9.850449	up
KIR3DL3	0.007881652	27.608913	down	17.119606	down	1.612707	up

KITLG	0.004934522	6.2074533	down	1.1776636	up	7.3102922	up
KLF12	8.00E-04	6.409878	down	1.3745602	up	8.810764	up
KLF3	0.007196833	1.5176562	down	4.408005	up	6.689837	up
KLHL14	1.09E-08	159.2065	down	19.63116	down	8.10989	up
KLHL5	0.003410083	1.9573686	down	3.578653	up	7.0047436	up
KLHL7	5.12E-05	35.6645	down	4.233876	down	8.423607	up
KMO	1.71E-13	236.06337	down	54.359653	down	4.342621	up
KPNA3	6.10E-06	13.830012	down	2.2781088	up	31.506273	up
KRAS	4.50E-12	14.512139	down	1.3210471	up	19.171223	up
KRIT1	9.59E-11	121.00392	down	14.98657	down	8.074157	up
KTELC1	5.24E-06	23.11791	down	15.097835	down	1.5312067	up
LAMB1	8.71E-06	21.627012	down	7.4199057	down	2.9147289	up
LAMP2	0.001239809	5.2560015	down	1.0154163	up	5.33703	up
LARP4	0.009858452	7.2839923	down	4.149282	down	1.7554827	up
LCORL	2.64E-08	181.3411	down	14.798675	down	12.253874	up
LEPR	8.25E-05	11.61754	down	1.4851083	down	7.822688	up
LFNG	0.00154863	4.9705286	down	1.6865714	up	8.383152	up
LGALS8	3.30E-10	12.158772	down	2.3452728	down	5.184375	up
LIG4	4.34E-09	47.895954	down	7.127392	down	6.7199836	up
LIN7C	5.98E-07	74.66467	down	5.855038	down	12.752212	up
LMBRD2	1.26E-07	42.713417	down	8.882486	down	4.808723	up
LNX2	0.001184876	11.066767	down	1.2263937	down	9.0238285	up
LOC389517	6.19E-05	30.220291	down	3.8523164	down	7.8447065	up
LOC400986	3.25E-06	20.030231	down	4.1007776	down	4.8844953	up
LOC440295	0.002048643	67.57112	down	14.920686	down	4.528687	up
LOC649159	0.009859664	21.845201	down	2.065604	down	10.575697	up
LOXL1	0.001091797	1.7497603	up	18.263783	up	10.437879	up
LPCAT4	1.71E-04	10.496793	up	46.757126	up	4.4544196	up
LPP	0.00422731	1.81944	down	11.011743	down	6.0522704	down
LRBA	2.25E-05	4.965517	up	7.1164956	up	1.4331832	up
LRRC41	9.49E-05	12.876652	down	5.590602	down	2.303267	up
LRRCC1	7.49E-06	9.134536	down	1.132945	up	10.3489275	up
LRRN2	0.005490519	22.002138	down	8.403005	down	2.6183655	up
LUM	1.02E-08	214.79869	down	10.248967	down	20.958082	up
LYPLA1	9.42E-08	399.4567	down	23.249031	down	17.181654	up
M6PRBP1	0.001523081	9.723795	down	5.018289	down	1.9376711	up
MAK10	0.009923156	2.375538	down	2.0057766	up	4.764799	up
MAML2	3.54E-05	2.7321782	down	2.583916	up	7.059718	up
MAN2A1	9.40E-07	69.97159	down	13.377403	down	5.2305813	up
MAP9	0.003974533	10.266039	down	3.3316138	down	3.081401	up
MARS2	6.22E-07	12.773468	down	1.3107413	up	16.742716	up
MATR3	3.02E-04	1.2734149	down	4.327333	up	5.51049	up
MBD2	0.009495194	9.130391	down	1.1638645	down	7.844892	up
MBNL3	1.87E-04	10.553734	down	1.2641286	down	8.348622	up
MCM8	1.93E-04	23.391054	down	2.6916099	down	8.690359	up
MCTP1	4.38E-06	12.204741	down	1.1294104	down	10.806294	up
ME2	1.47E-05	17.5825	down	1.8336841	down	9.588622	up
MED13	3.21E-05	10.258539	down	1.8127862	down	5.658991	up
MED23	0.005417526	4.8839235	down	1.011102	down	4.830298	up
MED30	7.23E-06	18.463022	up	111.39466	up	6.0333924	up
MED31	6.15E-09	403.7064	down	34.833733	down	11.589523	up
MEF2A	0.004415452	1.1514846	down	10.025066	up	11.543711	up
MET	2.60E-06	19.414341	down	7.3057513	down	2.6574051	up
METT10D	0.002912228	9.853692	up	15.992661	up	1.623012	up
METTL1	0.001330216	29.648531	down	5.47839	down	5.411906	up
MFF	0.001725928	18.361006	down	1.9070679	down	9.6278715	up
MFN1	0.003977393	16.017588	down	2.4632297	down	6.502676	up
MOBKL1A	0.002852561	9.310981	down	4.508898	down	2.065024	up
MOSPD2	2.20E-09	486.43158	down	67.09868	down	7.249493	up
MOXD1	0.007334051	21.313742	down	2.5787258	down	8.265222	up
MPDZ	2.87E-05	8.733337	down	2.4237306	down	3.6032617	up
MRC1L1	0.004563219	1.7223642	up	22.986298	up	13.345782	up
MRPL3	1.36E-06	42.637222	down	7.13509	down	5.97571	up
MRPS12	0.001736133	7.601594	down	1.5771123	down	4.8199444	up
MRPS16	0.00973183	1.6724702	up	6.701245	down	11.207633	down
MRPS28	0.005862697	1.4914746	up	17.222477	up	11.547282	up
MS4A4A	1.77E-09	52.302067	down	1.6558609	down	31.586025	up

MS4A7	9.88E-05	2.872869	up	15.16044	up	5.2771077	up
MSH2	0.003212148	2.483918	up	11.702062	up	4.71113	up
MST4	4.65E-04	6.4599204	down	1.8683835	up	12.069609	up
MTM1	1.12E-06	1.391843	up	94.294304	up	67.7478	up
MTMR9	4.96E-05	9.30774	down	1.9763287	down	4.7096114	up
MTX2	5.12E-08	26.983728	down	2.4727705	down	10.912346	up
MUC1	0.007696882	8.181167	down	4.6583314	down	1.7562441	up
MYADM	2.13E-04	4.1062875	down	2.1739745	up	8.926965	up
MYLK	1.20E-06	18.286156	down	1.9677991	down	9.292695	up
MYNN	0.006479343	17.98544	down	3.920522	down	4.587511	up
MYST4	0.006286535	8.624426	down	3.8666904	up	33.347977	up
N4BP2L1	0.00767875	7.796064	down	1.1935241	down	6.531971	up
N6AMT1	6.98E-04	8.429369	down	1.7085234	down	4.9337163	up
NAB1	0.007626717	7.284132	down	1.1189065	down	6.510046	up
NAP1L1	0.002751237	5.7457547	down	1.2047071	up	6.9219522	up
NAPEPLD	1.25E-10	290.15524	down	7.897009	down	36.74243	up
NAT11	0.003193242	3.1503613	up	50.628826	up	16.070797	up
NAT13	0.00676134	3.162337	down	1.413904	up	4.471241	up
NAV2	0.004129249	5.6218333	down	1.2648709	down	4.4445906	up
NBPF15	4.09E-04	3.1942167	down	3.8553326	up	12.314768	up
NCAPG2	6.26E-04	5.9330454	up	79.42693	up	13.387211	up
NCKAP1L	8.58E-04	6.9983354	down	32.479652	down	4.641054	down
NCOA1	4.95E-04	7.7209563	down	1.0618298	down	7.271369	up
NDRG1	0.001500237	8.090146	down	13.991383	down	1.7294351	down
NDRG4	4.96E-04	10.072089	down	1.2360748	up	12.449857	up
NDUFS7	0.002981367	1.5848469	up	5.2585316	down	8.333967	down
NEDD9	4.05E-07	12.268205	down	1.9509029	down	6.288476	up
NFAT5	6.90E-06	9.472188	down	1.2730764	down	7.440392	up
NFATC2	2.56E-06	13.405881	down	1.2140319	down	11.042445	up
NFATC3	0.004788925	3.2973022	down	1.6234404	up	5.3529735	up
NFIA	7.55E-04	18.464762	down	1.0405116	down	17.74585	up
NFXL1	3.28E-05	20.427988	down	4.7171674	down	4.3305626	up
NIN	1.38E-06	6.022748	down	1.5192481	down	3.9642954	up
NKG7	0.001432874	3.022726	up	3.747447	down	11.327506	down
NLGN4X	1.78E-07	137.42421	down	7.945553	down	17.295738	up
NNT	8.91E-04	2.727686	down	4.0158143	up	10.95388	up
NOL8	0.002590406	4.1103773	down	1.870514	down	2.197459	up
NOTCH2NL	1.75E-04	15.665	down	3.3258367	down	4.7100935	up
N-PAC	0.00346187	1.0552106	up	14.760106	up	13.987831	up
NQO1	1.13E-06	13.433853	down	2.288561	down	5.869999	up
NR1H3	0.007210864	1.7432098	down	11.243439	down	6.449847	down
NSUN6	0.003503544	11.104871	down	12.944696	down	1.1656773	down
NT5C	0.004214983	1.4111062	up	5.0594897	down	7.1394763	down
NTS	3.94E-07	165.26573	down	6.7430167	down	24.509161	up
NUCKS1	0.002361547	5.7921	down	11.153186	down	1.9255857	down
NUDT21	2.60E-04	5.727261	down	1.4824113	up	8.490156	up
NUFIP1	6.35E-04	39.52353	down	15.043396	down	2.627301	up
NUP43	2.13E-06	41.12042	down	7.0919256	down	5.7982016	up
NUS1	1.38E-05	8.8615885	down	1.8841668	down	4.703187	up
NUSAP1	2.68E-04	6.8090754	down	1.0127379	up	6.895809	up
OAS3	2.51E-07	126.159454	down	8.26494	down	15.264411	up
OLFM1	2.56E-05	29.158213	down	4.25994	down	6.844748	up
OPA1	1.72E-06	11.941727	down	1.344821	up	16.059486	up
ORC5L	8.90E-08	6.983898	down	1.8668504	up	13.037892	up
OXTR	0.002038054	17.838482	down	46.027496	down	2.5802362	down
P2RY13	1.15E-06	20.879519	down	2.6181147	down	7.97502	up
PAG1	1.76E-06	1.1712118	down	5.5300117	up	6.476815	up
PALM	0.008643085	9.486322	down	1.7710583	down	5.356301	up
PANK2	5.52E-05	6.172885	down	2.0828664	up	12.857293	up
PAQR8	6.99E-04	3.517141	down	8.769183	down	2.4932704	down
PARP12	0.00227428	1.2191415	down	8.662431	down	7.105353	down
PARP9	2.41E-05	71.75259	down	17.321856	down	4.142315	up
PARVA	7.69E-08	247.23334	down	9.589851	down	25.780725	up
PDCD10	0.002378464	6.2965646	down	1.462538	up	9.208966	up
PDCD5	2.35E-04	1.5486423	down	8.090751	up	12.529679	up
PDCD6IP	1.73E-04	43.0234	down	3.9710898	down	10.834155	up
PDE3B	6.49E-04	1.0468297	up	33.25751	up	31.769745	up

PDE5A	1.16E-06	11.281831	down	1.6449213	up	18.557722	up
PEMT	1.57E-05	8.662327	down	1.0171723	up	8.811079	up
PER2	2.70E-08	15.182093	down	1.5539488	down	9.770009	up
PES1	7.42E-05	12.714315	down	25.038574	down	1.9693213	down
PEX11G	1.49E-04	14.48946	down	23.36378	down	1.6124672	down
PHF14	3.85E-04	9.631312	down	4.026732	down	2.3918436	up
PHF3	3.00E-04	38.256657	down	4.0348635	down	9.4815235	up
PHKA2	6.22E-04	1.1365372	up	7.3392177	down	8.341294	down
PHOSPHO2	1.13E-13	211.928	down	10.28182	down	20.61192	up
PI15	9.40E-07	7.3512435	down	1.0285556	down	7.147152	up
PI4K2B	3.21E-09	15.732318	down	3.5230727	down	4.46551	up
PIAS2	3.65E-06	14.331547	down	1.7571716	down	8.156032	up
PICALM	3.13E-04	7.18382	down	1.0187378	down	7.051687	up
PIGQ	0.002960897	1.0294267	up	7.898721	down	8.131154	down
PIGU	0.007703219	1.3873187	down	7.44217	down	5.3644266	down
PIK3CA	9.32E-05	3.7560902	down	2.2704422	up	8.527986	up
PIK3R1	0.008839984	4.0413327	down	1.8703835	up	7.5588417	up
PKIA	3.38E-05	7.1112723	down	2.315107	up	16.46336	up
PLCL1	1.91E-06	40.642204	down	7.320416	down	5.5518975	up
PLD3	0.003207914	10.642531	down	1.2296128	down	8.655189	up
PLEKHG1	2.20E-06	99.23481	down	15.791914	down	6.2839007	up
PLEKHH3	0.004072717	22.8319	down	13.1146231	down	1.7367642	up
PLEKHO1	0.003336418	1.3467159	down	8.150619	down	6.0522184	down
PLSCR4	0.003514292	21.587084	down	5.3686056	down	4.0209846	up
PNPLA8	0.001587247	18.550701	down	3.0226085	down	6.1373158	up
POLG	3.94E-04	1.1935964	up	22.537111	up	18.88169	up
POLK	5.52E-04	14.247483	down	1.5928235	down	8.9447975	up
POLR2G	0.002288943	1.0156279	up	3.025785	down	3.0730715	down
POLR2J3	9.03E-05	9.367654	down	1.7078247	up	15.99831	up
POLR3F	3.77E-05	10.813741	down	6.1143355	down	1.768588	up
POMP	2.99E-08	271.48096	down	21.331226	down	12.726923	up
PPA2	0.008432304	5.9932437	down	1.346811	up	8.071766	up
PPIL4	2.54E-04	13.694382	down	1.0748713	up	14.7197	up
PPP1CB	0.008382075	1.6539217	down	4.811564	up	7.95795	up
PPP2R2D	1.69E-04	3.7548544	down	1.7788857	up	6.679457	up
PPT2	1.12E-05	22.466637	down	3.8161795	down	5.887207	up
PRDM4	0.005748785	1.4950874	down	10.724314	down	7.173035	down
PRKACB	1.13E-08	15.971311	down	1.0867783	down	14.496016	up
PRKAG2	1.13E-06	2.997834	down	1.5132383	up	4.5364375	up
PRKCB1	0.003439614	3.493342	down	1.3847489	down	2.5227256	up
PRKX	0.002009163	5.372691	up	8.666451	up	1.6130557	up
PRMT6	0.003053468	8.841437	down	2.3077857	down	3.8311348	up
PSAT1	1.95E-05	8.8213215	down	1.1514546	up	10.15735	up
PScdbp	5.51E-05	24.940912	down	1.5546597	down	16.042686	up
PSMB1	0.009982433	1.2877831	up	3.983861	down	5.130349	down
PSMB10	0.007183051	1.5658293	down	9.616911	down	6.1417365	down
PSMD1	0.001123151	3.2779691	up	3.9241211	down	12.863148	down
PSMD10	0.002145903	2.0157065	down	3.1240005	up	6.297069	up
PSMD6	3.05E-06	6.523827	down	1.973789	down	3.3052301	up
PSPH	7.04E-04	8.220119	up	21.99862	up	2.676192	up
PSRC1	6.02E-04	7.541325	down	2.1586294	down	3.493571	up
PTGFRN	3.24E-07	125.03998	down	14.123866	down	8.853099	up
PTPLAD1	5.31E-04	7.0569057	up	12.222071	up	1.7319307	up
PTPN22	1.11E-08	27.66733	down	1.5664712	down	17.662203	up
PTPRU	1.74E-04	21.717295	down	11.49789	down	1.8888068	up
PYGL	1.44E-04	6.9343495	down	1.5910488	down	4.358351	up
R3HDM2	0.003866316	7.4239974	down	1.557549	down	4.766462	up
RAB11FIP1	4.81E-11	8.213332	down	1.0559459	down	7.778176	up
RAB14	2.19E-07	31.366182	down	5.5596366	down	5.6417675	up
RAB30	2.31E-04	5.6773148	down	1.3136588	down	4.3217573	up
RABGGTB	1.69E-06	24.114546	down	9.35427	down	2.5779183	up
RAD17	9.80E-10	15.764736	down	1.1974355	down	13.165413	up
RAD50	2.10E-07	11.307503	down	2.0041196	up	22.66159	up
RAD54L	1.20E-04	8.542316	down	9.324137	down	1.0915232	down
RAG1AP1	8.22E-08	110.390396	down	22.24524	down	4.9624276	up
RAI1	0.001477566	3.294564	down	4.451799	up	14.666737	up
RALGPS2	0.00420607	12.850125	down	1.0342727	down	12.424311	up

RANBP2	2.90E-05	11.956906	down	1.5375684	up	18.38456	up
RAP1GDS1	0.002324897	5.9801173	down	1.3961884	up	8.349371	up
RBBP9	0.001302954	7.475199	down	2.0649567	down	3.6200273	up
RBL1	8.23E-10	5.555052	down	2.27847	up	12.657019	up
RBM3	0.006988636	10.974837	down	5.1557875	down	2.128644	up
RBMS1	8.80E-04	3.0370889	down	1.9745857	up	5.9969916	up
RBPJ	8.92E-04	5.1883717	down	2.4935017	up	12.937213	up
RCC2	0.008722604	3.2919636	up	3.7634346	down	12.389089	down
RCN1	4.68E-08	1931.6104	down	187.38063	down	10.308484	up
RCN2	0.001207017	3.7042944	down	1.8743887	up	6.943288	up
RDH11	1.63E-06	21.490473	down	10.045404	down	2.1393335	up
RECQL	3.71E-05	7.0416822	down	1.4022089	down	5.021849	up
RELN	1.19E-06	95.59824	down	7.5415096	down	12.676274	up
RFX5	5.33E-07	21.228926	down	5.6485868	down	3.7582722	up
RFXAP	0.00662855	6.99262	down	1.4685609	up	10.269088	up
RGPD5	0.001890577	10.783755	down	1.6457385	down	6.552532	up
RHEBL1	0.007252186	22.5372	down	10.359314	down	2.1755493	up
RHOJ	0.00369335	41.075268	down	5.6820483	down	7.228953	up
RIOK3	5.72E-05	7.644051	down	1.6435905	up	12.56369	up
RNASEH2B	0.002552729	1.58258	down	9.527301	down	6.0201073	down
RNASEN	1.89E-04	16.952	down	5.8214335	down	2.911998	up
RNF11	3.52E-09	106.87527	down	28.746521	down	3.717851	up
RNF138	0.005600598	15.289233	down	1.2903286	up	19.728134	up
RNF146	9.18E-04	4.1823926	up	21.163317	up	5.0600986	up
RNF38	0.002195766	4.3251867	down	1.204116	down	3.592002	up
RNF7	5.72E-06	16.398153	down	7.353568	down	2.229959	up
ROBO1	4.88E-04	16.772564	down	4.042655	down	4.148898	up
RPAP3	1.12E-08	26.437904	down	3.0988815	down	8.531435	up
RPL22	9.72E-04	4.9986415	up	41.404293	up	8.283109	up
RPL7	6.55E-05	1.7430243	down	8.760912	up	15.270482	up
RPS26	0.001252586	22.104454	up	11.528796	up	1.9173257	down
RPS6KC1	1.45E-12	29.431967	down	14.251197	down	2.0652277	up
RRP1B	1.52E-05	4.026398	down	5.681751	up	22.87699	up
RRP7A	0.001282253	2.8175774	down	17.236958	down	6.117653	down
RRS1	2.93E-04	4.6843753	down	5.9345093	up	27.799473	up
RSBN1L	4.18E-06	15.025451	down	1.0967731	up	16.479511	up
RUND C3B	0.002557344	1.6432617	down	17.837715	down	10.855064	down
RYK	1.67E-04	2.2418928	down	3.5815806	up	8.029521	up
SAMSN1	2.80E-05	8.686577	down	1.6891397	down	5.142604	up
SC5DL	7.01E-04	6.537944	down	1.0484343	up	6.854605	up
SCAMP1	2.84E-04	1.9808297	down	4.6856003	up	9.281375	up
SCMH1	0.001827465	5.87433	down	1.0055887	down	5.841682	up
SCML1	0.001537268	7.0845537	down	1.6290653	up	11.541202	up
SCNN1D	3.71E-04	1.289663	down	12.220806	down	9.47597	down
SCRIB	5.92E-05	8.95509	down	1.0431473	down	8.584683	up
SCYL1BP1	4.65E-06	20.571194	down	5.2053556	down	3.9519277	up
SDF4	6.89E-07	5.102552	down	2.6296375	up	13.417861	up
SDHD	0.001093202	7.437263	down	4.1244307	up	30.674475	up
SEC24C	0.003767617	5.644759	down	1.7614206	down	3.2046626	up
SEC62	2.73E-07	13.665146	down	2.3873982	down	5.723865	up
SEH1L	0.004251851	2.6577344	down	2.9345245	up	7.799186	up
SELM	0.003665327	1.7513821	up	7.8737764	down	13.789991	down
SENP6	2.80E-08	18.299578	down	5.733956	down	3.1914406	up
SENP7	0.003431266	4.3176417	down	2.81381	up	12.149023	up
SERAC1	0.001404165	15.370831	down	6.1535826	down	2.4978669	up
SERF1B	6.15E-06	114.98696	down	4.245132	down	27.086784	up
SERPINI1	1.04E-04	68.225105	down	15.913138	down	4.2873445	up
SETD3	4.03E-06	9.152396	down	1.1309292	up	10.350714	up
SETD6	5.09E-06	1015.6609	down	623.90845	down	1.6279002	up
SETDB2	2.95E-05	7.1602154	down	26.06232	down	3.6398795	down
SF3B3	0.005955674	3.4810174	up	1.448063	down	5.0407324	down
SF4	1.45E-04	1.4186026	down	7.087206	down	4.9959064	down
SFRP4	3.71E-09	645.5158	down	70.33453	down	9.177796	up
SFRS2B	0.001143766	1.5469866	up	6.8364787	up	4.419223	up
SFRS3	1.93E-07	24.722982	down	1.390048	down	17.78571	up
SGOL2	0.002171958	55.20704	down	5.8952947	down	9.364594	up
SH3BGRL	9.33E-06	26.52516	down	1.1126796	down	23.838997	up

SKI	0.003753592	3.3107417	down	2.5441647	up	8.423072	up
SLAMF8	6.26E-05	679.2688	down	1173.5913	down	1.727727	down
SLC10A7	1.47E-07	8.065574	down	1.503079	up	12.123195	up
SLC12A6	0.004253994	3.1686015	down	2.3791173	up	7.5384755	up
SLC15A4	0.002744256	3.8999882	up	20.188938	up	5.176667	up
SLC22A17	2.15E-04	8.498817	down	1.2768453	down	6.6561065	up
SLC25A23	0.002307631	2.4396906	up	4.344635	down	10.599566	down
SLC25A32	0.002937946	17.137173	down	2.985614	down	5.7399144	up
SLC25A40	0.009588216	2.7571132	up	22.022684	up	7.987586	up
SLC26A6	2.56E-05	14.273289	down	2.8242145	down	5.0538964	up
SLC29A1	1.52E-09	10.2297	down	3.786554	down	2.7015855	up
SLC30A5	0.004439674	14.013604	down	1.7273985	down	8.112549	up
SLC30A7	8.70E-04	2.2008038	down	11.535338	down	5.2414207	down
SLC41A3	0.005071448	7.1072893	down	1.3614538	up	9.676246	up
SLC4A5	0.009846691	16.100517	down	2.2384746	down	7.1926293	up
SLC6A9	5.55E-07	15.332633	down	3.9689453	down	3.8631504	up
SLC9A6	1.69E-07	11.971249	down	1.1739352	up	14.053468	up
SLCO3A1	2.94E-06	9.850855	down	1.0691134	down	9.214042	up
SLFN11	3.59E-07	71.14539	down	4.1624947	down	17.09201	up
SLK	0.005554502	8.88517	down	1.4707506	down	6.0412483	up
SLTM	2.62E-04	3.6996272	down	1.584603	up	5.86244	up
SMAD2	2.48E-04	16.294104	down	1.2305472	down	13.241345	up
SMC2	0.009035276	6.258391	down	1.2401171	down	5.046613	up
SMC6	0.005427342	17.837673	down	1.1931552	up	21.283113	up
SMG7	4.11E-06	3.6336079	down	1.1574938	up	4.2058787	up
SMPD1	1.41E-04	11.094001	down	2.1838887	down	5.07993	up
SMPDL3A	2.01E-06	90.51843	down	7.201459	down	12.569457	up
SNAPC4	9.07E-04	1.2094554	up	9.083944	down	10.986626	down
SNORD107	1.39E-04	20.249323	down	2.0026956	up	40.553215	up
SNRPD1	0.009445871	10.277269	down	2.311563	down	4.446026	up
SNRPN	1.10E-10	6.0401745	down	1.4836541	up	8.961529	up
SNX1	1.48E-05	2.4319503	up	13.213169	up	5.4331574	up
SP3	9.67E-05	4.6089344	down	2.701559	up	12.451309	up
SPAST	8.94E-06	8.06534	down	1.1734318	up	9.464127	up
SPC24	1.93E-04	1.0042573	down	15.117227	down	15.053143	down
SPCS3	0.001737695	42.13478	down	2.777251	down	15.171398	up
SPIC	3.23E-08	168.19083	down	11.336265	down	14.83653	up
SPOPL	1.70E-05	22.34085	down	2.1026425	down	10.625132	up
SPPL2B	0.003603679	6.5860186	down	1.8362278	down	3.586711	up
SQSTM1	0.002099883	2.2986104	down	14.846299	down	6.4588146	down
SRP9	0.002226583	4.255992	down	1.4425822	up	6.1396184	up
SRPRB	2.37E-05	26.215557	up	68.392334	up	2.608846	up
SSBP3	5.02E-05	5.075352	down	1.4636077	up	7.4283247	up
ST3GAL5	0.0092713	3.0759916	down	1.9154905	up	5.8920326	up
ST6GAL1	5.97E-04	4.802251	down	2.5717137	up	12.350014	up
ST6GALNAC3	5.92E-05	24.702171	down	8.771768	down	2.8160992	up
ST8SIA4	3.45E-04	7.9146743	down	1.3769864	up	10.898398	up
STAG2	2.15E-05	4.5220423	down	1.7371116	up	7.8552923	up
STAMBP	0.003216187	2.6281872	down	3.3215811	up	8.729737	up
STARD3	1.11E-04	12.877834	down	4.586416	down	2.807821	up
STAU1	0.004371808	2.3173866	down	2.5892754	up	6.0003524	up
STK17B	0.007832015	15.121467	down	1.7473718	down	8.653833	up
STRAP	0.002221307	4.6883545	down	1.0055181	up	4.7142253	up
STX2	0.003845002	1.6774983	down	6.473789	up	10.859771	up
STYX	1.58E-07	530.4886	down	75.47328	down	7.0288305	up
SULT1A1	7.45E-04	7.4111643	down	1.3344394	down	5.5537653	up
SUMF2	2.04E-04	7.7939963	down	2.0380912	down	3.8241646	up
SUMO1	2.18E-07	31.399881	down	1.5535663	down	20.211485	up
SUOX	9.41E-06	6.9373584	down	1.1747155	down	5.9055653	up
SUV420H1	0.006231028	4.7964387	down	1.0827773	down	4.429755	up
SYCP1	0.003136971	224.46432	down	51.643967	down	4.3463798	up
SYNE1	9.13E-08	17.009274	down	1.2625734	down	13.471909	up
SYNE2	0.002230475	4.3484006	down	2.79895	up	12.170956	up
SYNJ1	2.78E-04	2.0888796	down	3.063252	up	6.398765	up
SYN2BP	0.002357794	2.4766774	up	1.8647044	down	4.6182714	down
SYT11	0.00935805	1.2080003	up	4.395808	down	5.3101377	down
TADA1L	0.001455176	4.6171546	down	2.030439	up	9.374849	up

TAF1B	7.46E-04	26.991222	down	2.3801825	down	11.339978	up
TAF9	0.005208395	3.6693075	down	5.085628	up	18.660734	up
TANK	0.001362066	2.5658553	down	2.2945998	up	5.887611	up
TAOK2	2.33E-05	10.931411	down	2.340749	down	4.6700487	up
TAOK3	1.58E-08	1459.3153	down	103.75347	down	14.065223	up
TARDBP	1.83E-06	10.549396	down	2.2552018	down	4.677806	up
TAS2R14	0.007060847	5.658673	down	2.898415	up	16.401182	up
TBC1D22A	0.005599857	7.914468	down	2.1313534	down	3.7133532	up
TBL1X	0.009261122	1.0052005	up	7.6511955	down	7.690985	down
TBRG1	2.79E-04	2.2983956	up	22.137026	up	9.631512	up
TC2N	1.33E-05	9.135517	down	5.328204	up	48.675907	up
TCERG1	3.67E-05	4.2357664	down	1.9178729	up	8.123661	up
TCF12	0.001174474	5.227383	down	1.1713647	up	6.1231723	up
TCF7	0.00370217	1.2752731	down	5.2985783	up	6.7571344	up
TCP1	3.79E-12	22.603445	down	2.8443542	down	7.946777	up
TCTN1	0.006478699	10.08844	up	5.4727	up	1.8434117	down
TDO2	4.65E-05	76.98565	down	13.874537	down	5.5487013	up
TERF1	3.50E-04	9.139923	down	2.4233074	down	3.7716734	up
TFG	9.12E-05	3.4841151	down	2.2629988	up	7.884549	up
TFPI	4.88E-04	7.2029505	down	1.1407381	up	8.216681	up
TGFBR2	0.002047329	4.6393933	down	2.3302493	up	10.810942	up
THAP5	8.20E-09	46.291725	down	3.6403468	down	12.716297	up
THAP6	5.73E-04	6.109356	down	1.0096927	up	6.168572	up
TIA1	3.41E-06	188.68805	down	19.628876	down	9.612778	up
TIAL1	0.001795627	1.6368861	down	7.8093376	up	12.782996	up
TIMM22	4.58E-04	1.7783535	down	7.7498293	down	4.3578687	down
TIPRL	9.60E-05	2.0484483	down	4.6902337	up	9.607702	up
TLR3	0.004642209	56.188572	down	7.6077533	down	7.385699	up
TM4SF18	4.88E-11	150.3495	down	25.458818	down	5.905597	up
TMEM104	0.007229614	1.7107627	down	41.460464	up	70.929016	up
TMEM106B	2.07E-04	13.006642	down	1.5249091	up	19.833946	up
TMEM137	0.001013426	3.5679326	down	28.535751	down	7.99784	down
TMEM183A	5.67E-05	11.895105	down	4.381351	down	2.7149398	up
TMEM189	4.04E-04	7.9764543	down	24.212372	down	3.0354798	down
-UBE2V1							
TMEM19	6.05E-16	404.12213	down	53.722717	down	7.5223684	up
TMEM38B	0.005521221	22.167463	down	4.138439	down	5.3564796	up
TMEM41B	0.005605353	2.0247781	up	3.606849	down	7.303069	down
TMEM64	0.001839316	1.006199	up	16.737398	up	16.634285	up
TMEM69	1.45E-06	6.1254535	up	50.38219	up	8.225055	up
TMSB4X	3.05E-04	2.4892077	down	16.672798	up	41.50205	up
TNC	7.66E-05	9.045913	down	3.4609208	down	2.6137302	up
TNFAIP8	2.92E-05	16.28897	down	2.7411337	down	5.9424224	up
TNFRSF1B	3.54E-04	5.5427384	down	30.085102	down	5.4278398	down
TNIP3	0.001850497	1.4608194	up	6.9033813	down	10.084593	down
TOM1	0.005521505	2.0137942	down	13.295589	down	6.602258	down
TOP1	2.07E-04	16.0336	down	3.404917	down	4.708955	up
TOPORS	1.16E-06	77.31025	down	5.54056	down	13.953513	up
TPCN2	0.00385112	1.0582529	up	5.6552176	down	5.984651	down
TPI1	0.006767832	6.474049	up	1.0711734	down	6.9348297	down
TPK1	1.66E-04	10.618938	down	2.6232522	down	4.0480056	up
TPP2	1.44E-06	3.1247053	down	3.1084154	up	9.712883	up
TRABD	0.002094139	2.0375283	up	4.1379566	down	8.431203	down
TRAF5	2.71E-10	4.841076	down	3.352071	up	16.22763	up
TRAPPC2L	0.001729689	1.9559205	up	6.961032	down	13.615226	down
TRAPPC6B	4.37E-06	7.0665126	down	1.0150145	down	6.961982	up
TRAT1	1.09E-04	20.47111	down	2.9575875	down	6.9215574	up
TRIM3	1.74E-07	17.327156	down	2.509284	down	6.9052196	up
TRIM33	1.92E-05	8.900957	down	1.3160642	down	6.7633147	up
TRIM4	6.89E-04	6.8921475	down	1.0647311	down	6.4731345	up
TRPM2	2.67E-06	25.453693	down	2.9268909	down	8.696496	up
TRPT1	4.15E-05	16.68914	down	2.7049751	down	6.1697955	up
TSC1	3.90E-04	6.989248	down	1.7791383	down	3.9284456	up
TSC22D2	2.78E-07	8.655063	down	2.6950092	down	3.211515	up
TSC22D3	7.84E-04	2.9845226	down	2.509454	up	7.489523	up
TSNAX	1.22E-05	15.750429	down	4.2329097	down	3.7209456	up
TSPAN12	8.27E-11	307.26852	down	30.281181	down	10.147178	up
TSPAN13	9.42E-04	11.554177	down	1.1338136	up	13.100282	up

TSPAN33	0.00613541	2.501188	down	16.489416	down	6.592634	down
TSPAN4	0.001761541	16.38268	down	1.300723	down	12.595056	up
TSPAN7	0.001039907	87.62003	down	8.881055	down	9.865947	up
TSR1	2.45E-05	65.30981	down	3.794855	down	17.210089	up
TTC23	0.001620816	7.3842096	down	3.6497812	down	2.0231924	up
TTC39B	1.27E-06	98.98506	down	16.514227	down	5.993926	up
TTF1	3.36E-10	26.353401	down	3.6051302	down	7.309971	up
TTRAP	1.25E-04	5.5379086	down	2.2799292	up	12.626039	up
TUFM	7.82E-04	3.6293569	up	3.824123	down	13.879106	down
TWF1	0.002106424	4.5469346	down	1.0784723	down	4.216089	up
TXNRD2	0.004894615	2.0033112	down	12.318226	down	6.148934	down
TYW3	8.70E-05	8.997397	down	10.222054	down	1.1361122	down
UBE2D2	1.45E-06	5.7851043	down	2.6052413	down	2.2205637	up
UBE2D3	2.42E-08	10.865164	down	1.1240911	down	9.665733	up
UBE2H	1.97E-05	7.4031305	down	1.3136909	up	9.725424	up
UBE2Z	0.002731817	1.3880645	up	11.654188	up	8.395999	up
UBE4B	0.005822326	8.4463215	down	3.7183237	down	2.2715402	up
UBR5	0.00318293	8.255534	down	4.5141	down	1.8288326	up
UBR7	2.58E-04	4.61853	down	1.7280157	up	7.980891	up
UNC119	0.006902074	4.587935	down	1.3712082	down	3.3459072	up
UPF2	1.54E-04	11.068828	down	1.3227906	down	8.367785	up
UQCC	4.26E-04	5.6558146	down	1.0289153	up	5.819354	up
USP16	0.001374591	3.630336	down	1.5643557	up	5.679137	up
USP48	1.19E-04	8.408603	down	1.6513907	down	5.091831	up
USPL1	0.004945296	4.6374593	down	1.1363279	up	5.269674	up
UTP3	2.44E-06	247.37401	down	19.278603	down	12.831528	up
VAMP8	0.00243003	4.3750324	up	1.2482661	down	5.4612045	down
VARS2	0.001245543	1.625337	up	6.5147533	down	10.58867	down
VASH2	1.04E-05	114.04187	down	18.063295	down	6.313461	up
VEZT	4.59E-11	74.00654	down	15.173254	down	4.877434	up
VPS13A	3.47E-08	9.663795	down	1.178689	down	8.198767	up
VPS13B	4.38E-06	7.0657854	down	1.4157226	up	10.003193	up
VPS24	4.21E-05	6.1457205	down	1.899725	up	11.675179	up
WBP11	0.009260353	4.1503353	down	2.6407003	up	10.959794	up
WBP5	1.06E-08	68.87768	down	30.051939	down	2.2919543	up
WDR26	2.68E-05	8.021877	down	1.1101507	up	8.905493	up
WDR44	0.005568679	39.653145	down	5.6428657	down	7.02713	up
WDR46	0.00179891	7.6913476	up	2.4126773	down	18.556736	down
WDSUB1	6.15E-05	180.93266	down	36.461765	down	4.9622574	up
WHSC1	0.0012189	11.545975	down	2.6363404	down	4.379546	up
WIPF1	5.14E-04	2.9015427	down	6.0911565	up	17.673754	up
WWP1	5.87E-09	86.644775	down	23.274904	down	3.72267	up
WWP2	0.00105414	2.9178462	down	3.6091866	up	10.531052	up
XPO6	6.19E-09	18.474125	up	20.896225	up	1.1311076	up
XRCC5	0.001141931	1.1199814	up	14.1366415	up	12.6222105	up
YAF2	2.84E-05	8.718427	down	2.6534238	down	3.285727	up
YES1	0.004749542	4.0908623	down	5.3011575	down	1.2958535	down
YIPF4	4.85E-06	27.776245	down	4.6407657	down	5.985272	up
YME1L1	1.30E-04	4.047181	up	6.569345	up	1.6231902	up
YOD1	0.00716745	14.993594	down	3.292332	down	4.5540953	up
YPEL3	0.003913292	14.365424	up	98.21181	up	6.83668	up
YTHDF3	4.42E-07	6.116748	down	1.3097258	down	4.670251	up
YWHAE	0.006567453	4.0390725	down	1.2054291	up	4.8688154	up
ZAP70	0.00941424	3.9931872	up	5.7434764	up	1.438319	up
ZBTB11	0.005830909	9.577617	down	1.0353694	up	9.916371	up
ZBTB3	3.47E-05	3.579126	down	14.509221	down	4.053845	down
ZC3H7A	7.92E-10	463.68134	down	129.67134	down	3.5758195	up
ZCCHC6	8.55E-06	30.641006	down	33.206764	down	1.0837358	down
ZDHHC16	0.008849635	1.9925271	down	4.7530785	up	9.470638	up
ZDHHC4	0.009627339	30.245811	down	3.8074656	down	7.943817	up
ZFAND1	0.00343089	8.096212	down	1.8804401	down	4.305488	up
ZFAND2A	6.99E-04	1.0062547	down	8.323114	down	8.271379	down
ZFAND6	4.08E-08	105.78078	down	3.7741256	down	28.02789	up
ZFP106	0.004666306	1.3642471	up	6.2868414	up	4.608287	up
ZFP91	0.006881047	1.2046837	down	3.8671474	up	4.658689	up
ZFYVE1	0.001720764	8.695094	down	8.093691	down	1.0743052	up
ZMYND11	0.002739006	6.5577617	down	2.0223913	down	3.2425778	up

ZNF124	0.00266481	6.885966	down	1.1876531	up	8.178139	up
ZNF131	2.98E-04	12.154433	down	2.5474272	down	4.771259	up
ZNF141	6.21E-08	29.349707	down	1.0155233	up	29.805304	up
ZNF227	6.70E-07	12.667595	down	3.9416342	down	3.213792	up
ZNF23	6.45E-07	76.04954	down	17.593714	down	4.3225403	up
ZNF253	0.002447995	30.671535	down	2.5956028	down	11.816731	up
ZNF273	0.006807428	16.80808	down	2.403022	down	6.9945583	up
ZNF318	3.06E-07	21.514616	down	2.4030108	down	8.953189	up
ZNF322A	2.52E-06	15.518061	down	4.6302257	down	3.3514698	up
ZNF431	1.68E-06	90.29036	down	6.926899	down	13.034742	up
ZNF490	8.06E-09	475.23242	down	61.763958	down	7.6943297	up
ZNF493	1.33E-04	21.440052	down	5.9030714	down	3.6320155	up
ZNF526	6.59E-04	4.387784	down	10.010195	down	2.281378	down
ZNF567	3.37E-11	154.9765	down	14.825055	down	10.453688	up
ZNF593	0.001063756	1.2341977	down	11.589249	down	9.390107	down
ZNF653	0.00106378	1.8039771	up	5.3189297	down	9.595228	down
ZNF827	0.001880202	1.4905915	up	5.470114	down	8.153706	down
ZNF83	1.96E-04	7.862181	down	3.6259406	up	28.507801	up
ZNF93	0.003682921	1.5066208	up	11.371461	up	7.54766	up
ZSCAN18	2.06E-07	12.366672	up	15.575254	up	1.2594541	up

Supplementary Table 24. Genes differentially expressed between F-PTCL and AITL.

Gene ID	Corrected p-value	Absolute Fold Change	Regulation in F-PTCL
AASS	0.006721099	6.9508505	down
ABCA1	0.009255056	4.471113	down
ABCA10	0.001512908	7.4106607	down
ABCD2	0.002290321	6.078836	down
ABI3BP	0.002592176	8.837785	down
ACBD7	0.001505991	4.5303264	down
ADD1	0.005487896	5.024453	down
AIM2	8.70E-05	13.001065	down
ALDH6A1	7.15E-04	30.292324	down
ALDH7A1	0.003865223	8.697635	down
AMY2B	0.008165984	3.3694634	down
ANGPTL4	0.002918107	7.2624784	down
ANKRD35	9.77E-04	58.401836	down
ANKRD40	0.007821908	5.8272347	down
ANKS6	6.32E-05	18.939423	down
APLP2	0.006265898	15.759454	down
APOBEC3D	0.001018839	9.934807	down
APOBEC3F	0.005923716	3.2091925	down
AQR	0.001163615	12.736328	down
ARHGAP21	0.003212553	4.7678223	down
ARHGAP22	9.53E-04	11.024778	down
ARL16	0.007043136	9.75806	down
ARL6IP1	0.001867556	4.391882	down
ARMC1	7.15E-04	6.287192	down
ASB5	4.22E-04	42.96255	down
ATG12	0.008160952	4.8810673	down
ATP5L	0.006257816	6.8606515	down
ATPB4	0.008797346	5.274579	down
BACE2	0.005768979	5.311481	down
BAG4	0.007221074	3.8730369	down
BCL6B	0.003099599	6.637295	down
BRCA1	4.10E-04	8.163639	down
BRD7	0.008129506	6.194398	down
C11ORF58	7.62E-04	18.32515	down
C12ORF10	0.001795393	7.28373	down
C13ORF3	0.001512908	8.070674	down
C14ORF85	1.15E-04	67.8108	down
C15ORF29	0.005521033	4.8747907	down
C15ORF5	4.16E-05	21.765945	down
C17ORF55	2.64E-04	42.862545	down
C18ORF10	0.003550393	7.838923	down

C18ORF45	0.001344154	9.288338	down
C19ORF66	0.007456531	5.3172026	down
C1GALT1C1	7.72E-04	5.7198977	down
C1ORF110	0.006410764	9.589877	down
C1ORF218	0.006410764	4.3450704	down
C1QL2	0.003498111	24.732056	down
C20ORF94	4.79E-04	5.1433	down
C4ORF34	0.004506461	4.3440757	down
C5ORF34	0.004023642	12.555799	down
C7ORF27	0.008129506	6.0288734	down
C8ORF33	2.58E-04	6.623366	down
C9ORF169	1.39E-04	7.276296	down
CADM4	0.009034846	6.162319	down
CAPZB	0.002327481	23.211348	down
CCDC28B	9.53E-04	8.554726	down
CCNB1	0.009892512	5.5475936	down
CDH6	3.48E-04	17.941332	down
CDO1	0.006525365	10.504012	down
CDS1	0.007607385	6.003536	down
CELSR3	0.002564631	7.402844	down
CFI	5.33E-04	9.398326	down
CFLAR	0.005530739	4.9480195	down
CHCHD4	0.006285127	4.7701654	down
CHD9	0.001795393	7.444789	down
CHMP4A	0.009205915	6.538052	down
CIITA	0.004383729	5.2421994	down
CIT	0.001427465	8.584574	down
CLEC3B	0.006644404	11.210837	down
COL5A1	0.004023642	6.3481	down
COMM D8	0.003550393	7.491454	down
COPS2	0.001512908	11.230478	down
COQ2	0.009979644	25.968605	down
COTL1	0.006525171	8.595992	down
CPEB3	3.76E-06	19.95955	down
CPXM1	0.003740608	7.076955	down
CROT	0.001427465	5.676471	down
CSMD2	4.27E-04	20.137575	down
CSNK1G2	0.008560014	5.9608827	down
CTHRC1	4.40E-05	22.15206	down
CYP7B1	0.005837788	4.8154507	down
DAAM1	0.007880417	9.520425	down
DAB2	0.001018839	7.429707	down
DARS	0.007237782	4.112825	down
DBR1	0.001529687	4.1384196	down
DBT	0.009205915	4.8676763	down
DEPDC6	0.009607758	6.4172177	down
DHRS13	0.00505884	7.252834	down
DNAJC21	0.001163615	4.9249387	down
DSCC1	0.006440314	7.667918	down
DSEL	4.16E-05	25.306608	down
DTWD2	0.007821908	6.510927	down
DUSP3	4.89E-04	9.609001	down
EDEM3	7.15E-04	5.8986506	down
EEF1E1	0.009016617	6.6618366	down
EFCAB2	0.001795393	6.935688	down
EGLN2	0.008817447	4.5341926	down
EID2B	9.74E-06	48.621124	down
EIF2AK2	6.75E-04	9.760415	down
EIF3A	0.003177458	7.017942	down
EIF3C	0.003718566	7.323435	down
EIF5A2	0.00211369	38.130432	down
ELOVL2	0.005530739	11.639583	down
ENSA	0.003498111	5.633998	down
EOMES	0.008357832	6.321761	down
ERAL1	0.003498111	7.447069	down
ESPNL	0.003621221	12.869572	down
ETV6	0.003298047	8.728775	down

FAM103A1	5.69E-04	8.809606	down
FAM126A	3.00E-04	15.642905	down
FAM135A	0.00620863	9.553618	down
FAM164C	0.005553972	4.321063	down
FAM179B	0.003620393	5.40688	down
FAM46A	0.006273667	6.2907057	down
FAM53B	0.002277786	13.31916	down
FAM70A	0.006703681	5.5815744	down
FAM98A	9.77E-04	10.764453	down
FANCL	0.005130978	9.115642	down
FASN	0.005487896	5.3522096	down
FBXO5	0.006686966	11.124021	down
FEM1C	2.85E-05	14.872466	down
FH	0.00947703	4.131756	down
FLJ44124	0.0051334	8.588121	down
FN3KRP	0.009516406	18.471292	down
FOXN3	0.003498111	7.037565	down
GABPA	0.00469059	21.935917	down
GAGE5	2.64E-04	28.434034	down
GALNT1	0.001882699	7.9953594	down
GAS1	0.006665306	4.0365477	down
GCLM	4.62E-05	28.042463	down
GCN1L1	0.001970455	6.336624	down
GCNT1	1.44E-05	31.295786	down
GFPT1	4.89E-04	19.926119	down
GJC1	0.002311068	6.4021297	down
GNAI1	3.94E-04	24.286806	down
GNPNAT1	0.004264913	4.364096	down
GPR65	0.00673436	3.5078955	down
GSR	0.002166688	4.0615	down
GUCY1A3	3.34E-04	10.131008	down
HDHD2	0.002174057	7.8749986	down
HIPK2	0.004845828	7.231289	down
HLA-E	0.007825849	28.690632	down
HMHA1	0.009255056	4.7872653	down
HOXA2	4.08E-05	35.479454	down
HSPA2	0.006273667	5.2813625	down
HSPC268	0.002652978	17.389692	down
IGF1	1.88E-04	14.1034155	down
IL7	0.004156461	12.013782	down
IQCC	7.72E-04	12.422295	down
JARID1A	0.007078458	66.2011	down
KCNJ10	4.89E-04	7.7967143	down
KCNMB4	8.43E-04	8.641509	down
KCNT2	0.003826808	7.430913	down
KCTD17	4.79E-04	5.182059	down
KHDRBS3	4.62E-05	46.74356	down
KHSRP	0.004264913	4.8797398	down
KIAA1274	0.00211369	8.346205	down
KIAA1333	4.10E-04	24.689985	down
KIAA1524	0.002956321	6.7158546	down
KIAA1704	0.002918107	6.009364	down
KIAA1751	0.008400832	6.6624775	down
KIR2DL1	0.006760668	10.854722	down
KLHL14	0.003502828	11.503036	down
KMO	4.40E-05	26.816216	down
KRIT1	2.57E-07	19.790577	down
KTELC1	0.006337825	10.397751	down
L3MBTL2	0.009769705	3.2338376	down
LAMB1	0.004506461	5.543745	down
LARP4	0.004578318	4.2966576	down
LCORL	0.007638917	9.755965	down
LEPREL1	0.00201523	7.68939	down
LIG4	3.95E-04	5.532438	down
LOC389286	0.006273667	6.810984	down
LOC401252	0.007237782	6.5351396	down
LOC402110	0.002397922	17.058413	down

LOC440157	0.003212553	6.071294	down
LOC440295	0.001980803	14.393967	down
LOC441426	0.009255056	17.249702	down
LOC442582	0.001020258	18.748045	down
LOC54103	0.009518844	7.3338943	down
LONP2	0.004023642	5.3189163	down
LPP	0.008719726	6.191133	down
LSM2	0.00848006	4.0089626	down
LUM	0.003849729	6.7481155	down
LYPLA1	0.009046126	12.175904	down
M6PRBP1	0.009600718	4.109254	down
MAML3	0.00193337	8.5067215	down
MAN2A1	0.002915615	8.016293	down
MAN2B2	0.004844761	7.2362046	down
MBTD1	0.004260836	8.057388	down
MED31	0.0068116	14.412442	down
MET	0.00620863	5.7911243	down
MKRN1	0.007156577	3.5647945	down
MND1	0.001750089	7.2679687	down
MOBKL1A	0.002621011	6.0218325	down
MOSPD2	3.63E-04	25.38684	down
MTTP	0.004189321	13.093079	down
MYO10	5.66E-04	13.408863	down
NCBP1	0.00585091	6.858417	down
NEK2	0.008164501	9.597701	down
NEO1	4.40E-05	6.5865216	down
NLGN4X	0.002918107	6.784498	down
NOTCH2NL	9.76E-04	5.0161486	down
NSUN6	3.48E-04	13.238877	down
NUAK1	0.003177458	5.219131	down
NUCKS1	0.005620657	6.508262	down
NUP43	1.92E-06	12.984548	down
OXTR	7.09E-04	20.961843	down
PAQR8	0.00153319	7.150044	down
PBX2	0.005806869	4.2305865	down
PEAR1	0.004023642	7.604949	down
PES1	9.53E-04	14.513564	down
PEX11G	0.004399243	11.267722	down
PGAP1	3.94E-04	6.9355206	down
PHF13	0.005530739	4.8793325	down
PHF14	0.009516406	3.3742986	down
PHOSPHO2	0.002166688	10.834834	down
PIGM	0.007344679	8.893942	down
PIGX	0.005487896	7.0959525	down
PLEKHG1	0.002499568	11.7679205	down
PLEKHH3	3.25E-04	17.142418	down
POLR3F	0.001638724	5.163976	down
POMP	0.003669476	11.951405	down
PPIG	7.72E-04	6.7955914	down
PPP2R2A	0.007344679	3.120133	down
PRICKLE1	0.006482872	5.796452	down
PRR13	0.009313687	4.466944	down
PRSS23	0.003177458	8.944198	down
PSMC1	0.009255056	5.1416206	down
PTGFRN	0.0068116	5.914789	down
PTP4A2	0.004103434	6.8342104	down
PTPRU	0.006891795	7.0524616	down
QSER1	0.005620657	3.8569806	down
RAD54L	0.002397922	6.635993	down
RAG1AP1	0.003177458	11.003358	down
RBM41	0.009255056	5.004678	down
RCN1	0.001773111	58.72695	down
RELN	0.004264913	7.3180633	down
RHOJ	0.004524995	5.980872	down
RIC8B	0.003208943	14.38852	down
RNASEH2B	0.002499568	7.20803	down
RNASEL	0.004676314	3.5855713	down

RNASEN	0.003498111	6.4007926	down
RNF11	3.34E-04	16.78699	down
RNF150	0.002823318	8.134149	down
RORB	0.009255056	10.622409	down
RPS10	0.008797346	7.045753	down
RPS27L	0.001512908	6.9092183	down
RPS6KC1	8.81E-05	18.745535	down
RUND C3B	0.004578318	9.420786	down
S100A3	0.007711134	8.942829	down
SCYL1BP1	0.00577239	5.506925	down
SDAD1	0.001971543	5.329716	down
SEC63	0.007086346	3.972795	down
SELT	4.27E-04	13.3971195	down
SEN P6	0.007427083	4.9874196	down
SERF1B	0.006750406	8.329057	down
SETBP1	0.005083294	5.3412967	down
SETD6	0.00162084	223.82956	down
SETDB2	3.27E-04	16.13242	down
SF4	0.004453694	6.1089373	down
SFRP4	2.58E-04	34.795265	down
SH3BGRL2	0.002166688	14.539969	down
SH3BP4	0.009313687	6.506572	down
SKP1A	0.006871954	3.6610322	down
SLAMF8	0.008128945	137.59619	down
SLC19A3	0.008174583	7.510807	down
SLC25A13	0.009255056	5.241347	down
SLC30A7	0.001344154	8.956547	down
SLC35B4	0.009854952	5.390821	down
SLC36A4	0.003671266	4.410861	down
SLC38A5	0.009255056	3.9003642	down
SLITRK2	2.09E-04	14.258287	down
SNF8	0.00947956	5.330567	down
SNRPC	0.009607758	4.6638975	down
SNRPG	0.008504801	4.996765	down
SNW1	0.001283768	5.942991	down
SPC24	0.007546236	6.9834805	down
SPIC	3.94E-04	17.151617	down
SSPN	0.007156577	12.765097	down
STYX	0.002823318	27.293037	down
SUZ12	0.002983367	5.6309605	down
SYTL4	3.94E-04	12.557737	down
TAOK3	0.002371385	33.00952	down
TBL1X	0.004910842	5.5992155	down
TBX2	0.007078458	7.796086	down
TDO2	0.00440716	11.081358	down
TEX11	0.007711134	6.1001973	down
THAP5	0.005802979	5.0500827	down
TIA1	0.003225538	16.310478	down
TIMM22	0.006686966	5.5662274	down
TMEM137	0.001256493	15.128526	down
TMEM183A	0.005487896	4.363731	down
TMEM189-UBE2V1	0.002116912	13.029873	down
TMEM19	2.57E-07	32.272377	down
TMEM47	3.25E-04	14.154172	down
TNFRSF1B	0.006299525	12.061986	down
TNIP3	0.009569214	4.6899633	down
TPM3	0.005924117	5.4504294	down
TSPAN12	7.62E-04	21.84079	down
TSPAN33	0.009205915	6.4077077	down
TTF1	0.003453439	4.6966577	down
TYW3	0.002717147	7.1920743	down
UBE2M	0.004399243	4.692899	down
UBE2V2	0.003208943	9.669832	down
USP28	0.002915615	5.578052	down
UTP23	0.002376513	4.746803	down
VASH2	0.001901616	16.094357	down
VEZT	0.00193337	10.906304	down

WBP5	0.003099599	11.244993	down
WDR44	0.00846132	5.658135	down
WDR79	0.009358969	3.5898888	down
WWP1	0.002529311	14.063203	down
YIPF1	0.002956321	5.4660435	down
ZBTB1	0.005206829	5.1862197	down
ZC3H7A	0.002956321	29.289198	down
ZCCHC6	4.10E-04	18.155394	down
ZDHHC8	0.008452262	4.9656215	down
ZNF131	0.0015127	6.5522757	down
ZNF142	0.003745072	9.126152	down
ZNF167	0.009407196	4.751402	down
ZNF227	0.00211369	4.772507	down
ZNF23	4.40E-05	16.816093	down
ZNF490	8.43E-04	33.283813	down
ZNF493	0.002166688	6.2911015	down
ZNF526	0.002013522	8.138484	down
ZNF543	0.009034846	5.857266	down
ZNF557	0.001750089	8.613409	down
ZNF561	0.008716764	5.943809	down
ZNF567	0.001114671	15.420288	down
ZNF652	0.007696924	6.8548446	down
ZNF771	0.002918107	8.33634	down
ZYG11B	0.001931335	5.2407746	down
ADIPOR2	0.009516406	21.0461	up
AKR1B1	0.008719726	3.7689223	up
AKR1C2	0.006721099	10.1691	up
AMD1	0.006721099	4.9025664	up
ANKHD1	0.001971543	5.0964346	up
ANKRD9	0.002956321	7.7113457	up
ANXA5	0.006955957	16.032515	up
AP2B1	5.15E-04	15.976804	up
AP2M1	0.008716638	3.9503698	up
APBA2	0.004578318	20.990068	up
APBB1IP	0.007221074	5.711016	up
APOLD1	0.004012966	21.522852	up
AQP9	0.00425734	8.914484	up
ARMCX6	0.006410764	5.209512	up
ARRDC3	0.006122726	16.778696	up
ATP5F1	0.006721099	3.6082923	up
AXIN2	0.003177458	31.432663	up
BACH2	0.009616257	4.667967	up
BAZ1B	0.001283768	15.451679	up
BCL7C	0.007806727	4.8054714	up
BEX2	0.004954486	21.839859	up
BRF2	0.001283768	9.959711	up
C10ORF32	0.002416148	10.409831	up
C14ORF32	0.001998007	24.909534	up
C1ORF55	0.003498111	9.650796	up
C1QBP	4.89E-04	8.5476	up
C20ORF4	0.009548151	20.760876	up
C2ORF47	0.005911394	9.798617	up
C3ORF14	0.002290321	24.06436	up
C5AR1	0.00673436	15.858517	up
C5ORF25	0.008164501	11.418156	up
CASP6	0.003963402	4.028067	up
CCDC107	7.72E-04	30.068472	up
CCDC59	0.008921199	13.2924385	up
CCDC84	8.81E-05	79.893875	up
CCL22	0.008996708	19.531124	up
CCL23	0.009642038	5.329297	up
CCL3	0.001379336	15.196657	up
CCNL1	0.009484064	5.0891705	up
CD274	0.006703681	12.952867	up
CD58	0.009979644	10.508957	up
CDC2	0.006721099	5.3351145	up
CDK5RAP2	0.007156577	5.535153	up

CDKN2D	0.002277786	5.6594872	up
CENPH	0.003995729	5.340693	up
CHMP2A	0.008129506	5.7402115	up
CHMP6	0.006299525	9.703966	up
CIC	0.008752616	9.791438	up
CLASP1	0.005197869	28.49741	up
CLASP2	0.002522355	29.62007	up
CLIP4	0.002823318	22.020697	up
CLPTM1L	0.003498111	20.156614	up
CNOT8	0.007711134	3.6582751	up
CNPY3	0.00268214	18.267405	up
COG7	0.005245604	7.591311	up
COMMD9	0.008268533	10.968375	up
COPS4	0.006583526	15.082299	up
COPZ1	0.002661705	28.207102	up
COQ7	0.007347688	18.814882	up
CORO7	0.001867556	11.804779	up
COX7B	0.006721099	3.8473878	up
CXORF40A	0.001264581	14.514919	up
CYCS	0.005768979	15.653567	up
CYFIP2	0.009979644	3.3791854	up
D4S234E	0.00585091	6.9799743	up
DDX19B	0.001720097	9.951975	up
DDX21	0.003745072	12.597267	up
DNAJB6	7.15E-04	7.0230947	up
DNMT3A	0.006273667	6.737732	up
DPH3	0.004148494	7.020444	up
DPY30	2.58E-04	17.745598	up
DYM	0.004026739	22.51991	up
ECD	0.0040299	8.933097	up
EEF1B2	7.72E-04	4.398258	up
EEF1D	0.009516406	5.238196	up
EEP1	0.009516406	15.211833	up
EHD4	0.003911523	28.772253	up
EIF2S2	0.003272869	30.734167	up
EIF3F	0.006721099	4.0344014	up
ELF2	0.009467525	8.686361	up
ELK3	0.008797346	12.927707	up
ENTPD4	0.006273667	16.312376	up
ERN1	0.001867556	10.027168	up
FAM127B	0.009255056	9.094625	up
FAM162A	0.004190592	11.025533	up
FAM48A	6.92E-04	15.167932	up
FAM89A	3.34E-04	11.611632	up
FASTKD3	0.009255056	10.059738	up
FASTKD5	0.008797346	6.7576447	up
FOXO1	0.006873354	13.846647	up
GBE1	0.005172796	12.341494	up
GGNBP2	5.65E-05	62.049496	up
GMEB1	0.001919427	10.927252	up
GNPTG	0.002956321	10.117929	up
GPATCH4	0.006525365	7.5065994	up
GRINL1A	4.27E-04	9.736215	up
GTF2H4	0.00164392	24.32491	up
GUSBL2	0.004722433	6.0526247	up
HBXIP	4.40E-05	33.065296	up
HDGF	0.008125961	18.977495	up
HECTD1	0.009407196	8.080266	up
HK3	0.003849729	28.641922	up
HMGN1	0.006533589	11.042228	up
HNRPC	9.53E-04	9.067948	up
HNRPK	0.008797346	6.2411375	up
IARS	0.002361708	8.855911	up
ID2	0.00620863	4.763095	up
IIP45	0.008868565	27.962267	up
IL6R	0.006273667	10.037763	up
IMPACT	0.007156577	24.983097	up

ITGAM	0.001512908	10.035202	up
ITGB3BP	0.002719009	15.961721	up
JMY	0.007473841	7.351855	up
KIAA0141	0.007711134	9.479928	up
KIAA0247	0.008282234	8.521089	up
KIAA1128	0.001795393	11.447064	up
KIF2A	0.002956321	17.09515	up
KLF9	0.008995289	9.488094	up
KTN1	0.006490443	7.946556	up
KYNU	0.005018999	7.129059	up
LETMD1	6.83E-04	9.640929	up
LNPEP	0.005768979	3.9658847	up
LOXL1	0.005553972	13.190039	up
LRBA	0.003050032	7.4771338	up
LYRM2	0.001563511	18.623604	up
MAGOH	0.006337825	15.454308	up
MED30	8.81E-05	59.22387	up
MEF2A	0.00440716	7.503465	up
MFSD8	0.002267259	10.014574	up
MOAP1	0.008957885	8.551846	up
MOC52	0.007640815	6.458394	up
MORC3	0.006525365	12.431017	up
MPP7	0.002166688	21.049816	up
MRC1L1	0.004026739	12.85205	up
MRPL20	8.21E-04	48.818142	up
MRPL23	7.72E-04	29.162357	up
MRPL55	0.005083294	4.2663107	up
MRPS28	0.006873354	7.4213943	up
MS4A7	0.005620657	9.893232	up
MT1H	0.002311068	34.350796	up
MTHFD1L	0.00469059	9.433249	up
MTM1	0.003876145	16.335094	up
MYC	0.008383978	5.139362	up
MYD88	0.003498111	12.019675	up
NAAA	0.006347336	5.303448	up
NBR1	3.94E-04	18.236416	up
NCAPG2	0.003656701	29.210253	up
NCKAP1	0.006273667	7.9983687	up
NDUFA11	0.007546236	5.8516707	up
NELL2	0.001283768	23.405716	up
NIP30	0.008365646	15.253654	up
NLRC4	0.006273667	9.628864	up
NME6	0.009156768	6.706148	up
NPDC1	0.002918107	27.822905	up
NRD1	0.002213799	14.612283	up
NTN4	0.009255056	6.367585	up
NUMA1	0.009607758	5.407944	up
OAT	0.002661705	7.4686866	up
OSCAR	1.97E-04	20.551737	up
P4HA2	7.15E-04	8.820416	up
PABPN1	0.002376513	19.613274	up
PCBP1	0.004084435	7.754172	up
PCGF5	0.005173261	8.492847	up
PDE3B	0.004333112	13.668155	up
PGGT1B	0.005216889	4.8632555	up
PHLDA1	0.002311068	6.877027	up
PKD1	0.002652978	17.080986	up
PLEKHF2	0.003429672	5.0414157	up
PMS2	0.00268214	12.781322	up
PNMA1	0.007711134	7.775702	up
PPARA	0.004077315	9.680098	up
PPM1G	4.10E-04	10.687489	up
PRKX	0.001626937	10.287645	up
PSMA1	0.006525365	3.6164691	up
PSMD12	0.009255056	7.700241	up
PSPH	2.63E-04	17.412756	up
PXMP3	0.007711134	15.16036	up

RABEP1	0.008344029	15.109382	up
RBBP5	2.93E-04	43.420193	up
REEP3	0.007156577	11.642192	up
RNF146	0.004190592	9.127692	up
RNF4	0.009481185	6.6139364	up
RPL22	1.82E-04	19.032623	up
RPL34	0.009255056	5.6620927	up
RPL8	0.008627201	7.6106944	up
RPP38	0.007465011	6.4794436	up
RPS21	0.001283768	39.411095	up
RPS26	9.92E-05	32.98892	up
RPS7	0.003774964	12.732931	up
RUFY1	0.004026739	10.345824	up
SAMD3	0.007237782	5.1257014	up
SEC61G	0.001181684	11.130157	up
SEH1L	0.009034846	4.47619	up
SFRS2	0.006347336	3.177868	up
SFRS2B	0.005254331	5.4524736	up
SFT2D1	9.53E-04	30.565155	up
SH2D3A	0.002499568	14.893252	up
SLC15A4	0.001314587	16.96581	up
SLC25A40	0.00182446	14.469786	up
SNRPF	0.006265898	9.677233	up
SNX1	0.00240005	5.9364448	up
SNX25	0.009516615	7.481325	up
SNX5	4.27E-04	7.7886863	up
SORT1	0.005737121	7.419503	up
SPP1	0.008255319	12.164943	up
SRP14	0.00636012	5.6107802	up
SRPRB	0.001505991	25.656576	up
STARD7	0.002918107	4.8734803	up
SYPL1	0.009255056	3.9627783	up
TALDO1	0.006525365	23.500217	up
TBRG1	0.001505991	12.758599	up
TBRG4	0.009255056	7.1004543	up
TCTN1	0.006686966	5.1527348	up
THNSL1	0.003247789	18.00465	up
THOC7	0.006703681	7.836243	up
TM6SF1	8.10E-05	37.92788	up
TMEM14C	0.009979644	7.9732084	up
TMEM48	0.006347336	10.984599	up
TMEM64	6.55E-04	19.834202	up
TMEM69	0.001314587	24.32409	up
TMSB4X	0.007221074	5.69777	up
TNFRSF25	0.009376789	7.9491463	up
TNPO1	0.001283768	6.945177	up
TRAF3IP1	0.003498111	13.895607	up
TTC17	0.005553972	9.3417845	up
TULP3	0.007711134	17.077192	up
TXNDC14	0.006686966	13.20815	up
UBE2E3	0.004260836	5.4336123	up
UBE2Z	0.005487896	5.845522	up
UCHL5IP	0.003205248	6.614343	up
USP3	0.008357832	12.197942	up
WDR61	0.009358969	14.388639	up
WIPF1	0.006802904	4.9816713	up
XPO1	0.006373111	7.0369406	up
XPO6	0.002218735	7.7901487	up
YEATS2	0.006703681	12.133443	up
YME1L1	0.008917047	5.2307835	up
YTHDC1	0.006257816	3.8322124	up
ZBED2	0.001998007	37.774826	up
ZC3H15	0.009255056	5.9778433	up
ZCCHC14	0.009983876	10.501363	up
ZCCHC3	0.001899286	25.352436	up
ZNF295	0.008797346	23.723484	up
ZNF350	0.002921432	18.235462	up

ZNF512	0.009516406	22.665276	up
ZNF550	0.003778286	11.720262	up
ZSCAN18	0.001705727	8.766659	up
ZUFSP	0.001919427	12.769999	up

Supplementary Table 25. Genes differentially expressed between F-PTCL and Tfh-PTCL/NOS.

Gene ID	Corrected p-value	Absolute Fold Change	Regulation in F-PTCL
ACTN1	0.032651957	9.162927	down
ARMET	0.030497883	10.636738	down
C9ORF142	0.008475903	22.887108	down
DOK3	0.015336229	33.707104	down
FAM158A	0.017402537	15.228142	down
FAM38A	0.044065177	12.141764	down
FLJ33590	0.03327304	14.82872	down
IRAK1	0.03983541	10.90949	down
NDUFS7	0.03936868	8.333967	down
NKG7	0.009984055	11.327506	down
PSMD1	0.015925864	12.863148	down
RCC2	0.049700513	12.389089	down
SDSL	0.026798014	21.156904	down
SELM	0.029673908	13.789991	down
SLC25A23	0.0198869	10.599566	down
SNAPC4	0.042885497	10.986626	down
SPC24	0.021338666	15.053143	down
TRAPPCL	0.01688599	13.615226	down
TUFM	0.007843819	13.879106	down
VARS2	0.041499335	10.58867	down
WDR46	0.019348864	18.556736	down
ZNF653	0.028000334	9.595228	down
AASDHPPPT	8.07E-04	41.277176	up
ACSL5	0.021961661	7.4324985	up
AGL	0.001870222	13.543705	up
ALAS1	0.001051498	9.767095	up
ALDH6A1	0.02039886	10.994508	up
ANXA7	3.64E-05	40.392372	up
AP2A1	0.03167923	10.181193	up
ARFGEF1	0.048668984	7.4701123	up
ARID2	0.004780149	9.928244	up
ARL5A	0.014549244	9.049862	up
ATP6V1G2	0.007860205	11.110379	up
BFAR	3.05E-04	26.577612	up
BRWD1	0.046356093	5.8859763	up
C11ORF58	0.021391474	8.449126	up
C12ORF35	0.007745674	9.77064	up
C14ORF118	0.005698534	13.064511	up
C14ORF138	4.38E-04	18.437647	up
C14ORF43	0.012537808	7.4620814	up
C18ORF54	0.009466338	12.079316	up
C1D	5.02E-04	17.16907	up
C1GALT1C1	0.008882707	10.606838	up
C1ORF9	0.00838236	15.435501	up
C3ORF42	4.87E-04	18.550438	up
C6ORF204	0.019206485	6.1714954	up
C9ORF10OS	8.47E-05	32.76731	up
C9ORF5	0.033942744	12.83138	up
CAMK1D	0.049306374	8.945166	up
CAMK4	3.83E-04	40.382694	up
CAND1	0.01402145	11.286586	up
CAPRIN1	0.004135245	12.209074	up
CASP4	5.86E-04	14.70726	up
CASP7	0.0298692	9.471577	up

CBL	0.03706347	6.199753	up
CCBL2	0.014091983	6.705328	up
CCDC132	0.009961066	8.426201	up
CCDC75	0.04964969	10.867133	up
CCDC91	0.03512753	9.202882	up
CCNT2	4.45E-04	11.123002	up
CDC14A	0.002073128	13.715196	up
CDC2L5	0.00802759	9.967944	up
CDC42	0.012525885	11.098288	up
CDYL	0.009635665	13.891286	up
CENTB2	2.58E-04	18.135399	up
CENTD1	4.31E-04	23.371517	up
CHN1	2.27E-05	30.29738	up
CHORDC1	0.005117486	17.777973	up
CLEC2D	0.04525629	10.308395	up
CLTA	0.005595544	12.044148	up
CMTM3	0.003568086	8.541378	up
CNOT1	2.54E-04	13.108686	up
CNOT7	0.024104986	6.932718	up
COMMID10	0.01824176	10.954586	up
COMMID6	0.004976979	12.861322	up
CR2	0.015186134	25.68522	up
CTPS2	9.24E-04	16.736912	up
CYFIP1	0.03136223	7.499896	up
CYP20A1	0.010266114	11.954899	up
DCK	0.016406136	12.784302	up
DDHD1	0.024219202	17.90043	up
DDX21	0.020346805	21.651844	up
DST	0.001549506	12.828513	up
DTWD1	0.048062485	7.521082	up
DYNC2LI1	0.002310262	10.323492	up
DYRK1A	0.002618847	9.43213	up
EFNA1	7.42E-04	11.101642	up
EGFR	9.86E-04	13.83076	up
EIF1AX	0.030510424	8.746927	up
EIF3J	0.039439548	13.301756	up
EPB41	0.008182965	8.528528	up
EPB41L2	0.006198023	12.821627	up
ERMN	0.001211577	15.3513975	up
FAIM	0.014789138	8.915849	up
FAM108B1	0.003533945	10.087914	up
FAM116A	0.040596273	10.168262	up
FAM126B	0.002526283	14.150282	up
FAM134B	0.039423604	6.9451036	up
FAM135A	2.86E-04	40.914135	up
FAM49B	0.006612108	11.241121	up
FBXL5	0.010573233	8.84768	up
FBXO3	0.001707437	15.354269	up
FBXO30	6.85E-04	10.782243	up
FKBP9	5.38E-04	24.905056	up
FYB	9.89E-04	13.150131	up
GABPA	0.001725848	54.02769	up
GALNT7	0.004616549	22.558992	up
GFRA1	0.019593254	9.800043	up
GIMAP2	0.006579093	14.422142	up
GLMN	0.04389258	10.854096	up
GNAQ	0.00182405	36.411545	up
GNAS	3.99E-05	17.480091	up
GOLT1B	0.014576786	31.848818	up
GOSR2	0.005987098	14.441317	up
GPR162	0.04854598	6.4869947	up
GPR171	0.019456547	11.700031	up
HBXIP	0.040494666	9.077346	up
HECA	4.07E-07	24.14347	up
HIAT1	0.007237727	7.9011655	up
HK1	0.009167008	7.176962	up
HN1	0.046074625	20.770443	up

HSPD1	0.006317423	11.670771	up
IPO8	0.02395025	17.616047	up
ITGB1	5.53E-04	7.8162904	up
ITM2B	4.31E-05	21.194881	up
KIAA1199	0.042779103	28.80425	up
KIAA1370	0.001384766	14.814141	up
KIT	0.03743375	12.335301	up
KLF12	0.039620526	8.810764	up
KPNA3	2.26E-04	31.506273	up
KRAS	3.15E-06	19.171223	up
KRIT1	0.01222548	8.074157	up
LAMA3	0.008003891	12.8271055	up
LEPR	0.020601597	7.822688	up
LFNG	0.032402307	8.383152	up
LGALS8	0.041722108	5.184375	up
LIN7C	0.018642986	12.752212	up
LRP8	0.04905565	12.190844	up
LRRC1	0.010665879	10.3489275	up
LUM	3.22E-04	20.958082	up
MAML2	0.0098189	7.059718	up
MARS2	4.70E-04	16.742716	up
MCTP1	0.00814017	10.806294	up
ME2	0.033398382	9.588622	up
MFF	0.027835509	9.6278715	up
MS4A1	0.044877257	10.118098	up
MS4A4A	2.51E-06	31.586025	up
MST4	0.017647892	12.069609	up
MTM1	1.83E-04	67.7478	up
MTX2	0.009700547	10.912346	up
MYADM	0.00174102	8.926965	up
MYC	0.010495709	9.041944	up
MYLK	3.34E-04	9.292695	up
MYST4	0.005459053	33.347977	up
NAPEPLD	1.29E-04	36.74243	up
NBPF15	0.004330082	12.314768	up
NDRG4	1.99E-04	12.449857	up
NEDD9	0.038272757	6.288476	up
NFATC2	0.006347351	11.042445	up
NFIA	0.005338766	17.74585	up
NLGN4X	0.008505589	17.295738	up
NNT	0.028443443	10.95388	up
NTS	0.02140472	24.509161	up
NUDT21	0.019612119	8.490156	up
OAS3	0.002295236	15.264411	up
OLFM1	0.044097383	6.844748	up
OPA1	8.55E-04	16.059486	up
ORC5L	3.69E-04	13.037892	up
P2RY13	0.047715716	7.97502	up
PAG1	0.015161951	6.476815	up
PANK2	5.36E-04	12.857293	up
PARVA	0.005152434	25.780725	up
PDCD5	0.013747104	12.529679	up
PDE3B	0.013638238	31.769745	up
PDE5A	1.17E-04	18.557722	up
PEMT	0.009494056	8.811079	up
PER2	0.002117825	9.770009	up
PHOSPHO2	4.18E-05	20.61192	up
PI15	0.009325375	7.147152	up
PIK3CA	0.01747068	8.527986	up
PKIA	0.001123408	16.46336	up
PMS1	0.046308294	19.087858	up
POLG	0.041365776	18.88169	up
POLR2J3	9.28E-04	15.99831	up
PPIL4	0.005258972	14.7197	up
PPP2R2D	0.042560164	6.679457	up
PRKACB	1.43E-04	14.696016	up
PSAT1	0.014526144	10.15735	up

PSCDBP	7.47E-05	16.042686	up
PTPN22	3.05E-04	17.662203	up
RAB11FIP1	6.21E-04	7.778176	up
RAD17	1.61E-04	13.165413	up
RAD50	1.29E-04	22.66159	up
RAI1	0.010688429	14.666737	up
RALGPS2	0.044435494	12.424311	up
RANBP2	8.99E-04	18.38456	up
RAPH1	0.014703849	8.4397745	up
RBL1	8.44E-05	12.657019	up
RBPJ	0.002408673	12.937213	up
RCOR1	0.007719148	32.216034	up
RELN	0.004066379	12.676274	up
RIOK3	0.00952796	12.56369	up
RNF138	0.03886679	19.728134	up
RNF4	0.014938999	16.981974	up
RPAP3	0.011414674	8.531435	up
RPL7	0.00503679	15.270482	up
RRP1B	2.62E-04	22.87699	up
RRS1	0.002793369	27.799473	up
RSBN1L	0.002684305	16.479511	up
RYK	0.027394367	8.029521	up
SCAMP1	0.026224686	9.281375	up
SCGN	0.002081553	36.131283	up
SCML1	0.041291155	11.541202	up
SCRIB	0.03331376	8.584683	up
SDF4	2.60E-04	13.417861	up
SDHD	0.007074507	30.674475	up
SEH1L	0.03716784	7.799186	up
SENP7	0.033220008	12.149023	up
SERF1B	0.003061452	27.086784	up
SETD3	0.001779174	10.350714	up
SFRP2	0.006193906	42.93927	up
SFRS3	2.86E-05	17.78571	up
SH3BGRL	7.49E-04	23.838997	up
SLA	0.024993343	10.9353	up
SLC10A7	6.40E-04	12.123195	up
SLC41A3	0.010409465	9.676246	up
SLC9A6	6.44E-04	14.053468	up
SLCO3A1	0.012006078	9.214042	up
SLFN11	0.009661906	17.09201	up
SMC6	0.032854587	21.283113	up
SMPDL3A	0.010840488	12.569457	up
SNORD107	4.90E-04	40.553215	up
SNRPN	3.18E-04	8.961529	up
SOCS2	0.006703933	7.8000255	up
SP3	0.005744148	12.451309	up
SPAST	0.006361755	9.464127	up
SPIC	0.009852324	14.83653	up
SPOPL	0.003843804	10.625132	up
SSBP3	0.022611488	7.4283247	up
ST6GAL1	0.008441367	12.350014	up
ST8SIA4	0.029863885	10.898398	up
STAG2	0.017095156	7.8552923	up
STAMBP	0.036144394	8.729737	up
SUMO1	9.62E-04	20.211485	up
SUOX	0.02441466	5.9055653	up
SYNE1	3.04E-04	13.471909	up
SYNE2	0.040446144	12.170956	up
SYPL1	0.037388183	18.29962	up
TADA1L	0.027129823	9.374849	up
TAF9	0.0374676	18.660734	up
TAS2R14	0.029178554	16.401182	up
TC2N	6.89E-05	48.675907	up
TCERG1	0.006760553	8.123661	up
TCP1	0.002559799	7.946777	up
TFG	0.023799472	7.884549	up

TGFBR2	0.010612262	10.810942	up
THAPS	0.001529566	12.716297	up
TIPRL	0.01842422	9.607702	up
TMEM104	6.49E-04	70.929016	up
TMEM106B	8.78E-05	19.833946	up
TMEM128	0.03516394	16.539415	up
TMEM19	0.002633689	7.5223684	up
TMSB4X	0.004418903	41.50205	up
TOPORS	0.02619806	13.953513	up
TPP2	0.002498981	9.712883	up
TRAF5	9.02E-06	16.22763	up
TRAPPC6B	0.025020275	6.961982	up
TRIM3	0.005567181	6.9052196	up
TSC22D3	0.017641831	7.489523	up
TSPAN13	0.026092144	13.100282	up
TSPAN4	0.02809923	12.595056	up
TSR1	0.005438575	17.210089	up
TTC33	0.015244305	18.70002	up
TTF1	0.020189717	7.309971	up
TTRAP	0.008262022	12.626039	up
TUSC3	0.036112882	8.189791	up
TXK	0.006980763	24.003275	up
TXNL4A	0.008832347	24.957693	up
UBE2D3	0.001188838	9.665733	up
UBE2H	0.010766036	9.725424	up
VPS13A	0.00419009	8.198767	up
VPS13B	0.00383473	10.003193	up
VPS24	0.00646249	11.675179	up
WDR26	0.013391696	8.905493	up
WIPF1	0.00946921	17.673754	up
WWP2	0.014749949	10.531052	up
XRN2	0.03012715	23.389383	up
ZBTB11	0.036008757	9.916371	up
ZFAND6	7.41E-05	28.02789	up
ZFY	0.030169657	31.325817	up
ZNF141	9.51E-05	29.805304	up
ZNF318	0.001075414	8.953189	up
ZNF567	0.020276193	10.453688	up
ZNF83	0.002010679	28.507801	up

Supplementary Table 26. Genes differentially expressed between AITL and Tfh-PTCL/NOS.

Gene ID	Corrected p-value	Absolute Fold Change	Regulation in AITL
AIM2	0.002566941	23.48162	down
ALDH6A1	1.55E-05	48.15558	down
ANKRD35	2.97E-06	155.26956	down
APLP2	0.003657815	45.58968	down
APOBEC3G	8.40E-04	22.663546	down
AQR	8.54E-04	24.508722	down
ATP5L	0.03967707	11.2997055	down
C11ORF58	2.86E-04	24.138603	down
C14ORF85	0.001103142	149.10243	down
C15ORF5	0.03700855	18.255774	down
C20ORF96	0.045317184	128.80238	down
C5ORF34	0.04028918	44.67423	down
CAPZB	0.001680586	67.7006	down
CDH6	3.31E-04	48.682053	down
CPEB3	9.87E-04	33.154354	down
DHRS13	0.032171253	15.06404	down
EID2B	0.009678989	69.699135	down
EIF5A2	0.003201631	96.493546	down
ERAL1	0.042740557	10.915455	down
ETV6	0.044373468	15.039108	down
FAM53B	0.002020156	23.678072	down
FAM98A	0.04986558	13.817567	down

FBXO5	0.005901064	22.07946	down
FEM1C	7.73E-04	18.65839	down
FOXO4	0.045249026	16.194887	down
GCNT1	0.009365761	44.644897	down
GFPT1	5.15E-04	32.4352	down
GIMAP5	0.005055221	267.79944	down
GNAI1	3.00E-06	69.33706	down
HLA-E	1.20E-04	126.870316	down
HOXA2	1.52E-06	53.005295	down
JARID1A	0.024651164	283.76633	down
KCNJ10	0.049150266	11.204566	down
KHDRBS3	4.91E-07	163.35817	down
KIAA1333	0.007214521	34.416027	down
KLHL14	0.012276984	19.63116	down
KMO	1.30E-06	54.359653	down
KRIT1	0.005959029	14.98657	down
KTELC1	0.018496703	15.097835	down
MED31	0.004702204	34.833733	down
MOSPD2	3.83E-04	67.09868	down
NCKAP1L	0.01019731	32.479652	down
OXTR	0.01693197	46.027496	down
PES1	0.005020364	25.038574	down
PEX11G	0.01086219	23.36378	down
PHOSPHO2	0.015676547	10.28182	down
POMP	0.048381988	21.331226	down
RAG1AP1	0.011287431	22.24524	down
RCN1	0.00103686	187.38063	down
RNF11	7.99E-04	28.746521	down
RPS6KC1	1.44E-04	14.251197	down
RRP7A	0.033799168	17.236958	down
SETD6	7.10E-04	623.90845	down
SETDB2	0.001869267	26.06232	down
SFRP4	4.06E-04	70.33453	down
SLAMF8	0.001013491	1173.5913	down
SPC24	0.041140508	15.117227	down
STYX	0.003580729	75.47328	down
TAOK3	0.001891624	103.75347	down
TM4SF18	1.96E-04	25.458818	down
TMEM137	0.014504074	28.535751	down
TMEM189-UBE2V1	0.01013291	24.212372	down
TMEM19	2.45E-07	53.722717	down
TNFRSF1B	0.005939021	30.085102	down
TSPAN12	7.36E-04	30.281181	down
VEZT	0.001580042	15.173254	down
WBP5	4.84E-04	30.051939	down
WWP1	0.001683327	23.274904	down
ZBTB3	0.005124753	14.509221	down
ZC3H7A	2.15E-05	129.67134	down
ZCCHC6	0.002566889	33.206764	down
ZNF23	0.044095717	17.593714	down
ZNF490	0.001055645	61.763958	down
ZNF526	0.04116124	10.010195	down
ZNF567	0.003522322	14.825055	down
ANKRD9	0.002761816	21.909216	up
AP2B1	0.02397262	23.275143	up
APOLD1	0.005926091	61.081253	up
BAZ1B	0.005163072	23.257877	up
C11ORF46	0.035647195	22.80408	up
C1QBP	0.024113987	12.265031	up
CCDC84	0.00129678	128.052	up
CLASP2	0.010201118	80.66772	up
CNPY3	9.32E-04	38.411995	up
COQ7	1.62E-04	96.48538	up
CXORF40A	1.60E-04	24.014153	up
DDI2	0.028972138	9.440678	up
DNMT3A	0.002798959	23.469175	up
DPY30	3.72E-05	48.782364	up

FAM48A	0.006025021	23.848028	up
GGNBP2	1.39E-04	149.64116	up
HBXIP	2.75E-05	44.76022	up
HNRPC	0.048685484	12.152678	up
IIP45	0.02503481	108.87883	up
INCENP	0.027921667	14.045565	up
JMY	0.029629907	17.05962	up
LOXL1	0.04009175	18.263783	up
LPCAT4	0.002374276	46.757126	up
MED30	1.60E-04	111.39466	up
MS4A7	0.006395315	15.16044	up
MTM1	2.61E-04	94.294304	up
NAT11	0.023560397	50.628826	up
NCAPG2	0.004161646	79.42693	up
PDE3B	0.041418705	33.25751	up
POLG	0.036636703	22.537111	up
PSPH	0.015550672	21.99862	up
PTPLAD1	0.04920792	12.222071	up
RNF146	0.016585218	21.163317	up
RPL22	0.008697484	41.404293	up
SLC15A4	0.035324644	20.188938	up
SNX1	0.005495214	13.213169	up
SRPRB	7.43E-04	68.392334	up
TBRG1	0.013072972	22.137026	up
TM6SF1	0.04395993	41.096355	up
TMEM69	1.25E-04	50.38219	up
XPO6	1.73E-04	20.896225	up
YPEL3	0.010119362	98.21181	up
ZSCAN18	9.93E-04	15.575254	up